

STUDIES ON THE
GLYCOGEN PHOSPHORYLASE
SYSTEM

A Thesis submitted in partial fulfilment of the requirements
for the degree of Doctor of Philosophy

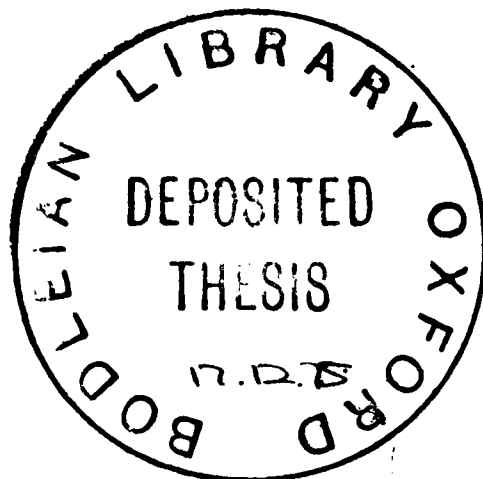
by

S.J.W. Busby, B.A.

St. John's College, Oxford

October, 1975

Department of Biochemistry



ABSTRACT

The rabbit muscle glycogen phosphorylase system consists of a complex set of interacting macromolecules and ligands. In vivo it is responsible for the regulated phosphorolysis of glycogen. This thesis describes some new approaches, based on the use of spectroscopic techniques, to the study of the regulation of the system.

Chapter 1 describes the components of the system; brief accounts of the properties of phosphorylase, phosphorylase kinase, phosphorylase phosphatase and other associated macromolecules are included. In addition some of the interesting unsolved problems concerning the system are raised. How does the structure of phosphorylase depend on the ligands that are present? What is the role of the pyridoxal phosphate cofactor in phosphorylase? What is the significance of the multiple aggregation states observed for phosphorylase? How do the enzymes that are involved in the phosphorylase cascade system interact with each other? Are the properties of these enzymes altered when they operate in the glycogen particle fraction or in the intact cell?

Chapter 2 introduces the spectroscopic techniques which have been used to investigate these problems. Fluorescence, ESR, and NMR methods are outlined and their relative merits are assessed. The applicability of these techniques to the problems outlined in Chapter 1 is critically estimated.

Chapter 3 describes the reaction of phosphorylase b with various reagents, some of which have spectroscopic properties that make them useful as probes of enzyme structure. It is shown that up to two sulphhydryl groups per phosphorylase subunit can react rapidly with iodoacetamide, 4-chloro-7-

nitrobenzofurazan, iodoacetamidosalicylic acid or 5,5'-dithiobis-(2-nitrobenzoic acid). In an attempt to clarify some of the inconsistencies that occur in the literature concerning the reaction of phosphorylase b with various sulphhydryl directed protein modifying reagents, it is shown that these fast reacting sulphhydryl groups can be blocked by preincubation of phosphorylase with cysteine or cystine.

The interactions of small regulatory ligands with phosphorylase, which had been labelled with the fluorescent probe iodoacetamidosalicylic acid, are discussed in Chapter 4. The quenching of probe fluorescence observed when ligands bind to labelled phosphorylase is used to quantify the interactions and to demonstrate cooperative effects between ligands. A description of a spin label probe, which may be covalently attached to phosphorylase, and which can also detect ligand induced changes in the enzyme is included. Experiments to determine the cause of the ligand induced changes in the spectral properties of the spin label and fluorescent probe are discussed. It is shown that when AMP is titrated into spin labelled phosphorylase a, the spin label can detect conformational changes in subunits to which no AMP is bound. A method is presented whereby the aggregation state of phosphorylase during this titration can be determined. It is demonstrated that when phosphorylase a is glycogen-bound, more than two subunits may interact together.

The properties of phosphorylase which had been modified with 5 diazo-1-H-tetrazole are described in Chapter 4. The spin label and fluorescent probes can be attached to the modified enzyme. It is shown that this modification, which specifically blocks a carboxyl group in the enzyme, weakens the binding of glucose-1-phosphate and glycogen to phosphorylase.

Chapter 4 also contains a study of the interaction of a spin labelled AMP derivative with phosphorylase. The effects of this derivative upon spin and fluorescent labels covalently attached to phosphorylase are described. It is shown that the spin labelled AMP derivative mimics IMP rather than AMP.

The phosphorus NMR signals obtained from the pyridoxal phosphate cofactor in phosphorylase b and a are presented in Chapter 5. A two component signal is seen for phosphorylase b alone. This is interpreted to represent a slow interchange between two or more enzyme conformations. Ligand induced changes in the spectra are also described and interpreted.

Chapter 6 discusses the changes in the ESR spectrum of spin labelled phosphorylase during the b to a conversion. In contrast, it is shown that when acetamidosalicylate phosphorylase b is converted to the a form no change in probe fluorescence is observed. However when the conversion is carried out in the presence of ligands, fluorescence changes occur which reflect differential ligand binding to the two forms of the enzyme. Experiments performed in the presence of glucose-6-phosphate directly demonstrate the presence of an intermediate active form of phosphorylase which binds glucose-6-phosphate tightly, unlike fully phosphorylated phosphorylase a. A method is described to detect protein-protein aggregation. It is based on the quenching of acetamidosalicylate fluorescence by nitrobenzofurazan when proteins labelled with these two probes aggregate. The method is used to show the time course of formation of tetrameric phosphorylase a from the dimeric species.

The extent to which the rabbit muscle glycogen particle fraction can simulate the environment experienced by phosphorylase in vivo is discussed in Chapter 7. An investigation of the conformation of spin labelled phosphorylase

in this cell free fraction, before and after transient activation, is described. Changes in the ESR spectra of the spin labelled enzyme during calcium dependent transient activation are correlated with changes in metabolite levels and phosphorylase a activity. The transient activation is associated with a loss of glucose-6-phosphate from phosphorylase b; newly formed phosphorylase a binds the nucleotides ADP, AMP or IMP. Lowering the $Mg^{2+} : Ca^{2+}$ concentration ratio during transient activation causes accumulation of ADP. Under these conditions ADP binding to phosphorylase a is potentiated. The chapter is concluded with a brief comparison of the glycogen particles prepared from normal and I strain mice.

An investigation of nucleotide inhibition of phosphorylase phosphatase in the glycogen particle fraction is included in Chapter 8. It is demonstrated that ADP and IMP inhibit the dephosphorylation of exogenously added and endogenous phosphorylase a. Inhibition is weaker than that previously reported for purified phosphatase and phosphorylase a. Using spin labelled phosphorylase a, it is demonstrated that in the glycogen particle fraction, ADP inhibition of phosphorylase phosphatase is not a consequence of the tight binding of ADP to phosphorylase a. It is shown that incorporation of phosphatase into the glycogen particle fraction causes large changes in some of the properties of the enzyme.

Chapters 1-8 deal with purified enzymes and cell-free systems. In contrast, Chapter 9 presents data from experiments with intact tissues. It is shown that phosphorus NMR can provide information on the concentrations, coordination and interconversion of phosphorus-containing metabolites in intact muscle. The shape of any particular signal indicates the number of

environments in which the corresponding compound finds itself, and is therefore a monitor for compartmentation of that compound. The multicomponent line-shape of the signal of inorganic phosphate intrinsic to muscle, or of phosphate 'dialysed' into the tissue indicates some form of compartmentation of this ion. The creatine phosphate resonance, in contrast, has only one component. The complexity of the inorganic phosphate line-shape is dependent on the integrity of the tissue. The origin of these effects is discussed.

Chapter 9 is concluded with a comparison of the phosphorus NMR spectra of red and white muscle and a discussion of the observed differences. Spectra of rabbit semitendinosus muscles exhibit a resonance which is not observed in spectra of rabbit white leg muscles. It is shown that this resonance is due to the presence of a phosphodiester. A partial purification of this metabolite is described but the exact nature of the compound is not defined.

The thesis is concluded with Chapter 10 which presents an assessment of the likely state of phosphorylase b and a in vivo. The discussion is not solely restricted to phosphorylase activation; the mechanism whereby phosphorylase activity is suppressed in resting muscle is critically discussed.

CONTENTS

<u>Chapter 1</u>	<u>The Glycogen-Phosphorylase System</u>	
A.	Historical	
B.	The Phosphorylase Cascade System	
C.	Phosphorylase	
	(i) Reaction Catalysed	
	(ii) Aggregation	
	(iii) Effectors	
	(iv) The Pyridoxal Phosphate Cofactor	
	(v) The Serine Phosphate	
	(vi) Crystallography	
D.	Phosphorylase kinase	
E.	cAMP dependent protein kinase	
F.	Phosphatases	
G.	Glycogen	
H.	The Glycogen Particle Fraction	
<u>Chapter 2</u>	<u>The Methods</u>	19
A.	Can the problems be solved?	
B.	Chemical Reactivity	
C.	Fluorescence Methods	
D.	Spin Label Probes	
E.	Nuclear Magnetic Resonance	
<u>Chapter 3</u>	<u>Covalent Attachment of Probes to Phosphorylase</u>	43
A.	The Reaction of Cysteine with Phosphorylase	
B.	The Reaction of Iodoacetamide with Phosphorylase	
C.	The Reaction of 4 Chloro 7 nitrobenzofuran with Phosphorylase	
D.	The Reaction of DTNB with Phosphorylase	
E.	The Reaction of Iodoacetamide Spin label with Phosphorylase	
F.	The Reaction of Iodoacetamidosalicylic Acid with Phosphorylase	
G.	Summary	

<u>Chapter 4</u>	<u>The Interaction of Ligands with Phosphorylase</u>	70
A.	Measuring Dissociation Constants of Enzyme Ligand Complexes	
B.	The Use of Spin Labelled Phosphorylase	
C.	The Probe Response to Ligand Binding	
D.	Do Probe Molecules Report Conformational Changes or Direct Interaction with Ligands?	
	(i) Using a labelled subunit with the AMP binding site blocked	
	(ii) How many subunits can one ligand molecule influence?	
E.	How many subunits interact in phosphorylase <u>a</u> ?	
F.	Spin labelled AMP - an activator of phosphorylase	
G.	The interaction of ligands with modified phosphorylase	
<u>Chapter 5</u>	<u>Phosphorus NMR Studies of Phosphorylase</u>	108
A.	Model Studies	
B.	The ^{31}P NMR Spectrum of phosphorylase <u>b</u>	
C.	The Effect of Ligands	
D.	Phosphorylase <u>a</u>	
E.	Conclusions	
<u>Chapter 6</u>	<u>The Phosphorylase <u>b</u> to <u>a</u> conversion</u>	120
A.	Studies using Spin Labelled Phosphorylase	
B.	Differential Ligand Binding to Phosphorylase <u>a</u> and <u>b</u>	
C.	The Conversion of Phosphorylase <u>b</u> to <u>a</u> catalysed by Non-Phosphorylated kinase	
D.	The kinetics of the Formation of phosphorylase <u>a</u> tetramers	

<u>Chapter 7</u>	<u>Protein-Glycogen Complexes - An Approach to the "In Vivo" Situation</u>	132
	<ul style="list-style-type: none"> A. The Contents of the Glycogen Particulate Preparation B. ESR Measurements C. Ca^{2+} Dependent Transient Activation D. Transient Activation at Lower $\text{Mg}^{2+}/\text{Ca}^{2+}$ Ratios E. Does Transient Activation in the Glycogen Particle Fraction tell us anything about Transient Activation <u>in vivo</u>? F. Ligand Induced Changes in Phosphorylase Conformation without Activation G. Trypsin Treatment of Glycogen Particles H. I-strain Mice Glycogen Particles 	
<u>Chapter 8</u>	<u>The Control of Phosphatase activity in the glycogen particle fraction</u>	161
	<ul style="list-style-type: none"> A. The Dephosphorylation of Extrinsically added phosphorylase <u>a</u> B. The Dephosphorylation of phosphorylase intrinsic to the glycogen particle fraction C. Discussion and Speculations 	
<u>Chapter 9</u>	<u>Observation of Tissue Metabolites using Phosphorus NMR</u>	178
	<ul style="list-style-type: none"> A. Model Studies B. Spectra of Intact Tissue C. Studies on Dialysed Muscle D. Red Muscle and the Unassigned Metabolite E. Partial Purification of the Unassigned Metabolite 	
<u>Chapter 10</u>	<u>Non-Covalent Regulation of Phosphorylase Activity - Unknowns and Inconsistencies</u>	207
	<ul style="list-style-type: none"> A. Non-Covalent Phosphorylase Inhibition B. Non-Covalent Phosphorylase Activation 	

<u>Appendix 1</u>	<u>Materials</u>	221
A.	Enzymes	
B.	Buffers	
C.	Reagents for Protein Modification	
D.	Materials for Enzyme Assays	
E.	Miscellaneous Reagents	
<u>Appendix 2</u>	<u>Technical Details</u>	224
A.	Phosphorylase assays	
B.	The molar concentration of Phosphorylase	
C.	Radioactivity Measurements	
D.	Absorption Measurements	
E.	Methods supplement to Chapters 4 and 6	
F.	NMR Spectrometers	
G.	Methods Supplement to Chapters 7 and 8	
H.	Freeze Clamp procedures	
I.	Muscle dialysis	
<u>Appendix 3</u>	<u>Are changes in the ESR Ratio always proportional to saturation functions?</u>	231

ACKNOWLEDGEMENTS

It is a well known fact that in any thesis, this is one of the most frequently perused sections. The collaboration, assistance and advice of many friends is, therefore, best recognised here.

I am especially indebted to my supervisor, Dr. G.K. Radda, who has provided an abundance of encouragement, stimulation and guidance.

The experiments with spin labelled phosphorylase were performed in collaboration with Dr. J.R. Griffiths and Dr. M.A. Hemminga. I am indebted to both these gentlemen for teaching me ESR techniques and for their patience and persistence.

I was introduced to phosphorus NMR by Dr. D.G. Gadian and Mr. P.J. Seeley, whose energetic, enthusiastic and thorough experimental skills have greatly contributed to the results described in Chapters 5 and 9.

Many of the results in Chapters 3 and 4 were obtained during fruitful collaborations with Mr. D.J. Brooks, Dr. O. Avramovic-Zikic, and Dr. W. Trommer.

The work has benefitted greatly from the efficient and expert technical skills of Mr. R. Gardener, Mrs. J. Johnson, Mrs. E.E. Richards, Mr. C.V.A. Dear and Mr. R. Harris.

In addition I should like to thank the other members and associates of the laboratory who, throughout my three years in Oxford, have offered friendship and help. In particular, I thank Mr. C.L. Bashford, Dr. R. Cecil, Dr. R.A. Dwek, Mr. S.J. Ferguson, the late Mr. J. Green, Mrs. L. Hemminga, Dr. D.I. Hault, Mr. N.P. Illsley, Dr. W.J. Lloyd, Mr. C.G. Morgan and Miss G.A. Ritchie.

The work was supported financially by an M.R.C. training award and a Senior Scholarship from St. John's College.

Abbreviations

Å	Angström Units
ADP	Adenosine-5'-diphosphate
AMP	Adenosine-5'-phosphate
ATP	Adenosine-5'-triphosphate
cAMP	Adenosine-3',5',-cyclic phosphate
DEAE	Diethylamino ethyl-
DHT	5-Diazo-1H-tetrazole
DTNB	5,5'-Dithiobis-(2-nitrobenzoic acid)
EDTA	Ethylene Diamine Tetraacetic Acid
ESR	Electron Spin Resonance
FDNB	2,4-Dinitro Fluorobenzene
G-1-P	α -D-Glucose-1-phosphate
G-6-P	D-Glucose-6-phosphate
Hz	Hertz
I ⁻	Iodide ions
IMP	Inosine-5'-phosphate
ISA	4 iodoacetamidosalicylic acid
MWC	Monod, Wyman and Changeux
Nbf	7-Nitrobenzofurazan -
Nbf-Cl	4-Chloro-7-Nitrobenzofurazan
nm	Nanometre
NMR	Nuclear Magnetic Resonance
P _i	Inorganic Phosphate
pp _a	Phosphorylase <u>a</u>
pp _b	Phosphorylase <u>b</u>
pp _a <u>b</u>	Hybrid phosphorylase (1 subunit <u>a</u> and 1 subunit <u>b</u>)
p.p.m.	Parts per million
R	the ESR ratio
S	Sedimentation coefficient
SA	acetamidosalicylate -
SDS	Sodium Dodecyl sulphate

τ	Correlation time
T_1	Spin-lattice relaxation time
T_2	Spin-spin relaxation time
TEA	Triethanolamine
Tris	Tris (hydroxymethyl) amino methane
UDPG	Uridine 5'-diphosphate α -D-glucose

Enzymes

Phosphorylase	2.4.1.1
Phosphorylase <u>b</u> kinase	2.7.1.38
Phosphorylase phosphatase	3.1.3.17
5' Adenylic acid deaminase	3.5.4.6
cAMP dependent protein kinase	2.7.1.37
Phosphoglucomutase	2.7.5.1
Myokinase	2.7.4.3
Glucose 6 phosphate dehydrogenase	1.1.1.49
Hexokinase	2.7.1.1
α -Amylase	3.2.1.1
Trypsin	3.4.4.4
Glycogen Synthetase	2.4.1.11
UDPG pyrophosphorylase	2.7.7.9
Alkaline phosphatase	3.1.3.1
Ribonuclease A	3.1.4.22
Oligonucleotide 5' nucleotido hydrolase	3.1.4.1

Chapter 1

THE GLYCOGEN - PHOSPHORYLASE SYSTEM

"....the highly developed situation is, by definition, low in opportunities of participation, and rigorous in its demands of specialist fragmentation from those who would control it". (2)

The rabbit muscle glycogen phosphorylation system consists of a complex set of interacting molecules. A full understanding of its operation and regulation requires not only a thorough characterisation of each component, but a clear picture of how these components interact and are influenced by the physiological environment. Whilst the conventional methods of enzyme assays, freeze clamp, isotope labelling and chemical analysis, can provide much basic information, it is clear that direct methods for studying unperturbed molecules in this system are needed. This thesis presents an attempt to investigate the enzymes concerned with glycogen breakdown with techniques which use spectral data to convey detailed molecular information.

This chapter outlines the present state of knowledge of the glycogen phosphorylase system, highlighting some of the points where there is uncertainty and ignorance, and the ensuing chapter introduces the spectroscopic techniques, pointing to their usefulness in approaching the outstanding problems.

A. Historical

In the 1931 issue of the Journal of Biological Chemistry, Carl and Gerty Cori wrote, "The observation that more muscle glycogen disappeared after epinephrine injection than could be accounted for as lactic acid, suggested that a substance intermediary between glycogen and lactic acid accumulated in muscle under these conditions". (3) This deduction gave impetus to a series of studies which, twenty five years later, had laid the foundations of our current knowledge of the glycogen phosphorylase system. Prompted by the discovery, by Emden, of hexose phosphates in muscle extracts (4,5), the Coris isolated and synthesised glucose-1-phosphate (6). By 1938, "The formation of glucose-1-phosphate and its conversion to glucose-6-phosphate had been shown to be the initial steps in the degradation of glycogen to lactic acid" (7,8) and hence the existence of phosphorylase and phosphoglucomutase was deduced (Fig. 1.1). Study of phosphorylase activity in tissue extracts revealed, for the first time, an allosteric effect - AMP and IMP stimulated the formation of glucose-1-phosphate from glycogen and inorganic phosphate (8,9,10).

Shortly afterwards, the crystallisation and preparation of phosphorylase were described (11,12). According to the preparation, two distinct forms of phosphorylase could be isolated. One form, the a form, crystallised readily and possessed activity in the absence of AMP. The other form, phosphorylase b, was more soluble and was inactive unless AMP was present. It was shown that tissues contain an enzyme which could convert the a form to the b form (13). Hence the idea that an enzyme could exist in two interconvertible forms became established.

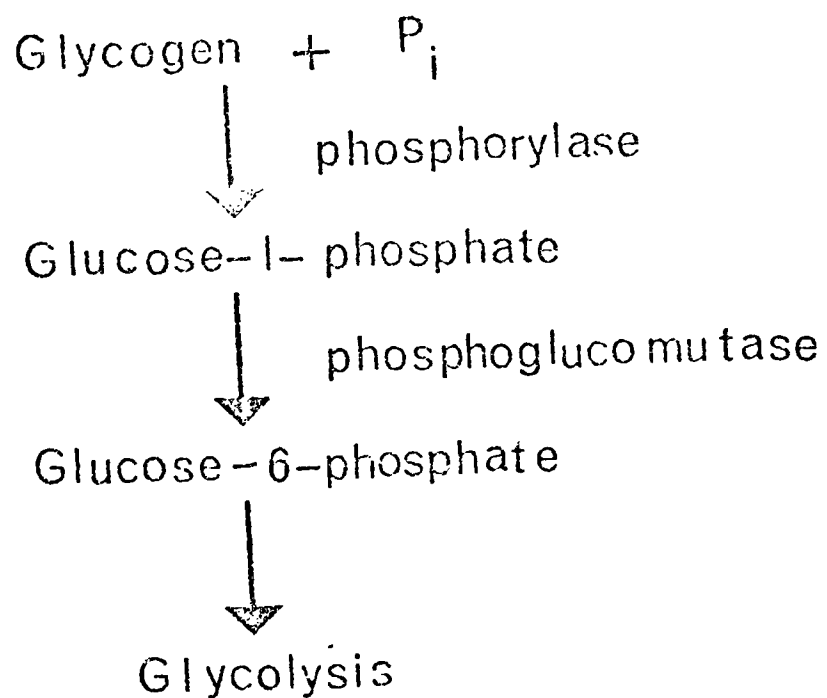


Figure 1.1 Glycogen provides sugar phosphates for Glycolysis

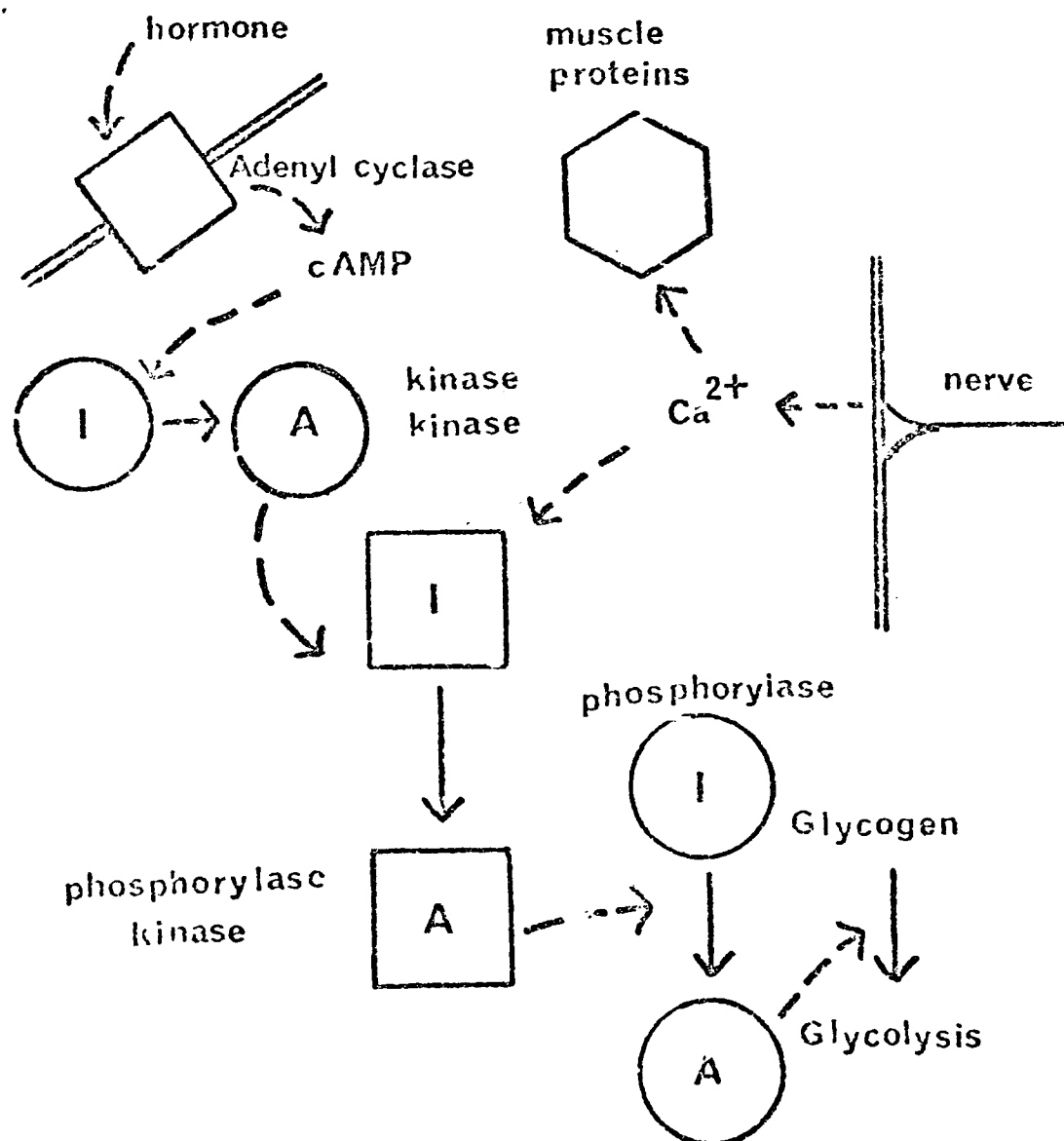


Figure 1.2 Switching on Glycogenolysis Scheme illustrating calcium and cAMP induced activation of the glycogen phosphorylase system (I = inactive form of enzyme, A = active form of enzyme)

Fischer and Krebs extended these observations when they demonstrated that the b to a conversion required ATP and Magnesium ions (14,15). This led to the discovery of phosphorylase kinase and the realisation that the b to a conversion proceeded by the covalent attachment of a single phosphate group onto one serine residue in each subunit (16,17,18).

B. The Phosphorylase Cascade System

Glycogen is the main energy storage polymer in white muscle. Glycogenolysis utilises the energy stored in the bonds of this polymer to produce the high energy compound, ATP. In order to provide energy when muscle contracts and to conserve energy when muscle relaxes, glycogenolysis must be controlled. Our understanding of this regulation is based upon the results of a large number of research groups whose work has developed and expanded the early observations of the Coris. A brief summary of current dogma is included here.

As is most logical, the first step of glycogenolysis, the phosphorylase step, is regulated (Fig. 1.2). In the resting muscle, phosphorylase, which is glycogen-bound, is assumed to be inactive and is in the b form (unphosphorylated). The main pathway for activation involves phosphorylation by ATP, catalysed by phosphorylase kinase. The activity of this latter enzyme is totally dependent upon the presence of calcium ions (19). Nervous stimulation of muscle leads to release of calcium from the sarcoplasmic reticulum, the increase in sarcoplasmic calcium concentration (about $2 \times 10^{-6} M$) being sufficient to stimulate both phosphorylase kinase activity and muscle

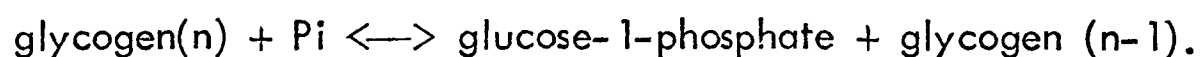
contraction (20,21) (see Fig. 1.2). ATP energised pumping of calcium out of the sarcoplasm causes muscle relaxation and deactivates phosphorylase kinase. Phosphorylase phosphatase then converts phosphorylase a to b, and further glycogenolysis is prevented.

Phosphorylase kinase activity is also enhanced when it is phosphorylated by cAMP dependent protein kinase (62). When adrenaline stimulates muscle, sarcoplasmic cAMP levels are raised, cAMP dependent protein kinase is activated and phosphorylase kinase is phosphorylated. Hence glycogenolysis in muscle may be stimulated by hormonal as well as nervous signals (22,23,24) (see Fig. 1.1). This sequence of effectors and enzymes is often referred to as a cascade because $< 10^{-10}$ M adrenaline in the plasma can produce levels of 10^{-8} M cAMP in the sarcoplasm which can activate 10^{-8} M cAMP dependent protein kinase and hence 4×10^{-6} M phosphorylase kinase and 8×10^{-5} M phosphorylase.

C. Phosphorylase

(i) Reaction Catalysed

The reaction catalysed by phosphorylase in vivo is:



Although the equilibrium of the reaction catalysed by glycogen phosphorylase is 4:1 in favour of glycogen synthesis, the low level of glucose-1-phosphate in the cell (due to the phosphoglucomutase equilibrium being 17:1 in favour of glucose-6-phosphate) and the high concentration of phosphate, ensure that the reaction catalysed by phosphorylase in vivo is glycogen breakdown. A

separate enzyme system involving UDPG is available for glycogen synthesis (25,26).

(ii) Aggregation

Although under most conditions phosphorylase b exists as a dimer of subunits, each of molecular weight 100,000 (27), AMP and divalent metal ions induce aggregation to a tetrameric form (28). In contrast, phosphorylase a, whilst normally tetrameric, is disaggregated to dimers by glucose, maltose or maltoheptaose. On the basis of this result, it has been suggested that glycogen-bound phosphorylase is always dimeric (29,30). However, as it is difficult to obtain definitive evidence concerning this point, the number of subunits which may interact together in vivo is open to doubt.

Ultracentrifugation and probe studies show that aggregation is a slow process, lagging behind the conformational changes associated, say, with the b to a conversion (31). However, the nature of the bonds responsible for aggregation and the arrangement of subunits in the aggregates are not known.

Phosphorylase, at low concentrations, may be reversibly monomerised if incubated in an imidazole citrate buffer. Monomerisation causes loss of enzymic activity and facilitates resolution of the cofactor, pyridoxal 5' phosphate (32).

(iii) Effectors

Undoubtedly one of the fascinating features of this enzyme is the way it interacts with a variety of ligands. Thus besides the substrates (Pi, glucose-1-phosphate and glycogen) many nucleotides, sugar phosphates and

metal ions bind to it. Some of these (notably AMP and IMP) are activators, others like ADP, ATP and glucose-6-phosphate are inhibitors. Substrates, activators and inhibitors show various forms of cooperativity (both homotropic and heterotropic) and the two types of phosphorylase (a and b) show distinct differences in their ability to interact with these ligands. Table 1.1 summarizes some of the information available about these interactions. Clearly some of the ligands shown cannot be biologically relevant and have only been studied to elucidate the specificity of binding and effector efficiencies. Nevertheless the complexity of the system is already obvious and many other variables (Table 1.11) have to be taken into account. In order to evaluate the physiological significance of these effects, it is necessary to know the dissociation constant of each ligand for each form of phosphorylase, the nature of any homo- or heterotropic effects and the concentration of each ligand in the tissue concerned, taking account of any compartmentation.

As phosphorylase activity can be regulated by covalent modification, many workers have found difficulty in understanding the reasons for the existence of such a large range of non-covalent effectors. These effectors may be merely remnants of an imperfect regulatory order, discarded by evolution in favour of regulation by covalent modification. Alternatively, regulation by covalent modification and non-covalent effectors may have distinct important complementary roles. If this is the case, it is necessary to establish the relation between the two modes of regulation. It is also necessary to estimate the importance of allosteric interactions in the maintenance of any physiological effects of small ligands. In phosphorylase most homotropic effects are weak (e.g. allosteric activation of phosphorylase b by AMP is described by a Hill

Table 1.1

The Interaction of Various Effectors with Phosphorylase

Effector	+ Phosphorylase <u>b</u>	+ Phosphorylase <u>a</u>
no ligand	no activity	50-60 units/mg activity *
AMP	activates to 80-90 units/mg * (12)	
IMP	activates (97)	binds but no effect on activity
ATP,ADP	inhibit AMP induced activity (98)	bind tightly but no effect on activity
G-6-P	strong inhibitor (98)	weak inhibitor
Phosphate, G-1-P (76)	substrates - bind weakly to both forms of phosphorylase	
Glycogen (106)	substrate - very tight binding to Phosphorylase <u>a</u> and <u>b</u>	
UDPG (99)	inhibitor - binds to the G-1-P site	
Gluconolactone (100)	inhibitor - supposedly a transition state analogue	
Glycerophosphate (101)	affects binding of other ligands	

* at 30°C. 1 unit \equiv 1 μ mole of phosphate released per minute, under standard assay conditions

Table 1.11
Miscellaneous Effectors of Phosphorylase

	Phosphorylase b	Phosphorylase a
Aggregation	dimer AMP induces tetramerisation (76)	tetramer (76) sugars induce dimerisation (29) dimer more active than tetramer (102) tetramer resistant to phosphatase (103)
Temperature	both forms are cold inactivated;	lowering temperature leads to aggregation
Divalent metal ions	promote aggregation (28). Ca and Mg ions essential for phosphorylation (19)	inhibit dephosphorylation (68)
Oxidation	oxidation of SH-groups leads to formation of inactive aggregates (104)	
Reduction	the lysine-pyridoxal phosphate bond may be reduced (36)	
pH value	optimum pH for activity is 6.4 With physiological metabolites present it is 7.0 (105)	
Ionic strength	-	high ionic strength disaggregates

coefficient of only 1.2 - 1.3) whereas heterotropic effects are strong (e.g. Glucose-1-phosphate can tighten the binding of AMP to phosphorylase b by a factor of up to 8). Hence it is possible that the critical interactions are those within, rather than between, subunits.

(iv) The Pyridoxal Phosphate Cofactor

Each phosphorylase subunit contains one molecule of pyridoxal 5' phosphate, covalently attached to phosphorylase by an imine bridge to a specific lysine residue (33,34). Although removal of the cofactor causes inactivation of phosphorylase (35), reduction of the imine bridge with borohydride results in an active adduct (36).

Reconstitution experiments with chemically modified pyridoxal analogues have helped to define the functionally essential features of the coenzyme (37). One observation of particular interest is that a monomer containing pyridoxal-5'-phosphate monomethyl ester confers activity on an inactive monomer containing unmodified cofactor whilst itself remaining inactive, when the two monomers are hybridised together in a dimer (38). This suggests that the phosphate may have a direct catalytic function in the enzyme.

The unusual fluorescence properties of this group have been variously interpreted as being due to interaction with a nucleophilic group and a hydrophobic pocket (42,43). Such an environment does shift the emission maxima of pyridoxal-shiff bases in the theoretically predicted direction. The observation that iodide ions cannot quench pyridoxal fluorescence efficiently by a collisional mechanism is also consistent with this. Spectroscopic observations using absorption (39,40) and fluorescence quenching techniques

(41) have indicated ligand induced changes in the environment of the heterocyclic chromophore. For example, addition of glucose-6-phosphate enhances the accessibility of the chromophore to I^- ions (41).

Despite this information, the role of pyridoxal phosphate in phosphorylase is still a puzzle. Suggestions for a possible function have included:

- a) the cofactor directly participates in the catalytic process
- b) the cofactor is responsible for maintaining the tertiary or quaternary structure of the enzyme
- c) correct folding of the polypeptide chain after it has been synthesised requires the presence of pyridoxal phosphate
- d) phosphorylase has a second enzymic activity dependent upon pyridoxal phosphate (which has never been discovered)
- e) the cofactor is important in regulating the amount of phosphorylase present in the tissue
- f) the presence of pyridoxal phosphate is the result of an olden evolutionary deployment which has become obsolete but has not been reversed.

Whilst evolutionary pressure to conserve pyridoxal phosphate would tend to exclude some of these explanations, no firm conclusions can be reached without more evidence.

(v) The Serine Phosphate

Proteolysis, by trypsin, of phosphorylase a results in a cleavage of the amino-end of the molecule: the resulting hexa-peptide contains the serine residue that is phosphorylated in the kinase catalysed

phosphorylation of the enzyme and is rich in basic amino acids (18,44).

The presence or absence of phosphate on this serine residue determines the conformation, activity and behaviour of the enzyme. Clearly this region of the enzyme must also have a recognition site for both phosphatase and phosphorylase kinase. However, the location and relation of this site to other parts of the enzyme is unknown.

(vi) Crystallographic Studies

As phosphorylase is an enzyme of large molecular weight, structural studies present considerable difficulties. These have been complicated by the fact that the most common crystal form of the enzyme contains the tetramer (45) (which is the predominant form of phosphorylase a and b at high concentrations, in the presence of AMP). Although the early electron microscopic studies suggested that the enzyme dimer was asymmetric more recent observations on the crystalline enzyme have suggested that the two subunits are identical (46). This is entirely consistent with all the chemical data available to date (47) and is confirmed by the recent X-ray crystallographic work on the enzyme. This was made possible by the discovery of a new tetragonal crystal form of phosphorylase b (48) which contains one monomer per asymmetric unit and in which two monomers are related by a crystallographic dyad axis to form the dimer. These crystals will grow in the presence of IMP or without any ligands, but not in the presence of AMP. The crystallographers' 6\AA resolution model shows that the molecule is ellipsoidal (with approximate dimensions of $127\text{\AA} \times 63\text{\AA} \times 63\text{\AA}$) and relatively compact. It also reveals the position of the heavy atoms (in two

mercury and one platinum derivatives) and a cavity on the enzyme surface (49). Whilst further crystallographic studies are likely to show details of the enzyme at higher resolution, they are unlikely to reveal, in the near future, any of the dynamic aspects of the structure e.g. the nature of ligand induced structural changes.

D. Phosphorylase kinase

This enzyme is responsible for phosphorylation of phosphorylase b. Apart from the recently demonstrated phosphorylation of troponin by this enzyme (50), its action appears to be specific for phosphorylase or a large peptide containing the key serine residue that may be isolated after proteolysis of phosphorylase b (51). The enzyme phosphorylase b kinase has a molecular weight of 1.26×10^6 and has a subunit structure of $(\alpha \beta \gamma)_4$ (52) or $[A B C_2]_4$ (53). Its activity is completely dependent on calcium ions (which it binds very tightly) and magnesium/ATP (19). Although the calcium / substrate / enzyme complex has a very low activity at neutral pH, its activity is 60-100 times higher at pH 8.4 (54). However the complex may be activated at neutral pH by phosphorylation on the β/B and α/A subunits of the kinase. Whilst two sites are phosphorylated, only one site need be phosphorylated for activation of kinase at neutral pH (55). Phosphorylase b kinase may also be activated at neutral pH by proteolysis or auto-phosphorylation. Proteolysis, cleaving the α/A subunit, may be effected with trypsin or with a calcium dependent proteinase (KAF) found in muscle homogenates (56-59).

In addition to binding sites for phosphorylase, calcium, ATP/magnesium

and magnesium, kinase contains binding sites for glycogen, cAMP dependent protein kinase and kinase phosphatase.

E. cAMP dependent protein kinase

Phosphorylation at both sites of phosphorylase b kinase is catalysed by cAMP dependent protein kinase. This dimeric enzyme has a regulatory and a catalytic subunit (60) - the regulatory subunit suppresses the activity of the catalytic subunit, so the dimer is inactive. Binding of cyclic nucleotide leads to dissociation of the dimer and release of the free catalytic subunit, which, on release, becomes active (61) and may then catalyse the phosphorylation of phosphorylase b kinase and glycogen synthetase (62). cAMP dependent protein kinase is non-specific with respect to protein substrates and it causes phosphorylation of a wide variety of proteins in a range of tissues (63,64). As cAMP production in muscle tissue is a result of hormone stimulation of membrane bound adenyl cyclase, it is easy to envisage how hormone action activates the glycogen phosphorylase system.

F. Phosphatases

Just as cAMP dependent kinase phosphorylates phosphorylase b kinase and glycogen synthetase, both these enzymes are dephosphorylated by kinase phosphatase. This enzyme has been little studied but has been partially purified (65). Its action on phosphorylase b kinase has been shown to be dependent on the number of sites which have been phosphorylated. Under some

circumstances, therefore, phosphorylase b kinase is resistant to phosphatase action (66).

Phosphorylase phosphatase has been studied in more detail. Its action on phosphorylase a is inhibited by AMP and IMP due to the binding of these nucleotides to phosphorylase a (67). In addition, magnesium ions, EDTA, glucose and glucose-6-phosphate affect phosphatase action (the latter ligand activating phosphatase) (68). It is possible to compare the effect of these ligands on the dephosphorylation of phosphorylase a and a phosphopeptide containing the keyseryl phosphate obtained by partial proteolysis of phosphorylase a (18). This allows one to deduce whether the effect of ligands is mediated by binding to phosphorylase a or to phosphatase (69).

It is generally assumed that active control of the glycogen phosphorylase system is effected by the kinases and that the phosphatases play a passive role, acting only to switch off components, after kinase activity has ceased. This point is discussed in Chapter 8.

G. Glycogen

The glycogen molecule consists of chains of glucose units joined by a 1 \rightarrow 4 bonds and branched by a 1 \rightarrow 6 bonds. Each glycogen molecule contains one "reducing" glucose residue and many non-reducing terminal residues (4-ends). The number of 4-ends depends upon the degree of branching by the chains i.e. the relative number of 1 \rightarrow 4 and 1 \rightarrow 6 bonds (see Fig. 1.3). Glycogen is very highly branched and, on average, contains only about 6-10 glucose units between branch points (70).

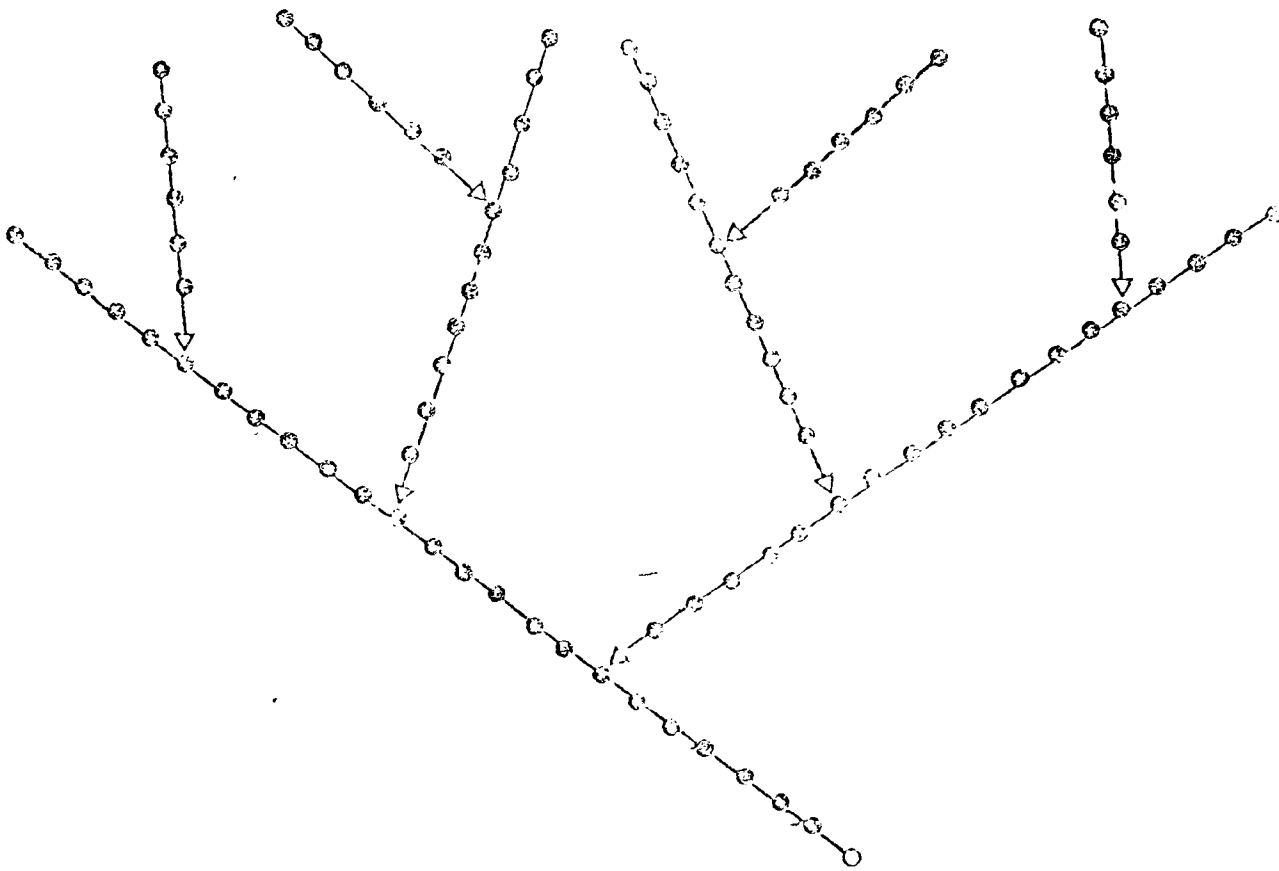


Figure 1.3 Schematic drawing of part of a glycogen molecule
 ● = α glucose, o = reducing glucose, - = 1,4-bond,
 —> = 1,6-bond

Although phosphorylase degrades glycogen sequentially from the non-reducing 4-ends, it cannot break 1 \rightarrow 6 bonds or 1 \rightarrow 4 bonds less than 4 residues away from a branch point (71) (see Fig. 1.3). However, because of the heavy branching of the molecule more than 10% of the polymer's glucose residues are at non-reducing termini. Hence, no matter how large a glycogen molecule becomes, a sizeable fraction of its glucose units is always available for immediate release as glucose-1-phosphate, provided that active phosphorylase is present.

Glycogen isolated from rabbit skeletal muscle has an average molecular weight of several million, and in the electron microscope appears as particles of diameter 40 μ (72). It is envisaged that in vivo, the enzymes concerned with glycogen metabolism cluster around the surface of the glycogen molecule. However, it must be remembered that, because of the high degree of chain branching, there is much space inside the glycogen, which may be occupied by water. It has been suggested that up to 4 grammes of water may be associated with one gramme of glycogen (73).

H. The Glycogen Particle Fraction

In vivo, the above components, together with the enzymes of glycogen synthesis, interact together to create a functional unit whose responses are geared to the needs of the cell. Many of these components, in vivo, are associated with molecules of glycogen.

To facilitate the study of this unit, Meyer et al. (74) have developed the preparation of a subcellular fraction from rabbit skeletal muscle, which

contains, principally, glycogen and the enzymes of glycogen metabolism. This preparation, the glycogen particle fraction, has been used to study the enzymes of glycogen breakdown in an environment supposedly approximating that found in vivo (75). A discussion of this fraction is included in Chapter 7.

Chapter 2

THE METHODS

A. Can the problems be solved?

The introductory chapter outlined the glycogen phosphorylase system, some of the outstanding problems associated with its study and some of the unanswered questions. Because most of these questions relate to the way in which the components of the system interact and behave in intact tissue, any real understanding requires many complementary pieces of data, some of which are accessible and some of which may never be. The approach which holds the promise of "most information" is X-ray diffraction, which, in principle, can provide the complete structure of many macromolecules. However, it is often impossible to apply the method to systems which bear any relation to the real biological situation. Also, it may be that the key to the understanding of complex bioorganisation will not be found at the level of the detailed molecular coordinates of, say, poly-peptide chains. Whilst it is hoped that this judgement is over pessimistic, the need for alternative ways of defining structural features, binding, associations and conformational changes at high resolution is apparent.

The problem is to describe the solution properties of components of the system in such a way that the same parameters could be extracted from in vivo experiments. For an enzyme like phosphorylase, this is a formidable problem for two reasons. Its large size restricts the number of methods that can provide meaningful information about the molecule. More importantly, it is possible

that the interaction or modification energies are distributed among a large number of covalent or non-covalent bonds so that both the overall and local changes in the enzyme will be small.

Spectroscopic measurements offer a possibility of studying aspects of enzyme structure in a range of environments. They often enable one to detect small conformational changes in enzymes, which can sometimes be related to specific molecular properties of the protein. Many spectroscopic measurements in enzyme systems are very simple and empirical in that they rely on the quantitation of a single spectroscopic parameter from one "reporter group" positioned on a protein. Although total structure cannot be obtained from such measurements, this simplicity and empiricism allows one to monitor the parameter in a range of systems, where more information-intensive methods, such as X-ray diffraction analysis, are inoperative. Moreover, as measurements can be made on opaque viscous samples containing high protein concentrations, without gross perturbation of the system, data can be obtained from preparations which are more closely related in the in vivo situation than dilute solutions of purified proteins.

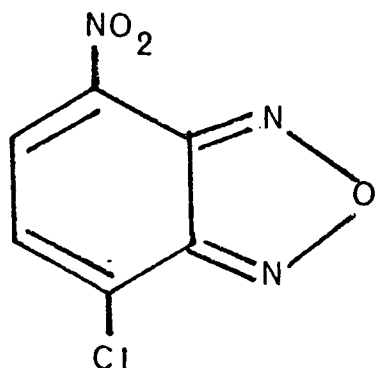
This thesis is primarily concerned with the applications of fluorescence, electron spin resonance (ESR) and nuclear magnetic resonance (NMR) to the understanding of the regulation of the rabbit muscle glycogen phosphorylase system. This chapter outlines some of the spectroscopic methods which have been used, and brief details of the methodology, potential and limitations of each technique are given.

B. Chemical Modification of Enzymes

In most enzymes some amino acids may easily be chemically modified. For example the nucleophilic properties of cysteine, lysine and histidine residues facilitate reactions with a wide variety of reagents containing carbon-halide bonds. Although many such reactions often cause inactivation or denaturation of the enzyme, it is often possible to select conditions and reagents so that a fully active or functional modified protein may be prepared. A large number of protein modifying reagents which contain spectroscopically useful groups are now commercially available e.g. fluorescent and spin label probes, ^{13}C and ^{19}F derivatives. Hence, this type of reaction is the starting point of many of the investigations into the structure and function of enzymes which are based on spectroscopic probe methods.

In many cases, the usefulness of "labelled" enzymes depends upon the specificity of attachment of the probe to the protein. Whilst a protein molecule may contain, say, thirty or more residues which could potentially react with a given reagent under a particular set of conditions, very often, modification is restricted to a small number of sites. Although steric effects due to the tertiary structure of the protein are the cause of much of this selectivity, the exact specificity of any reaction is likely to be caused by a large number of interacting factors, which, in most cases, are not understood. The specificity of any reaction may be investigated in two ways. Either, the distribution of the label between the various sites on the enzyme may be determined by protein chemistry or the kinetics of the reaction may be studied. Whilst the former method is often more rigorous, the kinetic approach is more practicable for the study of large proteins and labile reagents.

For example, the reagent 4 chloro 7 nitrobenzofurazan (Nbf-Cl) (I) reacts specifically with the sulphhydryl groups of phosphorylase (78).

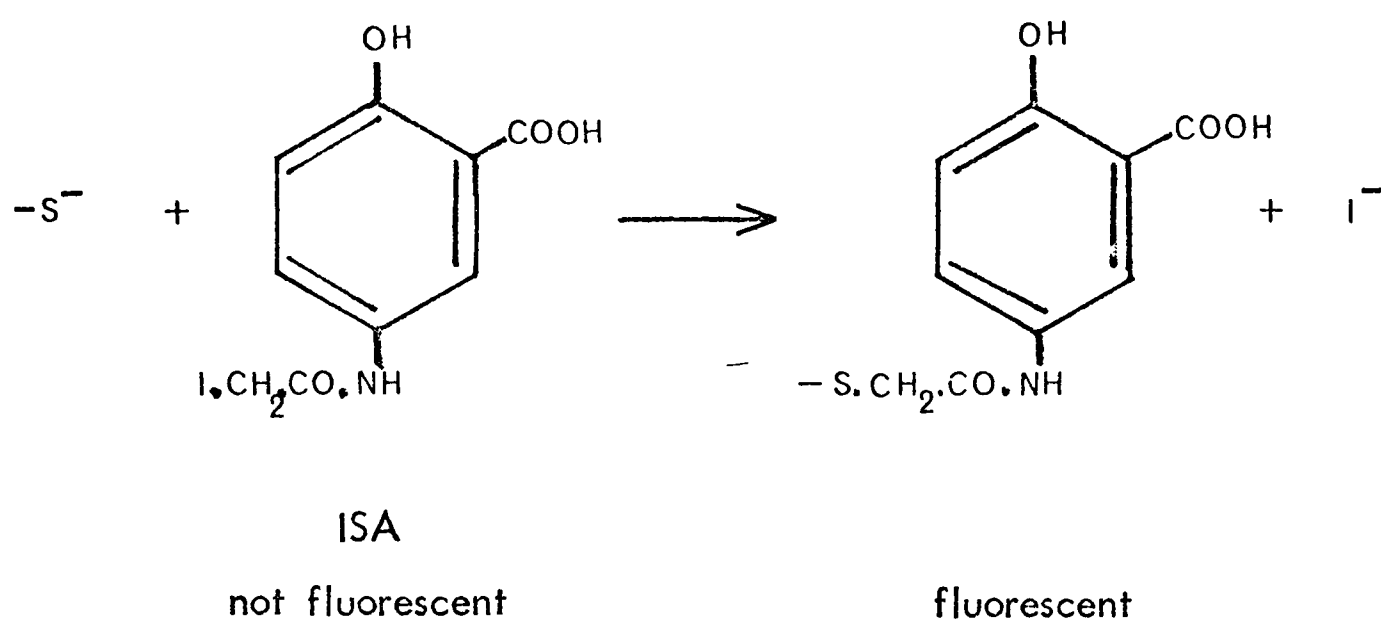
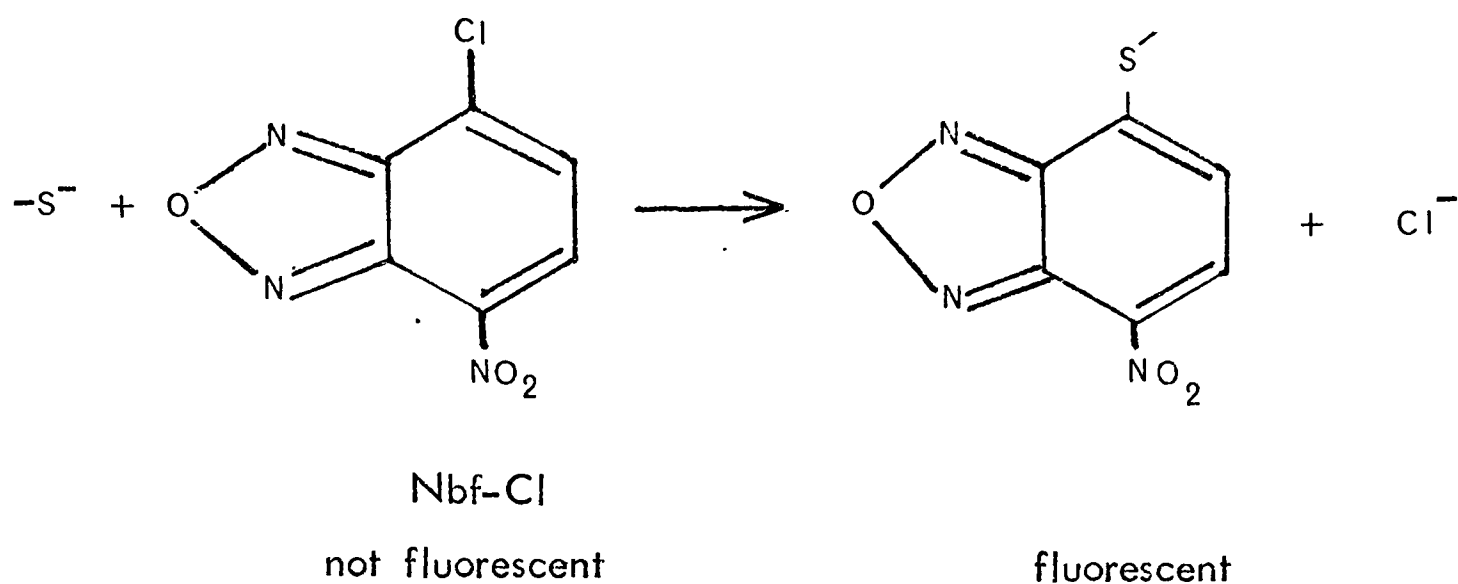


I

The reaction is accompanied by a large change in the absorption and fluorescence spectra of the chromophore and, hence, the rate and extent of the reaction can be simply monitored. Alternatively, if radioactively labelled reagents (e.g. ^{14}C iodoacetamide) are used, the extent of any reaction can be estimated from a measurement of the radioactivity incorporated into the protein.

C. Fluorescence Methods

Proteins may be studied by fluorescence methods if light emission can be observed from aromatic amino acids, substrates, cofactors or reporter groups which may be covalently or non covalently attached. Two reporter groups, Nbf Cl and Iodoacetamidosalicylic acid (ISA), which may be covalently attached to phosphorylase, are described in this thesis. Both react with the sulphhydryl groups of phosphorylase by nucleophilic displacement of a halide ion, to give fluorescent adducts which are fully catalytically active.



Fluorescence is a result of electron transitions from excited states to the ground state of a molecule. In principle, for any fluorescent molecule, several parameters can be measured and in some cases these parameters can give information about the environment around the fluorophore. For example the relative positions of the excitation and emission wavelength maxima can indicate the polarity of the environment. Measurements of fluorescence polarisation and lifetime can reveal some of the motional characteristics of the fluorophore.

An alternative use of fluorescence is to monitor changes in any parameter as a function of some perturbant. Information about the system may then be abstracted without a detailed physical interpretation of the observed parameter.

For example, on excitation of acetamidosalicylate (SA) phosphorylase at 320 nm, fluorescence at 400 nm is observed. Moreover, this fluorescence is quenched by up to 30% on addition of some ligands to phosphorylase. This provides a sensitive way of monitoring and quantifying ligand interactions with different forms of phosphorylase (79).

Fluorescence measurements may also give distance information. The fluorescence of any group may be quenched if its emission has spectral overlap with the absorption of a second fluorescent group positioned nearby (81). The efficiency of quenching increases as the distance between the two groups decreases. The distance range over which quenching occurs is determined by the overlap integral, the orientation of the two groups and the dielectric constant of the medium. For example, from the excitation and emission spectra of acetamidosalicylate (the donor) and Nbf (the acceptor) shown in Fig. 2.1, it may be deduced that acetamidosalicylate fluorescence will be quenched 50% if an Nbf group is placed 25–30 Å from it, provided that the two groups have random averaged orientations (82, 157). As well as the quenching, a life time change in the donor group fluorescence and an increase in the fluorescence of the acceptor group should be observed.

Fluorescence measurements can, in principle, be made on labelled phosphorylase in a wide range of environments. However because of scatter and inner filter effects, in practice, such measurements must be made in clear solutions at low protein concentrations. Despite these problems, in some cases, studies can be extended to more cloudy solutions (containing, say, glycogen) by the use of front face fluorescence or by measurement of fluorescence life time (107).

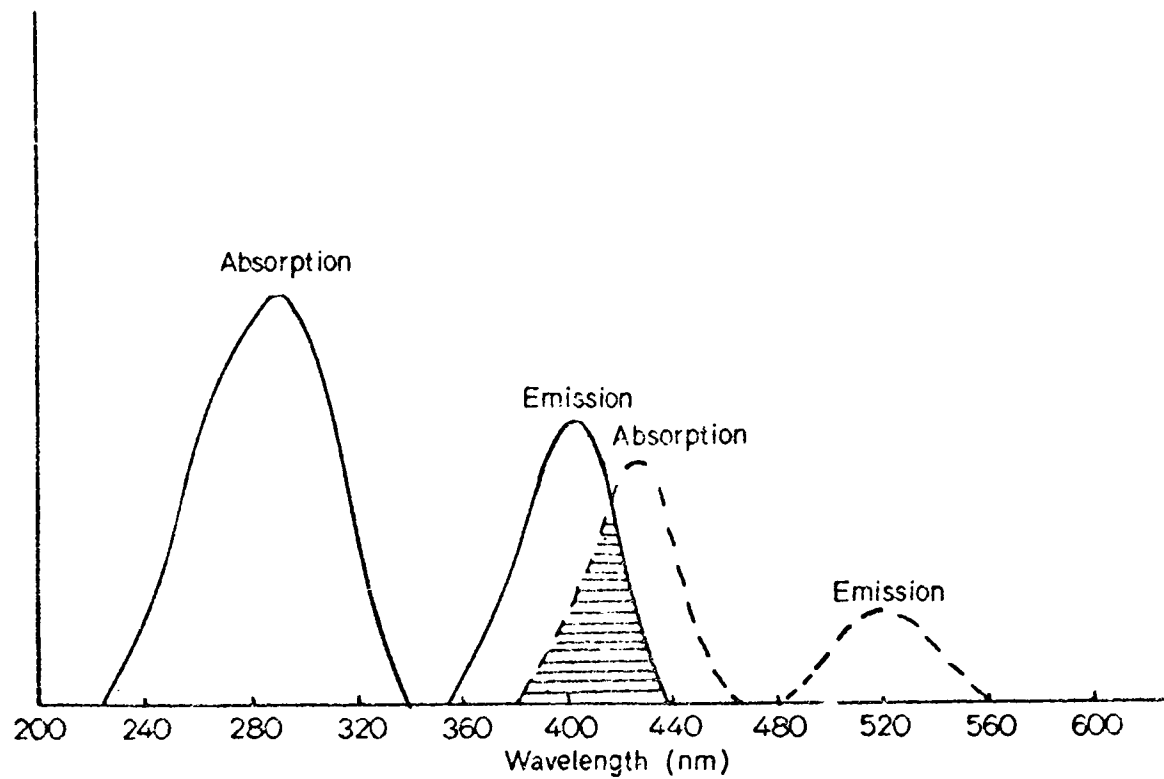


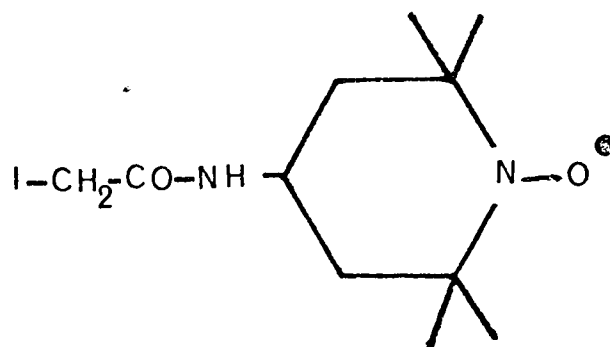
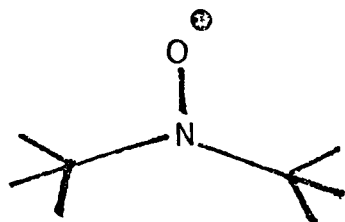
Figure 2.1

The absorption and emission bands of acetamidosalicylate N-acetyl cysteine (full lines) and Nbf N-acetyl cysteine (broken lines). The absorption and fluorescence spectra of the acetamidosalicylate and Nbf moieties when attached to phosphorylase b are identical to the spectra shown in the figure.

It must be stressed that the above uses of fluorescence can often be a matter of "trial and error", because there is no way of predicting which fluorescent probes attached to which groups will "report" changes in any enzyme. For example, when the above probes were attached to 5' adenylic acid deaminase no ligand induced fluorescence changes were observed although it was known that activity linked conformational changes were occurring.

D. Spin Label Probes

The spin label method, first introduced for the study of macromolecules by McConnell and his associates (83), relies on the electron spin resonance (ESR) properties of stable free organic nitroxide radicals of the type:



iodoacetamide spin label

When a spin label is placed in a magnetic field, the magnetisation associated with the free electron of the nitroxide group is distributed between two energy levels. The energy difference ($h\nu$) between these two levels is given by:

$$h\nu = g \beta H$$

where g is the splitting factor,

β is the Bohr magneton,

and H is the applied magnetic field.

When microwave energy (of frequency, ν) is applied to the system the magnetisation associated with the electron is excited from one level to the other and energy is absorbed. Because of coupling between the magnetisation of the electron (spin quantum number = $\frac{1}{2}$) and the magnetisation due to the nuclear spin of the nitrogen atom (spin quantum number = 1) each energy level is further split into three sub-levels. Hence if the microwave energy is scanned through a range around ν whilst the applied magnetic field is maintained at a constant value, H , three separate absorption bands may be measured. In fact, in most ESR machines the frequency of the microwave source remains constant and the magnetic field is varied continuously.

ESR signals consisting of three symmetrical lines are obtained from spin labels, such as those shown above, which are tumbling rapidly in solution ($\sim 10^{-11}$ sec). However when motion is more restricted, the line shape is considerably altered. This can be used to derive information about the mobility of the labels. In addition, the splitting of the lines (i.e. the separation of the three components in Hertz) is a measure of the polarity of the environment of the radical (84). In favourable cases, the ESR signal can be used to obtain information about the orientation of the molecule with respect to a laboratory axis related to the magnetic field (85).

The iodoacetamide spin label derivative shown above may be covalently linked to phosphorylase by reaction with the sulphhydryl groups of the protein (90). When the probe is attached to phosphorylase, the line shape of the observed ESR spectrum is sensitive to the conformation of phosphorylase around the probe, which in turn is determined by the state of activation of the

enzyme (80). ESR spectra of labelled enzyme in the presence or absence of AMP are shown in Fig. 2.2. Similar changes are seen when other ligands are added to phosphorylase. These effects, originally discovered by Dr. N.C. Price, and investigated in greater detail by Drs. J.R. Griffiths and R.A. Dwek (88,89), were analysed by characterising each ESR spectrum by the ratio, R . This is the ratio of the amplitudes of the low field and centre peaks in the differentiated form of ESR spectra. The ratio R was observed to change during titrations with ligands, and if R_o was the ratio for the unliganded enzyme and R_∞ was the ratio exhibited when the enzyme was saturated with any ligand, the fraction of enzyme (X) binding the ligand when the ratio observed was R_x , was taken as:

$$X = \frac{R_x - R_o}{R_\infty - R_o} \quad (101)$$

This method for handling data has been retained in this thesis. The ratio method was originally developed because technical difficulties and machine fluctuations made absolute peak heights difficult to measure reproducibly. However subsequent studies have revealed that during some titrations both the centre peak and low field peak amplitudes alter. Although this apparently casts doubt upon the validity of using the observed ratio changes as a proportionate measure of ligand saturation of labelled enzyme, it is easy to show that if the proportionate change in the centre peak height is no more than 20% and the ratio R does not change by more than 40%, the equation

$$X = \frac{R_x - R_o}{R_\infty - R_o} \text{ is valid to within 10\% (91) (see Appendix 3).}$$

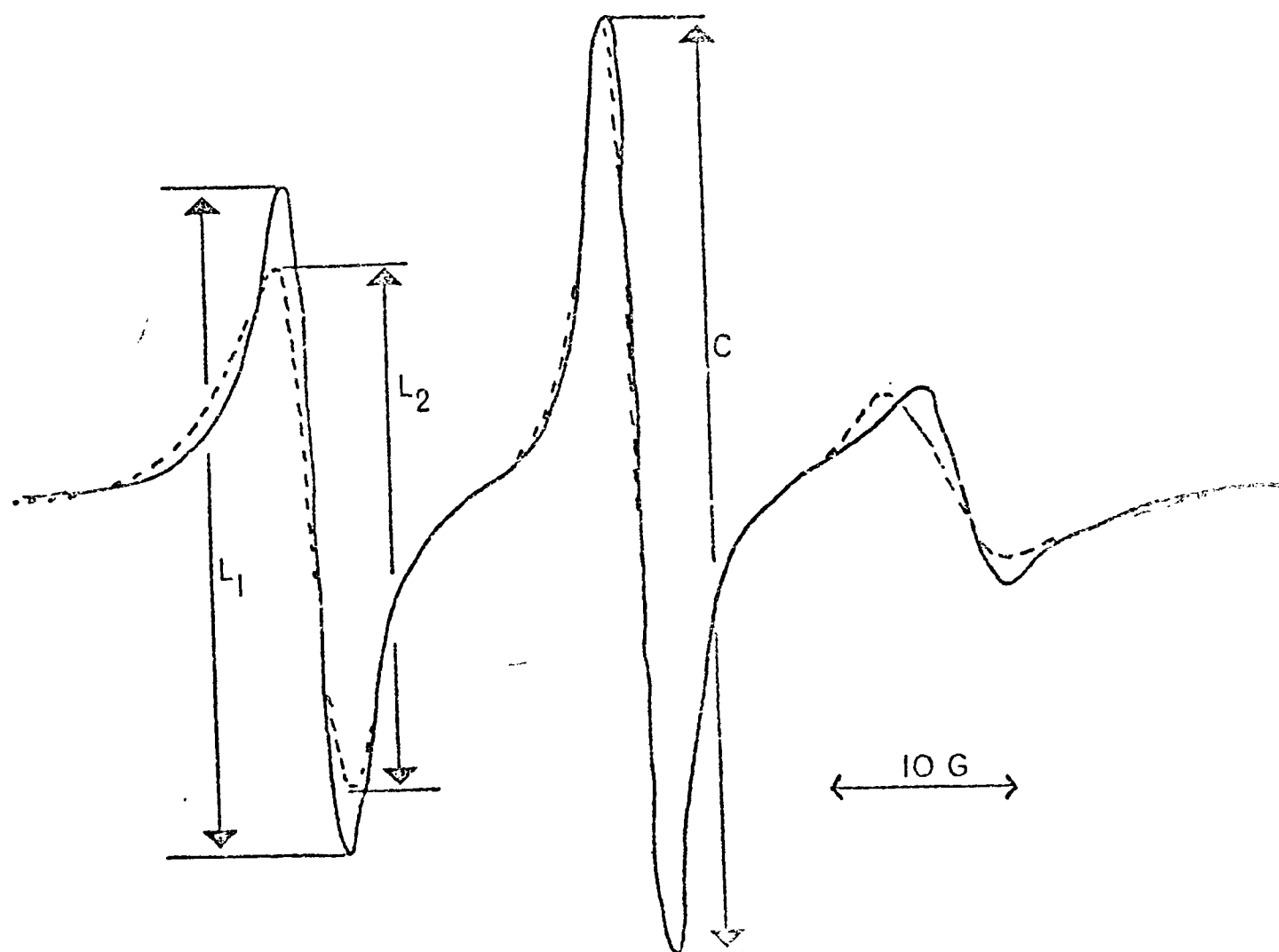


Figure 2.2 ESR spectrum of spin labelled phosphorylase b in the presence (dotted line) or absence (full line) of AMP. 22°C, 50 mM TEA, 100 mM, KCl, 1 mM EDTA pH 7.0 buffer plus or minus 1 mM AMP. Ratio (R) = L_1/C or L_2/C .

The advantage of ESR over fluorescence is that measurements can be made with very opaque solutions without loss of efficiency (for example, the glycogen particle fraction). In addition, there are no technical problems associated with experiments at high protein concentrations: ESR titrations could easily routinely be performed with 70-80 μM spin labelled phosphorylase (the physiological concentration). The two disadvantages of ESR as compared to fluorescence are that continuous readout of probe parameters cannot be obtained and that more probe is needed to obtain spectra. As with fluorescence, finding a useful combination of probe and point of attachment can be a matter of "trial and error".

E. Nuclear Magnetic Resonance

NMR is similar, in principle, to ESR. However because the magnetisation of nuclei rather than electrons is studied it operates in different field and frequency ranges. When placed in a magnetic field, nuclei which have spin quantum numbers $\neq 0$ orientate themselves with respect to the field. They may then be displaced from this orientation by the absorption of energy, which may be applied in the form of radiofrequency radiation (the displacement is known as resonance). Nuclei in different chemical environments experience different magnetic fields and hence resonate at different energies. Thus the abscissa of an NMR spectrum represents a range of resonance energies and the ordinate shows the number of nuclei resonating at each energy in the range. An NMR spectrum presents an analysis of a molecule in terms of the different magnetic environments around each atom.

NMR spectra can be recorded by scanning radiofrequency radiation through a range of energies and recording the absorption of energy at each frequency. This method, known as continuous wave NMR, is, however, not normally used, as most biochemical applications of NMR require the maximum sensitivity of the technique. Signal/noise may be increased by the use of Fourier Transform NMR. A brief description of this technique is included at this point, as it is conceptually completely different to continuous wave NMR, and as it is relatively unfamiliar to most biochemists. Excellent reviews by Coxon (92), and Carrington and McLauchlan (94) are available.

The sample is placed in a strong magnetic field. The magnetisation vector of a nucleus in any particular environment is orientated with respect to the applied magnetic field and precesses around the direction of the field (the z direction) with a particular frequency. This frequency is the resonance frequency for the nucleus in that environment. Nuclei in different magnetic environments have different resonance frequencies. In this state there is no net magnetisation in the plane perpendicular to the z axis (the $x - y$ plane). However on application of a short pulse of radiofrequency energy the magnetisation vectors from the orientated nuclei move away from the z direction (see Fig. 2.3) and magnetisation may be detected in the $x - y$ plane. Each magnetic component is still precessing around the z direction with a frequency equal to its resonance frequency. Hence, if the magnetisation detector is placed along, say, the y axis, each magnetic component is detected as a sinusoidal signal. Moreover the sinusoidal signal from each component decays with time due to (i) reversion of the magnetisation from the $x - y$ plane to the z direction (spin lattice

relaxation described by the relaxation time, T_1) and (ii) individual nuclei with the same frequency of precession around the z axis eventually randomising the direction of their magnetisation vectors in the $x - y$ plane (spin spin relaxation described by the relaxation time, T_2) (see Fig. 2.3).

Hence each nucleus in each different environment may give rise to a damped sinusoidal magnetic oscillation at the detector, the frequency of which is related to its resonance frequency. The decay of magnetisation measured at the detector (the free induction decay) is the sum of the damped oscillations from the many sets of magnetic centres, expressed in the time domain. Fourier transformation of the decay results in data which express the intensity of each oscillation in the frequency domain.

The spectra resulting from a Fourier Transform or a continuous wave operation can therefore be identical. Fourier Transform NMR is preferred as free induction decays from successive pulses of radiation can be accumulated more quickly than the energy range of a continuous wave spectrometer can be swept. Signal/noise is thus increased by operation in the Fourier Transform Mode.

Many different nuclei may be observed by NMR, the biochemist finding ^1H , ^{19}F , ^{13}C , ^{31}P and ^{15}N most useful. Proton NMR has been most studied as, in principle, it can give readout from all the protons in a sample, thus providing structural and dynamic information about any molecule. For each resonance, several parameters can be measured.

1) Line position - the resonance position of any particular set of atoms provides information about the chemical environment of that set. For example, protons attached to an aromatic ring always resonate at a frequency removed

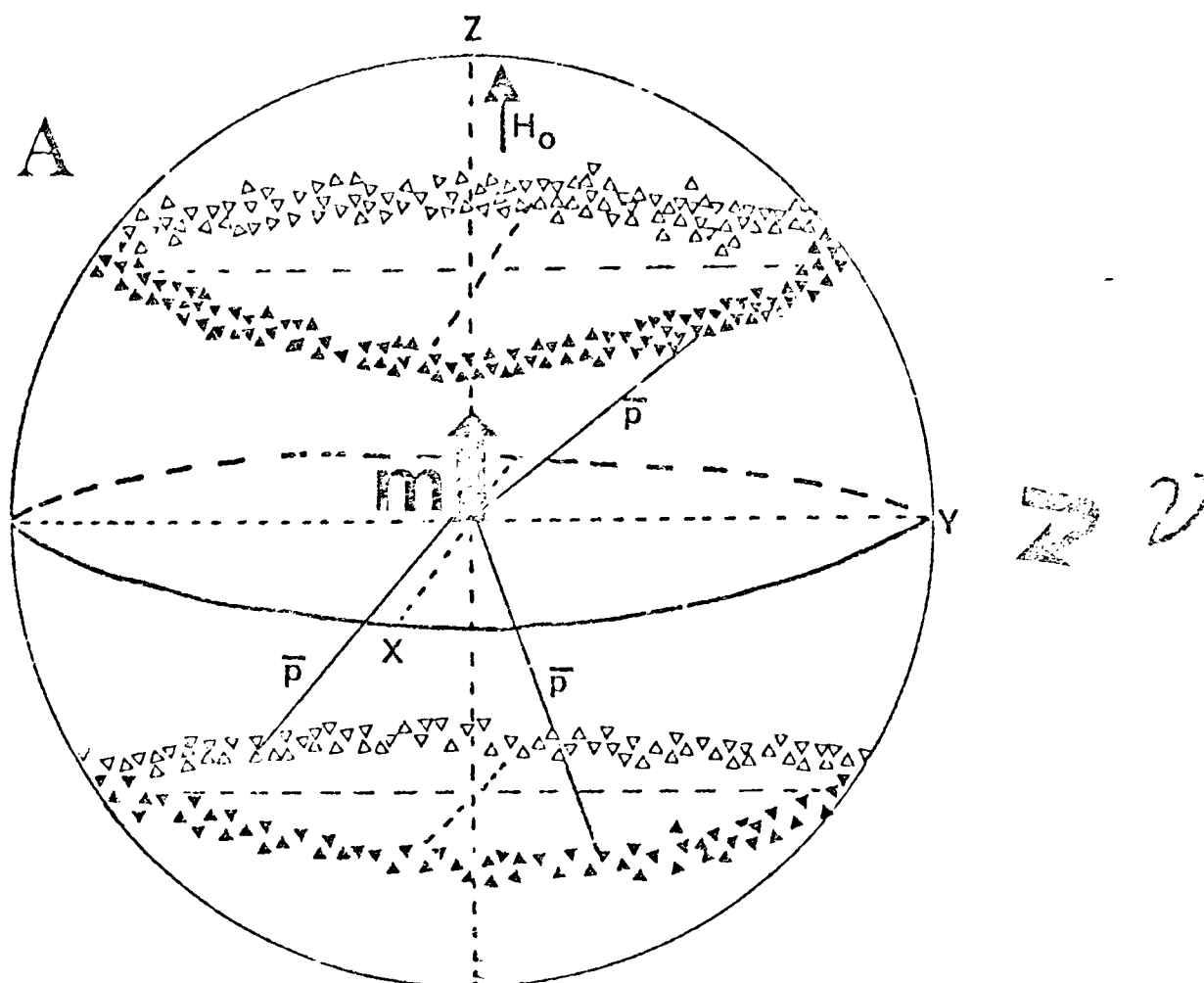
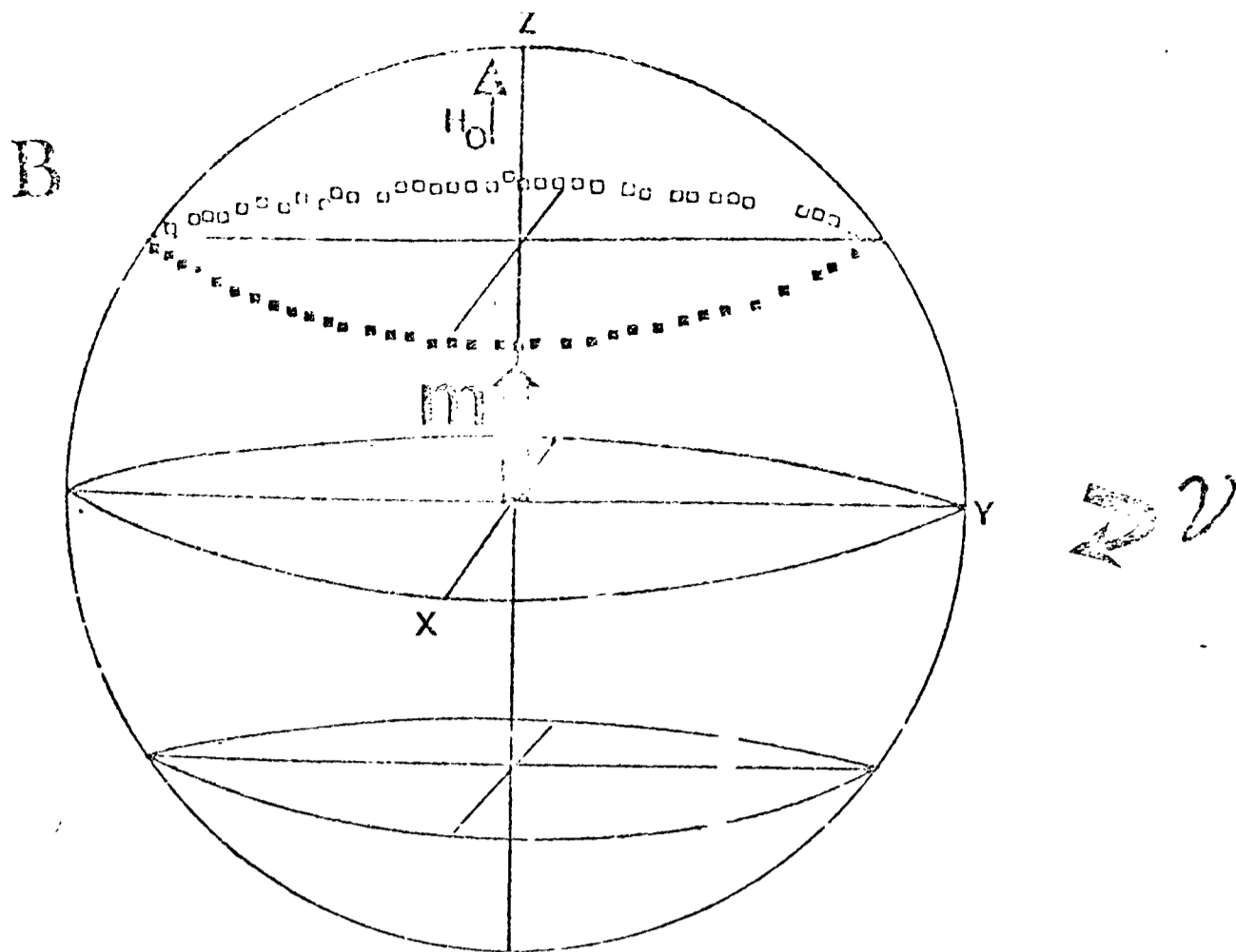


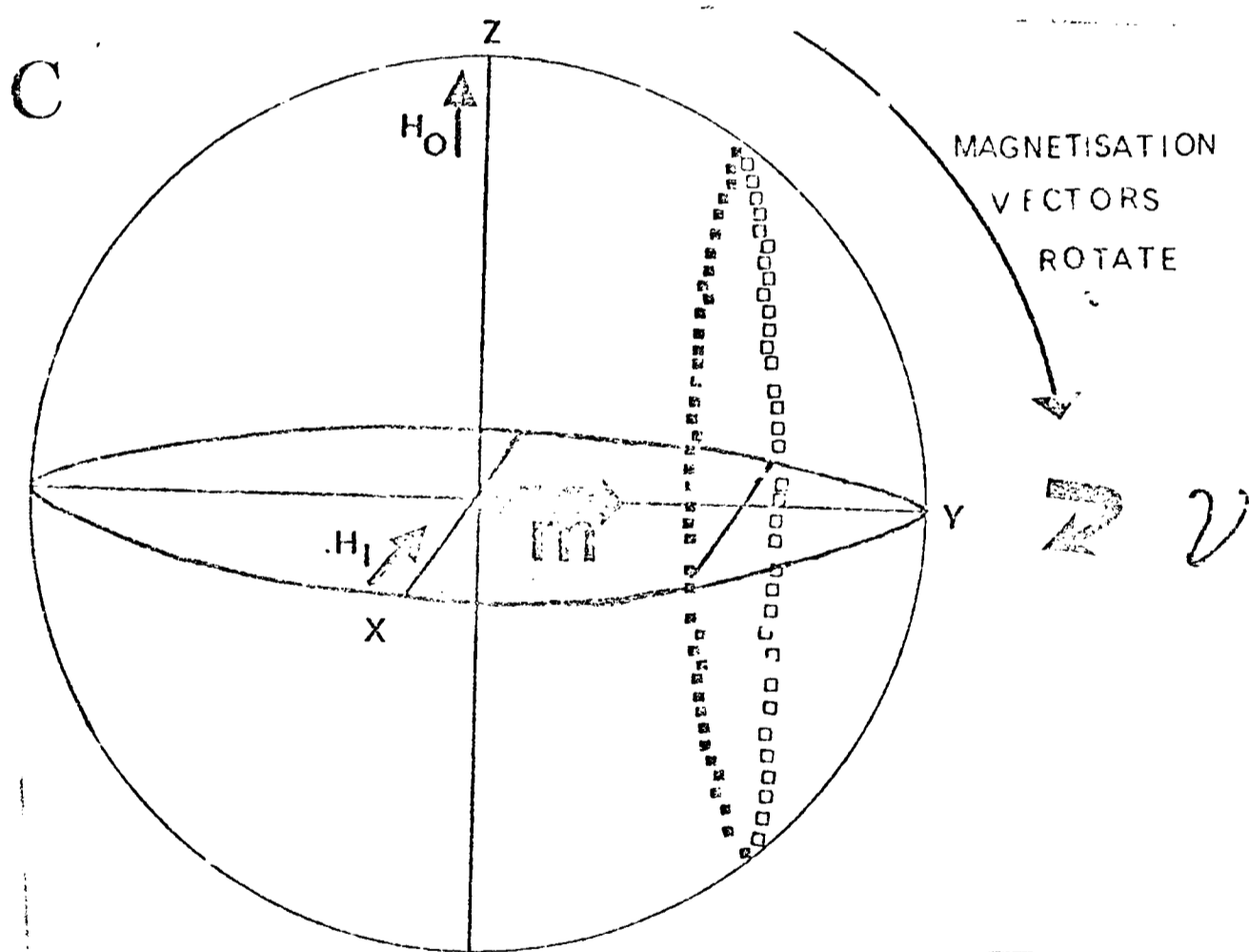
Figure 2.3 The NMR Experiment

A - a magnetic field H_0 is applied to the sample in the z direction. The magnetization vectors from each nucleus orientate themselves with respect to this field. Lines joining the triangles and the centre of the sphere represent individual magnetization vectors - three such vectors, marked \bar{p} are shown. The vector from each nucleus precesses around the z axis with a frequency ν - about 129×10^6 times per second in the case of phosphorus nuclei if H_0 is 7.5 Tesla. In this illustration, all the nuclei are in identical environments and all precess at ν cycles per second.

There will be a slight excess of nuclei with vectors whose orientations lie with rather than against H_0 . Hence a resultant net magnetization, m , exists in the z direction. There is no resultant magnetization in any direction in the x - y plane (the difference in populations between the two states of orientation of the vectors is greatly exaggerated in this figure).
 x, y and z refer to laboratory axes.

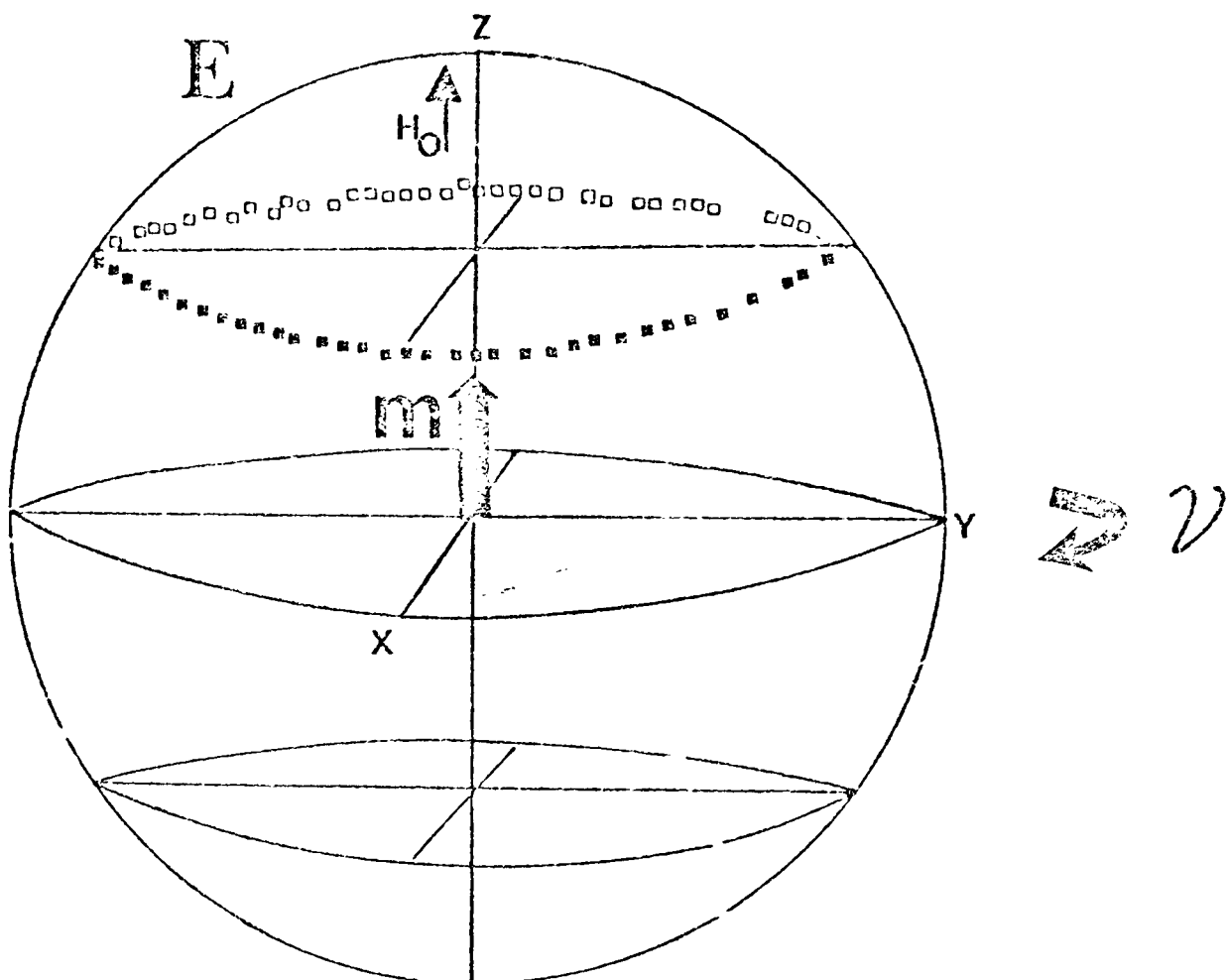
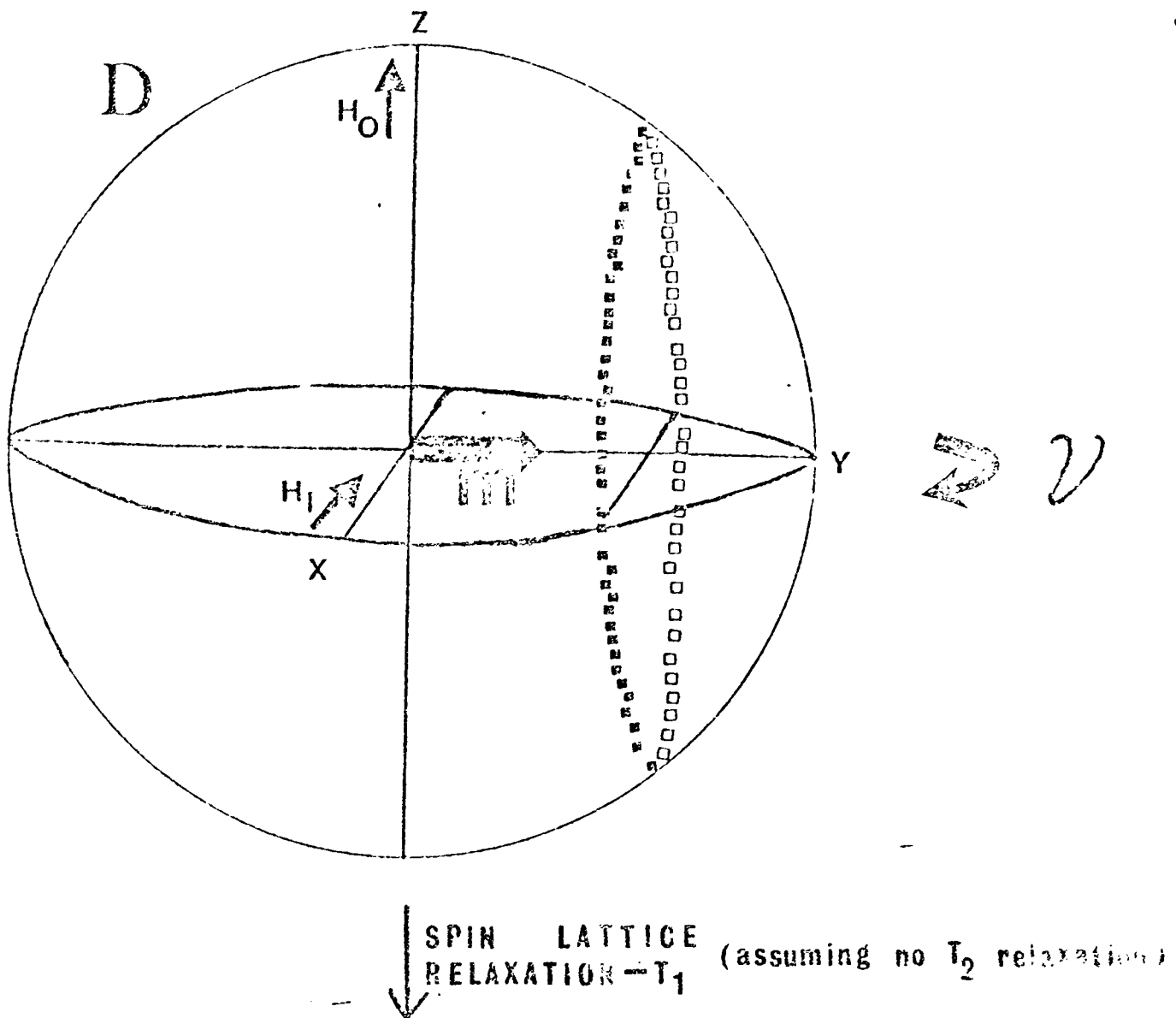


B - This simplifies figure A and considers only the excess of nuclei whose magnetization vectors lie with H_0 over nuclei whose vectors lie against H_0 . The net resultant magnetization vector lies in the z direction and there is no net magnetization in the x - y plane.

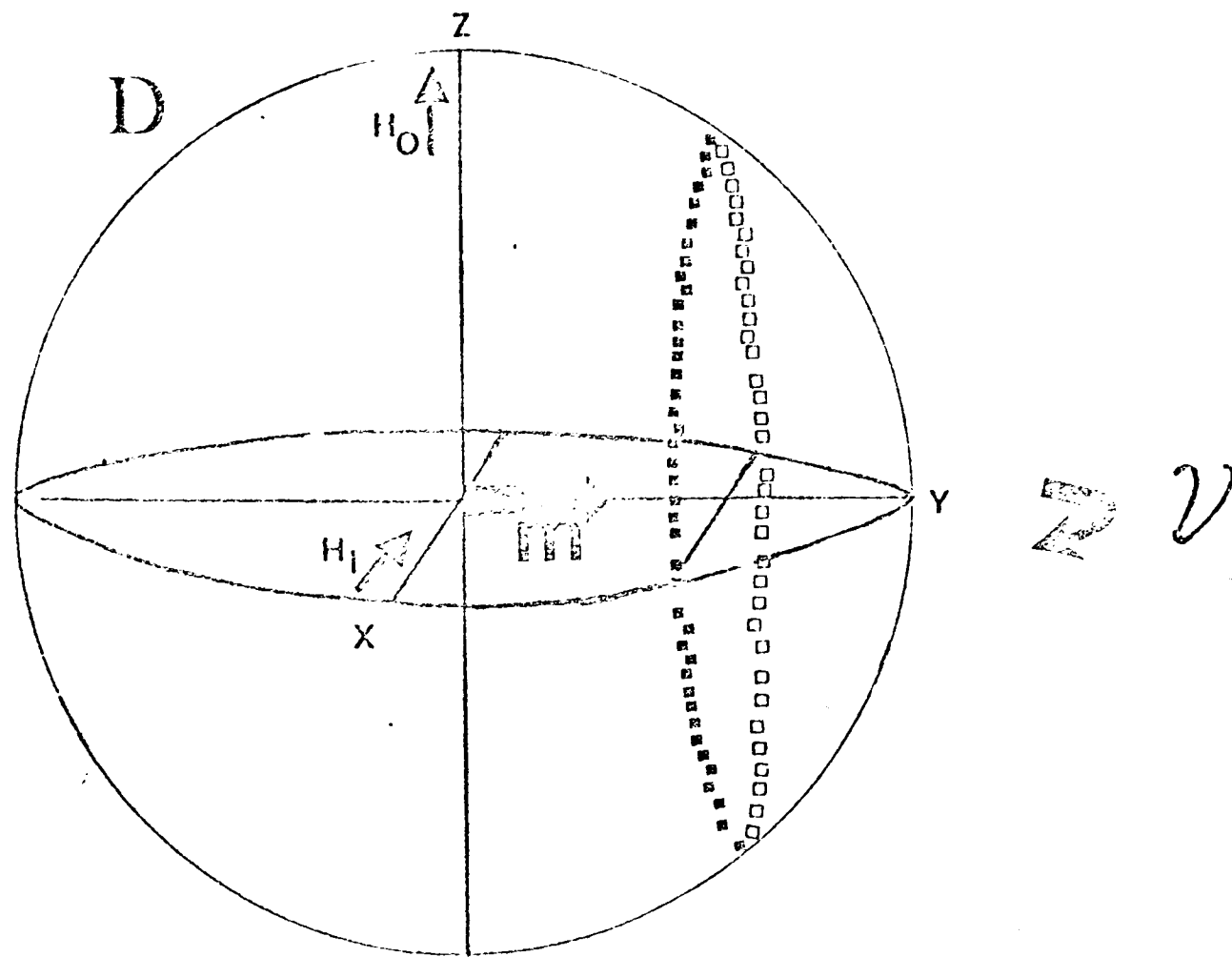


C - A 100μ second pulse of radiation of frequency ν is applied in the x direction (H_1). This causes the orientation of each vector to rotate by 90° around the x axis, as shown. The angle of rotation is dependent upon the pulse length. Whilst rotation is occurring, each vector still precesses around the z direction with a frequency ν . Each vector will precess 12,900 times around the z direction in 100μ seconds.

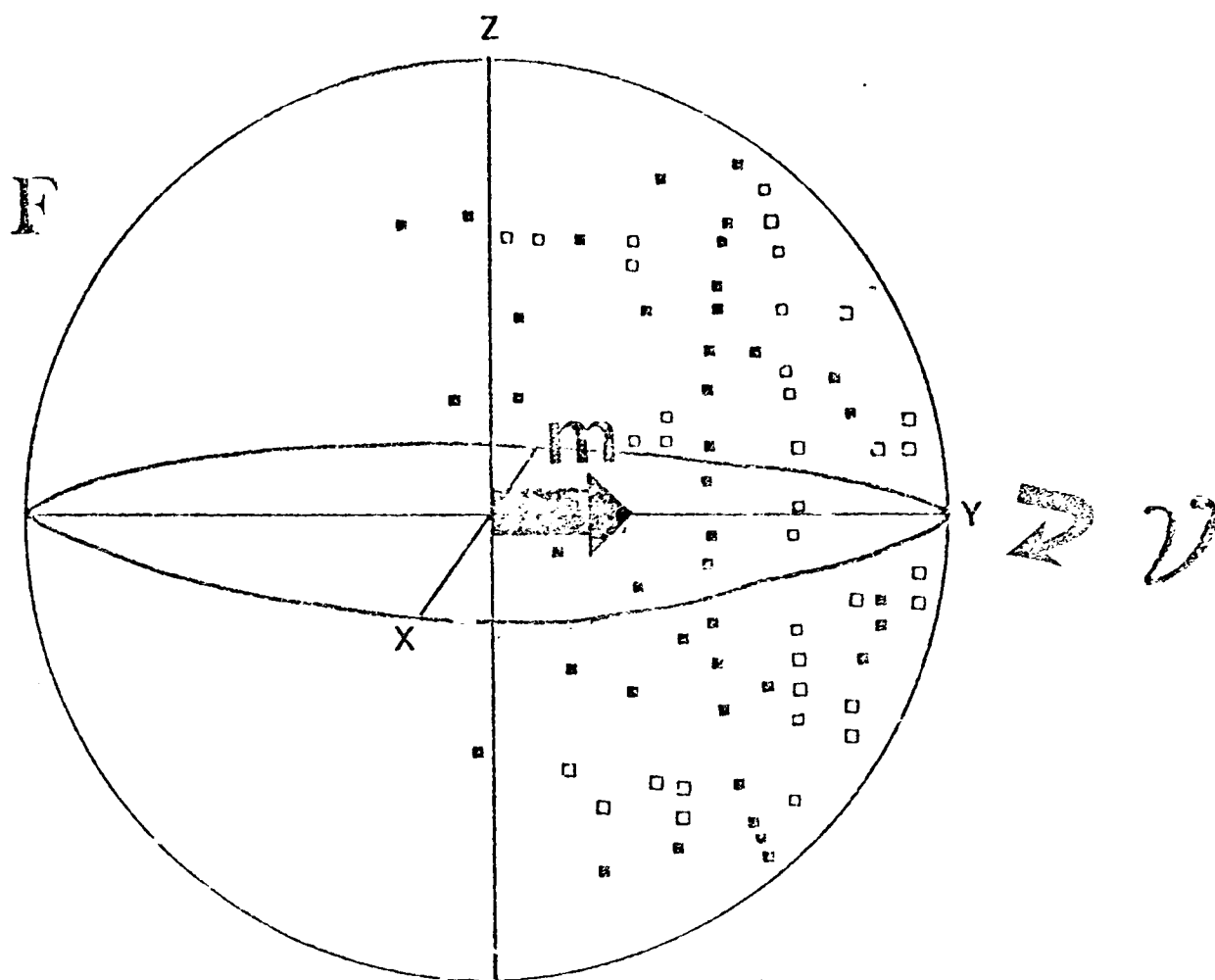
Rotation causes the resultant net magnetization vector to be tipped out of the z direction. After a 90° rotation the net vector, m , lies in the x - y plane and, like the vector from each nucleus, precesses at frequency ν around the z direction. A magnetization detector which monitors, say, magnetization in the y direction thus records a sinusoidal signal of frequency, ν .



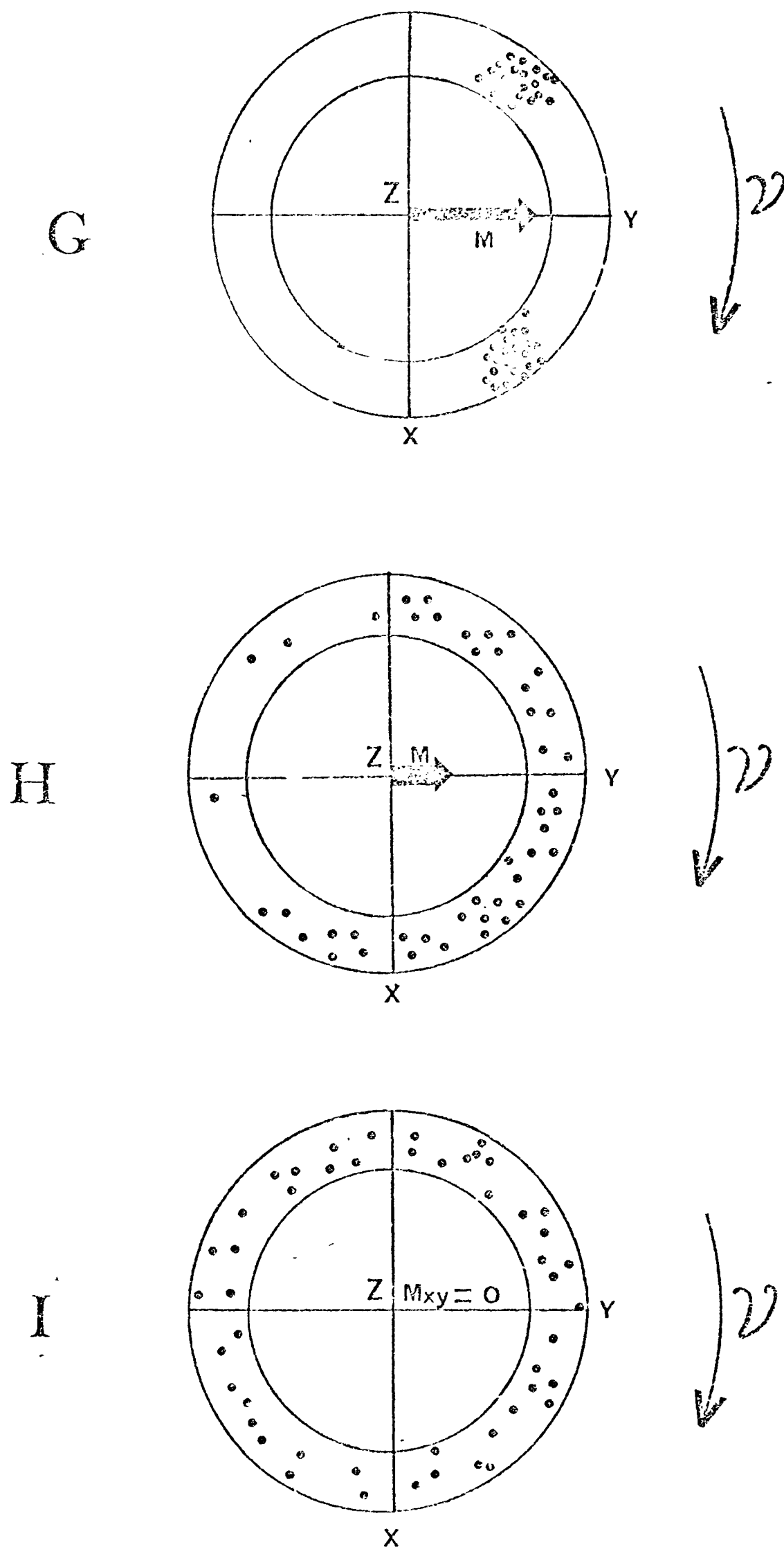
D \rightarrow E - After H_1 radiation has been switched off, the individual magnetization vectors return to their original orientations. Hence net magnetization (m) in the x-y plane diminishes and reappears in the z direction. The decay of net magnetization from the x-y plane due to this process is exponential and has a half time, T_1 , the spin-lattice relaxation time. T_1 may be several seconds; during this time the magnetization vector may precess 10^9 times around the z direction.



↓ SPIN - SPIN RELAXATION - T_2 (assuming no T_1 relaxation)



D \rightarrow F - After H_1 is switched off, the individual magnetization vectors continue to precess around z at a frequency, ν . Provided that each vector precesses at exactly ν , the resultant magnetization in the x - y plane, m , will remain constant. Due to spin spin interactions and magnetic inhomogeneities, slight differences in ν occur between the vectors from different nuclei. This causes a gradual randomisation in the directions of the vectors and a decay in the resultant magnetization in the x - y plane, m . This decay is exponential and is characterised by the spin-spin relaxation time T_2 . T_2 may be several milliseconds; during this time each magnetization vector may precess 10^6 times around the z direction



G-H-I - This figure describes the T_2 process. It represents a cross section of the sphere in D , containing the x - y plane. Immediately after H_1 is switched off, individual magnetization vectors are rotating at frequency ν in phase around the z axis. Gradually, as they lose coherence, the net magnetization vector in the x - y plane is reduced. In I complete randomisation of the vectors has occurred and the net magnetization in the x - y plane is zero. During this process each individual vector and the resultant magnetisation, m , may precess $10^7 - 10^8$ times around the z axis.

T_2 relaxation does not generate magnetization in the z direction.

from the resonance position of, say, the methyl protons of alanine (108).

Another example concerns ^{31}P resonances from phosphate groups. The frequency of these resonances is dependent upon the state of ionisation of the phosphate and the nature of adjacent groups (109).

2) Intensity - the intensity of any particular resonance (defined by the area under the resonance and normally obtained by computer-aided integration of a spectrum) is proportional to the concentration of nuclei responsible for the resonance. Such information can be useful in defining the structure of unknown molecules or for simple assay of compounds whose spectral characteristics are known.

3) Relaxation Rates - The rate of return of the magnetisation from the $x - y$ plane to the original orientation may be measured. Relaxation can be measured in terms of two parameters, the spin-lattice relaxation rate (T_1) and the spin-spin relaxation rate (T_2). The width of a resonance in an NMR spectrum is directly related to T_2 .

Relaxation rates are dependent upon the fluctuation of magnetic fields in the vicinity of the nucleus and are related to τ_r , the rotational correlation time, τ_m , the exchange correlation time and τ_s , the electronic spin-spin correlation time. These correlation times simply describe the time scale of magnetic fluctuations due to molecular rotation, exchange from one environment to another, or interactions with neighbouring magnetic centres (110).

4) Line Shape - Suppose that a nucleus can exist in two environments. If half the nuclei are permanently in one environment and the remainder are

in the other, two resonances may be seen in an NMR spectrum. If the two resonances cannot be completely resolved a complex line shape will be observed. Two components will also be observed if the nucleus is "jumping" from one environment to another with a frequency much less than the frequency separation of the two resonances (i.e. the nucleus is in slow exchange relative to the NMR time scale). If the jumping frequency is much greater than the frequency separation of the two components, a single line will be observed (Fig. 2.4). Very complex line shapes can thus be produced by nuclei which can "experience" several different magnetic environments and which are not in fast exchange between these environments (94).

5) Splitting Patterns - Resonances from unique atoms in one environment are often split into several components due to magnetic coupling with other nuclei. The magnitude and extent of such coupling and the splitting between the components produced can provide information about the arrangement of atoms in molecules (95).

Allied to angular and distance dependent perturbation techniques (96) proton NMR should, in principle, be able to provide much of the structural and dynamic information one would like to know about molecules in solution. Of course there are a large number of theoretical and practical problems associated with such analyses. On the theoretical side, the translation of the above parameters into real molecular terms requires a great deal of complex theory and supposition. On the practical side, firstly, most NMR experiments require that each nucleus which is to be observed must be present at concentrations greater than 1 mM (a concentration which is prohibitive for some studies). Secondly deuterium oxide, rather than water must be used as

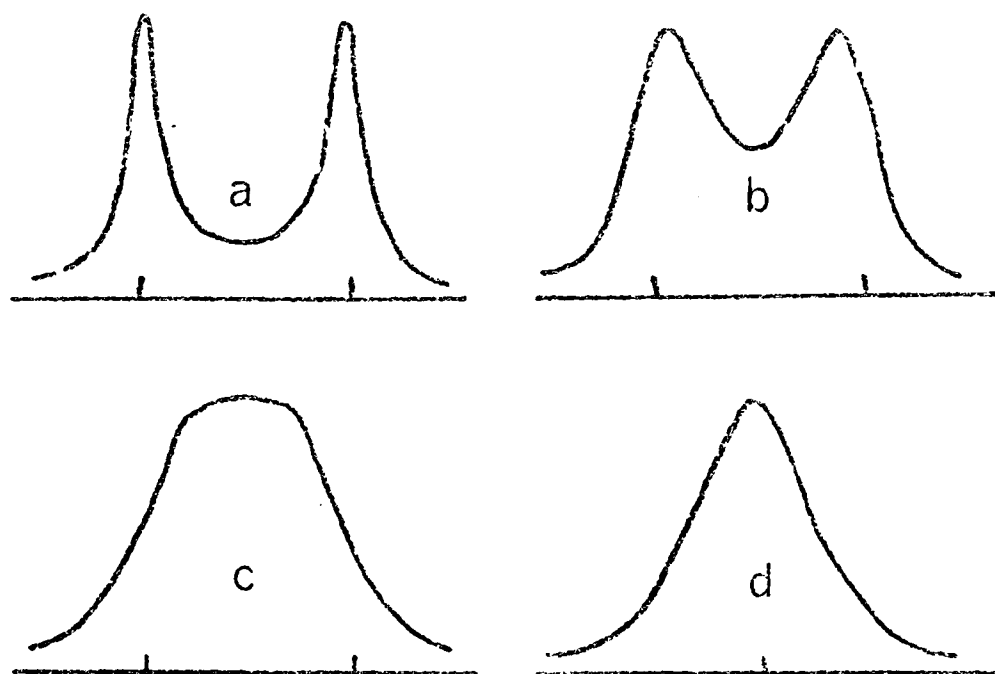


Figure 2.4 Line shape for jumping spin. The ratio of the jumping rate to the line splitting takes the values (a) $1/10$ (b) $1/5$ (c) $1/2\sqrt{2}$ (d) $1/2$. (from 94)

a solvent. This requirement restricts the use of proton NMR in the study of fresh animal tissues and makes the study of a large range of systems very difficult and expensive. Thirdly, as biological molecules are very complex and contain large numbers of protons, the resolution available at realistic magnetic fields is not sufficient to enable the separation of many of the resonances. This is particularly critical with large proteins (such as phosphorylase), which tumble very slowly, causing the line widths of resonances to broaden.

With the present theory and expertise available, many proton NMR spectra are uninterpretable and much information is lost simply because of the complexity of the spectra. Moreover the drawbacks of low sensitivity, complexity and the need for the use of deuterated solvents prevent the study of many molecules in their biological environments.

Many of these problems can be circumvented by the use of phosphorus NMR. Although it has only $1/15$ the sensitivity of proton NMR, it is attractive because studies may be made in aqueous solution and the spectra are relatively simple due to the small number of different chemical environments in which phosphorus atoms are found. In addition, the chemical shift range is much larger for phosphorus than for protons (87).

The selection of phosphorus in preference to proton NMR sacrifices potential information in favour of simplicity, adaptability and a view of some situations not available to proton NMR. Chapters are devoted to phosphorus NMR studies of the pyridoxal and serine phosphates in phosphorylase and to the observation of phosphorus resonances from subcellular fractions and whole tissues. Many of the studies described only take account of Resonance Frequency and

Intensity measurements and are thus only quick easy assays of phosphorus containing compounds. However some of the studies on whole tissue and phosphorylase include a consideration of line width and line shape.

As the applications of phosphorus NMR described in this thesis have only recently been discovered, many of the sets of observations reported here are incomplete. However they are presented as, perhaps, one of the uses of NMR that is most illuminating to the biochemist.

Chapter 3

THE COVALENT ATTACHMENT OF PROBES TO PHOSPHORYLASE

One of the best ways of attaching reporter groups to proteins is by utilising the reactivity of cysteine residues. A large number of fluorescent and spin labelled reagents which can react specifically with sulphhydryl groups in proteins are available (111). Many measurements on labelled enzymes may be made without an accurate knowledge of the number or locations of attached probe groups. Hence the validity of most of the results in this thesis does not depend upon absolutely specific labelling of particular groups. In contrast, measurement of the distance between probes on an enzyme surface necessitates absolute specificity in the attachment of each probe to the protein (112).

There has been a good deal of confusion concerning the number of sulphhydryl groups in phosphorylase which can react with modifying reagents. The one fact on which most workers are agreed is that of the 9 cysteine groups per phosphorylase monomer, up to 4 can react with iodoacetamide or DTNB under conditions where the enzyme is not denatured (113-116). This is an encouraging start as, obviously, the ease with which specific labelling can be achieved decreases as the number of groups available for reaction increases. It is at this point that confusion strikes the literature. Perhaps the most reliable source of data is that of Madsen and his colleagues who, from a long sequence of studies, found that 2 sulphhydryl groups per phosphorylase monomer reacted relatively rapidly with iodoacetamide without causing loss of enzyme

activity. In addition, Madsen et al. found that 2 further sulphhydryl groups per monomer reacted more slowly causing loss of enzyme activity (117, 118, 47). Buc-Caron (119) observed a similar pattern of reactivity between DTNB and phosphorylase b (i.e. two fast reacting groups and two slowly reacting groups associated with loss of enzyme activity). However Kleppe and Damjanovich (120) and Sanner and Tron (121) suggested that the fast phase of reactivity accounted for only one sulphhydryl group. Simultaneously Johnson (122), Robinson (123) and Salmon showed that with iodoacetamide and Nbf-Cl the fast reaction phase also consisted of only one group (78,124).

In order to resolve these conflicts, a series of studies on the reactivity of the sulphhydryl groups of phosphorylase was initiated and is described in this chapter. The observation which accounts for these discrepancies is that phosphorylase will react with cysteine; a sulphhydryl protecting reagent which is often used in the enzyme preparation and is recommended in the procedure used by most workers in the field (125). Reaction with cysteine leads to blockage of one or more of the fast reacting sulphhydryl groups of phosphorylase. Most workers who have found only one fast reacting sulphhydryl group have used enzyme prepared in the presence of cysteine.

The following pages list the experiments performed to investigate this problem. The kinetics of the reactions of the sulphhydryl groups of phosphorylase were investigated either by measuring the incorporation of radioactive reagent into the protein, or by monitoring spectral changes that took place as the reactions occurred.

A. The reaction of cysteine with phosphorylase

Fig. 3.1 shows the time course of incorporation of radioactive cysteine into phosphorylase b, in the presence or absence of oxygen. Radioactive ^{14}C -cysteine was added to a freshly prepared and neutralised cysteine solution which was then incubated with phosphorylase. After various times, aliquots were removed and passed down a small Sephadex G25 column to remove free cysteine. After determination of the protein concentration, the amount of cysteine incorporated into phosphorylase was deduced from radioactivity measurements. Fig. 3.1 also shows results obtained when free cysteine was removed by dialysis into 1% formic acid, after acidification of aliquots of the incubation mixture to pH 3 with equal volumes of 1% formic acid. One cysteine group is incorporated per monomer, followed by slower incorporation of another group. At time $t = 4$ hours the enzyme was $> 95\%$ active.

Phosphorylase labelled with about one equivalent of ^{14}C cysteine was dialysed into a series of media containing thiols or protein unfolding reagents. Radioactivity associated with the protein after dialysis was measured and is expressed as a percentage of the original radioactivity in Table 3.1. Treatment with cold cysteine or 2 mercapto ethanol causes loss of radioactive cysteine from phosphorylase. In contrast, radioactive cysteine is not lost from the enzyme when it is dialysed into SDS or guanidinium hydrochloride solutions at acid pH, where disulphide exchange is slow.

Together with the fact that the presence of oxygen is necessary for cysteine incorporation, these results indicate that it is likely that an - S - S - covalent bond is formed between phosphorylase and the incorporated cysteine.

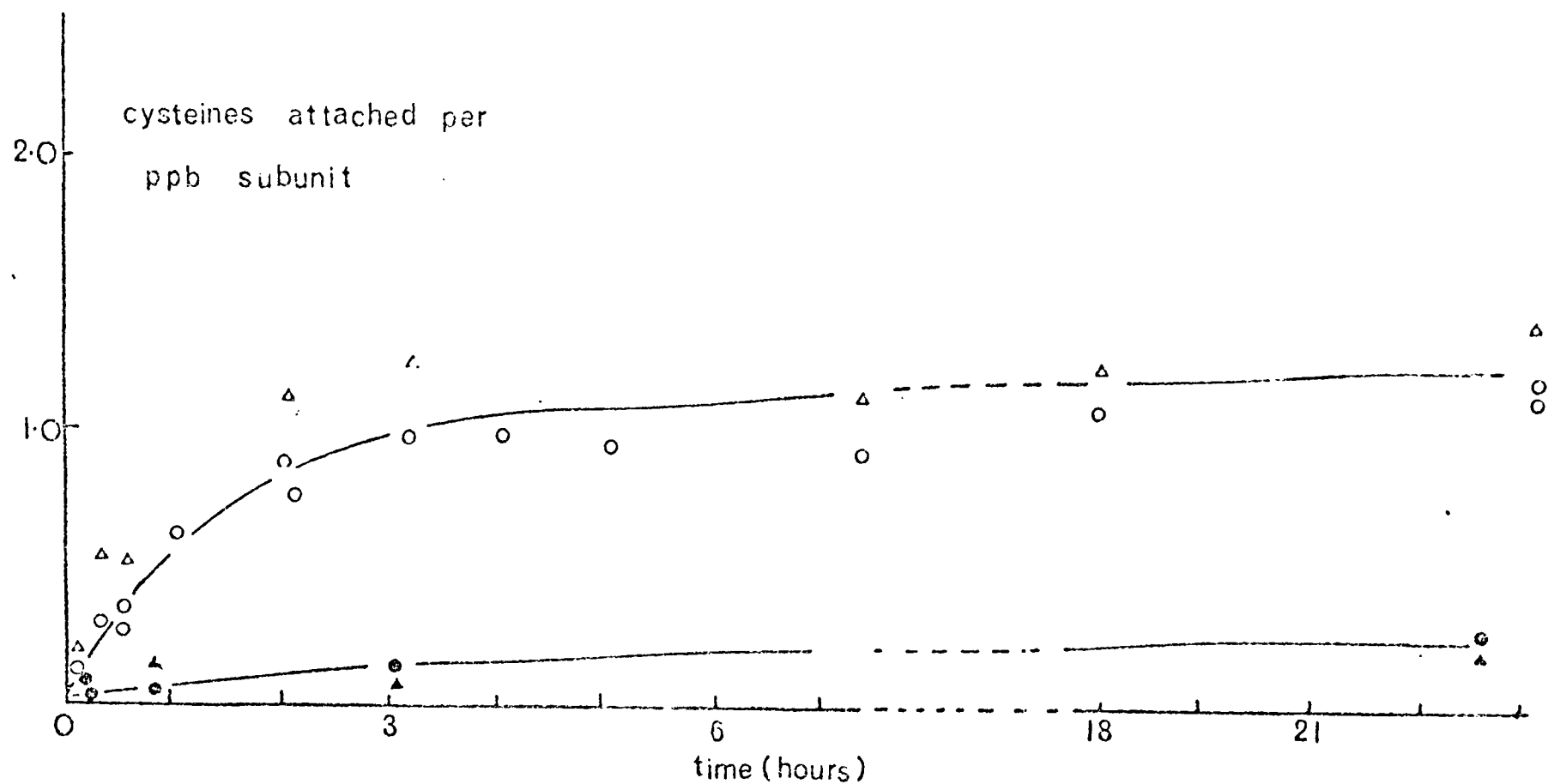


Figure 3.1

Incorporation of ^{14}C cysteine into phosphorylase b

1.31 mM ^{14}C cysteine was added to 106 μM phosphorylase b in TEA buffer pH 7.5, at $t = 0$. After various times aliquots were removed from the incubation mixture. Unreacted ^{14}C cysteine was removed from some aliquots with a small Sephadex column (Δ). To other aliquots, an equal volume of 1% formic acid was added and unreacted cysteine was removed by dialysis (o). ^{14}C cysteine incorporated into phosphorylase was monitored in each sample and is plotted in the figure.

The closed symbols (\blacktriangle, \bullet) show a similar experiment performed with nitrogen saturated solutions.

All experiments in this chapter were performed at 20°C.

Table 3.1

Treatment of ^{14}C cysteine phosphorylase b with various reagents

1 ml of 50 μM phosphorylase, containing 1 equivalent of ^{14}C cysteine, was dialysed into 3 x 1 litres of various media. Radioactivity associated with the protein was determined before and after dialysis.

Dialysis Medium	% of counts associated with phosphorylase after dialysis
50 mM triethanolamine 100 mM KCl pH 7.5	100
0.4M imidazole adjusted to pH 6.2 with citric acid	100
2M Guanidinium hydrochloride	pH 2.0 100 pH 7.5 3
5M urea	pH 2.0 100 pH 7.5 2
1% sodium dodecyl sulphate	pH 2.0 100 pH 7.5 7
50 mM triethanolamine pH 7.5 + 2 mM cold cysteine	3.5
50 mM triethanolamine pH 7.5 + 5 mM β mercaptoethanol	2
50 mM triethanolamine pH 7.5 + 1 mM Dithiothreitol	90

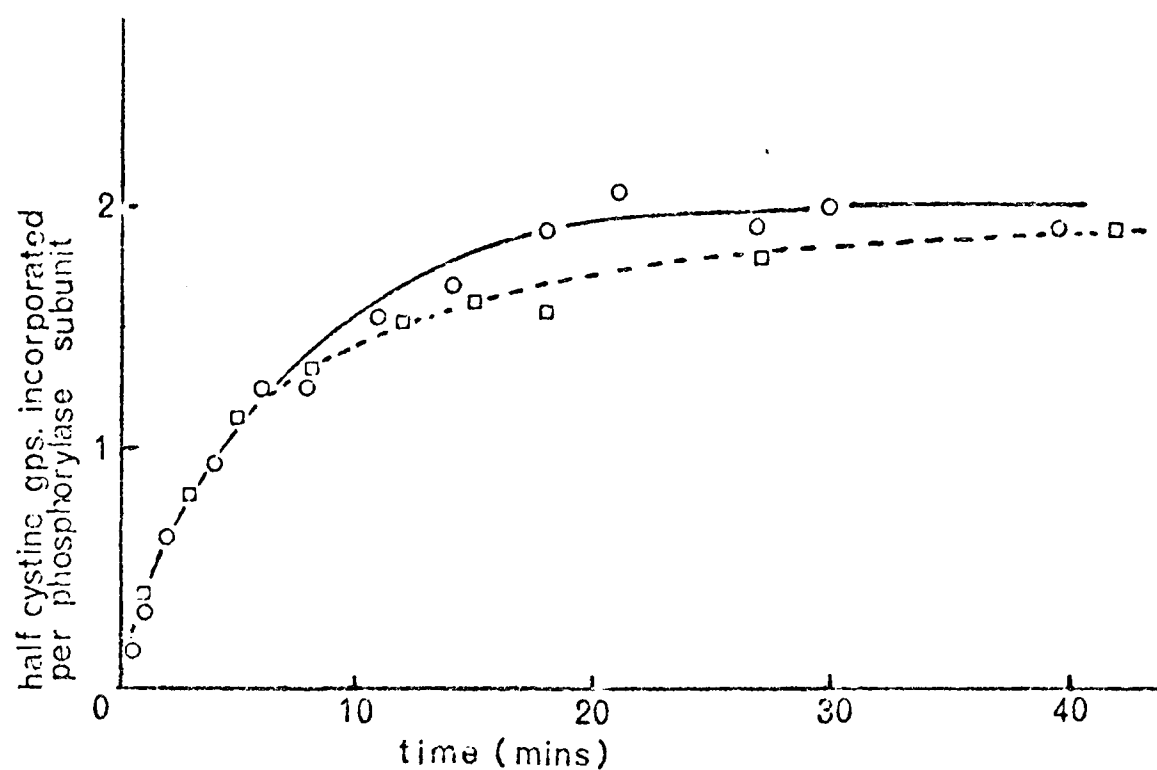


Figure 3.2 Incorporation of ^{14}C cystine into phosphorylase b

$580\ \mu\text{M}$ ^{14}C cystine was added to $80.6\ \mu\text{M}$ phosphorylase b in TEA buffer pH 7.5, at $t = 0$. After various times aliquots were removed from the incubation mixture and unreacted ^{14}C cysteine and ^{14}C cystine was removed with a small Sephadex column. ^{14}C half cystine incorporated into phosphorylase was monitored in each sample and is plotted in the figure. The experiment was performed using air-saturated (o) or nitrogen-saturated (□) buffers at 20°C .

At room temperature and 1 atmosphere, the concentration of oxygen dissolved in buffer is only about $200 \mu\text{M}$ (126). Hence kinetic analysis of Fig. 3.1 could give misleading conclusions as the level of oxygen present could become depleted during the course of the reaction.

The experiment was, therefore, repeated using radioactive cystine. This was prepared by adding a solution of 1 mM cystine at pH 7.5 to radioactive cysteine. From the data shown in Fig. 3.2, it is apparent that two half cystine groups are rapidly incorporated per phosphorylase monomer. The course of the reaction is unaffected by the presence of oxygen.

The reaction of cysteine with phosphorylase may proceed by two mechanisms

- (i) Cysteine slowly oxidatively dimerises to cystine which then reacts with phosphorylase by disulphide exchange.
- (ii) Cysteine and a sulphhydryl group of phosphorylase oxidatively react directly together.

In view of the rapid reaction of phosphorylase with cystine it is impossible to define whether the second mechanism occurs exclusively and whether the first cysteine that is incorporated into the enzyme blocks one unique sulphhydryl group per monomer or is shared between the two fast reacting sulphhydryl groups.

B. The Reaction of Iodoacetamide with Phosphorylase

Fig. 3.3 shows the time course of the reaction which occurred when 6.42 mM iodoacetamide was incubated with 100 μ M phosphorylase b. Aliquots were removed from the reaction mixture at various times and equal volumes of 1% formic acid were added. After dialysis and a redetermination of the protein concentration, the radioactivity associated with phosphorylase was measured. 1.7 - 1.8 sulphydryl groups per monomer reacted rapidly with iodoacetamide under these conditions. At $t = 1$ hour, the enzyme was > 90% active.

Fig. 3.4 shows a similar experiment performed at lower iodoacetamide concentrations, where the reaction was second order with respect to iodoacetamide and phosphorylase. The data were analysed using a PDP 11 computer programme written by Mr P.J. Seeley. The programme takes the equation:

$$-\frac{dA}{dt} = k_1 (S_o - SA_1)A + k_2 (S_o - SA_2)A + k_3 (S_o - SA_3)A \dots$$

where, $\frac{dA}{dt}$ is the rate of removal of iodoacetamide

A is the concentration of iodoacetamide present at time, t

S_o is the initial concentration of each sulphydryl group,

n groups react with iodoacetamide with 2nd order rate constants of $k_1, k_2,$

$k_3 \dots k_n$

and $SA_1, SA_2, SA_3 \dots SA_n$ are the concentrations of iodoacetamide which

have reacted with each of these groups at time, t.

The operator estimates values of $k_1, k_2, k_3 \dots$ and selects a time increment Δt , which is small compared to the half time of the fastest reacting

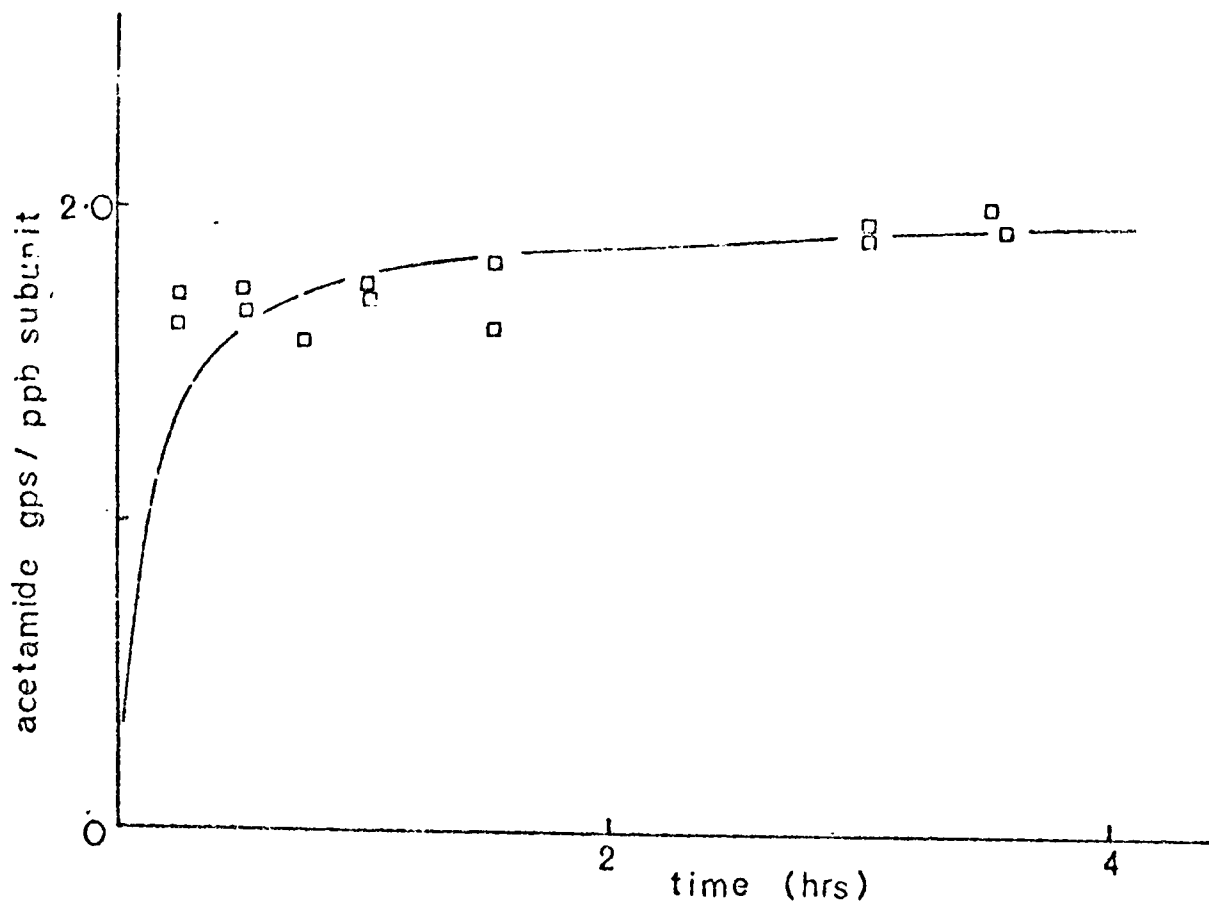


Figure 3.3

The reaction of iodoacetamide with phosphorylase b

6.42 mM ^{14}C iodoacetamide was added to 100 μM phosphorylase b in TEA buffer pH 7.5, at $t = 0$. After various times, aliquots were removed from the reaction mixture and the reaction was stopped by the addition of an equal volume of 1% formic acid. After dialysis the ^{14}C acetamide incorporated into phosphorylase was assayed and is plotted in the figure.

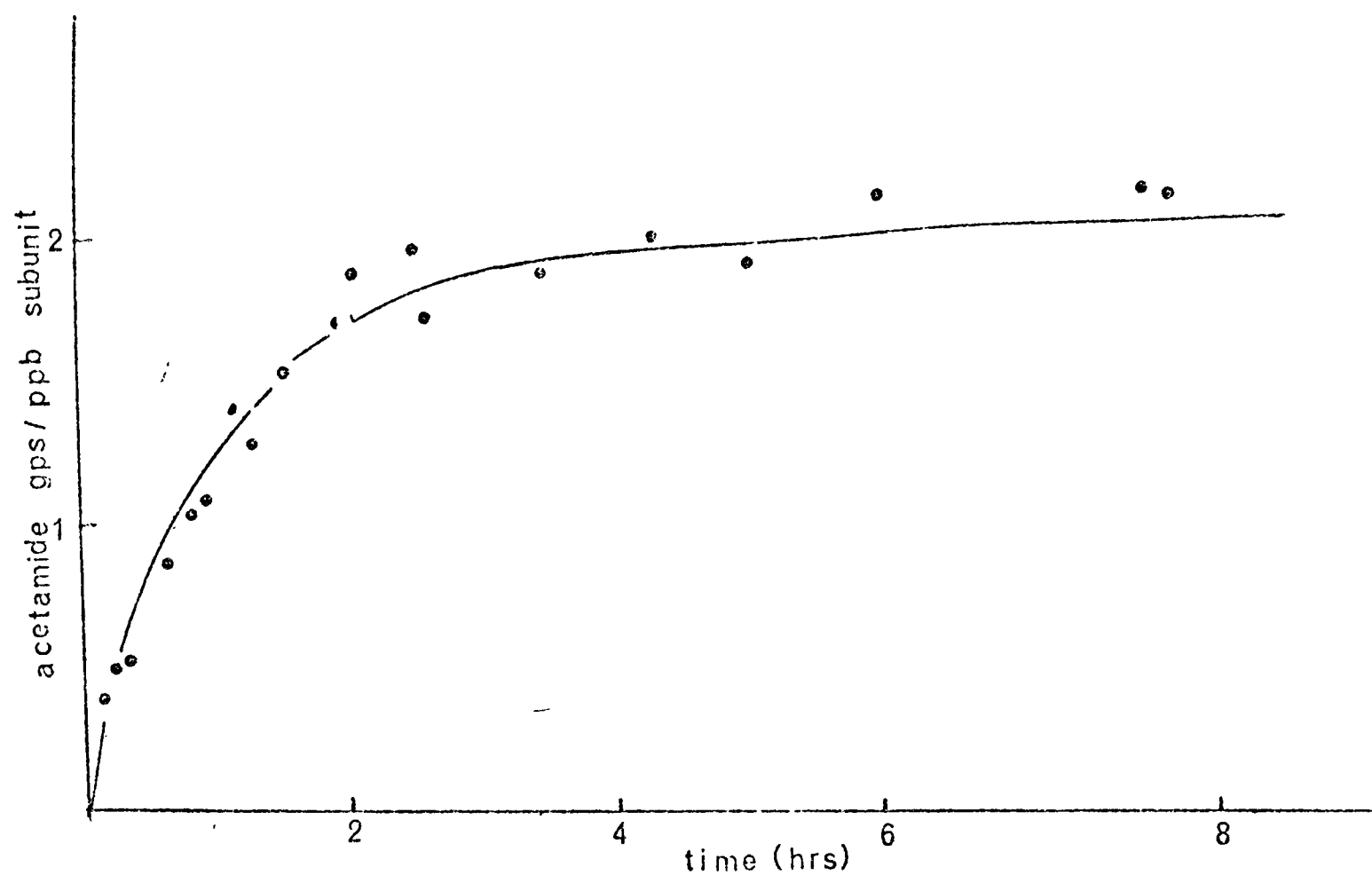


Figure 3.4

The reaction of iodoacetamide with phosphorylase b

672 μM iodoacetamide was added to 90 μM phosphorylase b - the experimental procedure was as described in Fig. 3.3. The continuous line represents a curve simulated by the PDP II programme described in the text, assuming that 4 groups / phosphorylase subunit react with iodoacetamide with rate constants of 105, 50, 0.2 and 0.2 $\text{l. moles}^{-1} \text{min}^{-1}$.

group. The computer now calculates $\frac{dSA_1}{dt}$, $\frac{dSA_2}{dt}$, $\frac{dSA_3}{dt}$ $\frac{dSA_n}{dt}$ for the time increment 0 to $0 + \Delta t$ taking A as A_0 , the initial concentration of iodoacetamide. SA_1 , SA_2 , SA_3 SA_n and A are then calculated for time $t = \Delta t$. The calculation is now repeated for the time increment Δt to $2 \Delta t$ and new values of SA_1 , SA_2 , SA_3 SA_n and A are calculated for $t = 2 \Delta t$. The programme thus computes the reaction time course of the incorporation of acetamide into phosphorylase assuming rate constants k_1 , k_2 , k_3 k_n . This is displayed on a multichannel analyser where it can be compared to the experimental data. The continuous line in Fig. 3.4 is such a comparison.

The data in Fig. 3.4 cannot be analysed in terms of a unique pair of rate constants. Sets of pairs of rate constants ranging from $k_1 = 120 \text{ M}^{-1} \text{ min}^{-1}$ $k_2 = 40 \text{ M}^{-1} \text{ min}^{-1}$ to $k_1 = 80 \text{ M}^{-1} \text{ min}^{-1}$ $k_2 = 80 \text{ M}^{-1} \text{ min}^{-1}$ fit the data equally well.

Whilst the actual values of the rate constants are not important, it is obvious that the reaction must be analysed in terms of two rather than one fast reacting groups per monomer. If enzyme which had been incubated with cysteine was used in these experiments, less than two acetamide groups per monomer were rapidly incorporated.

C. The Reaction of Nbf-Cl with phosphorylase

Fig. 3.5 shows the time course of the reaction of Nbf-Cl with phosphorylase b, under conditions where the reaction is kinetically pseudo first order with respect to Nbf-Cl. The number of Nbf groups incorporated

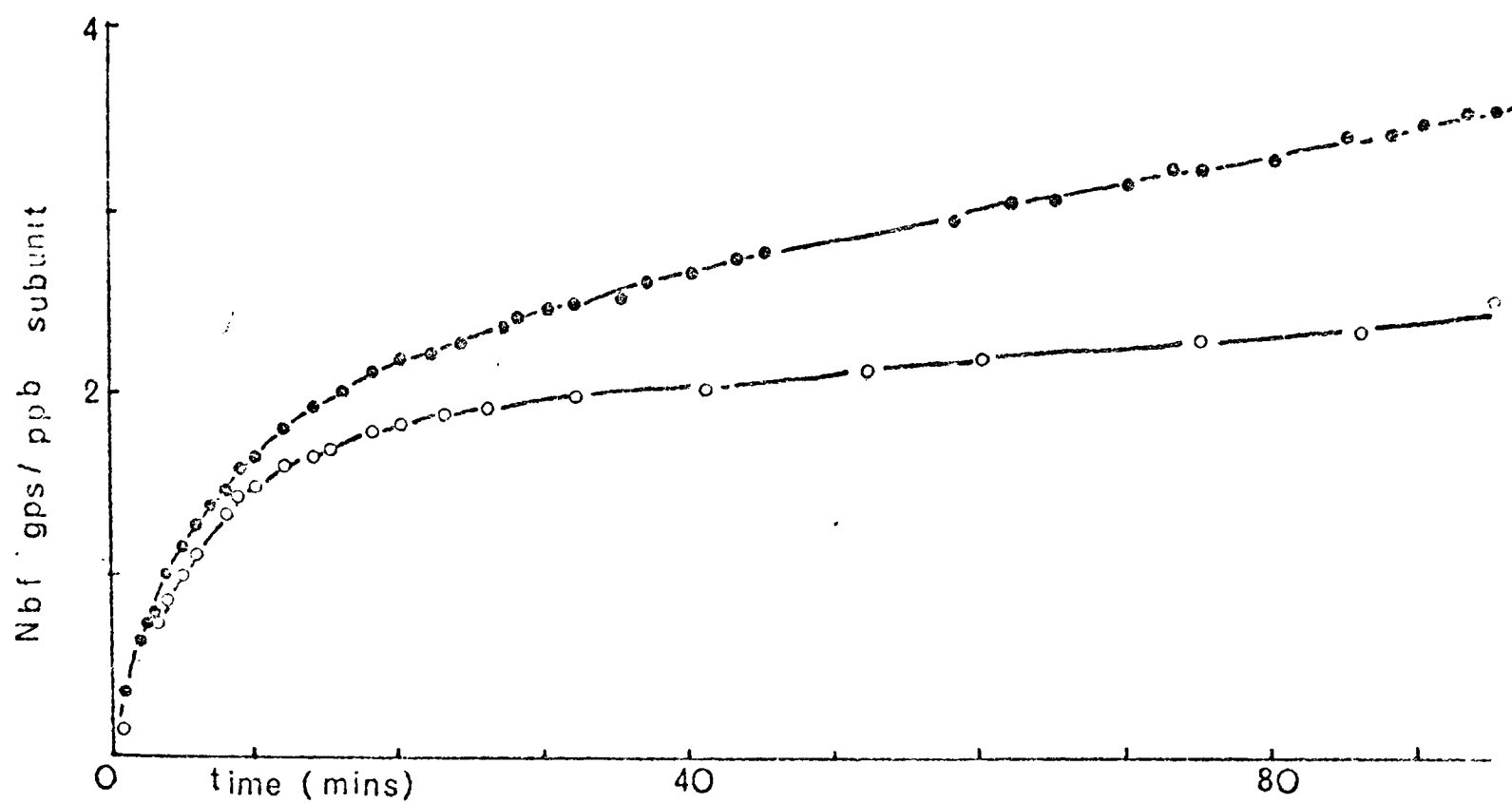


Figure 3.5

The reaction of Nbf-Cl with phosphorylase b

At $t = 0$, $371 \mu\text{M}$ Nbf-Cl was added to $10 \mu\text{M}$ phosphorylase b in TEA buffer pH 7.5 plus (○) or minus (●) 1 mM AMP. The number of Nbf groups per phosphorylase subunit was calculated at each time point from 420 nm. absorption measurements.

per phosphorylase monomer was calculated from measurements of the increase in optical density at 420 nm characteristic of the formation of S-Nbf adducts, taking an extinction coefficient of 1.3×10^4 , as reported by Salmon (124) and Birkett et al. (127).

The reaction, which involves the simultaneous modification of four or more sulphhydryl groups, cannot be unambiguously analysed. The situation is complicated by a slow denaturation of the enzyme after 3-4 Nbf-Cl groups per monomer have reacted. Because of the cloudiness produced by this denaturation, the curve in Fig. 3.5 does not converge to an "infinity value" and, therefore, in order to make a kinetic analysis the later points have to be discarded and an estimate of the end point has to be made. The curve can be fitted to various sets of k values, using the PDP 11 programme described in section 2.B. If end points of between 3.0 and 4.0 groups are assumed, all possible computer fits necessitate the existence of about two groups per monomer which react an order of magnitude faster than any other group.

This is confirmed by the experiment described in Fig. 3.6. The reaction of Nbf-Cl with unmodified phosphorylase and phosphorylase with 1.9 acetamido groups attached per monomer was studied. From the figure it is apparent that the incorporation of 1.9 acetamide groups per monomer (as described in the previous section - Fig. 3.3) blocks the "fast phase" of the reaction of Nbf-Cl with phosphorylase. The difference between the two curves in Fig. 3.6 is thus the time course of incorporation of Nbf-Cl into the rapidly reacting groups of phosphorylase, and is shown in Fig. 3.7. A semi logarithmic

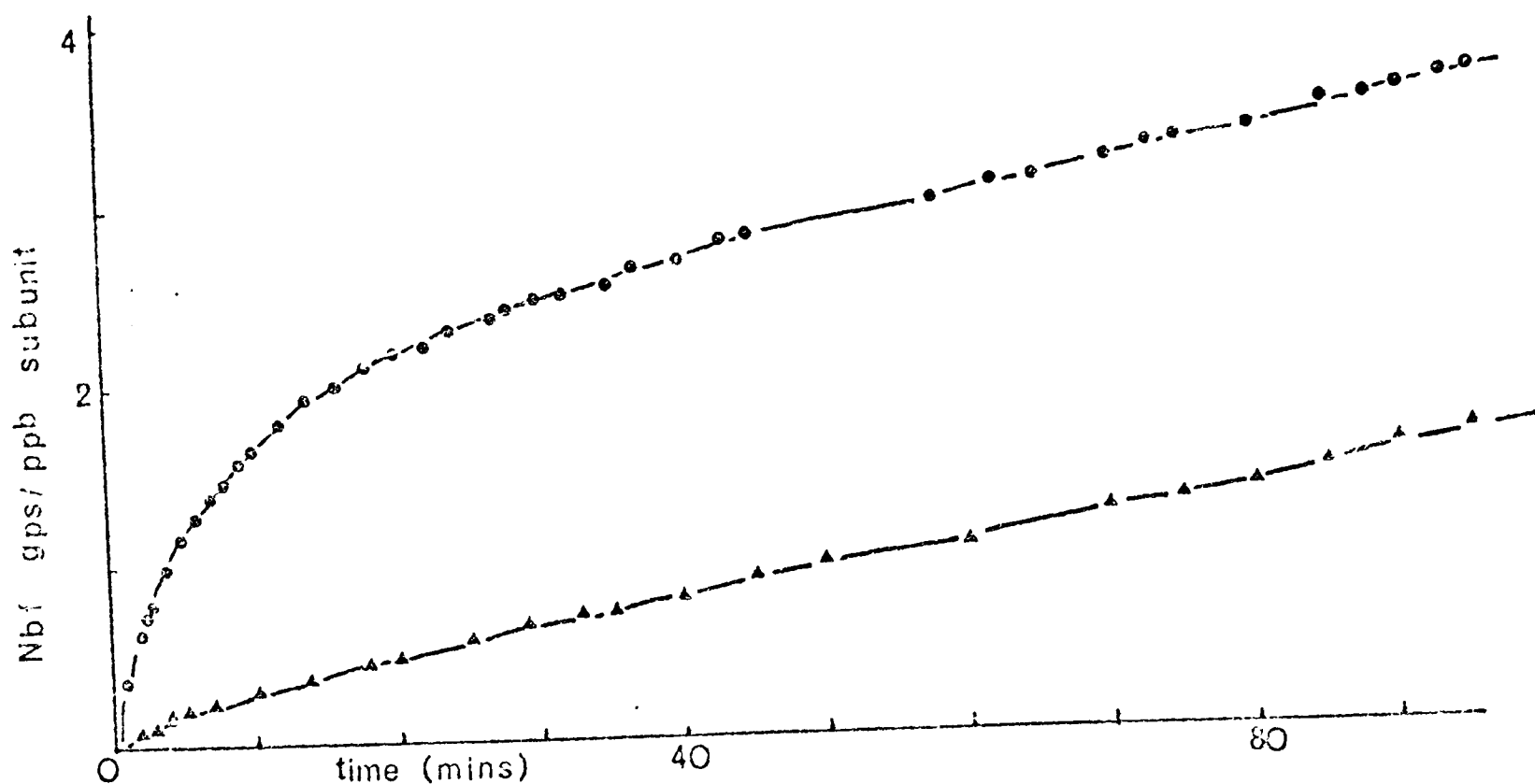


Figure 3.6 The reaction of Nbf-Cl with phosphorylase b (●) and (Acetamido)_{1,9} phosphorylase b (▲)

Conditions are described in the legend to Fig. 3.5.

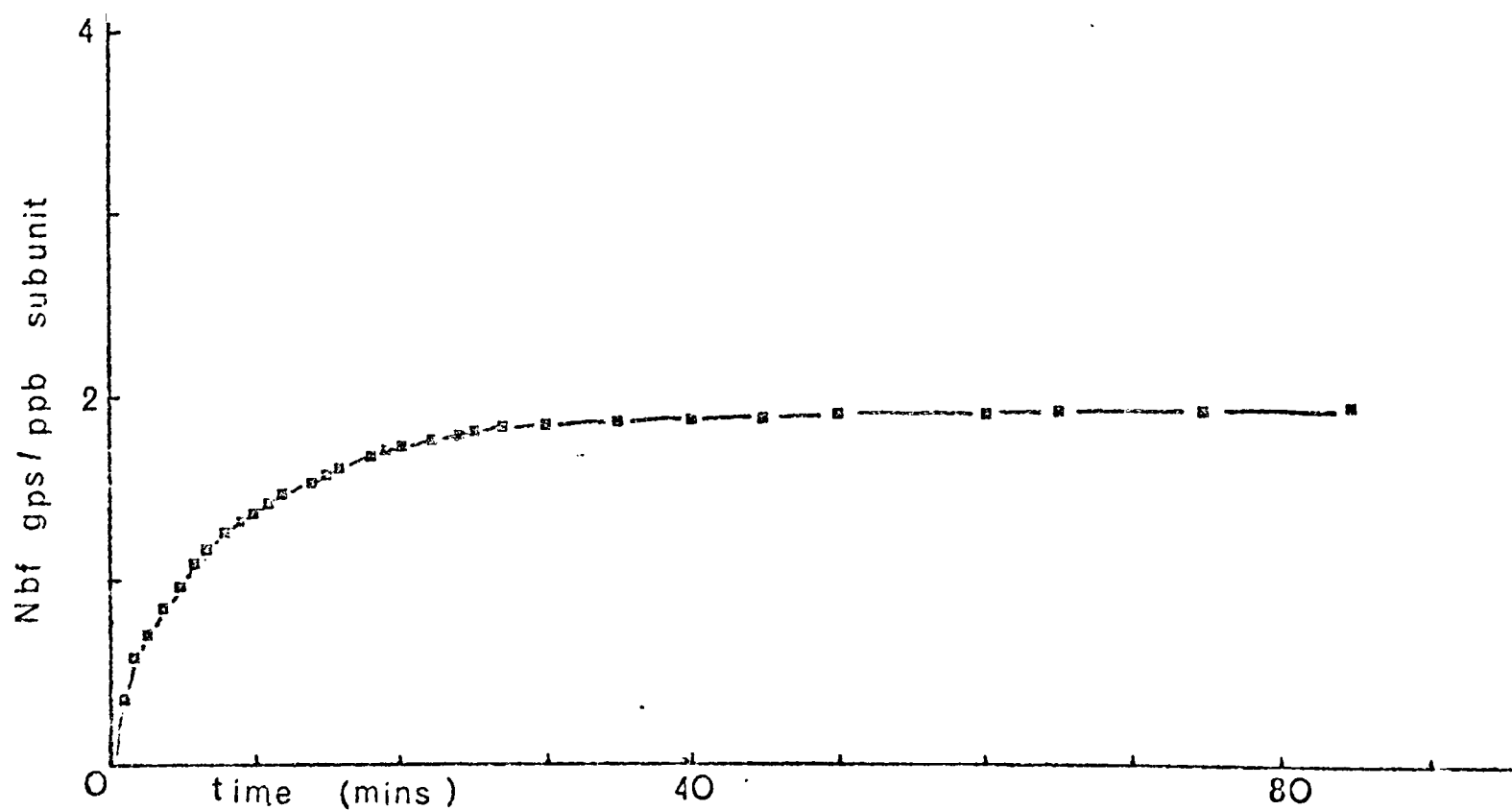


Figure 3.7 The reaction of Nbf-Cl with the two rapidly reacting groups of phosphorylase b

Data was obtained from subtraction of the two curves shown in Fig. 3.6.

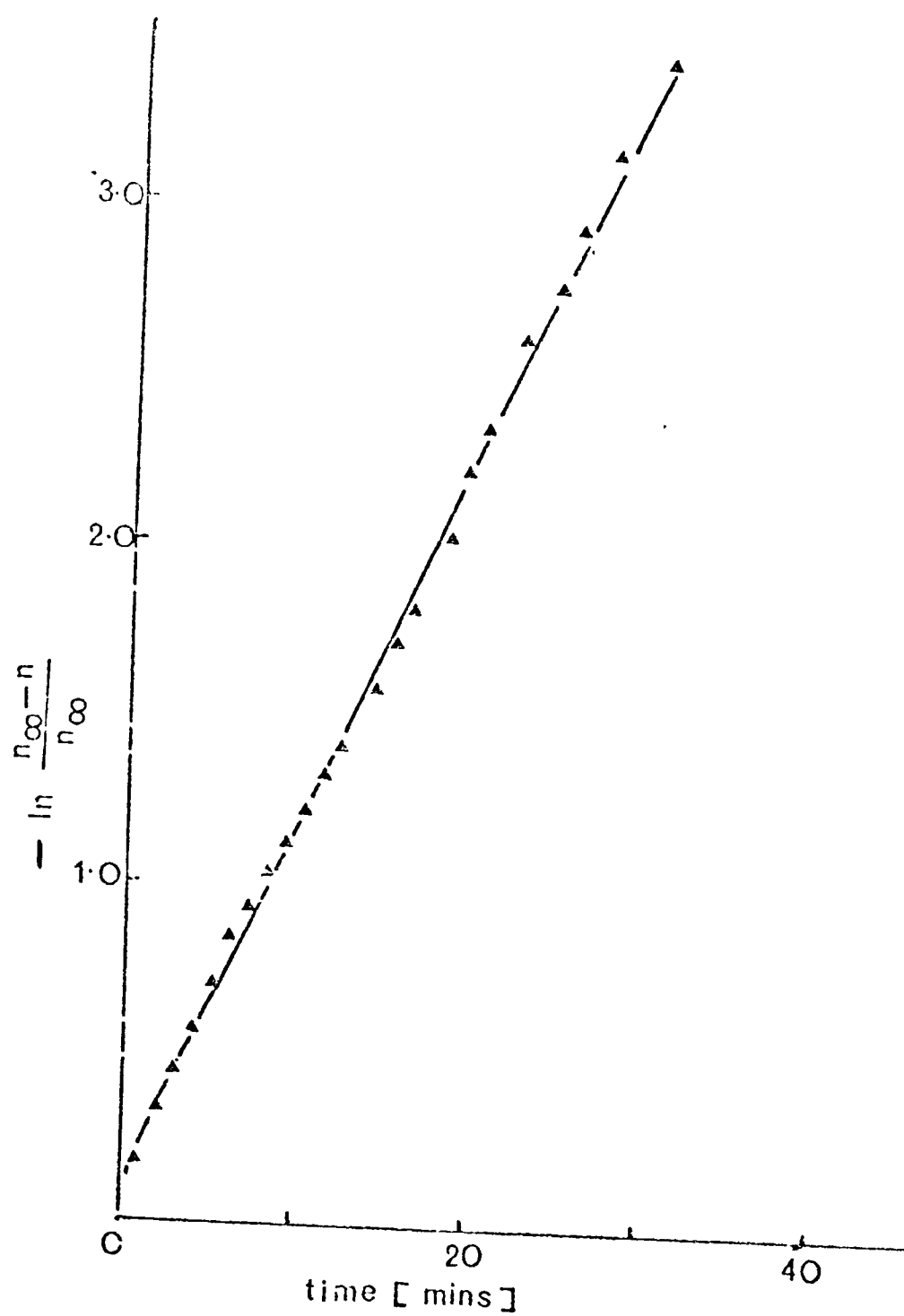


Figure 3.8

Semi logarithmic plot describing the reaction of Nbf-Cl with the two rapidly reacting groups of phosphorylase b

Data obtained from Fig. 3.6. $n_{\infty} = 1.95$.

plot of the data from Fig. 3.7 is shown in Fig. 3.8. This shows that the fast phase of the reaction of Nbf-Cl with phosphorylase may be described in terms of 1.95 groups per monomer reacting with a rate constant of $300 \text{ M}^{-1} \text{ min}^{-1}$. It is difficult to analyse the slow phase of the reaction shown in Fig. 3.6 as the number of groups involved cannot be accurately determined. However if it is assumed that 2 slowly reacting groups are present which react at the same speed, rate constants of $35 \text{ M}^{-1} \text{ min}^{-1}$ are obtained.

Several cautionary points must be made about this analysis.

- (i) It relies upon the likely proposition that the 1.6 - 2.0 groups per monomer which react rapidly with Nbf-Cl are the same as those which react rapidly with iodoacetamide.
- (ii) The estimate of the number of rapidly reacting groups falls in the range 1.6 - 2.0 and is always slightly less than the integer 2. This may be due to a 10% error in the subunit molecular weight of the enzyme or in the extinction coefficient of the S - Nbf adduct. Alternatively, slow oxidation of the rapidly reacting sulphhydryl groups may take place after sulphhydryl protecting reagents have been removed.
- (iii) It is impossible to distinguish between two groups reacting with one rate constant and two groups with slightly differing rate constants.
- (iv) These analyses assume that chemically identical cysteine residues in different subunits have similar reactivities and that all simultaneous reactions proceed independently.
- (v) It is assumed that the extinction coefficient of the S - Nbf moiety is the same for all groups on the protein.

Despite these reservations, the conclusion that the reaction of Nbf-Cl

with phosphorylase is best described in terms of 1.6 - 2.0 rapidly reacting sulphhydryl groups per monomer, seems inevitable. This conclusion was confirmed by a further experiment. From Fig. 3.5, it is apparent that AMP affects the reaction of Nbf-Cl with phosphorylase, primarily by reducing the rate of reaction of the "slowly reacting" set of groups. Fig. 3.9 shows the course of the reaction of Nbf-Cl with unmodified phosphorylase b and phosphorylase b with 1.9 acetamide groups per monomer incorporated, both in the presence of AMP. Again, the incorporation of 1.9 acetamide groups per monomer blocks the fast phase of the reaction. The difference between the two curves (shown as the dotted line in Fig. 3.9) represents a fast reaction phase of 1.70 groups per monomer.

An alternative approach to the determination of the number of groups in the rapidly reacting set is to plot the data from Fig. 3.5 semi-logarithmically (Fig. 3.10) according to the method of Freedman and Radda (129). As single straight line plots are not obtained it is evident that the data do not describe single pseudo first order rate processes. If it is assumed that either reaction can be described in terms of two sets of groups, the extrapolations shown indicate the number of groups reacting in each fast set. Using these extrapolations, values of 1.75 and 1.60 groups in the fast reacting set are obtained, with and without AMP respectively. These values are in reasonable agreement with the other methods of analysis.

In the introduction to this chapter, it was noted that workers who had used enzyme prepared in the presence of cysteine had found only one sulphhydryl group in the first reaction phase. The reaction of Nbf-Cl with phosphorylase, into which known amounts of cysteine had been incorporated, was therefore

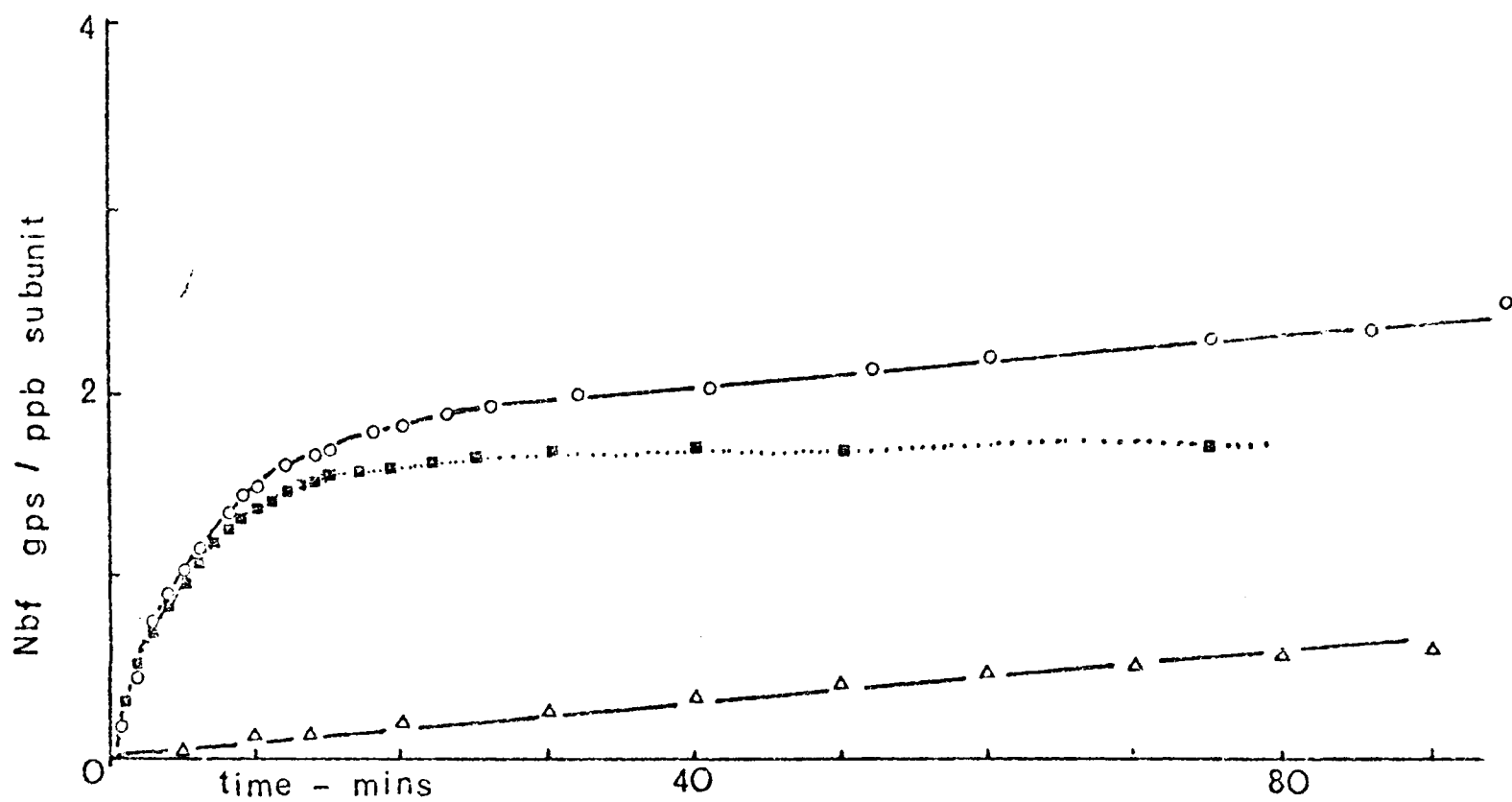


Figure 3.9

The reaction of Nbf-Cl with phosphorylase b in the presence of AMP

The reaction of Nbf-Cl with phosphorylase b (o) and (Acetamido)_{1.9} phosphorylase b (Δ) was monitored as described in the legend to Fig. 3.5. The difference between the two curves, representing the modification of the two fast reacting groups of phosphorylase, is also plotted (■).

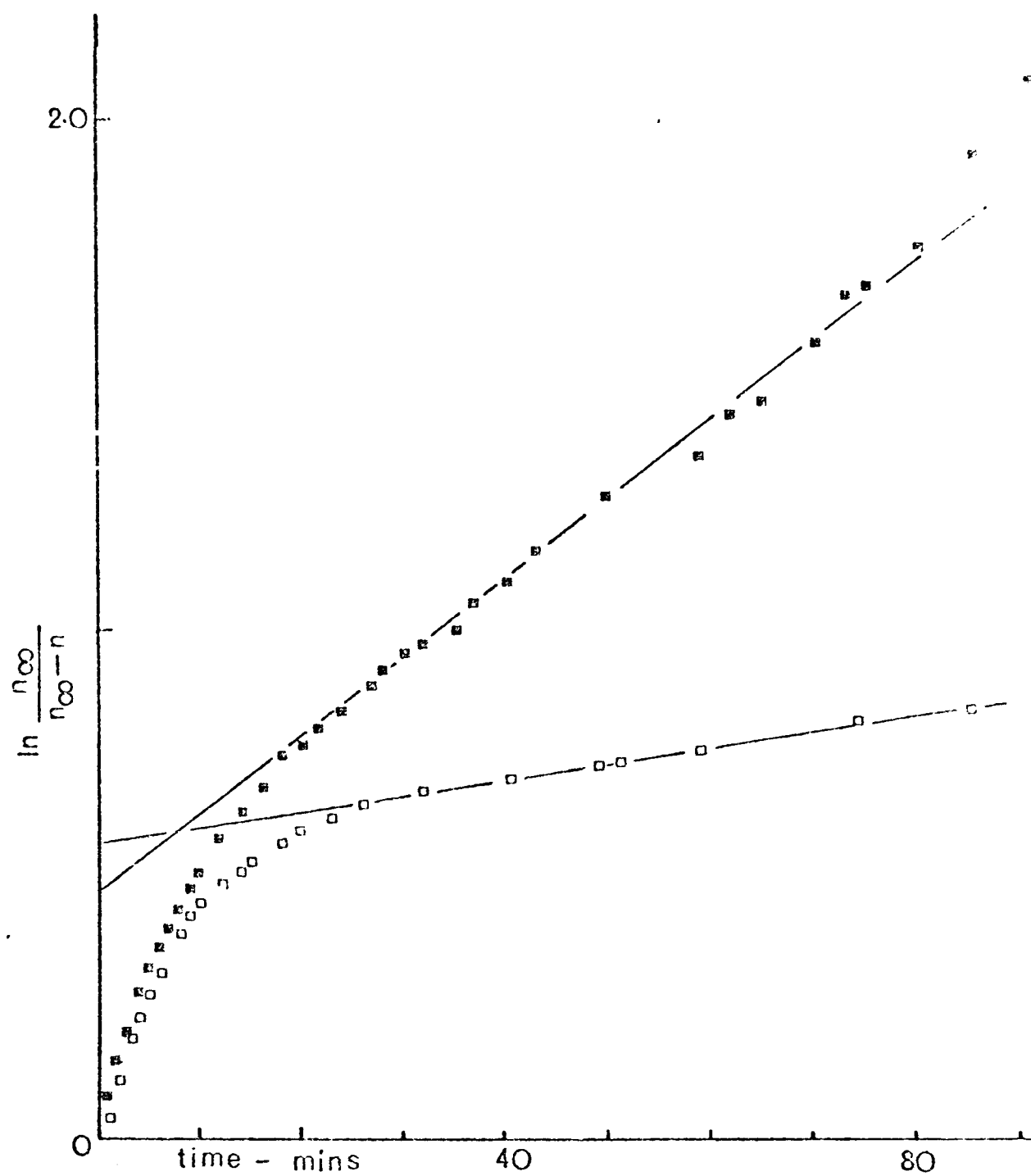


Figure 3.10 Semi logarithmic plot describing the reaction of Nbf-Cl with phosphorylase b

Data from Fig. 3.5 is plotted semilogarithmically assuming $n_{\infty} = 4$. Data is shown for the experiment with (\square) or without (\blacksquare) 1 mM AMP.

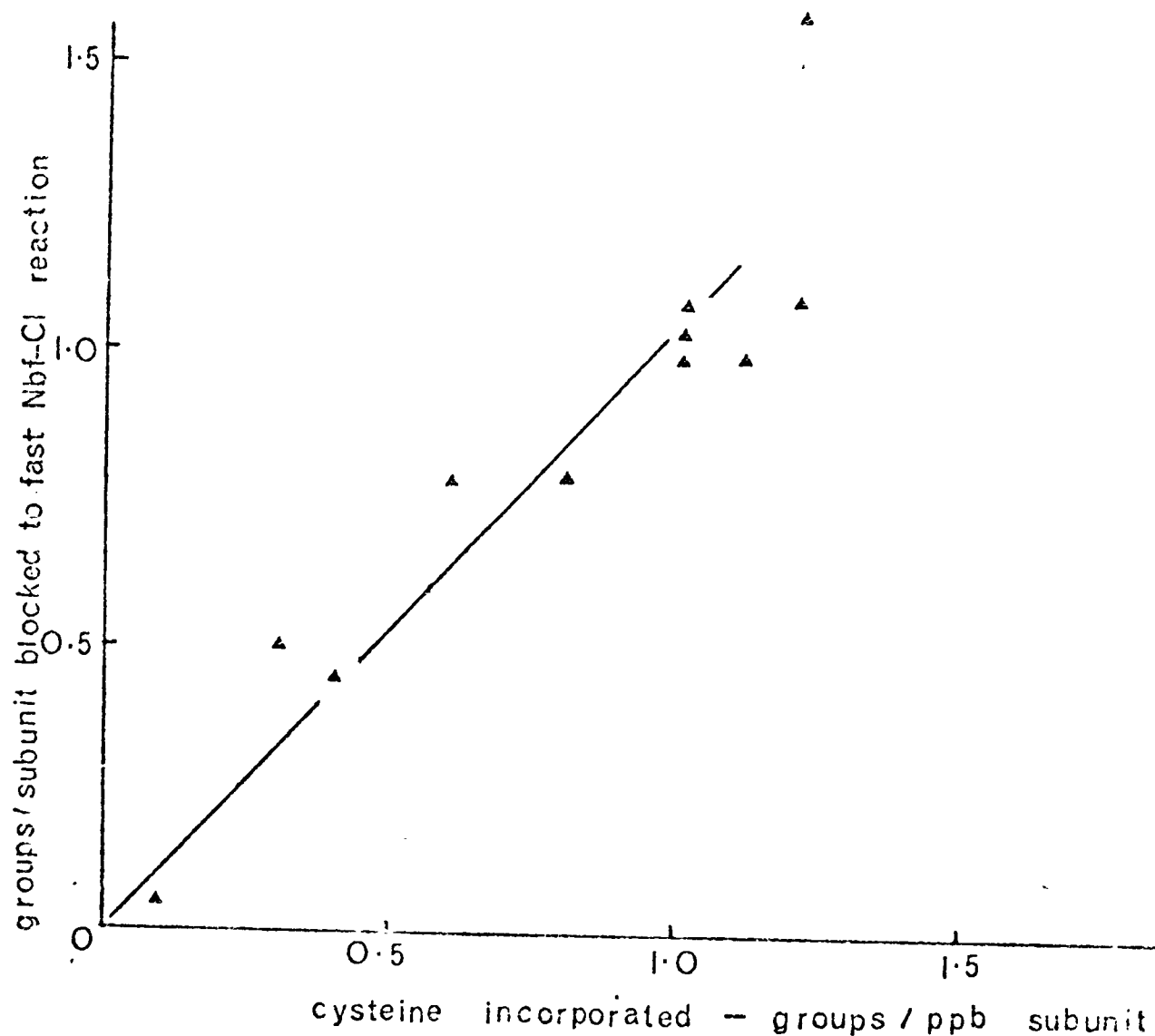


Figure 3.11 Correlation of ^{14}C cysteine residues incorporated into phosphorylase b and the number of groups blocked to reaction with Nbf-Cl

^{14}C cysteine was determined in phosphorylase samples taken from the experiment described by Fig. 3.1. The kinetics of the reaction of Nbf-Cl with each sample were examined under the conditions shown in Fig. 3.5. The reduction in the number of fast reacting groups, due to the cysteine incorporation, was deduced and is shown in the figure.

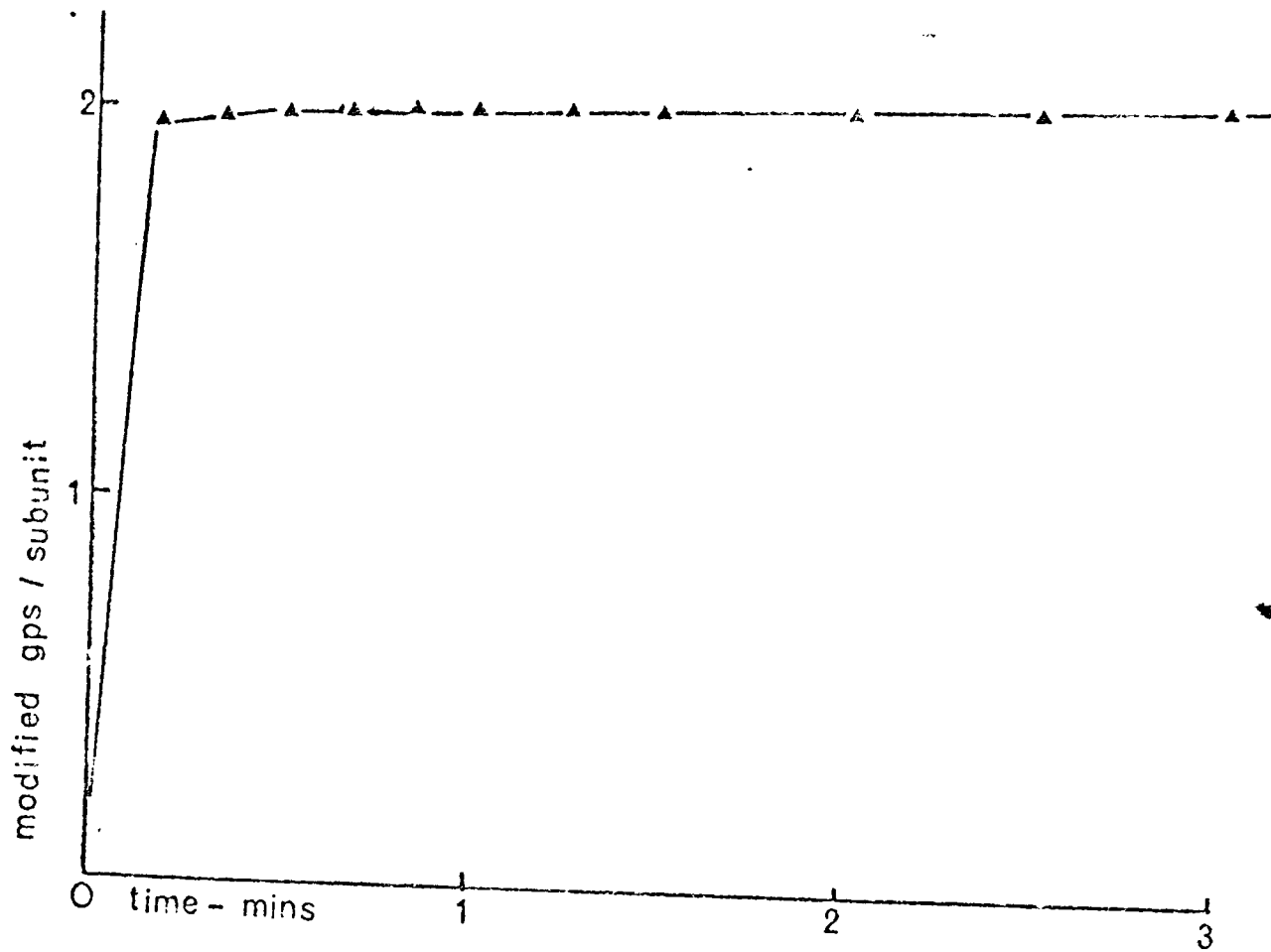


Figure 3.12 The modification of phosphorylase b with DTNB

At $t = 0$ $22.8 \mu\text{M}$ phosphorylase b was added to a solution of 1 mM DTNB in 50 mM Tris 1 mM EDTA pH 8.2. Groups modified were quantified from optical density measurements at 412 nm .

studied. Incorporation of cysteine into phosphorylase causes a reduction in the number of "fast phase" sulphhydryl groups which react with Nbf-Cl. Fig. 3.11 correlates this reduction with the number of cysteine groups incorporated per monomer. Within experimental error, a 1:1 correlation exists between the number of cysteine groups attached to phosphorylase and the reduction in the number of groups reacting with Nbf-Cl.

D. The Reaction of DTNB with Phosphorylase

The time course of the reaction of DTNB with phosphorylase b is shown in Fig. 3.12. The number of half DTNB groups incorporated per monomer was calculated from the increase in absorption at 412 nm associated with the reaction, using a molar extinction coefficient of 1.36×10^4 (128). Rapid reaction of two sulphhydryl groups per subunit is observed.

Two sets of authors have previously reported that only one sulphhydryl group per monomer reacts rapidly with DTNB (120, 121). It is interesting to note that both sets of authors used enzyme which had been prepared in the presence of cysteine.

E. The Reaction of Iodoacetamide Spin Label with Phosphorylase

At the same time as the above studies, the incorporation of iodoacetamide spin label into phosphorylase was investigated by Drs. J.R. Griffiths and N.C. Price (90). Their results, included here for completeness, are based upon the analysis of the time course of incorporation of ^{14}C labelled

reagent into phosphorylase. In triethanolamine buffer at pH 7.5, two fast reacting and two slowly reacting groups were found with rate constants $k_1 = 150 \text{ M}^{-1} \text{ min}^{-1}$, $k_2 = 15 \text{ M}^{-1} \text{ min}^{-1}$ and $k_3, k_4 = 0.1 \text{ M}^{-1} \text{ min}^{-1}$.

F. The Reaction of Iodoacetamidosalicylic acid (ISA) with phosphorylase

This was followed by monitoring the increase in fluorescence due to the formation of the thioacetamidosalicylate adduct. Fig. 3.13 shows the increase in fluorescence observed when ISA is added to unmodified phosphorylase or phosphorylase with 1.9 acetamide groups attached. The effect of incorporation of 1.9 acetamide groups into phosphorylase is to remove the initial fast reaction of ISA with the protein. Of course, this does not prove that 2 SA moieties are added to the enzyme during this fast phase. However if 2 equivalents of ISA are incubated with phosphorylase b for 24 hours and the iodide produced is removed by dialysis, no fast phase in the kinetics of incorporation of iodoacetamide or Nbf-Cl into di SA labelled phosphorylase is observed. This indicates that the fast phase fluorescence increase in the reaction represented in Fig. 3.13 is due to the addition of about 2 SA moieties to phosphorylase.

The difference between the two curves in Fig. 3.13 represents the fluorescence increase due to the reaction of ISA with these two fast phase groups. A semi logarithmic plot of this difference is shown in Fig. 3.14. The most simple explanation of these data is that the fast phase of the reaction is due to one group reacting with a rate constant of $3400 \text{ M}^{-1} \text{ min}^{-1}$ and another group reacting with a rate constant of $700 \text{ M}^{-1} \text{ min}^{-1}$.

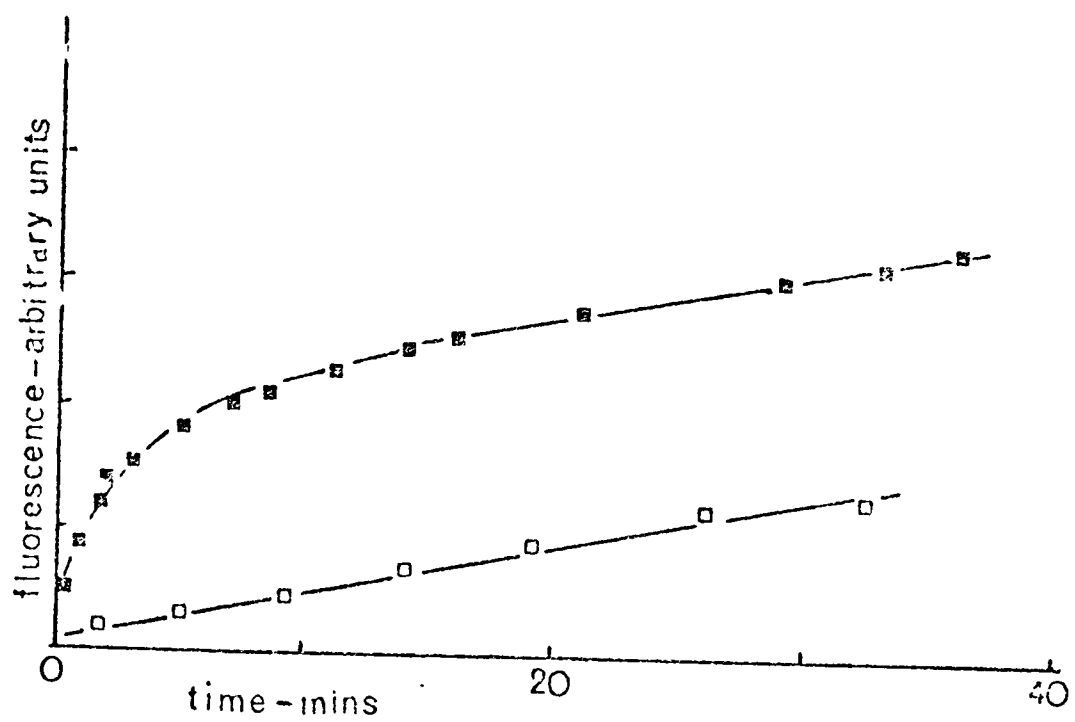


Figure 3.13 Increase in fluorescence during the reaction of ISA with phosphorylase b (■) or (acetamido)_{1,9} phosphorylase b (□). 355 μM ISA was added to 10 μM enzyme at $t = 0$. Fluorescence at 400 nm upon excitation at 320 nm was monitored continuously as a function of time.

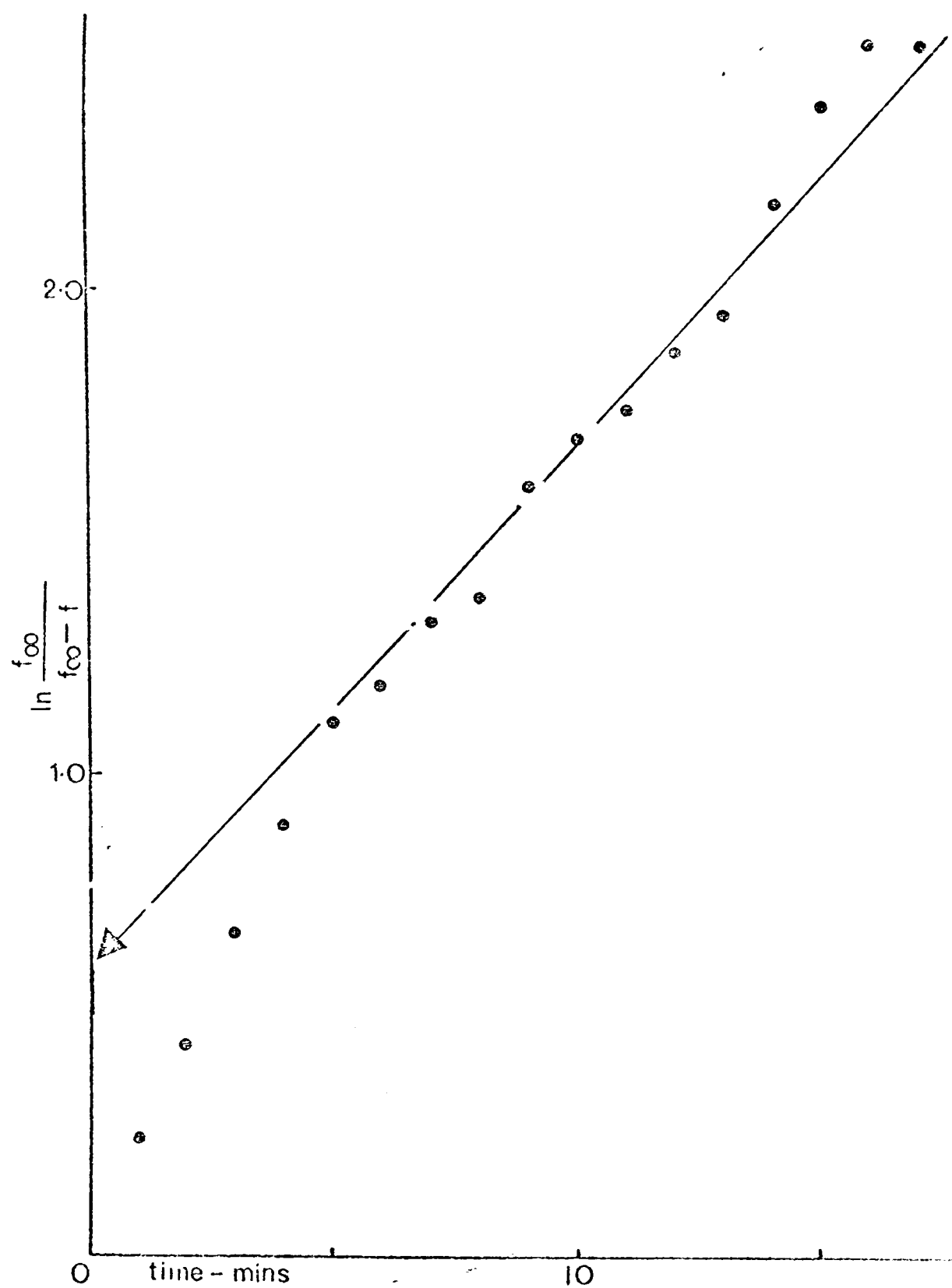


Figure 3.14 Semi logarithmic plot of the fast phase fluorescence increase during the reaction of ISA with phosphorylase b

Data was obtained from the difference between the curves in Fig. 3.13.

G. Summary

The reactivity of the sulphhydryl groups of phosphorylase towards a variety of reagents has been studied. The reactions of these reagents were analysed in terms of two components, a fast phase and a slow phase. The fast phase accounts for the reaction of up to 2 sulphhydryl groups per subunit. Incorporation of cysteine into phosphorylase, probably via an - S - S - bridge, can block some or all of the fast phase reactivity.

In view of the complexity of the analysis, it is difficult to give unambiguous values for the rate constants of the groups in the fast reacting phase. The relative values of the rate constants for the two groups depend upon the reagent used. Sets of values which are consistent with the above data are shown in Table 3.II.

Considerable care must be taken in the analysis of results which require specific labelling of phosphorylase as the enzyme does not, as was once thought, contain only one highly reactive sulphhydryl group per monomer. If one equivalent of any reagent reacts with phosphorylase, it will distribute itself between the various reactive groups. The nature of this distribution will depend upon the rate constants for the reaction of these groups with the reagent.

Table 3.11

The reactivity of the sulphhydryl groups of phosphorylase b

Sulphhydryl group	Remarks	Rate constant* for reaction with		
		iodoacetamide	iodoacetamide spin label	Nbf -Cl Iodoacetamidosal.
1	not associated with activity loss	70-110 ⁺	150	300
2	not associated with activity loss	40-80 ⁺	15	300
3	reaction of groups 3 and 4 are associated with activity loss	< 0.5	0.1	35
4	and disaggregation	< 0.5	0.1	35

These rate constants are subject to the assumptions of the analyses referred to in the text

* in $M^{-1} \text{ min}^{-1}$

+ whilst these two k values are not identical, they are too close to permit accurate analysis

Chapter 4

THE INTERACTION OF LIGANDS WITH PHOSPHORYLASE

A. Measuring dissociation constants of enzyme ligand complexes

The interaction of a number of ligands with phosphorylase is important in the regulation of glycogen breakdown (75). However there are a number of difficulties in defining the importance and extent of such interactions under physiological conditions. Firstly, while extensive kinetic and some equilibrium binding studies have pointed to the possibility of multiple effector and substrate binding sites, the nature of the interactions between different ligands is not fully understood (101, 130, 131). Although, in principle, it should be possible to quantify all the ligand interactions using established methodology, in practice, the complexity of the system, experimental difficulties and the tedium of conventional techniques have prevented such definition. Secondly, the a and b forms of phosphorylase have different affinities for given ligands. There is evidence that during the conversion of phosphorylase b to a, intermediate forms, which have additional regulatory properties, exist (132). Finally, there is the possibility that the interactions are altered by protein-protein contacts which only occur in the glycogen particle fraction (133).

Clearly a simple rapid method of detecting ligand binding to phosphorylase is required. Covalently bound probes whose spectral properties alter as ligands bind to phosphorylase provide such a method. The two probes which have been used in these studies are acetamidosalicylate and the

acetamide spin label, both of which were described in Chapter 2.

Acetamidosalicylate phosphorylase b was prepared by incubation, at room temperature, of one equivalent of ISA with phosphorylase in triethanolamine KCl buffer at pH 7.5 for 20 hours, followed by dialysis to remove iodide and unreacted reagent. Acetamidosalicylate phosphorylase b is a fully active dimer which sediments with an S_{20} value of 8.3S.

On excitation at 320 nm (Fig. 2.1) the salicylate label has a fluorescence emission maximum at 400 nm. Binding of glucose 1-phosphate (but not glucose or glycogen) and effector ligands to the labelled enzyme reduces the intensity of salicylate emission. In titrations with varying amounts of ligands the fluorescence changes can be used to obtain apparent binding constants for substrates and effectors. These binding constants together with the limiting fluorescence quenching produced by the ligands are summarized in Table 4.1. Fluorescence titrations utilising the quenching of light emission from acetamido-salicylate-phosphorylase b by ligands were carried out using 0.1 mg/ml enzyme ($1 \mu\text{M}$). As the minimum concentration of ligand added in most titrations was $20 \mu\text{M}$, it could be assumed that the free ligand concentration was equal to the total ligand concentration added. However, during the titration of AMP into labelled phosphorylase a, because binding is very tight, concentrations of ligand in the range $1\text{-}20 \mu\text{M}$ were added. Hence this assumption could not be made and the exact value for the apparent binding constant could not be calculated. In other cases, the apparent binding constants shown (Table 4.1) are the values of the total ligand concentration required to produce half of the total fluorescence quenching. Corrections were made for dilution of the enzyme during titrations. About

Table 4.1

Fluorescence changes when various ligands are titrated into labelled phosphorylase a and b Binding followed by the quenching of the salicylate fluorescence of the labelled protein. 50 mM triethanolamine- KCl buffer pH 7.5, 1 μ M acetamidosalicylate-phosphorylase at 18°C (from (79))

Acetamidosalicylate-phosphorylase <u>b</u>		Acetamidosalicylate-phosphorylase <u>a</u>	
ligand	k_{app}	ligand	quenching
	mM		%
AMP	0.070	AMP	21
ADP	0.100	ADP	20
ATP	2	-	-
IMP	5	IMP	15
Glucose-1-phosphate	10	-	-
Glucose-6-phosphate	0.040	Glucose-6-phosphate	18
Phosphate	1.0		
β -Glycerophosphate	5.0		
Glucose, gluconolactone, maltotetraose and glycogen		No effect	

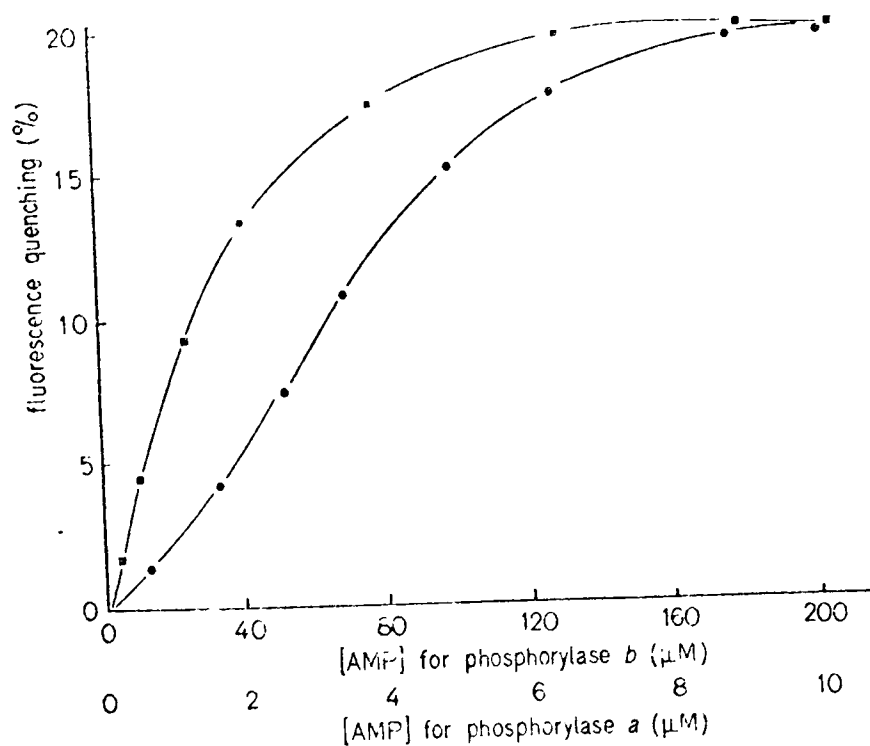


Figure 4.1 Fluorescence changes as AMP binds to acetamido-salicylate-Phosphorylase b (●) and a (■). 50 mM triethanolamine - KCl buffer pH 7.5, 1 μ M acetamido-salicylate phosphorylase at 18° C.

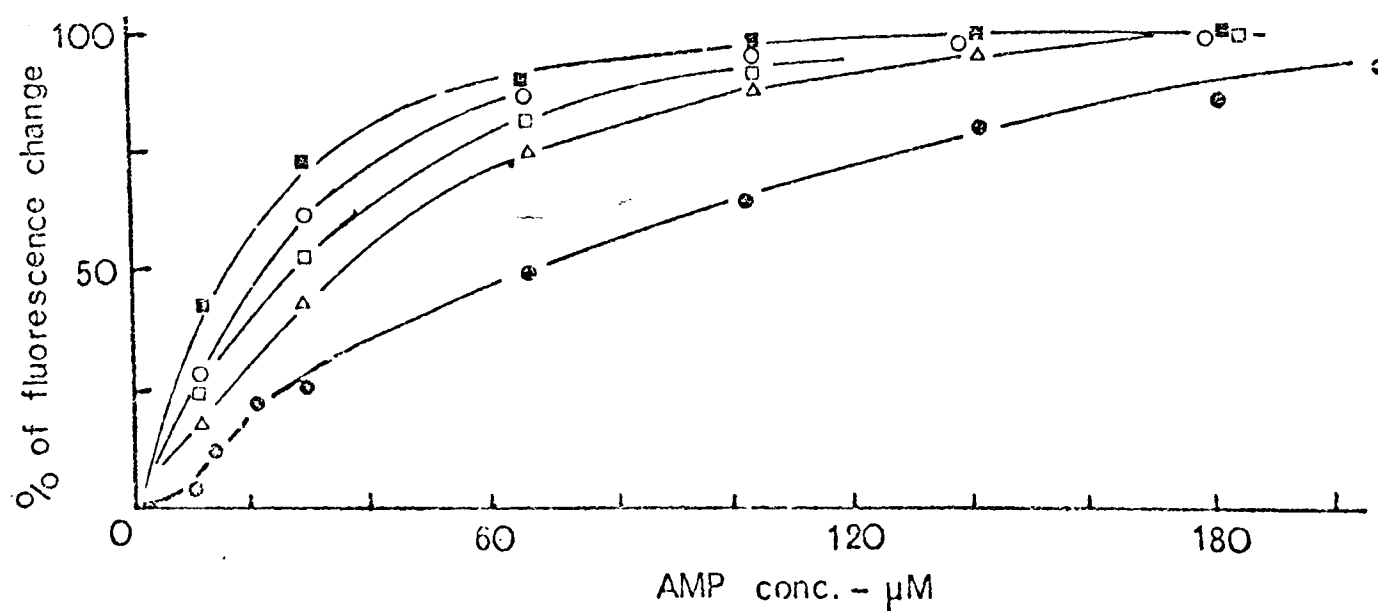


Figure 4.2 Fluorescence changes as AMP binds to acetamido-salicylate-phosphorylase b in the presence of various glucose-1-phosphate concentrations. 50 mM triethanolamine - KCl buffer pH 7.5, 1 μ M acetamido-salicylate-phosphorylase b at 18° C. Concentration of glucose-1-phosphate: 0 (●), 5 mM (Δ), 10 mM (\square), 15 mM (\circ) and 20 mM (\ominus).

20% of the fluorescence emission (excitation 320 nm; emission 400 nm) of acetamidosalicylate phosphorylase b is due to protein fluorescence. Control titrations were therefore performed using unlabelled phosphorylase to check that the fluorescence changes seen with the labelled enzyme were not due to changes in protein fluorescence.

Fig. 4.1 shows the change in 400 nm fluorescence when labelled phosphorylase b and a are titrated with AMP. While the limiting quenching is the same in both cases, the titration curves demonstrate tighter binding of AMP to the latter form of the enzyme, in agreement with earlier equilibrium dialysis experiments (130,134). The heterotropic interactions between glucose-1-phosphate and AMP are demonstrated by the fluorescence titrations shown in Fig. 4.2. One ligand tightens the binding of the other, in contrast to the interaction between glucose-6-phosphate and AMP, where glucose-6-phosphate weakens the binding of AMP (135).

2,4 Dinitrofluorobenzene modified phosphorylase has been reported not to bind AMP, but to bind sugar phosphates in the same way as the native enzyme (136). Phosphorylase desensitized in this way was prepared by a modification of the method of Baumert et al. (137). 20 mgs/ml phosphorylase b (in 50 mM triethanolamine - 100 mM KCl buffer, pH 7.5) was incubated with 10 mM 2,4 dinitrofluorobenzene for 45 minutes at room temperature. Excess reagent was removed by dialysis. After addition of 20 mM 2-mercaptoethanol the solution was warmed to 30°C for 60 minutes. After removal of 2-mercaptoethanol by dialysis the 2,4 dinitrofluorobenzene modified phosphorylase was labelled with the acetamidosalicylate group (as described above). Addition of AMP, ADP, ATP or IMP causes no change in the

fluorescence of the probe whilst the quenching by glucose-1-phosphate and glucose-6-phosphate is unaltered, as are their apparent binding constants to the enzyme. This result confirms that the AMP binding site of phosphorylase b may be blocked without affecting the sugar phosphate binding sites.

Glucose-6-phosphate weakening of AMP binding to phosphorylase b is therefore not a result of simple competition for one binding site.

Table 4.1 shows that the binding of the substrates, phosphate and glucose-1-phosphate to phosphorylase is relatively weak and that the inhibitor, glucose-6-phosphate, binds tighter than the activator, AMP. It is interesting to note that ADP, which inhibits AMP induced activation of phosphorylase b, also binds relatively tightly. Compared to phosphorylase b, phosphorylase a binds nucleotides more tightly and glucose-6-phosphate less tightly. This point will be iterated several times throughout this thesis, as the regulation of phosphorylase activity by ligands depends upon the relative amounts of nucleotides and sugar phosphates bound.

At this point, it is necessary to make several reservations about this simple use of fluorescence. The apparent dissociation constants were deduced from the concentration of ligand required to produce half of the fluorescence change.

(i) Because of the possibility of cooperative effects, multiple binding sites or multiple enzyme conformations, it is unlikely that the values obtained represent dissociation constants for simple equilibria.

(ii) With the instrumentation available at present, studies of acetamidosalicylate phosphorylase attached to glycogen could not be made.

In addition measurements had to be made at very low protein concentrations.

(iii) The exact values of limiting quenching vary from one labelled enzyme preparation to another by up to 25%. This is because small differences in the amount of label attached to phosphorylase cause variations in the relative amounts of protein and acetamidosalicylate fluorescence. However, within experimental error the apparent dissociation constants do not vary. This experimental error can be up to 20% because of the difficulties associated with the measurement of very small fluorescence changes.

Despite these reservations, the method provides a simple, quick way of monitoring enzyme-ligand interactions, and has considerable advantages over more conventional techniques.

B. The Use of Spin Labelled Phosphorylase

Similar titrations may be performed with spin labelled phosphorylase, using the changes in the ESR ratio, R , to detect ligand binding. These titrations have been undertaken by Drs. J.R. Griffiths and R.A. Dwek. Their results, which are listed in Table 4.11, are in good agreement with the results from titrations monitoring acetamidosalicylate fluorescence. There are only two major discrepancies. When detected by the fluorescent probe, the binding of inorganic phosphate to phosphorylase b and IMP to phosphorylase a appear to be much tighter than when monitored by the spin label probe. Possible explanations for these observations include the existence of multiple binding sites for these ligands in the enzyme or a non-linearity in probe response during sequential ligand binding to an oligomeric phosphorylase molecule. For example, with one probe, the spectral

Table 4.11

Dissociation constants and limiting ESR ratios of various ligands for spin labelled phosphorylase b and a complexes. (From (101))

Ligand	Phosphorylase <u>b</u>		Phosphorylase <u>a</u>	
	Apparent K_D (mM)	ESR ratio	Apparent K_D (mM)	ESR ratio
None	-	0.68	-	0.58
AMP	0.085	0.52	0.002 & 0.010	0.51
ADP	0.131	0.63	0.035	0.51
ATP	3.0	0.64	0.88	0.52
IMP	2.0	0.70	6.50	0.69
Phosphate	6.1	0.55	0.48	0.49
G-6-P	0.031	0.44	5.90	0.50
Glycerophosphate	3.6	0.58	-	0.56
UDPG	4.0	0.65	13.0	0.49

change observed when one ligand molecule binds to a dimeric phosphorylase molecule may be less than one half of that seen when two ligand molecules bind to the enzyme dimer. With the other probe, the full spectral change may occur after only one ligand molecule has bound to an enzyme dimer.

C. The probe response to ligand binding

The preceding discussion has been concerned with the affinity of binding of ligands to phosphorylase, investigated by the use of probe methods. It is now necessary to discuss the effects of these ligands on phosphorylase and the "view" these probes have of the enzyme before and after ligand binding.

It is a fundamental assumption of most theories of enzyme regulation that the interaction with the modulator ligand leads to an isomerisation (conformational change) in the protein structure. The main concern of the various theories has been to account for the observed cooperativities (positive or negative) between identical or non-identical ligands (homotropic and heterotropic cooperativity). The two most widely discussed theories formulate cooperative interactions in terms of structural changes which involve a concerted change in all subunits or a sequential change that depends on the extent of ligand occupancy of the subunits (138, 139). While these two models differ in many important features, they have one aspect in common. That is that the structural equilibria between the different states can be described by a relatively small number of well defined unique conformations of the enzyme. In many cases this type of description has succeeded in accounting for the observed thermodynamic equilibria and kinetic behaviour of

regulatory enzymes. At the same time it is possible that the "distinct" conformational models should only be considered as the best approximations one can make on the basis of available structural evidence. An alternative, but not necessarily contradictory view, considers that the multiplicity of interactions and the variety of effects that are observed for some enzymes "show that multimer proteins are unlikely to be limited to a very small number of conformations" (140). At any moment during any titration, phosphorylase may be interconverting between a large number of conformations and the ESR ratio or fluorescence intensity observed from probe molecules may be an average of many different interactions. Hence it is not possible to assign much structural meaning to the observed spectral parameters. Investigation of multiple conformations may be facilitated by the fact that different methods give an average in different time domains. The next chapter describes how NMR measurements may be exploited to give a simple demonstration of conformational multiplicity.

When a ligand binds to phosphorylase, the protein adopts a new set of conformations. The effects of ligands on the various probes which have been attached to phosphorylase are listed in Table 4.III. The changes could occur for several reasons:

(i) When phosphorylase adopts a new set of conformations, the amino acids around the probe molecule alter their conformation and changes in the spectroscopic properties of the probe are seen. For example, the difference in the ESR ratio observed for spin labelled phosphorylase b and a must be due to an effect of this kind.

Table 4.III

The effect of ligands on the various probe parameters of phosphorylase b and a
(From 79, 101 and 124)

Ligand	% Quenching of Acetamidosalicylate fluorescence	% Quenching of NBD fluorescence	ESR ratio
Phosphorylase <u>b</u>			
None	-	-	0.68
AMP	20	10	0.52
ADP	15	-	0.63
ATP	14	no effect	0.64
IMP	14	no effect	0.70
G-1-P	12	5	0.65
G-6-P	12	24	0.44
UDPG	no effect	no effect	0.65
Glucose	no effect	no effect	0.68
Glycogen	-	-	0.65
Glycerophosphate	14	-	0.58
Phosphate	14	-	0.55
Phosphorylase <u>a</u>			
None	-	-	0.58
AMP	21	-	0.51
G-1-P	-	-	0.58

(ii) The ligand could interact directly with the motion of the probe, causing spectral changes. Whilst there is no proof that this does not take place, there are several reasons for supposing that it is unlikely. It is difficult to see how the binding site for so many ligands could be close to, say, the acetamidosalicylate group. It is unlikely that the spectral changes seen with the spin labelled enzyme are due to direct interaction of ligands with the probe because IMP, which binds to the same site on the protein as AMP, causes very little change in the ESR spectrum.

(iii) The spectral changes could be the result of aggregation changes following ligand binding. As aggregation changes are slow and spectral changes occur instantaneously, this can be discounted (31). In addition, glucose, which reverses all aggregation changes, does not alter the effects of ligands on the ESR and fluorescent label spectral parameters.

Two attempts have been made to prove whether changes in label spectral parameters reflect conformational changes or the actual presence of ligand. In both cases an experiment was designed to attempt to observe a change in the spectral readout of a label attached to a subunit to which no perturbing ligand was bound.

D. Do probe molecules report conformational changes or direct interaction with ligands?

(i) Using a labelled subunit with the AMP binding site blocked

The probe acetamidosalicylate was attached to phosphorylase b in which the AMP binding site had been blocked by 2,4 dinitro fluorobenzene (FDNB). Subunits of this species were then

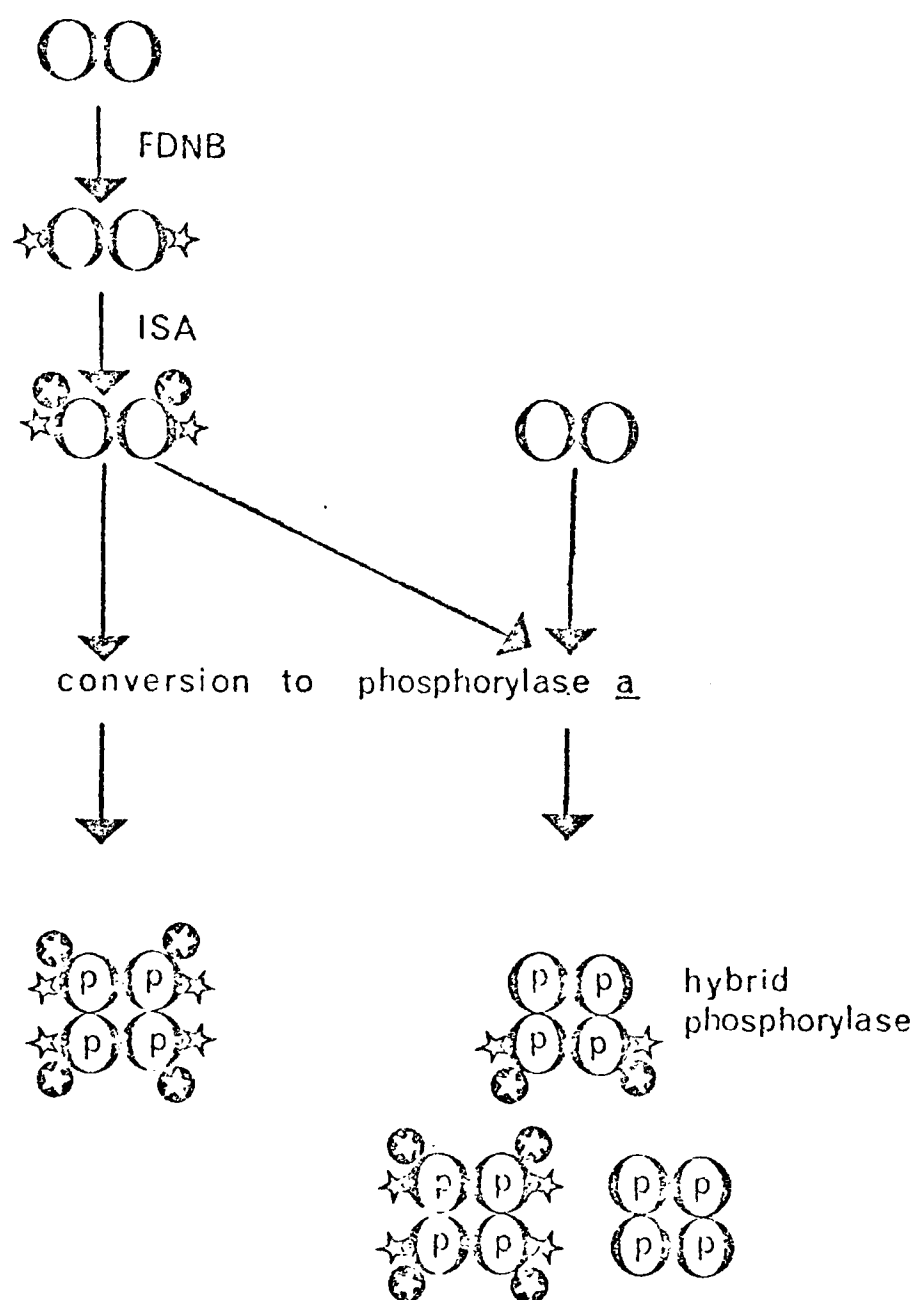


Figure 4.3

The preparation of hybrid labelled phosphorylase a

O represents a phosphorylase b subunit and ⊙ represents a phosphorylase a subunit. ☆ represents an FDNB blocked AMP binding site in phosphorylase b and ⊙ with a star represents an SA probe molecule. The figure is described in the text.

Table 4.IV

Species	activity (% of maximum possible)	is SA fluorescence quenched by AMP?
FDNB modified SA ppb	inactive	no
FDNB modified SA ppa	90% activity stimulated 30% by AMP	yes
FDNB modified ppb mixed with unlabelled ppb and converted to a form	90% activity stimulated 30% by AMP	yes

hybridised with native phosphorylase which contained no label and an AMP binding site. The hybridisation was performed by conversion of a mixture of FDNB blocked SA phosphorylase b and unmodified phosphorylase b to the a form. After phosphorylation, it was hoped that "mixed" tetramers would be formed (see Fig. 4.3). In these mixed tetramers, the probe acetamidosalicylate would only be attached to subunits whose AMP binding site was blocked. Hence, any AMP induced change in acetamidosalicylate fluorescence would be indicative of a conformational change transmitted to the probe via the subunit interface as AMP bound to a neighbouring unmodified subunit.

Unfortunately, it was impossible to reach any such conclusions from the result. This was because a product whose 400 nm fluorescence was quenched by AMP was obtained when FDNB blocked SA phosphorylase b was converted to the a form, in the absence of unmodified phosphorylase. Conversion of FDNB blocked SA phosphorylase b to a appears to generate an AMP binding site which is "seen" by the fluorescent probe (see Table 4.IV).

(ii) How many subunits can one ligand molecule influence?

AMP binding to phosphorylase a is very tight. Hence, if a high concentration of, say, spin labelled tetrameric phosphorylase a is titrated with AMP, at the beginning of the titration, most of the AMP will be enzyme bound. During the titration the ESR ratio changes from R_0 to R_∞ . At any point in the titration, when the ratio observed is R , the proportion of enzyme subunits "influenced" by AMP is $R - R_\infty / R_0 - R_\infty$. Hence the concentration of subunits "affected" by AMP can be calculated.

The ratio, $n = \frac{\text{the concentration of subunits affected by AMP}}{\text{the concentration of AMP added}}$,

will be a measure of the MINIMUM NUMBER OF PHOSPHORYLASE SUBUNITS WHOSE CONFORMATION IS ALTERED BY ONE AMP MOLECULE.

n will equal the number of subunits affected by one AMP molecule only if three conditions are fulfilled:

- a) all the AMP is bound
- b) no tetramer has more than one AMP molecule bound
- c) the ESR ratio (R_S) shown by a subunit whose conformation is altered by an AMP molecule bound to a neighbouring subunit, is equal to the ESR ratio shown by a subunit which has an AMP molecule bound to it (R_∞).

Even at the beginning of the titration, conditions (a) and (b) will not be wholly fulfilled. Any deviation from these conditions will cause n to fall below the actual number of subunits affected by the binding of one AMP molecule. Hence n is the MINIMUM number of subunits whose conformation is altered by one AMP molecule.

During titrations of AMP into spin labelled phosphorylase α , as the concentration of AMP increases, n decreases. It is useful therefore to define n_0 as the value of n extrapolated to zero AMP concentration. Measurements of n and n_0 can be exploited in two different ways.

- 1) As n_0 can never be greater than the number of subunits in the protein, it is a measure of the lowest possible number of subunits in the enzyme oligomer.

- 2) If the value of n or n_0 is greater than 1, the spin label must be detecting conformational changes which occur in a subunit due to the presence of an AMP in another subunit of the oligomer.

Table 4.V

Results of a typical titration of AMP into spin labelled phosphorylase a

ppa concentration (μ M)	AMP concentration (μ M)	R	n
58.7	0	0.694	-
57.7	3.9	0.652	3.05
56.8	7.7	0.628	2.39
55.9	11.4	0.608	2.07
55.0	16.9	0.577	1.87
54.15	22.3	0.549	1.76
53.3	52.0	0.530	0.82
52.5	198	0.502	0.22
51.8	975	0.500	0.05
51.0	1740	0.490	0.03

Data from a titration of AMP into spin labelled phosphorylase a are shown in Table 4.V. They indicate that one AMP molecule can affect at least 3.05 phosphorylase subunits. This must mean that the spin label can detect a conformational change in a subunit where AMP is not bound.

E. How many subunits interact in phosphorylase a?

The opening chapter expounded some of the unknowns concerning the aggregation state of phosphorylase. Whilst it is known that glucose disaggregates tetrameric phosphorylase a to dimers, the state of aggregation of phosphorylase a when bound to glycogen is uncertain. Clearly, the experimental approach outlined in the previous section offers the possibility of investigating this problem. A determination of n_o under different conditions was, therefore, made in order to derive information about the state of aggregation of phosphorylase a.

Spin-labelled phosphorylase a, prepared in an oxygen-free environment, was titrated with AMP in different media. In Fig. 4.4 values of n_o , calculated from the titration data, are plotted against the concentration of AMP added. In triethanolamine buffer the value for n_o is greater than 2.5, which is consistent with phosphorylase a being a tetramer. In the presence of glucose, phosphorylase a dissociates into dimers (29,30) and under these conditions a value of n_o less than 2 is found, confirming that the parameter n_o is lower than the actual number of interacting subunits in the oligomer. When phosphorylase a is in the presence of glycogen, under the conditions of the experiment, more than 95% of the protein is bound to the glycogen. From the titration data, in this case, n_o is between 3 and 4. This indicates that

when phosphorylase α is bound to glycogen more than 3 subunits can interact together and that the enzyme is unlikely to be a dimer.

Fig. 4.5 shows ultracentrifugation data from spin-labelled phosphorylase α prepared in nitrogen or air saturated buffers. Enzyme prepared in nitrogen saturated buffers exists predominantly in tetrameric form (Fig. 4.5c) and only a very small amount of higher aggregates. This enzyme can be wholly dissociated into dimers with glucose.

In the case of enzyme prepared in the air, besides the tetrameric form, higher aggregates are present (Fig. 4.5a). Neither the tetramer nor these higher aggregates can be dissociated with glucose. In the presence of β mercaptoethanol the higher aggregates disappear and only the tetramer is observed (Fig. 4.5b). This result shows that the remaining free sulphhydryl groups in spin-labelled phosphorylase α oxidize in the air, giving disulphide bridges between subunits. As a result, higher oligomers as well as tetramers, are present. Glucose has no effect on the aggregation state of phosphorylase α when the subunits are covalently linked together. β -mercaptoethanol reduces the disulphide bonds between the subunits, removing the higher aggregates of the enzyme and leaving the tetrameric form. When the spin-labelled enzyme is prepared in nitrogen-saturated oxygen-free buffers, the normal tetrameric form of phosphorylase α is obtained as the sulphhydryl groups do not oxidize.

Fig. 4.6 shows values of n as AMP is titrated into spin-labelled phosphorylase α prepared in air-saturated buffers. The value of n_0 is higher than 2.5 in triethanolamine buffer and in the presence of glucose and glycogen. This result shows that glucose does not cause dimers to form, in agreement

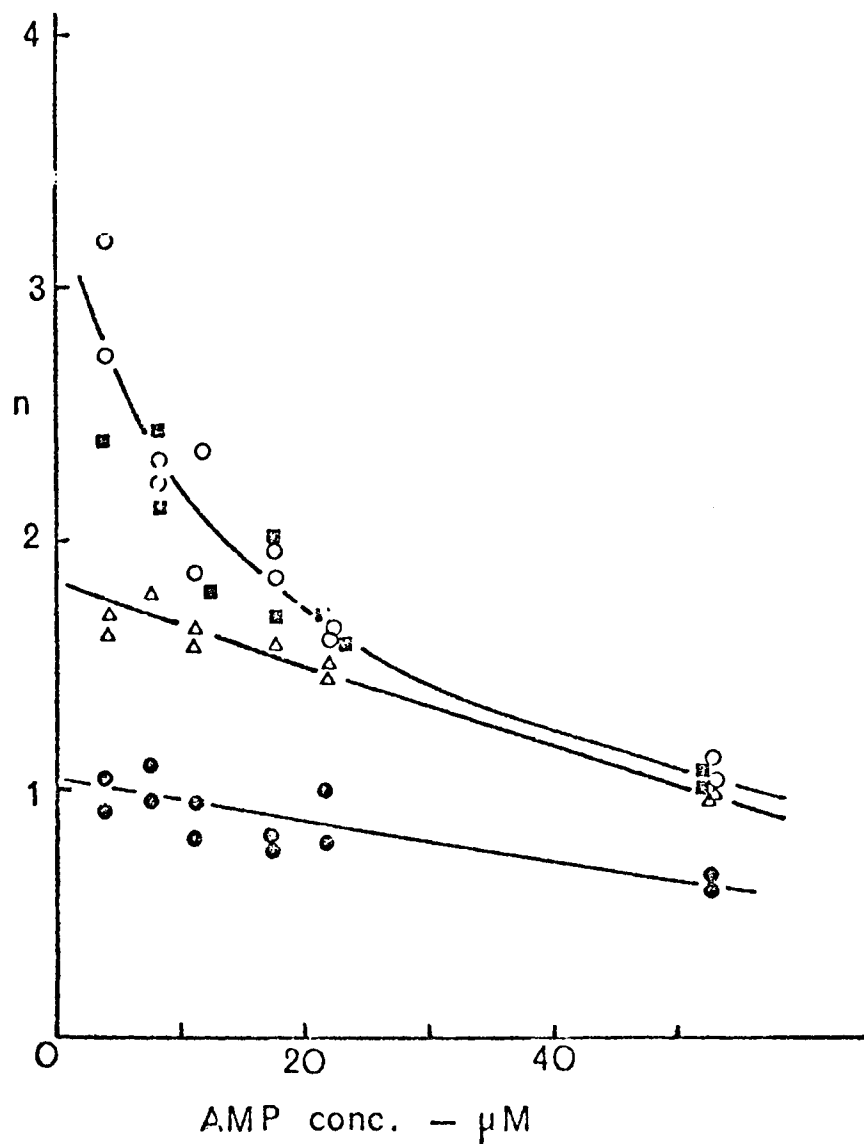
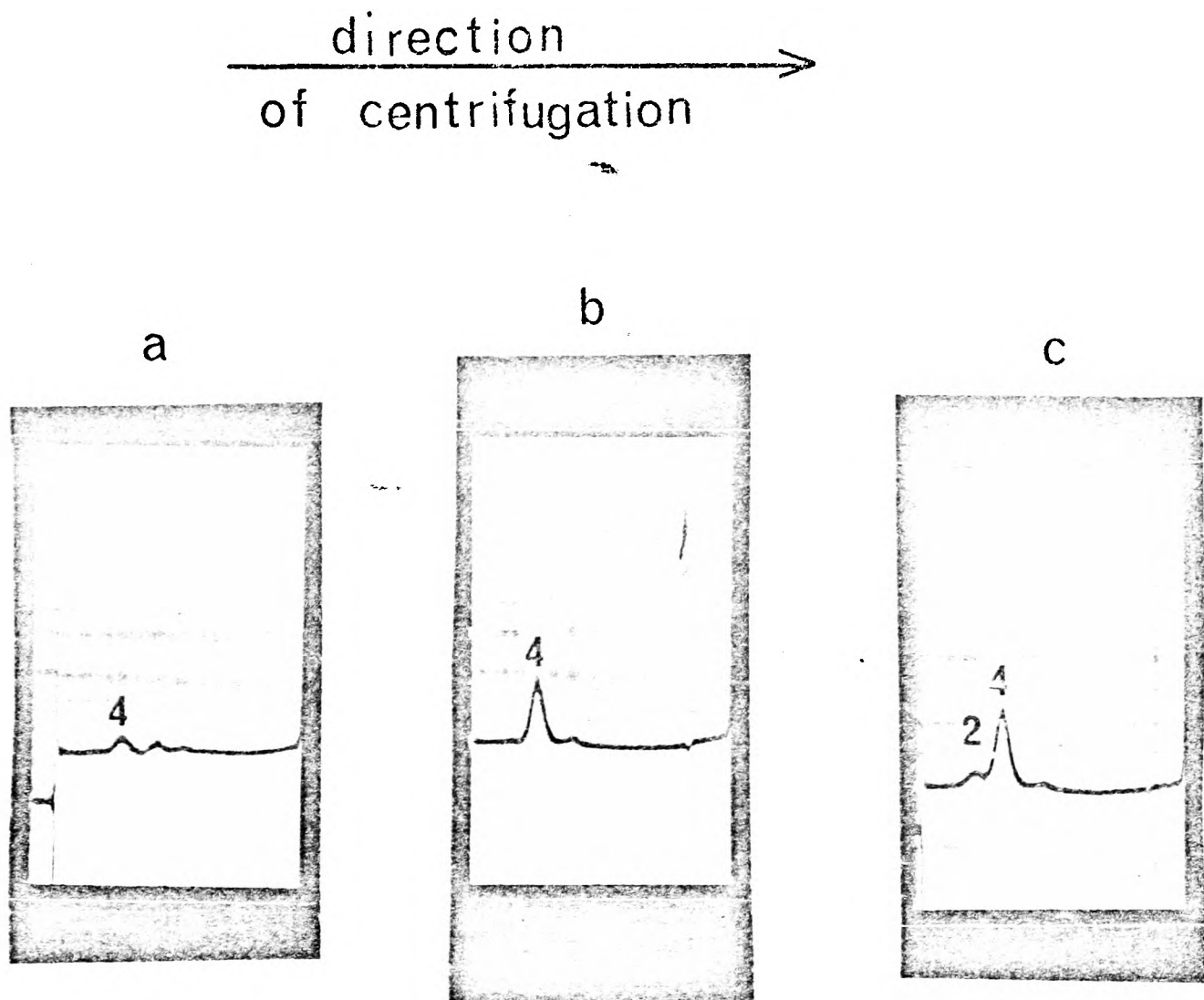


Figure 4.4

Variation of n with AMP concentration

AMP was titrated into $68 \mu\text{M}$ spin labelled phosphorylase α , prepared in the presence of nitrogen saturated buffers, in 50 mM TEA, 100 mM KCl, 1 mM EDTA, pH 7.5 (■) or the same buffer system containing 2% glycogen (o) or 100 mM glucose (Δ). The other buffer system used was 0.4 M imidazole adjusted to pH 6.4 with citric acid (●).

Throughout the titration, the ESR ratio was recorded, and n was deduced as described in the text.



2 marks the dimeric species , $S = 9$.
4 marks the tetrameric species , $S = 13$.

Figure 4.5 Ultracentrifugation traces of spin labelled phosphorylase a
50 μ M enzyme in triethanolamine (50 mM), KCl (100 mM), EDTA (1 mM) was centrifuged in a Beckman Model E Ultracentrifuge at 56000 r.p.m. at 20°. Photographs were taken using Schlieren optics 20 minutes after the plateau speed was reached. (a) spin labelled phosphorylase a prepared in air saturated buffers, (b) spin labelled phosphorylase a prepared in air saturated buffers; 5 mM mercaptoethanol was present during the centrifugation, (c) spin labelled phosphorylase a prepared in nitrogen saturated buffers.

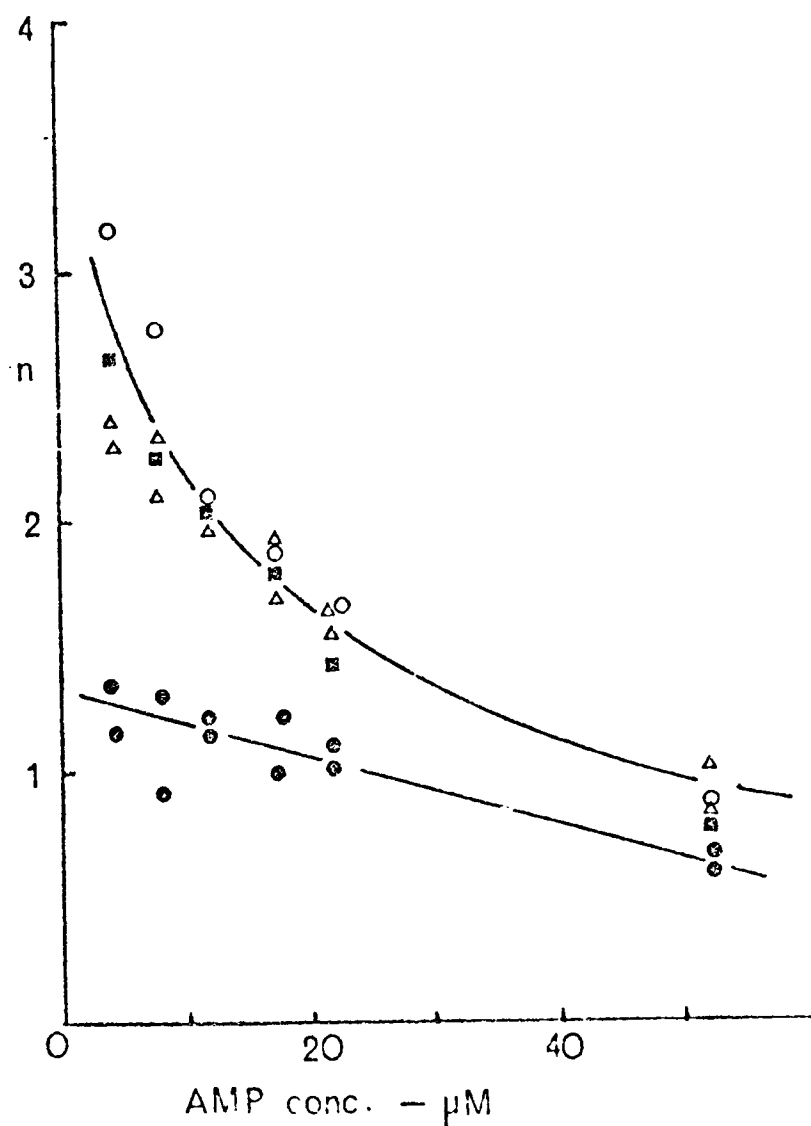


Figure 4.6

Variation of n^- with AMP concentration

AMP was titrated into $59 \mu\text{M}$ spin labelled phosphorylase α , prepared in the presence of air saturated buffers, in 50 mM TEA, 100 mM KCl, 1 mM EDTA pH 7.5 (■), or the same buffer system containing 2% glycogen (o) or 100 mM glucose (Δ). The other buffer system used was 0.4 M imidazole, adjusted to pH 6.4 with citric acid. (●)

with the ultracentrifugation data. An interesting point to note is that, although the interactions between the subunits in the enzyme prepared under nitrogen and in the air are different, the curves in Figs. 4.4 and 4.6 are quite similar, suggesting that the disulphide bridges between the subunits in the enzyme prepared in the air do not alter the cooperativity to a great extent. These titrations, could not be performed in the presence of β mercaptoethanol as sulphhydryl protecting reagents reduce the spin label.

The titrations of spin-labelled phosphorylase α , prepared under nitrogen and in the air, were also carried out in the presence of imidazole citrate buffer. The results, given in Figs. 4.4 and 4.6, show that the value of n_o is around 1. At this high enzyme concentration the presence of imidazole citrate does not monomerise phosphorylase. However the value for n_o of 1 indicates that imidazole destroys the cooperative interactions between the subunits.

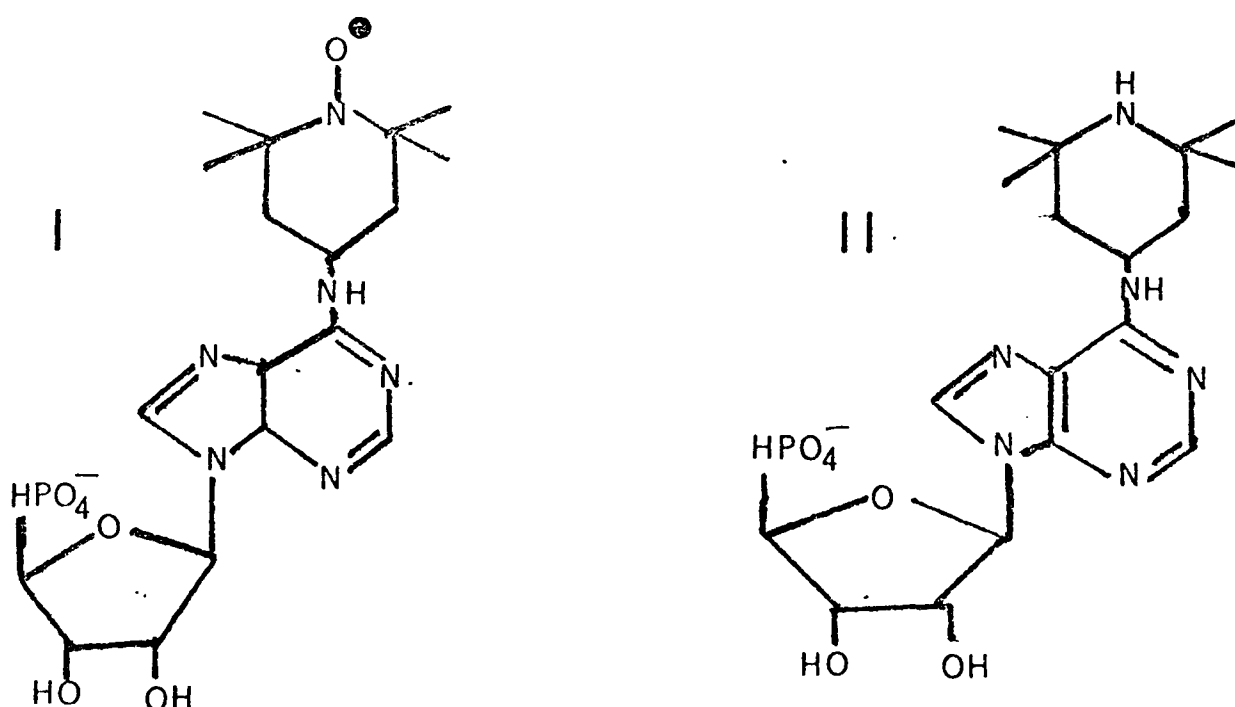
The conclusions from this series of experiments are:

- (i) in glycogen-bound phosphorylase α at least 3 subunits can interact with one another, exactly as in the absence of glycogen. The results indicate that higher aggregates than dimers are possible in glycogen-bound phosphorylase α .
- (ii) the cooperative interaction between the subunits that is detected by the spin label probe is diminished by imidazole citrate.
- (iii) when spin labelled phosphorylase α is exposed to air, the sulphhydryl groups oxidise and higher aggregates are formed, due to the formation of disulphide bonds between subunits, but the cooperativity of the system is largely unaltered.

F. Spin labelled AMP - an activator of phosphorylase

A logical way to extend these studies is to use effector or substrate derivatives which are either fluorescent or spin labelled. In principle, the spectroscopic parameters observed could be used to provide information about the nature of the ligand binding sites or to detect conformational changes at these sites resulting from the binding of other ligands to the enzyme (77, 141). In addition, using electronic energy transfer or spin-spin interactions it should be possible to triangulate the ligand binding sites from the other sites on the protein (142). One problem is that the introduction of bulky spin labelled or fluorescent groups on to a ligand may grossly weaken binding of the modified nucleotide to phosphorylase or prevent the activity-linked conformational changes from taking place.

This section introduces a spin labelled AMP derivative [N^6 -(2,2,6,6-tetramethylpiperidin-4-yl-1-oxyl) adenosine 5' monophosphate] (I) and its diamagnetic analogue (II) and presents an analysis of their interaction with phosphorylase.



The effects of these derivatives are compared to the effects of AMP and IMP, which activate phosphorylase in different ways. AMP activates phosphorylase b and tightens the binding of the substrate glucose-1-phosphate (97). It also stimulates phosphorylase a activity by 30%. In contrast IMP, whilst not stimulating phosphorylase a, activates phosphorylase b. However, IMP binds to phosphorylase b an order of magnitude weaker than AMP, activates to only 60% of the AMP induced activity, and does not tighten glucose-1-phosphate binding (97). Many other nucleotide analogues act like IMP rather than AMP (143).

Fig. 4.7 shows the increase in phosphorylase b activity as the concentration of the spin labelled AMP derivative is raised. Data are given for assays at 16 mM and 100 mM glucose-1-phosphate and activity is expressed as a percentage of the maximum activity observed with AMP present. It is evident that at both glucose-1-phosphate concentrations the spin labelled AMP derivative activates phosphorylase to only 60% of the maximum AMP induced activity. The figure also shows that the activity induced by IMP is 60% of the activation by AMP. With IMP, however, 60% activation only occurs at 100 mM glucose-1-phosphate, whereas with the spin labelled AMP analogue 60% activation occurs at both 16 mM and 100 mM glucose-1-phosphate. From the curve it is evident that the concentration of the spin labelled AMP derivative required for $\frac{1}{2}$ maximum activation is $150 \pm 20 \mu\text{M}$ at 16 mM glucose-1-phosphate and $60 \pm 20 \mu\text{M}$ at 100 mM glucose-1-phosphate.

Fig. 4.7 also shows the increase in phosphorylase b activity as the concentration of the diamagnetic analogue of the spin labelled AMP derivative is raised. Within experimental error, activation by the diamagnetic analogue

is identical to activation by spin labelled AMP.

Similar experiments were performed with phosphorylase a. Neither spin labelled AMP nor the diamagnetic analogue cause any stimulation of phosphorylase a activity. Again, this is similar to IMP; whilst AMP stimulates phosphorylase activity by 30%, IMP causes no stimulation.

Fig. 4.8 shows the ESR spectrum of the spin labelled AMP derivative in the presence of phosphorylase a. The sharp triplet ESR spectrum arises from free labelled AMP, while the broad component is from the spin label bound to the enzyme. The distance of the outermost peaks in this spectral component is about 56 Gauss, indicating that the bound spin labelled AMP is almost completely immobilised (84). The same ESR spectrum is found for spin labelled AMP in the presence of excess phosphorylase b.

When AMP or IMP is added to solutions containing phosphorylase and spin labelled AMP the broad ESR signal disappears, while the sharp spectrum increases in intensity, suggesting that spin labelled AMP competes at the nucleotide binding site on the enzyme.

Fig. 4.9 gives the titration data as phosphorylase b or a is added to spin labelled AMP. The parameter f in Fig. 4.9 is defined by:

$$f = \frac{hV}{h_0V_0}, \quad (1)$$

where h is the height of the centre line of the ESR spectrum of spin labelled AMP and V the sample volume. h_0 and V_0 are the height and volume before any enzyme is added. f may be interpreted as the fraction of free spin labelled AMP.

In Fig. 4.9 there is a regular decrease of f with increasing amounts of enzyme, showing the binding of spin labelled AMP to the enzyme. Since

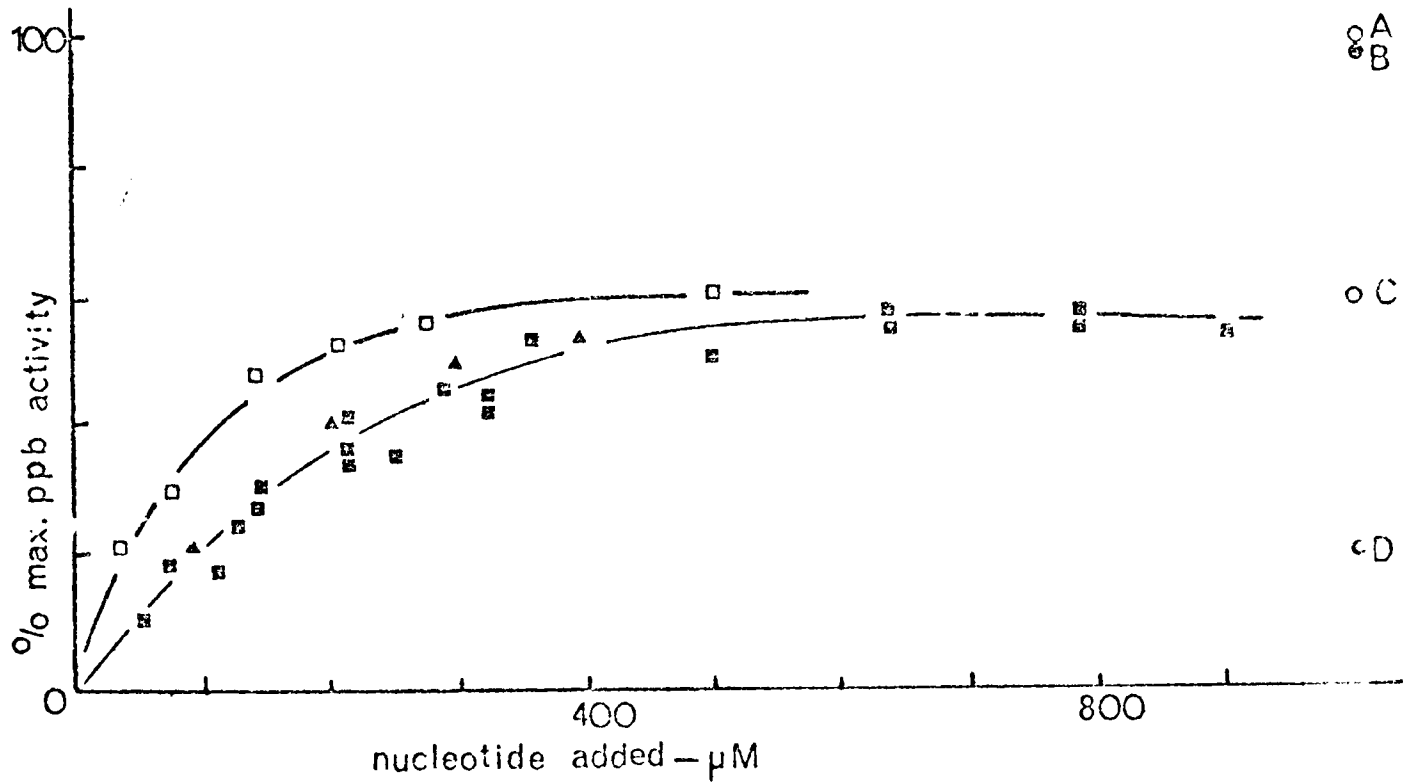


Figure 4.7

Nucleotide activation of phosphorylase b activity

Phosphorylase b activity is measured at varying concentrations of the spin labelled AMP derivative (\square, \blacksquare) or the diamagnetic analogue (\triangle) at 16 mM (\blacksquare, \triangle) or 100 mM (\square) glucose-1-phosphate concentration. Activity is expressed as a % of the maximum AMP stimulated activity. Points A and B represent phosphorylase b activity at 2 mM AMP concentration and points C and D represent phosphorylase activity at 15 mM IMP assayed at 16 mM glucose-1-phosphate (B and D) and 100 mM glucose-1-phosphate (A and C). Assays performed at 20°C.

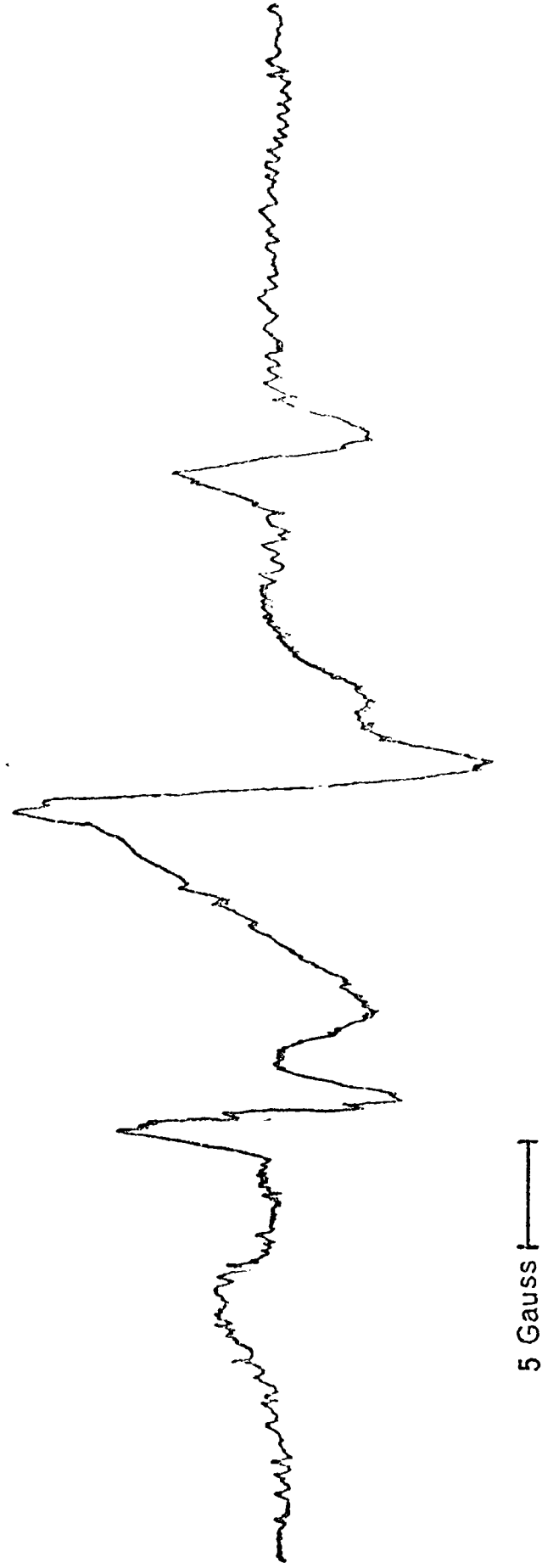


Figure 4.8 ESR spectrum of bound and free spin labelled AMP

The ESR spectrum of 17 μ M spin labelled AMP derivative in the presence of 131 μ M phosphorylase α in triethanolamine - KCl buffer pH 7.0.

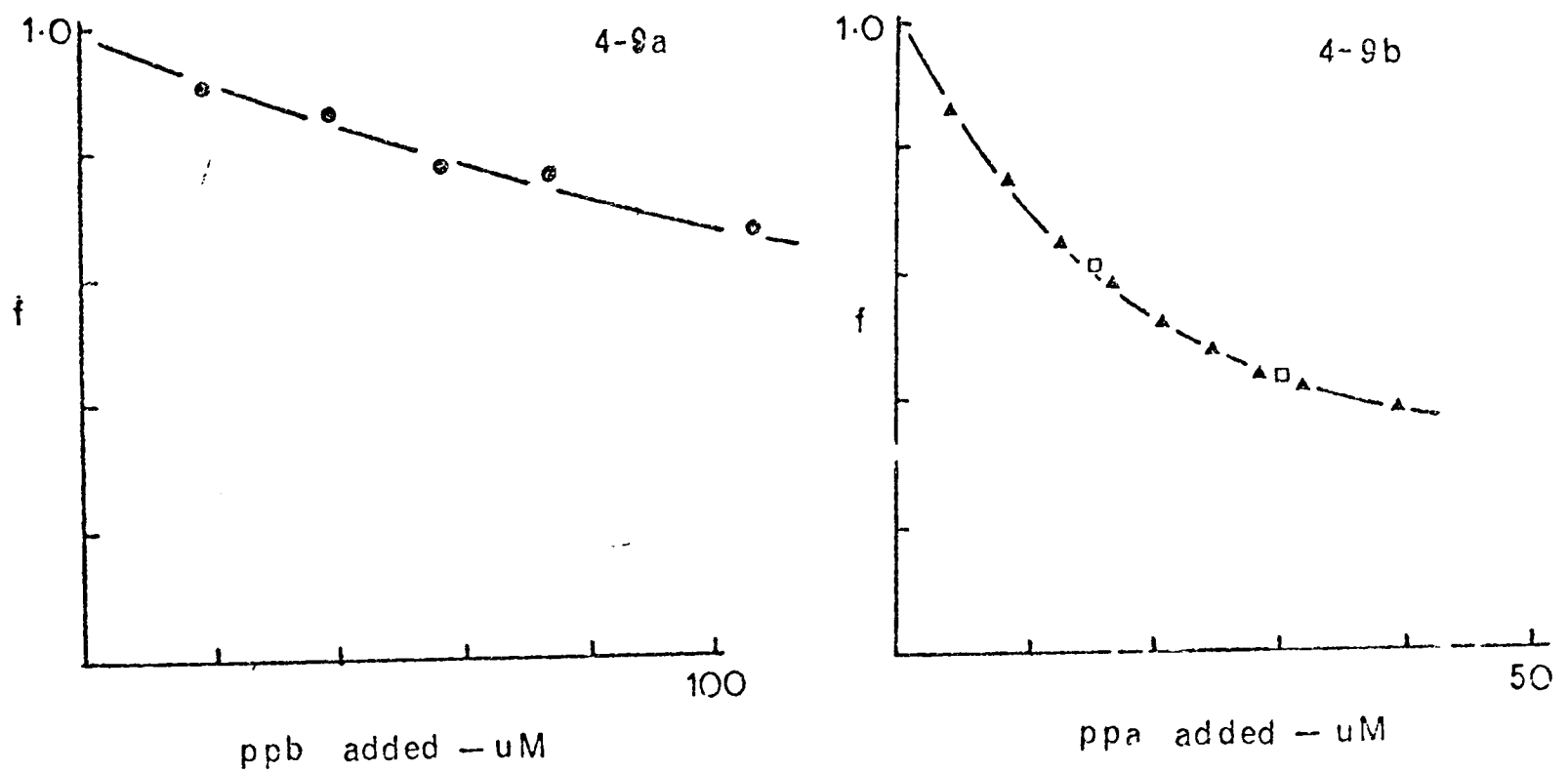


Figure 4.9

Decrease in free spin labelled AMP concentration as phosphorylase is added

f (the fraction of the free spin labelled AMP derivative) is shown at increasing concentrations of phosphorylase b (●), phosphorylase a (▲), and reduced spin labelled phosphorylase a (□). The spin labelled AMP derivative concentration was $100 \mu\text{M}$ in Fig. 4.9a and $20 \mu\text{M}$ in Fig. 4.9b. f was calculated as described in the text. Triethanolamine - KCl buffer pH 7.0 was used.

the curve in Fig. 4.9b is much steeper than the curve in Fig. 4.9a, it is evident that the binding of spin labelled AMP to phosphorylase a is tighter than the binding of the spin label to phosphorylase b.

The dissociation constant K_D can be calculated from the titration data by assuming that each enzyme subunit binds a single molecule of ligand and that there is no interaction between the sites, giving

$$K_D = \frac{f}{1-f} E_t - fS_t \quad (2)$$

E_t is the total enzyme concentration and S_t the total ligand concentration. Note that Eqn. (2) only gives good values for K_D as long as the intensity of the ESR spectrum of bound spin labelled AMP is negligible compared with the intensity of the spectrum of the free spin label. The dissociation constants with spin labelled AMP are $175 \pm 25 \mu\text{M}$ for phosphorylase b and $15 \pm 5 \mu\text{M}$ for phosphorylase a.

When AMP or IMP are titrated into acetamidosalicylate phosphorylase b or a, quenching of acetamidosalicylate fluorescence occurs.

Table 4.VI shows the apparent dissociation constants of the spin labelled AMP derivative and phosphorylase b and a as calculated from measurements using the ESR spectra of the spin labelled analogue or the fluorescence of acetamidosalicylate covalently attached to phosphorylase. They are compared to the literature values for AMP and IMP.

The ESR spectrum from a spin label covalently attached to phosphorylase gives information about the conformation of the enzyme (144). The spectrum is characterised by the ratio, R , described in Chapter 2. Table 4.VII shows the value R for spin labelled phosphorylase b and a in the presence of AMP,

Table 4.VI

Dissociation constants for phosphorylase and nucleotides

	Phosphorylase <u>b</u>	Phosphorylase <u>a</u>
Spin labelled	175 \pm 25 μ M *	15 \pm 5 μ M *
AMP derivative	150 \pm 20 μ M ⁺	15 \pm 5 μ M ⁺
AMP	70 μ M (79) 85 μ M (88)	10 μ M (79) 2 and 10 μ M (144)
IMP	5 mM (79) 2 mM (88)	6.5 mM (88)

* value deduced using ESR signal from spin labelled AMP derivative

+ value from measurements of the fluorescence of acetamidosalicylate phosphorylase

Table 4.VII

ESR ratios shown by spin labelled phosphorylase in the presence of saturating quantities of nucleotides (From (148))

Ratio shown by:	Spin labelled phosphorylase <u>b</u>	Spin labelled phosphorylase <u>a</u>
No nucleotide	0.66	0.62
With diamagnetic analogue of spin labelled AMP derivative (900 μ M)	0.66	0.67
With AMP (1 mM)	0.52	0.51
With IMP (15 mM)	0.66	0.68

Values shown are subject to an error of ± 0.01

IMP or the diamagnetic analogue of the spin labelled AMP derivative. The changes induced in the ESR spectrum by the analogue are similar to those induced by IMP.

From this series of experiments several conclusions may be reached.

The spin labelled AMP derivative binds tightly to phosphorylase b and a. Dissociation constants deduced by observing changes in the ESR spectrum of spin labelled AMP agree with the constants obtained by monitoring the changes in acetamidosalicylate fluorescence when spin labelled AMP is titrated into acetamidosalicylate phosphorylase. Similar binding constants and activation patterns were observed when spin labelled AMP was replaced by the diamagnetic analogue. This indicates that the nitroxide part of the spin labelled derivative is not crucially important in the binding of the derivative to phosphorylase or in the ensuing conformational changes. Moreover binding causes conformational changes in phosphorylase. The affinity of binding of the derivative to phosphorylase is similar to that of AMP and stronger than that of IMP. According to the probes used, the conformations induced in the enzyme by spin labelled AMP are similar to those induced by IMP. Attachment of the bulky spin label group to the adenine nucleotide clearly alters its interaction with phosphorylase but does not invalidate its use as a nucleotide analogue.

G. The interaction of ligands with modified phosphorylase

The ability to specifically block any particular ligand binding site on a large allosteric enzyme provides a useful tool in the study of that enzyme. Although, the literature contains numerous descriptions of chemical

modifications which alter the overall allosteric properties of phosphorylase, FDNB is the only reagent which has been reported to affect just one allosteric site.

In a search for modifications which specifically block other ligand binding sites, the interaction of effectors and substrates with phosphorylase, which had been modified with 5-diazo-1H-tetrazole (DHT) was studied. The incorporation of approximately 1 mole of this reagent per mole of enzyme subunits gives complete inactivation as a result of modification of a specific carboxyl group (145,146). Ligand binding to the modified enzyme was investigated using the ESR and fluorescence techniques outlined above, with DHT modified phosphorylase characterised and provided by Dr. O. Avramovic-Zikic.

The acetamidosalicylate group was introduced by incubation of DHT phosphorylase with one equivalent of iodoacetamidosalicylic acid. The acetamido-salicylate fluorescence is quenched by AMP, IMP, glucose-6-phosphate and glucose-1-phosphate. The apparent K_D values are collected in Table 4.VIII and are compared with the results obtained previously for active phosphorylase b. Comparison of the apparent K_D values for active and DHT-modified phosphorylase b shows that the only significant difference is in the binding of glucose-1-phosphate. This is seen both by the change in K_D and by the decrease in the effectiveness of glucose-1-phosphate in tightening AMP binding.

The ESR spectrum of spin-labelled DHT-phosphorylase b is very similar to that of the native enzyme and addition of AMP causes a similar immobilization of the spin label to that shown for the active enzyme. The

Table 4.VIII

Apparent dissociation constants of various ligands for DHT modified phosphorylase b determined by the quenching of salicylate fluorescence of the labelled protein (From (149))

Ligand	app mM	app mM
AMP	0.070 ± 0.010	0.083 ± 0.007
AMP + 23 mM Glucose-1-phosphate	0.010 ± 0.003	0.019 ± 0.006
Glucose-6-phosphate	0.040 ± 0.010	0.050 ± 0.010
Glucose-1-phosphate	10 ± 2	> 20

Table 4.IX

Comparison of "apparent dissociation constants" for native phosphorylase b and catalytically inactive modified phosphorylase b derived from spin label analysis (From (149))

Ligand	SPIN LABELLED PPB K app mM	SPIN LABELLED DHT PPB K app mM
AMP	0.085 ± 0.004	0.085 ± 0.012
AMP + Glucose-1-Phosphate (37 mM)	0.0095 ± 0.0014	0.0149 ± 0.006
AMP + Glycogen (1.7%)	0.023 ± 0.002	0.049 ± 0.008
Pi	6.1 ± 0.4	4.2 ± 0.8

apparent dissociation constants derived from ESR measurements are collected in Table 4.IX. These results show that, in agreement with the fluorescence measurements, AMP binding and the AMP induced conformational change are unaffected by the modification of phosphorylase b with DHT. At the same time the heterotropic cooperativity between AMP and glucose-1-phosphate and AMP and glycogen is diminished in the modified enzyme. This is evidenced by the smaller effect of these two substrates in tightening AMP binding in the DHT-enzyme than for native phosphorylase b.

Direct evidence for the decrease in the affinity of phosphorylase b towards glycogen as a result of DHT-modification is given in Fig. 4.10. The binding of glycogen to phosphorylase b can be followed by the large increase in light scattering when enzyme and glycogen are mixed (147). This increase is practically abolished in the DHT-modified enzyme.

Modification of phosphorylase b by DHT (in approximately 1 group per enzyme subunit) does not interfere with the binding of the activators AMP and IMP and of the inhibitor glucose-6-phosphate nor does it alter the resulting conformational changes as defined by the ESR spectrum of the spin label. Modification does, however, influence the binding of the substrates to different extents. There is a decrease in glucose-1-phosphate binding and a considerable effect on glycogen binding. Presumably as a consequence of this, the heterotropic effect of the latter two substrates on AMP binding is also diminished.

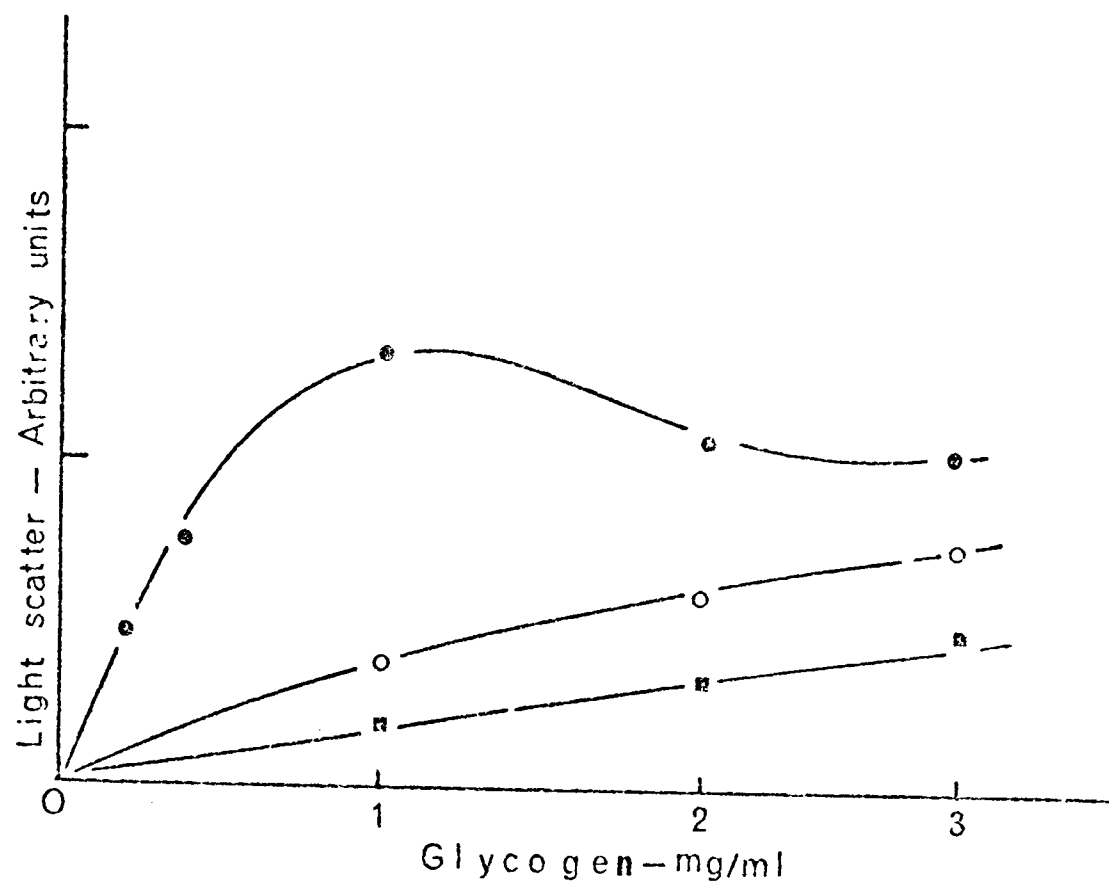


Figure 4.10 Effect of glycogen on light scattering in the presence of $10 \mu\text{M}$ phosphorylase b (● - ●), $10 \mu\text{M}$ DIT-phosphorylase b (○ - ○) or in buffer alone (□ - □). Buffer consisted of 50 mM^- triethanolamine-HCl KCl (100 mM) and EDTA (2 mM) at pH 7.5. Light scattering measurements were made on a Hitachi spectrofluorometer - the excitation and emission wavelengths were set at 500 nm.

Chapter 5PHOSPHORUS NMR STUDIES OF PHOSPHORYLASE

The study of enzyme conformation, by the use of covalently attached spectroscopic probes, raises an interesting problem. Obviously, it is necessary to attach the probe at a position where it does not interfere with the properties of the enzyme. However, it is also desirable that the probe be positioned so that it can detect changes which are vital to the function of the enzyme. The studies in the previous chapter assumed that, because probe parameters may be altered by very small perturbations, important conformational changes in the enzyme could be detected, whilst the consequences of these changes remained unaffected. An approach, which does not rely on these assumptions utilises the intrinsic spectral properties of phosphorylase. The pyridoxal phosphate cofactor is an ideal target for such an approach. One cofactor molecule is specifically attached to one lysine residue per phosphorylase subunit and it contains the only phosphorus atom in phosphorylase b. As it has been found in all glycogen phosphorylases studied to date, it, presumably, has an important role in the enzyme.

This chapter described the use of high sensitivity phosphorus NMR spectroscopy to observe both the state of pyridoxal phosphate in phosphorylase b and a and the response of the cofactor to enzyme-ligand interactions.

A. Model Studies

Fig. 5.1 shows ^{31}P NMR spectra of a solution of pyridoxal 5' phosphate recorded at different pH values. A single resonance is observed which, as the pH increases, moves to higher frequency. This pH induced shift is a result of interconversion between the mono- and dianionic forms of the phosphate group (93). The resonance of the dianionic form of pyridoxal phosphate occurs 120 Hz from the resonance of the monoanionic form.

At pH values where significant quantities of both forms exist, a single resonance is observed, with a line position intermediate between the positions found for the mono- and di-anionic forms. A single line is observed because the fast exchange condition applies (see Chapter 2) i.e. the rate of interconversion of the two species is \gg the frequency separation of the resonances from the two species. The position of the resonance is an indication of the relative amount of the two forms present. Hence pK values can be deduced from such titrations.

If the two forms of pyridoxal phosphate could not interconvert, two lines would be observed at positions corresponding to the frequencies of the mono-anionic and di-anionic species. If the rate of interconversion was \approx the frequency separation of the resonances from the two forms, a complex line shape would be produced (see Fig. 2.4).

In Fig. 5.2, the data from Fig. 5.1 are presented graphically, together with data from similar pH titrations of serine phosphate, pyridoxal phosphate conjugated to ethanolamine, glucose-6-phosphate and AMP. As these molecules all contain phosphate esterified to a methylene group their resonance frequencies are similar.

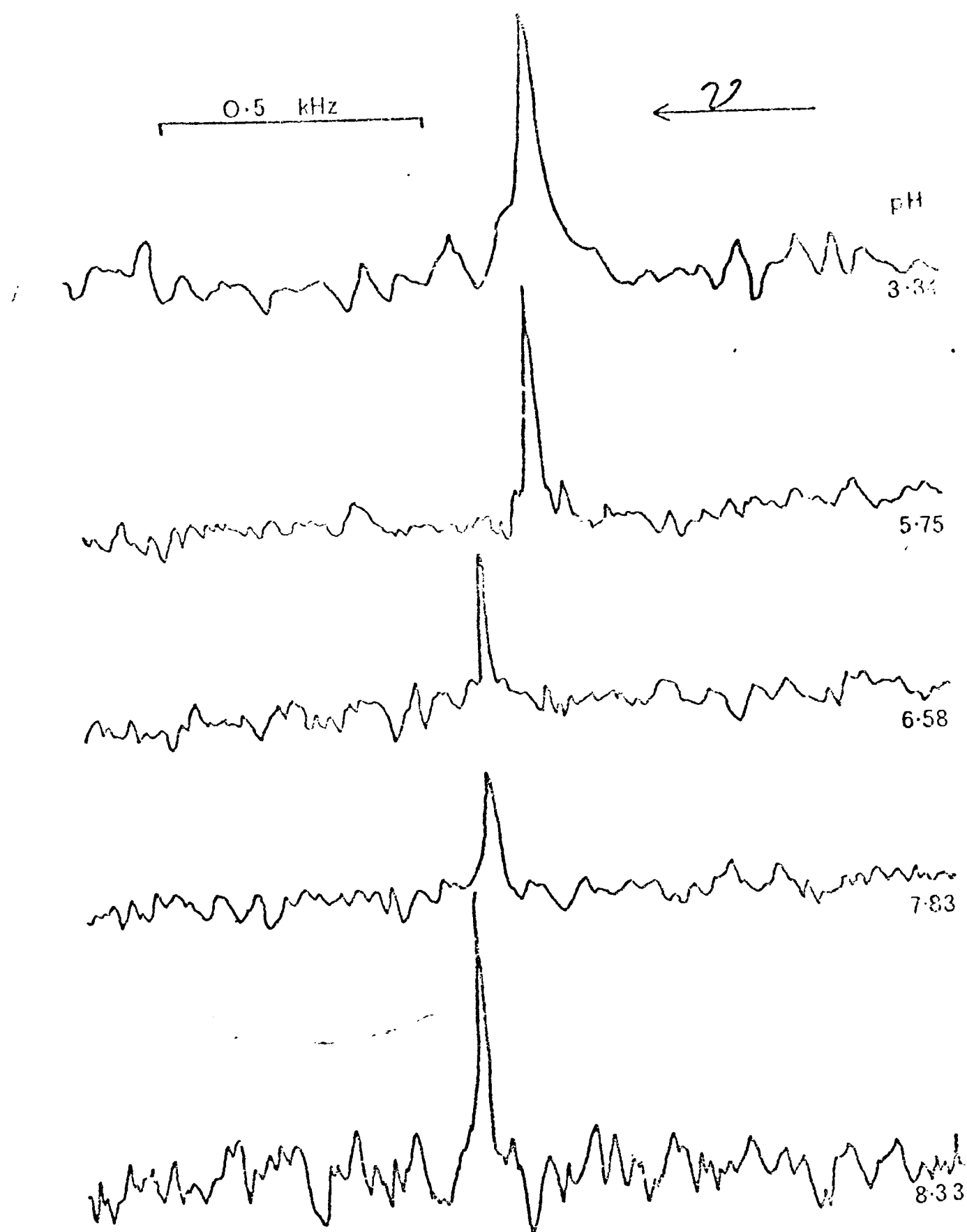


Figure 5.1

2.1 Tesla Phosphorus NMR Spectra of Pyridoxal 5' Phosphate

The spectra were recorded without proton irradiation with an external deuterium oxide lock. The sample consisted of 30 mM pyridoxal 5' phosphate in TEA, KCl, EDTA buffer at various pH values.

ν indicates the direction of increasing frequency in each spectrum.

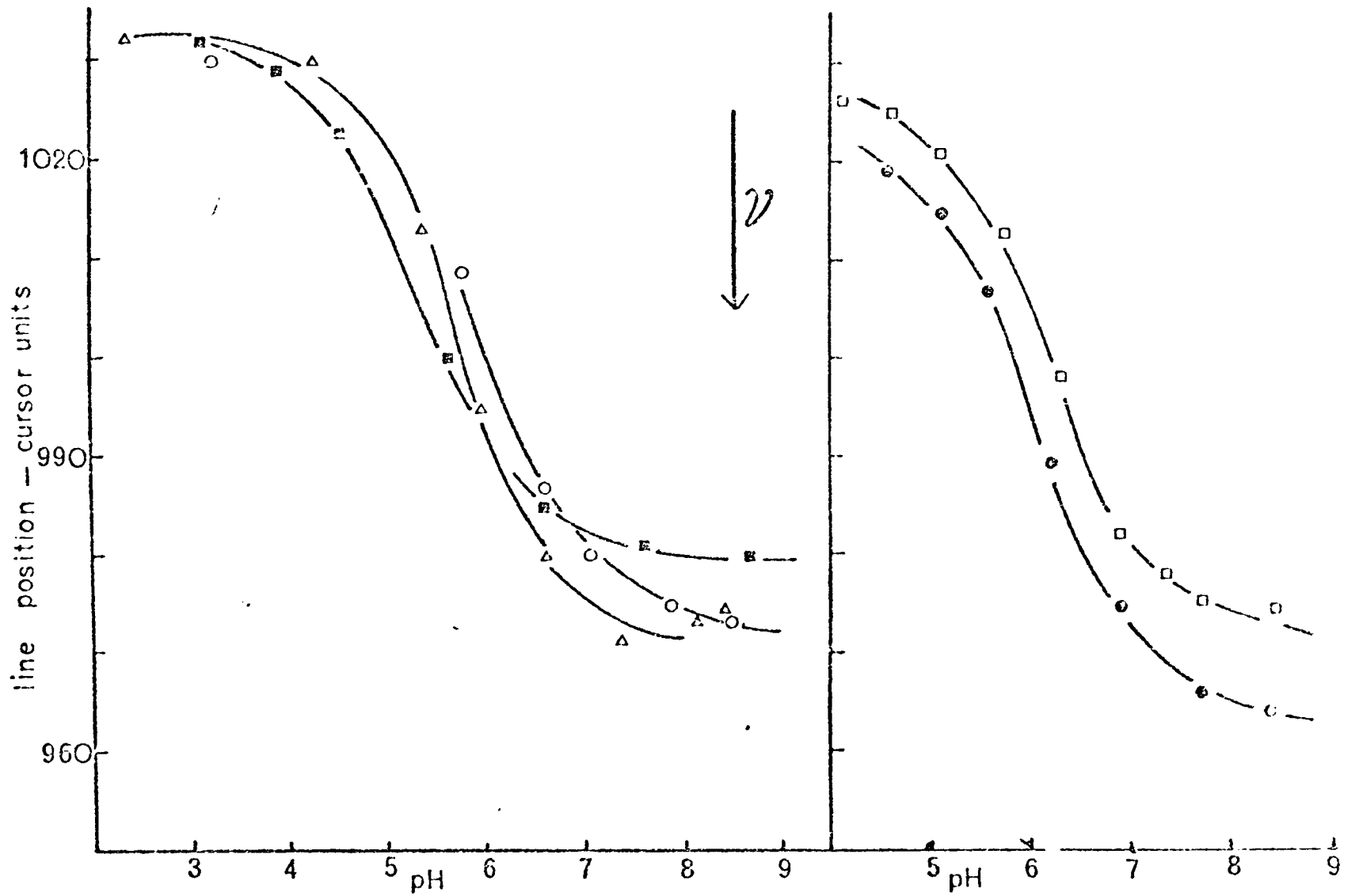


Figure 5.2

pH titrations of phosphorus containing compounds by phosphorus NMR

Spectra were recorded at 2.1 Tesla as in Fig. 5.1. Titration data are shown for pyridoxal 5' phosphate (o), serine phosphate (Δ), pyridoxal 5' phosphate in the presence of 1.6 mM ethanolamine (\boxplus), AMP (\square) and Glucose-6-phosphate (\odot).

The pK values for the interconversion of the mono- and di-anionic forms of these molecules are all in the range 5.5 - 6.5. Therefore, if these molecules are free in solution at pH values above 7, the phosphate will be in the dianionic form.

B. The ^{31}P NMR spectrum of phosphorylase b

^{31}P NMR spectra of phosphorylase b recorded on two spectrometers each operating at a different magnetic field strength (7.5 Tesla and 2.1 Tesla) are shown in Fig. 5.3. The figure also shows the resonance positions of the mono- and di-anionic forms of amine bound pyridoxal phosphate (P^- and P^{--}), recorded on the same machines.

The most apparent feature of the spectra is that the signal arising from a single phosphate residue per subunit has more than one component. This observation implies that the phosphate residue of the coenzyme experiences at least two different environments, i.e. that the phosphorylase b subunit has a minimum of two forms (conformations), which on the NMR time-scale are not rapidly interconvertible. At 2.1 Tesla two peaks are resolved in the phosphorylase b spectrum. They correspond in frequency to the resonances of the dianion and monoanion forms of both pyridoxal-5'-phosphate and a pyridoxal-5'-phosphate-butylamine conjugate. Assuming that these signals correspond to two interconverting forms of the enzyme, a lower limit can be placed on the 'lifetime', τ , for the interconversion from the theory of chemical exchange. (τ is the reciprocal of the sum of the forward and backward rate constants for interconversion.) At 2.1 Tesla (36.43 MHz) the

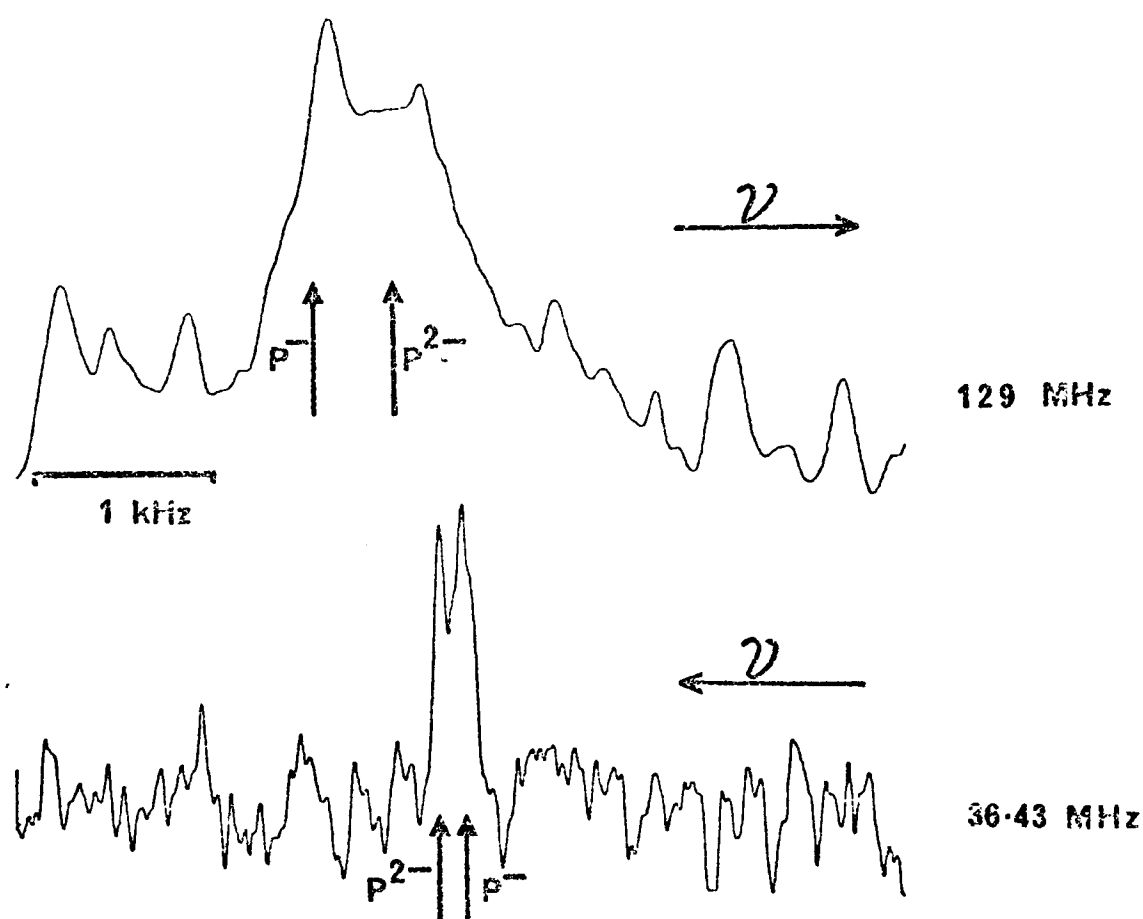


Figure 5.3

Phosphorus NMR Spectra of Phosphorylase *b* at 7.5 and 2.1 Tesla

The spectra in Figures 3-6 were recorded at 20°C without proton irradiation. External deuterium oxide was used for the field-frequency lock. P^- and P^{2-} indicate the resonance positions of the monoanionic and dianionic forms of the butylamine conjugate of pyridoxal phosphate (10 mM). ν indicates the direction of increasing frequency in each spectrum.

The spectrum at 7.5 Tesla is that of a sample of 2.0 mM phosphorylase *b* in 50 mM triethanolamine hydrochloride, 100 mM potassium chloride, 1 mM EDTA, pH 7.78. Radiofrequency radiation was applied as 18,102 45° pulses at intervals of 2 s. The 2.1 Tesla spectrum was recorded from a sample of 1.0 mM phosphorylase *b* in the triethanolamine buffer system at pH 7.50. 6700 70° pulses were applied at 8 s intervals. From (152).

two peaks are separated by approximately 150 Hz and hence $\tau (> 1/2\pi\Delta\nu)$, where $\Delta\nu$ is the frequency separation in Hz) must exceed about 1 ms. As the pK_a of free pyridoxal phosphate is 6.2, a signal corresponding to the dianionic form of the cofactor would be expected at the pH of the above experiments (7.5). If the two components of the signal observed at 36.43 MHz do in fact correspond to the two states of ionisation of the phosphate group, it is likely that proton exchange requires a concomitant conformational change in the enzyme, which is the rate limiting step in the interconversion between these states.

Whilst throughout this chapter it is suggested that the two components of the signal could correspond to the two states of ionisation of the phosphate group, current data do not provide sufficient evidence to prove this hypothesis. The ideas forwarded here are the simplest explanations which fit the available data.

Fig. 5.3 shows that the total width of the resonance is larger at 7.5 Tesla than 2.1 Tesla (approximately 900 and 200 Hz respectively). The difference in the linewidths at the two field strengths cannot be accounted for by chemical exchange alone and must, at the high magnetic field strengths employed here, contain contributions from chemical shift anisotropy of the phosphorus resonance, as observed in other systems (150). Magnetic relaxation due solely to anisotropy of the phosphate group generates a signal linewidth which is proportional to the square of the applied magnetic field intensity and hence accounts for the major proportion of relaxation at 7.5 Tesla, whilst being subordinate to dipolar relaxation at the lower frequency (151).

C. The Effect of Ligands

Addition of the activator AMP, or of the inhibitor glucose-6-phosphate, results in a dramatic change in the NMR signal of pyridoxal phosphate. Fig. 5.4 and 5.5 show spectra of phosphorylase b in the presence of AMP or Glucose-6-phosphate recorded at 2.1 Tesla and 7.5 Tesla respectively.

The assignments shown were deduced from spectra recorded at differing relative concentrations of ligand to enzyme. The pyridoxal phosphate resonance of phosphorylase b saturated with glucose-6-phosphate consists predominantly of one signal of frequency corresponding to that of the dianion form of pyridoxal phosphate. The cofactor signal has a minor component at the monoanion frequency. In contrast, in AMP-saturated phosphorylase b the major portion of pyridoxal phosphate magnetisation is at the monoanion frequency though there may be some absorption at the dianion position which is obscured by the AMP signal. Both effectors reduce the linewidth of the pyridoxal phosphate signal as compared to the unliganded enzyme. These results could be most simply explained by a reduction in the number of conformations accessible to the phosphorylase-ligand complex.

D. Phosphorylase a

Phosphorylase b may also be activated to the a form by phosphorylation of a single serine residue. The phosphorus NMR spectrum of phosphorylase a is shown in Figure 5.6. The composite signal from both the seryl and pyridoxal phosphates is narrower (approximately 120 Hz) than the

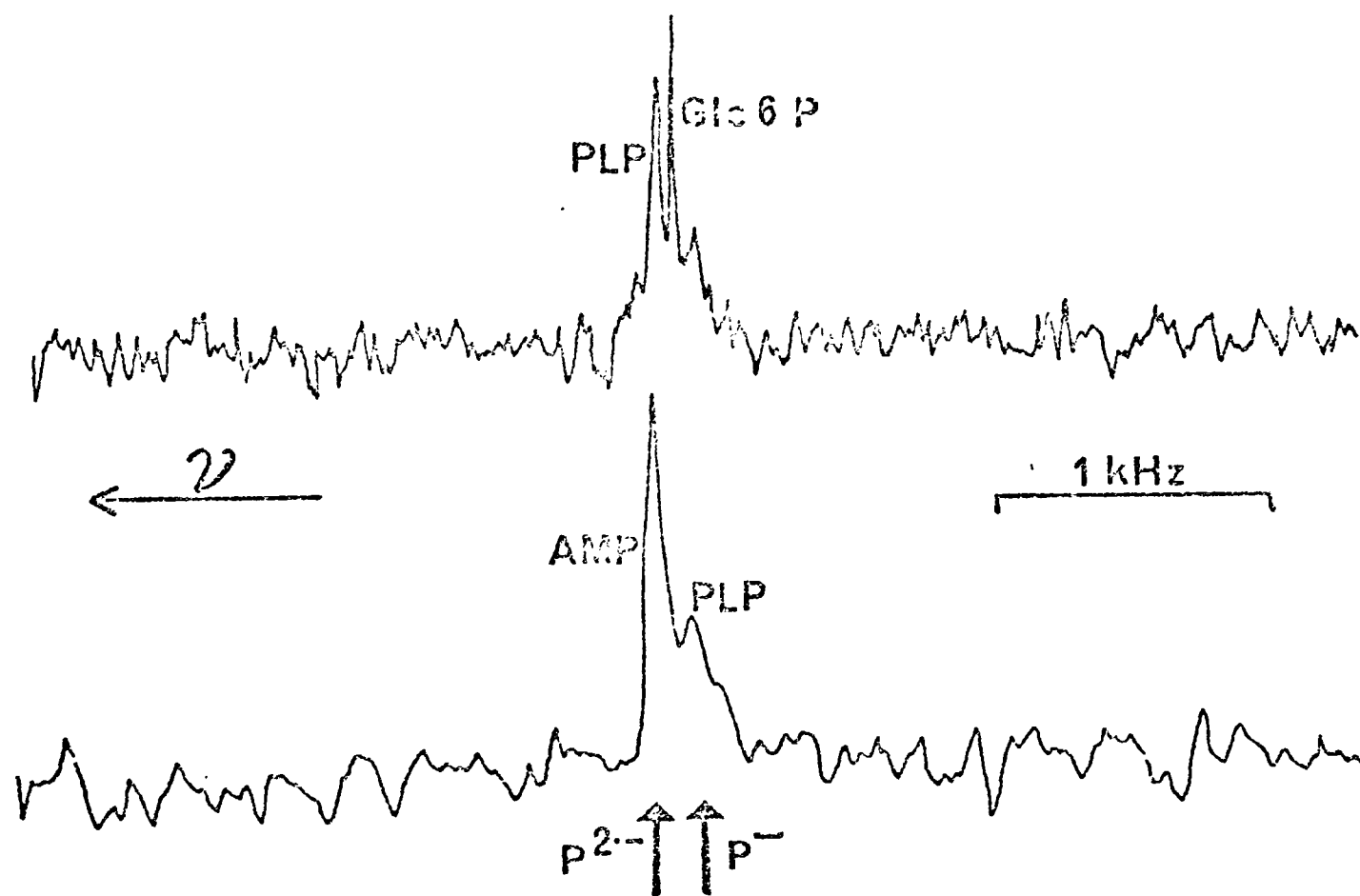


Figure 5.4 2.1 Tesla Phosphorus NMR Spectra of Phosphorylase b in the Presence of Glucose-6-Phosphate or AMP

The upper spectrum is that of 1.11 mM phosphorylase b and 1.14 mM glucose-6-phosphate in the triethanolamine buffer system (see Fig. 5.3) at pH 7.81. 10,976 pulses were applied at 6 s intervals. The lower spectrum was recorded from a sample of 1.2 mM phosphorylase b and 1.2 mM AMP in triethanolamine buffer at pH 7.5, and is the accumulated magnetization from 10,164 pulses applied at intervals of 3 seconds.

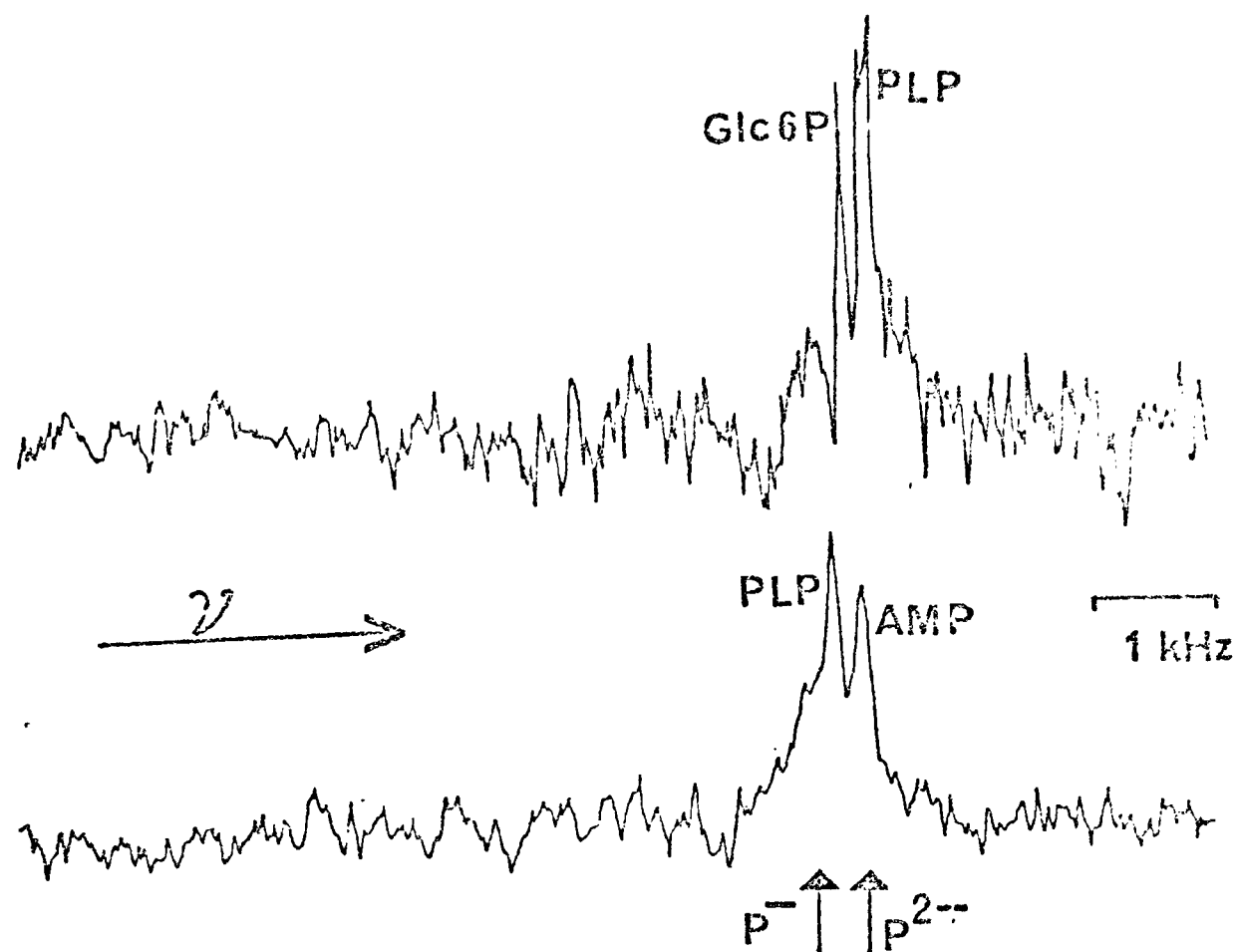


Figure 5.5 7.5 Tesla Phosphorus NMR Spectra of Phosphorylase \bar{b} in the Presence of Glucose-6-phosphate or AMP

The upper spectrum is that of 1.11 mM phosphorylase \bar{b} and 1.14 mM glucose-6-phosphate in the triethanolamine buffer system (see Figure 5.3) at pH 7.89. 10722 45° pulses were applied at 6 s intervals.

The lower spectrum was recorded from a sample of 1.16 mM phosphorylase \bar{b} and 1.7 mM AMP in triethanolamine buffer at pH 6.8, and is the accumulated magnetization from 14400 45° pulses applied at intervals of 2 s.

Other details are given in Figure 5.3.

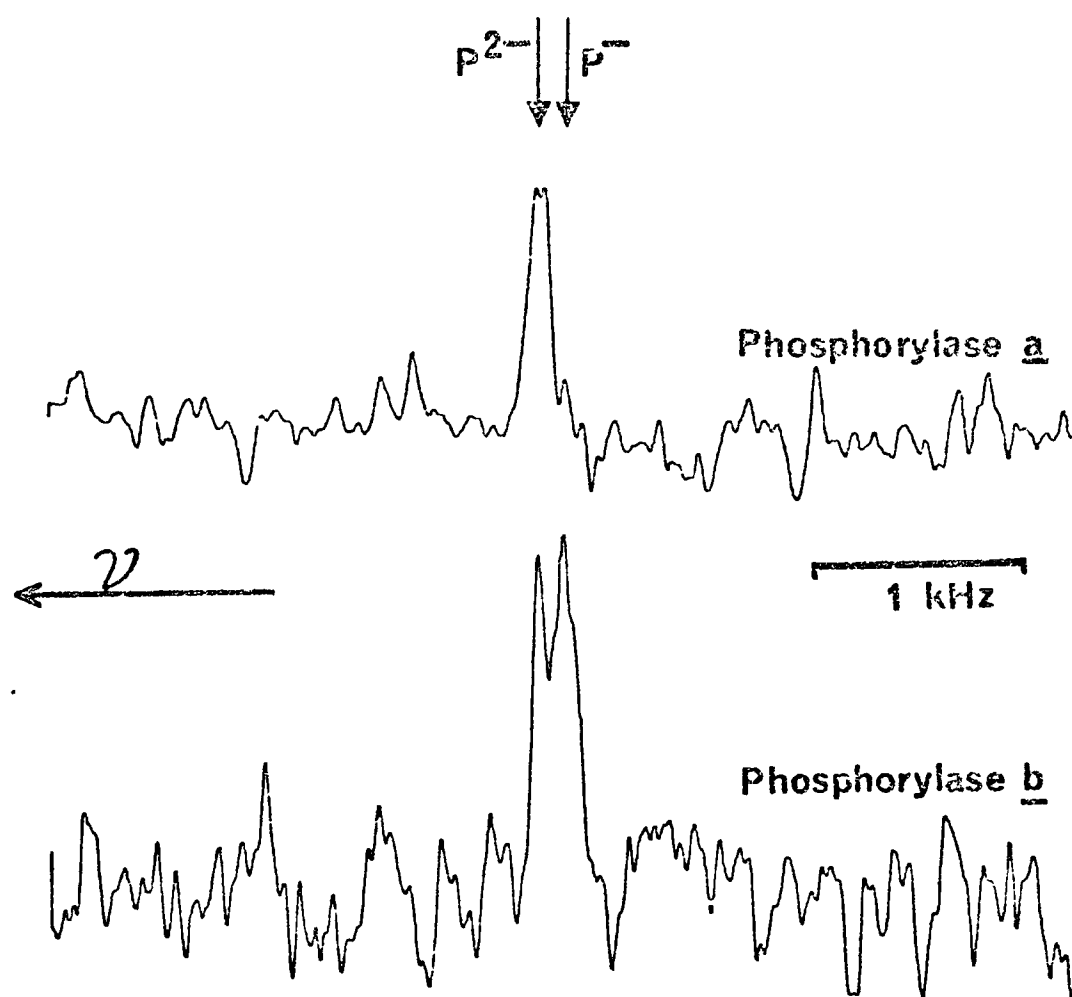


Figure 5.6

2.1 Tesla Phosphorus NMR Spectra of Phosphorylase a and b

6800 pulses were applied at 10 s intervals to a 0.723 mM sample of phosphorylase a in triethanolamine buffer at pH 7.5 (80° pulses were used).

The phosphorylase b spectrum is the same as that shown in Figure 5.3.

Other details are given in the legend to that figure.

signal from phosphorylase b alone and corresponds in frequency to the dianion form of pyridoxal phosphate (or the amine conjugate). Assignments of both phosphates to the single phosphorylase a resonance is based on an experiment in which the intensity of the enzyme signal was compared to that of a standard concentration of pyridoxal phosphate. The chemical shifts of the phosphates correspond to the value for the pyridoxal phosphate in phosphorylase b in the presence of the inhibitor glucose-6-phosphate.

E. Conclusions

Pyridoxal phosphate in phosphorylase b undoubtedly experiences more than one 'chemical environment'. On the simplest assumption that the two component signal seen for phosphorylase b alone at 36.43 MHz represents a slow interchange between two enzymic conformations, an upper limit of 1 kHz can be given for the rate of exchange between these forms. Addition of ligands (AMP or glucose-6-phosphate) shifts the pyridoxal phosphate into one of the environments. There is apparently no direct relation between the characteristics of the pyridoxal phosphate resonances and enzymatic activity, in view of the fact that activation by AMP or by covalent phosphorylation produce opposite changes in the spectrum.

Chapter 6

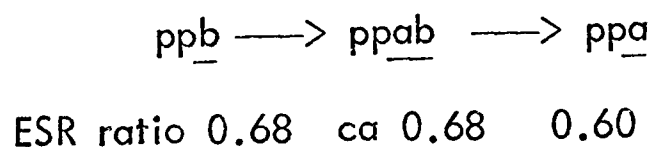
THE PHOSPHORYLASE b TO a CONVERSION

In skeletal muscle, phosphorylase b to a conversion is responsible for the initiation of glycogen breakdown. Incorporation of one phosphate / phosphorylase monomer from ATP/Mg⁺⁺ to the enzyme is catalysed by the calcium activated enzyme phosphorylase b kinase and locks phosphorylase in an "active conformation". Although this favours the formation of tetrameric enzyme, adoption of the tetramer aggregation state is not necessary for activity (102). Phosphorylase a can bind all of the ligands which are effectors of phosphorylase b yet with different affinities. For example the nucleotides ATP, ADP, and AMP bind more tightly to the a form than to the b form whereas glucose-6-phosphate binds more weakly.

It has been suggested that during the b to a conversion, hybrids consisting of one phosphorylated and one non phosphorylated subunit are transiently produced. These hybrids (the ab form of phosphorylase), have properties characteristic of phosphorylase b and a. Like phosphorylase a, they exhibit AMP independent activity and like phosphorylase b, this activity is inhibited by 1mM Glucose 6 phosphate. To date the ab form has been detected solely by activity measurements (153-156). In this section, it is shown that the spin label and fluorescent probes, described in Chapter 2, can detect the b to a conversion and provide further evidence for the existence of the ab form.

A. Studies using Spin Labelled Phosphorylase

The characteristic ESR ratio of the spin label probe differs for phosphorylase b and a ($R_b = 0.68$, $R_a = 0.60$), reflecting the difference in the conformation between the two forms. The lower ratio exhibited by spin labelled phosphorylase a cannot be due to aggregation as addition of glucose does not affect the ratio, whilst converting tetrameric phosphorylase a to a dimeric form. The difference in the ratio shown by phosphorylase b and a may be used to follow the kinetics of b to a conversion (see Fig. 6.1). During the conversion of phosphorylase b to a, the ab form of phosphorylase is transiently produced. Careful measurements over the first few minutes of the conversion show a transient lag in the ESR ratio change, behind activity changes. The most likely interpretation of this observation is that the ratio shown by the ab form is close to that of phosphorylase b, the reaction sequence being:



Using this assay procedure, the activities of different forms of phosphorylase kinase at different pH values may be deduced. If non-phosphorylated kinase is used, a lag in the production of phosphorylase is seen due to auto-activation of kinase (158).

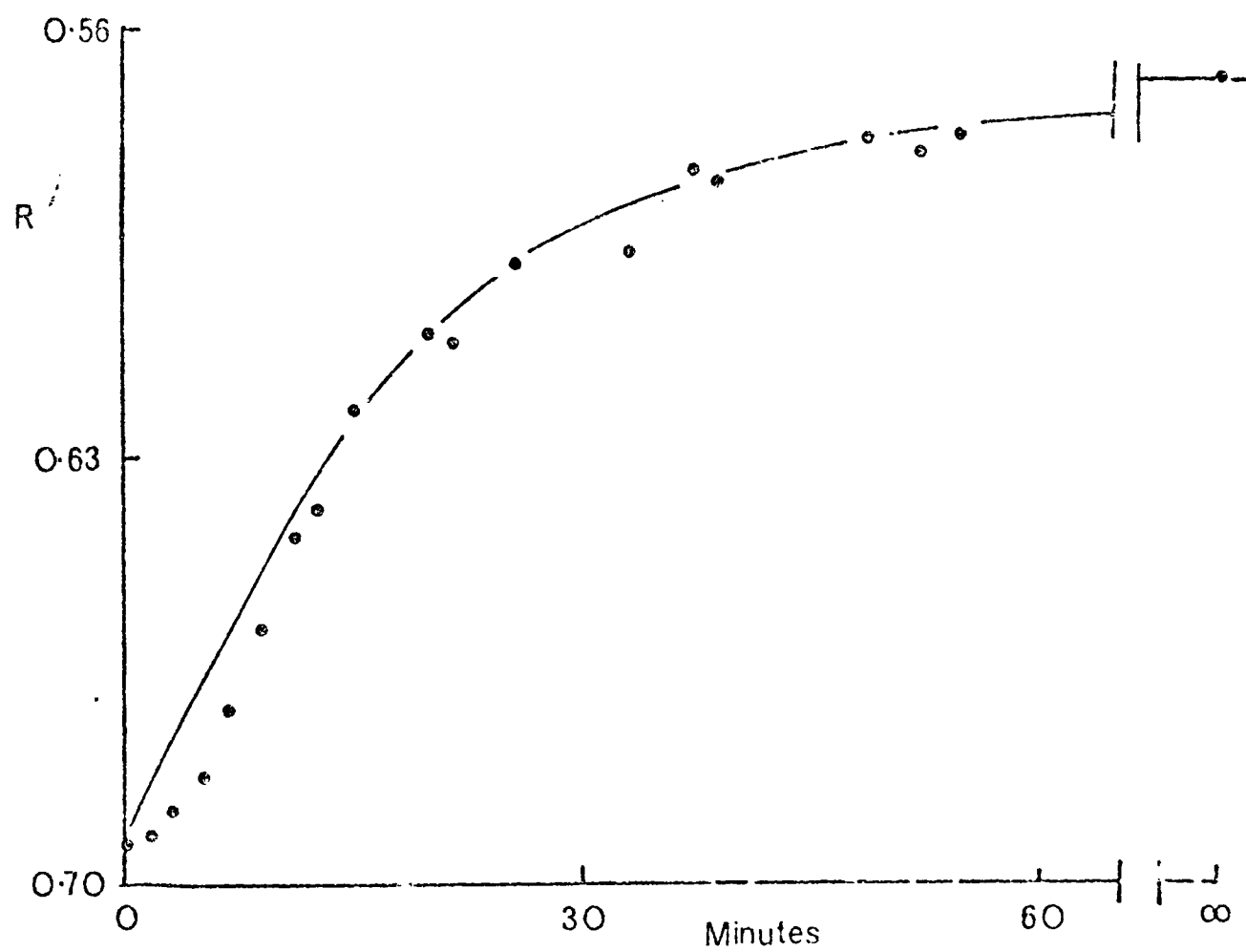


Figure 6.1 Changes in the ESR ratio on conversion of spin labelled phosphorylase b to a (120 μ M phosphorylase b, 2.9 mM ATP, 9.8 mM Mg^{2+} , 7.5 μ M Ca^{2+} plus activated phosphorylase kinase). The full curve was calculated assuming only the b and a forms were present.

B. Differential ligand binding to phosphorylase a and b

Acetamido-salicylate-phosphorylase b may be converted into the active a form; the conditions for the conversion are: 5 μM labelled phosphorylase b, 1 nM phosphorylated-phosphorylase kinase, 5 mM MgCl_2 , 5 μM CaCl_2 and 50 μM ATP in 50 mM triethanolamine-HCl buffer containing 100 mM KCl at pH 8.2. Under these conditions the interconversion takes about 5 min and no change in the salicylate fluorescence is seen. When the interconversion is carried out in the presence of 25 μM AMP a decrease in salicylate fluorescence is observed due to the tighter binding of AMP to the a form, the uptake of AMP by the newly formed labelled phosphorylase a resulting in fluorescence quenching (Fig. 6.2). Conversely, addition of glucose-6-phosphate (400 μM) to the reaction mixture produces an enhancement in the salicylate fluorescence during the b to a conversion (Fig. 6.2). This is because glucose-6-phosphate is released from phosphorylase a, being weakly bound to phosphorylase a compared to phosphorylase b. The rate of the interconversion (as assayed by the appearance of phosphorylase a activity) is unaffected by AMP and glucose-6-phosphate at the concentrations used in the experiments described above.

The fluorescence change in the presence of AMP followed exactly the same time course as the appearance of activity, while when glucose-6-phosphate was present there was a considerable lag before the expulsion of the inhibitor. This clearly implies that glucose-6-phosphate binds to a form of the enzyme which is already active but cannot be phosphorylase a, i.e. that during the interconversion hybrids are formed which are still subject to inhibition by glucose-6-phosphate but bind AMP as tightly, or nearly as tightly, as the

Figure 6.2 Fluorescence changes as AMP or glucose-6-phosphate bind to acetamidosalicylate-phosphorylase during b to a conversion with phosphorylated phosphorylase b kinase at pH 6.8 or pH 8.2 (continuous lines). 50 mM triethanolamine-KCl buffer with no EDTA pH 6.8 or pH 8.2, 5 μ M acetamidosalicylate-phosphorylase b, 5 mM $MgCl_2$, 5 μ M $CaCl_2$, 50 μ M ATP, and 25 μ M AMP or 400 μ M glucose-6-phosphate. 1 nM phosphorylated phosphorylase b kinase was added at zero time. Percentage conversion of phosphorylase b to a at pH 8.2 (●) from activity measurements.

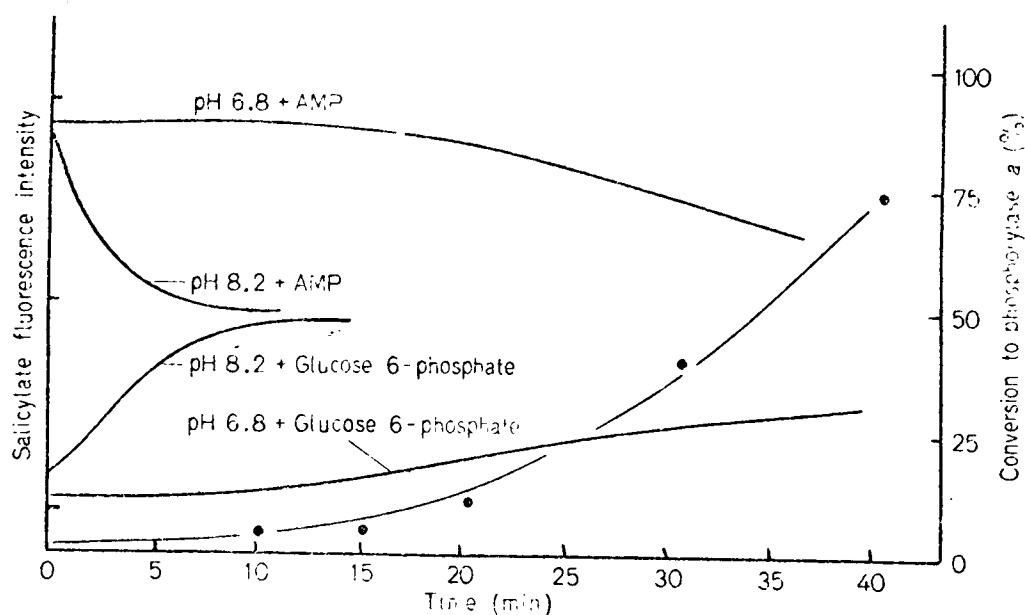
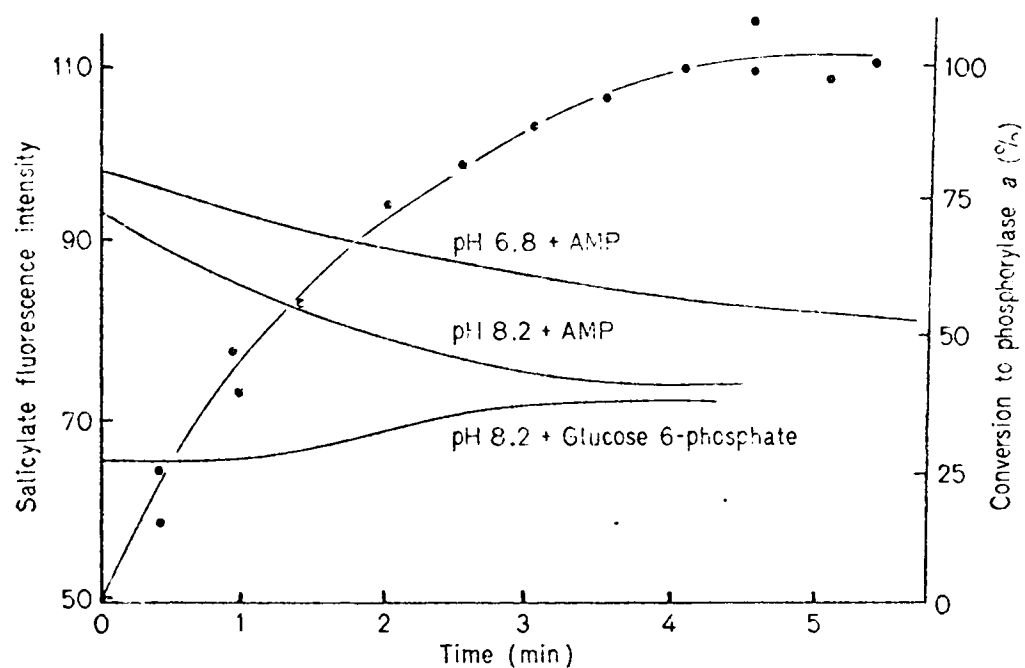


Figure 6.3 Fluorescence changes as AMP or glucose-6-phosphate binds to acetamido-salicylate-phosphorylase during b to a conversion with non-phosphorylated phosphorylase b kinase at pH 6.8 or pH 8.2. Conditions as for Fig. 6.2 except 1 nM non-phosphorylated phosphorylase b kinase was used (continuous lines). Percentage conversion of phosphorylase b to a at pH 6.8 (●) from activity measurements.

completely phosphorylated form.

In activity assays (where activities are measured by taking aliquots of the reaction mixture and diluting them so that essentially no glucose 6-phosphate or AMP is present in the assay mixture) this lag does not appear. If the aliquots that are taken from the reaction mixture are assayed at 100 mM Glucose 1 phosphate, in the presence or absence of glucose 6-phosphate (1 mM), it is found that glucose 6-phosphate inhibits activity only during the first few minutes of the conversion. This confirms the observation of Hurd *et al.* (153) who suggested that the intermediate singly phosphorylated phosphorylase dimer binds glucose 6-phosphate (and AMP) relatively tightly. The fluorescence experiments provide a direct demonstration of this, since the lag seen in the fluorescence change in the presence of glucose 6-phosphate corresponds to the time period during which glucose 6-phosphate inhibition is present. The fluorescence method, however, provides a more accurate measure of the time course for the appearance of a form of phosphorylase which is active but still binds both glucose 6-phosphate and AMP.

Fig. 6.2 also shows that the initial velocity of the conversion at pH 8.2 is three times faster than at pH 6.8. The exact ratio of initial velocities at the two pH values varies with the phosphorylase concentration.

C. The Conversion of Phosphorylase b to a Catalysed by Non-phosphorylated Kinase

Conversions were also studied at pH 6.8 and 8.2 using non-phosphorylated phosphorylase b kinase (Fig. 6.3). At pH 6.8 in the presence

of AMP or glucose 6-phosphate the change in the fluorescence of labelled phosphorylase during the conversion showed a lag phase that corresponded to a similar delay in the appearance of phosphorylase a activity. Increasing the amount of kinase in the reaction mixture diminished the duration of the lag while addition of cyclic AMP or preincubation of kinase with phosphorylase and ATP did not abolish the lag. Preincubation of kinase with ATP, magnesium and calcium abolished the lag phase in the activity changes.

At pH 8.2 the changes seen were similar to those observed when phosphorylated phosphorylase b kinase was used. In the presence of glucose 6-phosphate the lag phase was still apparent but it was not present when fluorescence was followed in the presence of AMP or in the activity assays.

The ratio of the initial activity of non-phosphorylated kinase at pH 8.2 to that at 6.8 was over 100. Table 6.1 summarises these observations.

The continuous assay method for phosphorylase kinase described here has facilitated the study of non-linear progress curves more precisely than was possible with the previous technique based on phosphorylase a activity measurements. The disadvantages of the fluorescence method are the need to use phosphorylase concentrations much lower than that of AMP and glucose 6-phosphate and the need to maintain a low ADP concentration. The method is also very susceptible to interference by contaminating enzymes such as 5'-adenylic acid deaminase and ATPases. While the pH 6.8 to 8.2 ratios for the activity of phosphorylated kinase are similar to those reported by Cohen (52) in the case of non-phosphorylated kinase at pH 6.8 it is evident that autophosphorylation is appreciable (161) over a short time period even at low ATP concentrations. This effect is distinct from the lag phase observed

Table 6.1

Summary of the various lag effects during the conversion of phosphorylase b to a seen using the fluorescence of acetamido-salicylate-phosphorylase in the presence of AMP or glucose 6-phosphate at pH 6.8 and pH 8.2 using phosphorylated or non-phosphorylated phosphorylase b kinase

50 mM triethanolamine - KCl buffer pH 8.2 and pH 6.8 at 18°C were used with no EDTA present, 5 μ M acetamido-salicylate-phosphorylase b, 1.0 nM phosphorylase b kinase, 5 mM MgCl₂, 5 μ M CaCl₂ and 50 μ M ATP, with 25 μ M AMP or 400 μ M glucose 6-phosphate present were concentrations used to follow the conversion by salicylate fluorescence.

Kinase	pH	Fluorescence assay		Activity assay (+ glucose 6-phosphate or AMP)
		+AMP	+glucose 6-phosphate	
Activated	6.8	no lag	lag	no lag
	8.2	no lag	lag	no lag
Non- activated	6.8	lag	lag	lag
	8.2	no lag	lag	no lag

by Kim and Graves (162) as preincubation of the kinase with phosphorylase b does not affect the activation lag period. Because of the contribution of autophosphorylation to activity, care must be taken when defining the pH 6.8 activity of non-phosphorylated kinase. The pH 8.2 to 6.8 activity ratios of over 100 are only seen when kinase is rapidly prepared since trace quantities of proteolytic enzymes will also activate phosphorylase b kinase causing the ratio to drop.

It has been suggested (52) that, in vivo, the low pH 6.8 activity observed with non-phosphorylated phosphorylase b kinase is not sufficient to account for the rapid phosphorylase a production in glycogen particles following flash activation with calcium, magnesium and ATP and in muscle tissue on electrical stimulation (163).

It is possible that in vivo and when in glycogen particles, the activity of phosphorylase kinase, when bound to glycogen (51) or other proteins, is increased. It is however difficult to relate the activity of non-phosphorylated kinase seen here to that in vivo because of the high concentration found in muscle and the possibilities of phosphorylation during electrical stimulation.

D. The Kinetics of the Formation of Phosphorylase a Tetramers

The rate of formation of the phosphorylase a tetramer has been previously followed using a non-covalent fluorescent probe 2-(N-methylanilino)-naphthalene-6-sulphonate (31). The use of this probe depended on a detailed comparison of the sedimentation behaviour of the different aggregation states of the enzyme with the fluorescence characteristics of the probe. Another

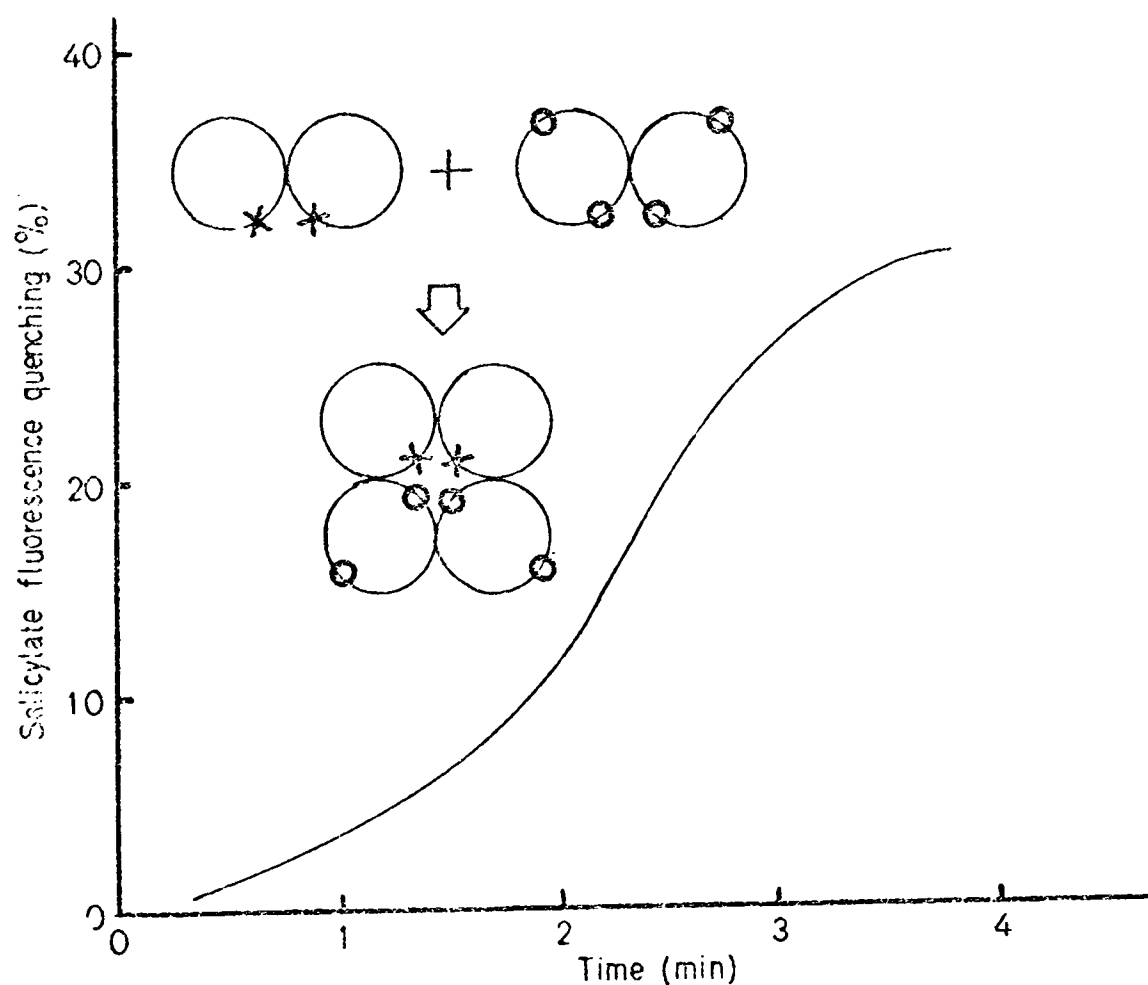


Figure 6.4 The quenching of acetamidosalicylate fluorescence by singlet energy transfer to Nbf moieties due to the tetramerization of acetamidosalicylate-phosphorylase and Nbf phosphorylase dimers during phosphorylase b to a conversion. Tris-KCl buffer pH 8.5, 1 μ M acetamidosalicylate-phosphorylase b, 2 μ M nitrobenzoxadiazole phosphorylase b, 5 mM MgCl_2 , 5 μ M CaCl_2 , 50 μ M ATP, and 1 nM phosphorylated phosphorylase b kinase. The inset illustrates the experiment. Nbf and acetamidosalicylate moieties are represented by o, and * respectively.

method utilises the fact that the fluorescence emission band of the acetamido-salicylate group on phosphorylase overlaps with the absorption band of the Nbf group which can also be attached to the enzyme (Fig. 2.1). If the two probes are closer than 3.0 nm apart, from theoretical considerations one may expect energy transfer to take place between them, with a consequent quenching of the acetamido-salicylate fluorescence. When a solution of acetamido-salicylate phosphorylase b (0.1 mg/ml) is mixed with Nbf phosphorylase b (0.2 mg/ml) no significant change in salicylate fluorescence is observed. After converting this mixture to phosphorylase a a 30% quenching of salicylate fluorescence is observed which can be reversed by the addition of glucose (50 mM). Glucose is known to disaggregate phosphorylase tetramers and does not affect the fluorescence of acetamido-salicylate-phosphorylase a (Table 4.1). No change in acetamido-salicylate fluorescence is observed if acetamido-salicylate-phosphorylase a (0.1 mg/ml) is added to Nbf-phosphorylase a (0.2 mg/ml). Quenching associated with the interconversion therefore can be attributed to energy transfer in the hybrid tetramers of phosphorylase a. Fig. 6.4 shows the kinetics of the production of this quenching as phosphorylation takes place, using activated phosphorylase kinase at pH 8.5. The time course of the appearance of the quenching lags considerably behind that of the activity changes, but corresponds to the results obtained using the non-covalent probe.

The heterologous protein-protein interaction between phosphorylase b kinase labelled with Nbf and phosphorylase b labelled with iodoacetamido salicylic acid has also been observed (112). Nbf phosphorylase b is titrated into kinase labelled with 6-7 acetamidosalicylate groups per $\alpha\beta\gamma$ unit. As the two proteins aggregate, the Nbf groups on the phosphorylase come close

to some of the acetamidosalicylate groups on the kinase, causing a quenching of salicylate fluorescence. A useful control is to repeat the experiment with kinase labelled only with 2-3 acetamidosalicylate groups per $\alpha\beta\gamma$ unit. Very little quenching is observed, as the first few acetamidosalicylate groups which attach to phosphorylase kinase are too far from the phosphorylase-attached Nbf groups to be quenched. It would be interesting to perform such experiments using phosphorylase a and phosphorylase phosphatase. Using this method it may be possible to see the interaction between phosphorylase kinase and phosphatase suggested by Bot et al. (159).

It is important to note that these methods report proximity of proteins and not, primarily, the effect of one protein on the conformation of the other. Efforts with this system to observe conformational changes in one protein as a result of binding to another have proved abortive to date (160).

This section shows how the application of relatively simple and empirical probe techniques can give useful information about a set of enzyme interactions and interconversions. In the next section an attempt is made to show how these methods may be applied to the phosphorylase system, when found in a more complex environment.

Chapter 7PROTEIN-GLYCOGEN COMPLEXES - AN APPROACH TO
THE "IN VIVO" SITUATION

In the previous sections it was shown that in solution phosphorylase exhibits complex behaviour showing a multiplicity of conformations, interactions with a variety of ligands and several different possible modes of regulation of its activity. All these properties of the system raise interesting enzymological questions but, as in any field of enzymology, can only point to their possible biological significance. The biochemist is often forced to use teleological arguments to support the importance of his studies by assuming that no specific behaviour is accidental but is "designed" by the process of evolution to meet a particular biological problem. While this is a convenient argument for justifying a study on isolated systems (which undoubtedly has a value in its own right) the experimental problems in demonstrating the relation between in vitro and in vivo observations remain formidable.

In attempting to understand the regulation of glycogen metabolism in vivo we are fortunate in having a "half-way-house". Meyer et al. have demonstrated that a particulate fraction can be prepared from rabbit skeletal muscle which is rich in glycogen and contains phosphorylase, phosphorylase kinase and a number of other enzymes associated with phosphorylase control (74). In these "glycogen particles" transient activation of phosphorylase b takes place on addition of Mg/ATP provided that Ca^{++} ions are present (164). Whilst there is little direct evidence that phosphorylase and the other enzymes in the cascade are bound to glycogen in vivo, the high concentration of glycogen in muscle and the tight binding of phosphorylase to it make this likely. The glycogen particle fraction

can be prepared by three methods - direct centrifugation, acid precipitation and acetone precipitation. The components of a typical fraction prepared by the acid precipitation method are listed in Table 7.1. In different preparations the glycogen / phosphorylase / glycogen synthetase ratio remains roughly constant, reflecting tight binding of phosphorylase and synthetase to glycogen. Electron microscopy shows the fraction obtained by the acid precipitation method as a mixture of densely staining particles of glycogen and sarcoplasmic vesicles (165). Zonal centrifugation of the mixture led to a separation yielding two fractions. One contained particles of glycogen and associated proteins (30-40 $m\mu$ diameter) and the other contained the sarcoplasmic vesicles, to which smaller particles of glycogen were attached (10-20 $m\mu$ diameter). Incubation of the latter fraction with glucose-1-phosphate led to synthesis of glycogen. Electron microscopy showed that the newly formed glycogen was attached to the membrane-bound glycogen particles (166). The free glycogen particles contained phosphorylase, phosphorylase b kinase and glycogen synthetase but the latter was not present in the membrane-bound glycogen particle fraction.

In whole muscle tissue glycogen was seen in particulate deposits, whose size was the same as those particles seen in the glycogen rich fractions. Some of the densely staining particles of glycogen were associated with parts of the sarcoplasmic reticulum in ordered arrays (165). All these observations suggest that the glycogen particles prepared by acid precipitation are similar to those in the intact tissue.

Membrane-bound carbohydrates are not uncommon. In pigeon retina tissue all the cells' glycogen is intimately associated with highly ordered arrays

Table 7.1

The Contents of a Typical Glycogen Particle Fraction

Glycogen	(20 mg/ml)
Phosphorylase <u>b</u>	(70 μ M)
Phosphorylase <u>b</u> kinase	(4 μ M)
Glycogen synthetase	(4 μ M)
Phosphorylase phosphatase	
Kinase phosphatase	
cAMP dependent kinase kinase	
Ca ²⁺ dependent kinase activating factor (KAF)	
Sarcoplasmic reticulum ATPase	
AMP deaminase	
Myokinase	
Phosphoglucomutase	
Creatine kinase	
Glucose-6-phosphate	(400 μ M)
IMP	(10 μ M)

The preparation of the fraction is described in Appendix 2 G.

of endoplasmic reticulum (1). Lipid-sugar complexes have been shown to be important in the initiation of synthesis of bacterial peptido-glycan (167, 168) and plant cell wall cellulose (169). Further evidence for membrane/glycogen complexes in muscle has been inferred from electron microscopic examination of tissue samples from patients suffering from thyrotoxic periodic paralysis (170). In such cases, it is observed that glycogen was actually enclosed by the sarcoplasmic reticulum and subsarcolemmal blebs filled with glycogen were formed, thus impairing the function of the membrane and, hence, the muscle.

Utilising kinetic measurements, some properties of the enzymes in the glycogen rich particulate fraction have been shown to be different from those of the purified enzymes (164, 171-173). These studies, which have been previously reviewed (75, 133) showed that the system was clearly amenable to more detailed structural and mechanistic studies.

The initial papers concerning glycogen particles raised a number of questions: (i) do small metabolites bind to phosphorylase b and so regulate its activity in the glycogen protein complex, (ii) does either form of the enzyme undergo a protein-protein interaction with any other component of the complex and (iii) do small metabolites bind to phosphorylase a and modify its properties? Since the glycogen particle fraction is an opaque, viscous suspension which is not accessible to normal spectroscopic methods, most studies have used enzyme activity as their only probe. All three of the questions are to some extent concerned with the conformation of the enzyme. The results described in this chapter centre around the use of spin labelled phosphorylase to investigate the conformation of the enzyme when in the glycogen particle fraction.

A. The Contents of the Glycogen Particulate Preparation

The contents of a typical glycogen particulate preparation are listed in Table 7.1. Precise details of each assay are included in Appendix 2 Section G. It is interesting to note that:

(i) The ratio of phosphorylase kinase activity at pH 8.2 to that at pH 6.8 is 8-12, indicating that 10-20% of it is activated either by proteolysis or phosphorylation (52).

(ii) The glycogen particulate fraction shows a high 5'-adenylic acid deaminase activity. Little activity was found in the supernatant after the fraction was centrifuged down during the preparation. This is in accord with the results of Brody and Costello (176), who found that 5'-adenylic acid deaminase behaved as though it were particle bound. Possibly it binds to elements from the sarcoplasmic reticulum which sediment with the glycogen particulate preparation. The high level of this enzyme prohibits the study of the effect of AMP on the system as 1 mM AMP is converted to IMP in less than 15 seconds in the glycogen particulate preparation.

The experiments described in this chapter rely upon two additional sets of observations. The first is that glycogen particles take up externally added phosphorylase (174). In order to show that labelled phosphorylase was taken up by glycogen particles and that it could displace the native phosphorylase from the particles, the glycogen-rich fraction was centrifuged in the presence of labelled phosphorylase b. By comparing the label concentration with the phosphorylase activity in the supernatant it was possible to deduce the amount of labelled enzyme taken up and the amount of native phosphorylase displaced. Since the spin label moiety on phosphorylase is slowly reduced by

glycogen particles, in these experiments, phosphorylase labelled with a fluorescent probe (4-iodoacetamidosalicylic acid) was used. This label binds to the same sulphhydryl group as the spin label and the acetamidosalicylate-phosphorylase b has identical enzymic properties to the spin-labelled enzyme. Different concentrations of fluorescent acetamidosalicylate-phosphorylase b were added to a glycogen particle suspension and centrifuged for 100 min at 80,000 g. The supernatant was removed from the glycogen particle pellet and the amount of acetamidosalicylate-phosphorylase b in the supernatant was deduced from fluorescence measurements. The overall phosphorylase concentrations in the supernatant and the pellet were derived from measurements of activities of diluted aliquots of each fraction. A plot of the amount of labelled phosphorylase b bound to glycogen particles vs. the concentration of added labelled enzyme is shown in Fig. 7.1. When 50 μ M labelled phosphorylase b is added, 95% of it is taken up into the glycogen particles. At high concentrations of labelled phosphorylase b, native enzyme was displaced from the particles, demonstrating that extrinsically added phosphorylase takes up the positions on the particle originally occupied by intrinsic phosphorylase b.

The additionally bound phosphorylase may contain any one of the covalent labels described in Chapter 3. Thus one is in a position to make specific spectroscopic observations on the bound enzyme. For technical reasons so far, these have been restricted to using ESR measurements on spin labelled phosphorylase.

A second set of observations utilises ^{31}P NMR. This technique allows quantification of the levels of the different phosphate containing compounds in the glycogen particles and the changes in these levels during transient

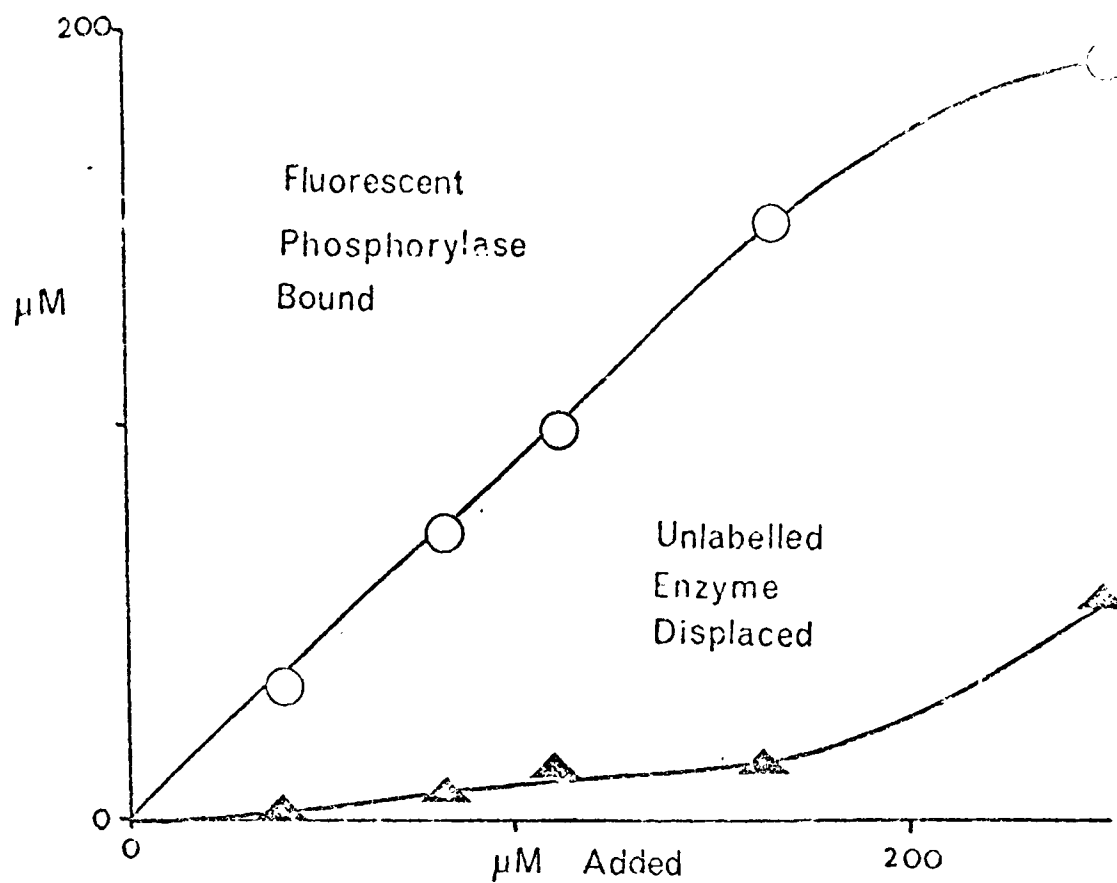


Figure 7.1

(o) Amount of acetamidosalicylate phosphorylase b bound to aliquots of a glycogen particle suspension and (Δ) unlabelled phosphorylase b displaced after pelleting glycogen particles by centrifugation in the presence of various concentrations of fluorescent. labelled phosphorylase b

activation (175). By coupling these observations with activity measurements, insight can be gained into the various interactions in glycogen particles.

B. ESR measurements

The ESR spectrum of spin labelled phosphorylase b bound to glycogen particles is similar to that of the free enzyme but the value of R (see Chapter 2) is generally lower. If however glycogen particles are extensively dialysed, removing all small ligands, the ratio returns to the same value as was found for phosphorylase in the presence of glycogen. In contrast spin labelled phosphorylase a bound to dialysed glycogen particles exhibits a ratio significantly different to that from enzyme in a simulated glycogen medium. Table 7.11 lists the ESR ratio exhibited by various spin labelled phosphorylase-ligand complexes in the glycogen particle fraction and in a simulated glycogen particle medium (i.e. a medium consisting of phosphorylase, glycogen, sugar phosphates and nucleotides in concentrations similar to those found in the glycogen particle fraction). Apart from the anomalous ratio seen with unliganded phosphorylase a, the conformation of the enzyme as reported by the ESR ratio is the same in the glycogen particles as in the simulated medium. By titrating ligands into spin labelled phosphorylase attached to the glycogen particles, it is possible to deduce the relevant binding constants.

It must be remembered that the spin label probably samples only a localised conformation of phosphorylase and it is conceivable that two identical ESR ratios could be obtained from different forms of the enzyme. Nevertheless, the results show that, as judged by the spin label, the conformation of

Table 7.11

Ratio Exhibited by Spin Labelled Phosphorylase in the Presence of Saturating Amounts of Different Ligands in the Glycogen Particle Fraction and in a Simulated Glycogen Particle Medium Consisting of 2% Glycogen and 400 μ M Glucose-6-phosphate in Triethanolamine Buffer pH 7.0

Ligand added	Spin Labelled Phosphorylase <u>b</u>		Spin Labelled Phosphorylase <u>a</u>	
	Ratio in Glycogen Particles	Ratio in Simulated Medium	Ratio in Glycogen Particles	Ratio in Simulated Medium
No ligand added (before dialysis)	0.48	0.45	0.70	0.58
No ligand added (after dialysis) *	0.65	0.65	0.70	0.58
Glucose-6-phosphate added (11.7 mM)	0.48	0.45	0.50	0.50
IMP added (21.2 mM)	0.69	0.69	0.69	0.69
ADP added (11.7 mM)	0.62	0.63	0.52	0.51
ATP added (27 mM)	0.62	0.64	-	-

* Measurements made after the glycogen particles / simulated medium had been dialysed into triethanolamine buffer pH 7.0 to remove glucose-6-phosphate.

Table 7.III

The Anomalous Ratio in Modified Glycogen Particles

50 μ M spin labelled phosphorylase α was added to samples of variously treated glycogen particles. After addition, the ESR ratio was recorded as a function of time and extrapolated to time zero.

<u>treatment</u>	<u>Ratio (at t = 0)</u>
Control particles	0.70
1 mg/ml trypsin for $\frac{3}{4}$ hour followed by 1 mg/ml trypsin inhibitor	0.69
1 mg/ml pronase for 1 hour	0.60
particles dialysed into 50 mM TEA, 100 mM KCl, 1 mM EDTA pH 7	0.69
heat treated particles (50°C for 10 minutes)	0.60
1% Glucose added	0.61
particles dialysed into 5M urea. Urea was then removed by dialysis into TEA buffer pH 7	0.60
particles diluted 10 times into TEA buffer pH 7	0.61

phosphorylase in the presence of IMP, ADP, ATP and glucose-6-phosphate is the same in a solution of purified glycogen as in the glycogen particle fraction. Preliminary studies indicate that incorporation into the glycogen particle fraction does not grossly alter the affinity of phosphorylase for these ligands (177).

It is not yet clear why spin labelled phosphorylase a exhibits an anomalous ESR ratio in the glycogen particle fraction. The most obvious explanation is that the effect is due to an interaction between phosphorylase and a macromolecular component in the glycogen particles such as a protein or glycogen. Since the anomalous ESR ratio cannot be produced by adding purified proteins or carbohydrates to spin labelled phosphorylase a, it could be that the change in conformation is due to an interaction with one or more as yet unpurified proteins on the surface of the glycogen.

Table 7.III lists the ESR ratio observed when spin labelled phosphorylase a is added to glycogen particles which have been variously treated. The anomalous ESR ratio is observed in dialysed or trypsin treated particles but is not observed in pronase treated or diluted glycogen particles. Interestingly the presence of 1M Glucose removes the anomalous ratio. Possibly this is due to the high concentration of glucose competing phosphorylase a off the surface of the glycogen. Glucose has no effect on the ESR ratio of spin labelled phosphorylase a in the simulated glycogen particle medium.

C. Ca²⁺ Dependent Transient Activation

Fig. 7.2 shows a series of ³¹P NMR spectra recorded during a calcium dependent transient activation of the glycogen particle fraction. Phosphate-containing ligand concentrations have been deduced using similar spectra recorded during transient activations under a variety of conditions.

At this stage it is important to mention two points. The first is technical and relates to the way the data were collected in the kinetic experiments. In order to reduce the time necessary for accumulating the spectrum at each point, a relatively rapid pulse sequence was used in the Fourier transform mode. This can result in truncation errors and consequently a systematic error in the absolute concentrations of the substrates. But for each substrate the time course of the reaction will follow the true variation in concentration.

The second point is that only in cases where the ligand is in rapid exchange between the free and bound forms is "total" ligand measured. In the slow exchange situation the resonances of the bound ligands would be too broad to be observed under the conditions of the experiments described above (although in fact it is possible to study bound ligands by ³¹P NMR). Since it is not yet known which of these conditions is applicable in the glycogen particle and since the measured ligand concentrations are in considerable excess over the concentrations of the enzymes, to the first approximation, the measurements represent free ligands. To relate these to the way the small molecules modify the enzyme functions (and in particular those of phosphorylase) it is necessary to correlate the NMR observations with activities and the ESR measurements.

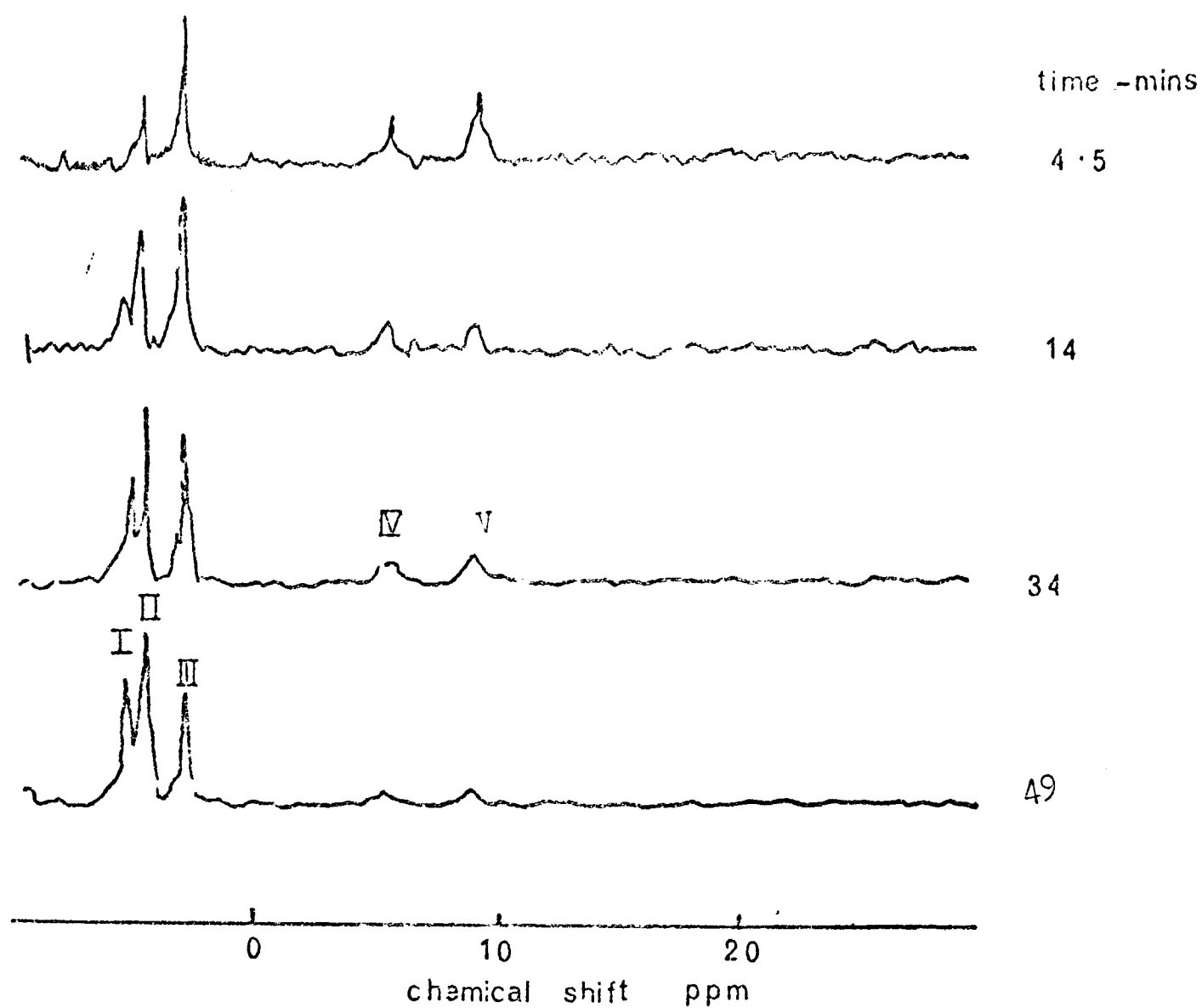


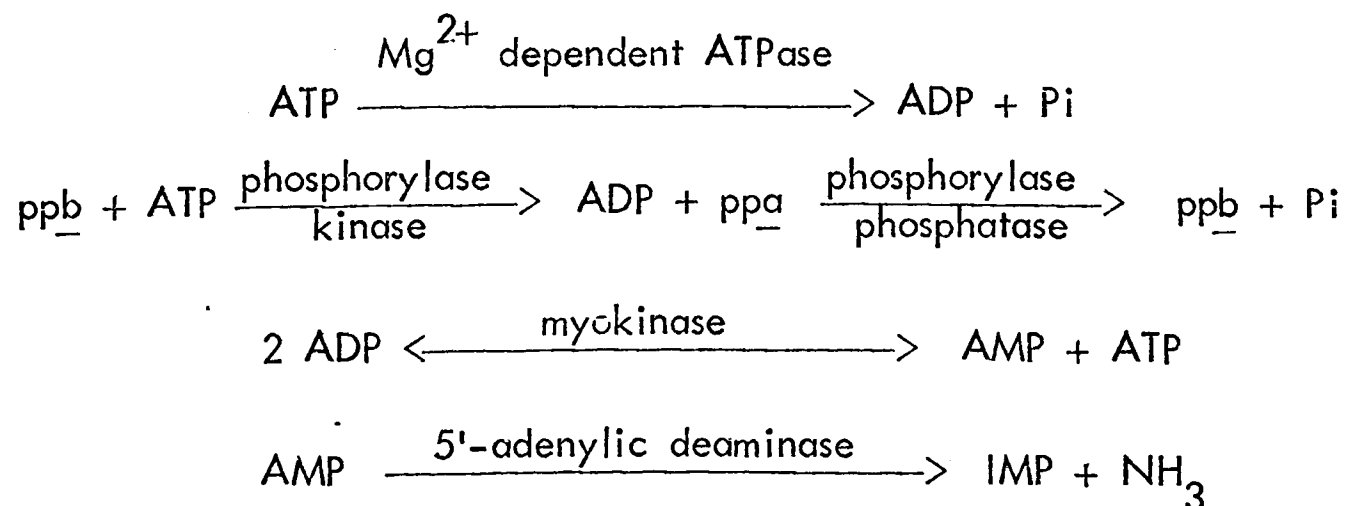
Figure 7.2

Series of phosphorus NMR spectra recorded at different times during calcium dependent transient activation

5 mM $MgCl_2$, 2 mM $CaCl_2$, 20 μM spin labelled phosphorylase b and 27 mM ATP (added at $t = 0$) were added to the glycogen particle fraction. Each spectrum is 50 scans with a pulse interval of 3 seconds. Spectra were recorded at 129 MHz with a sweep width of 5 KHz. Peak I is due to glucose-6-phosphate, II to AMP and IMP (NMP), III to inorganic phosphate, IV and V to ADP.

Fig. 7.3 shows the time course of changes in phosphorylase activity throughout transient activation. Changes in the ESR ratio (R , see Chapter 2 section D) from added spin labelled phosphorylase \underline{b} and associated changes in the concentrations of phosphate-containing small ligands, deduced from spectra similar to those shown in Fig. 7.2 are also shown in Fig. 7.3. The measurements illustrated in Fig. 7.3 were made concurrently on identical samples. A large ATP concentration was used to extend the duration of transient activation and to ensure that the concentrations of metabolites would be high enough to be observable during the process.

It is evident that rapid ATP utilization leads to a small transient accumulation of ADP and a large rise in nucleotide monophosphate levels. Unfortunately, AMP and IMP resonances have the same chemical shifts and using phosphorus NMR it is impossible to separate these two components in a mixture. However, from the high level of 5'-adenylic acid deaminase (which catalyses an irreversible reaction (198)) it is clear that no sustained accumulation of AMP concentration could take place. The nucleotide interconversions which take place during transient activation in the glycogen particle fraction are:



FLASH ACTIVATION OF PHOSPHORYLASE IN GLYCOGEN PARTICLES

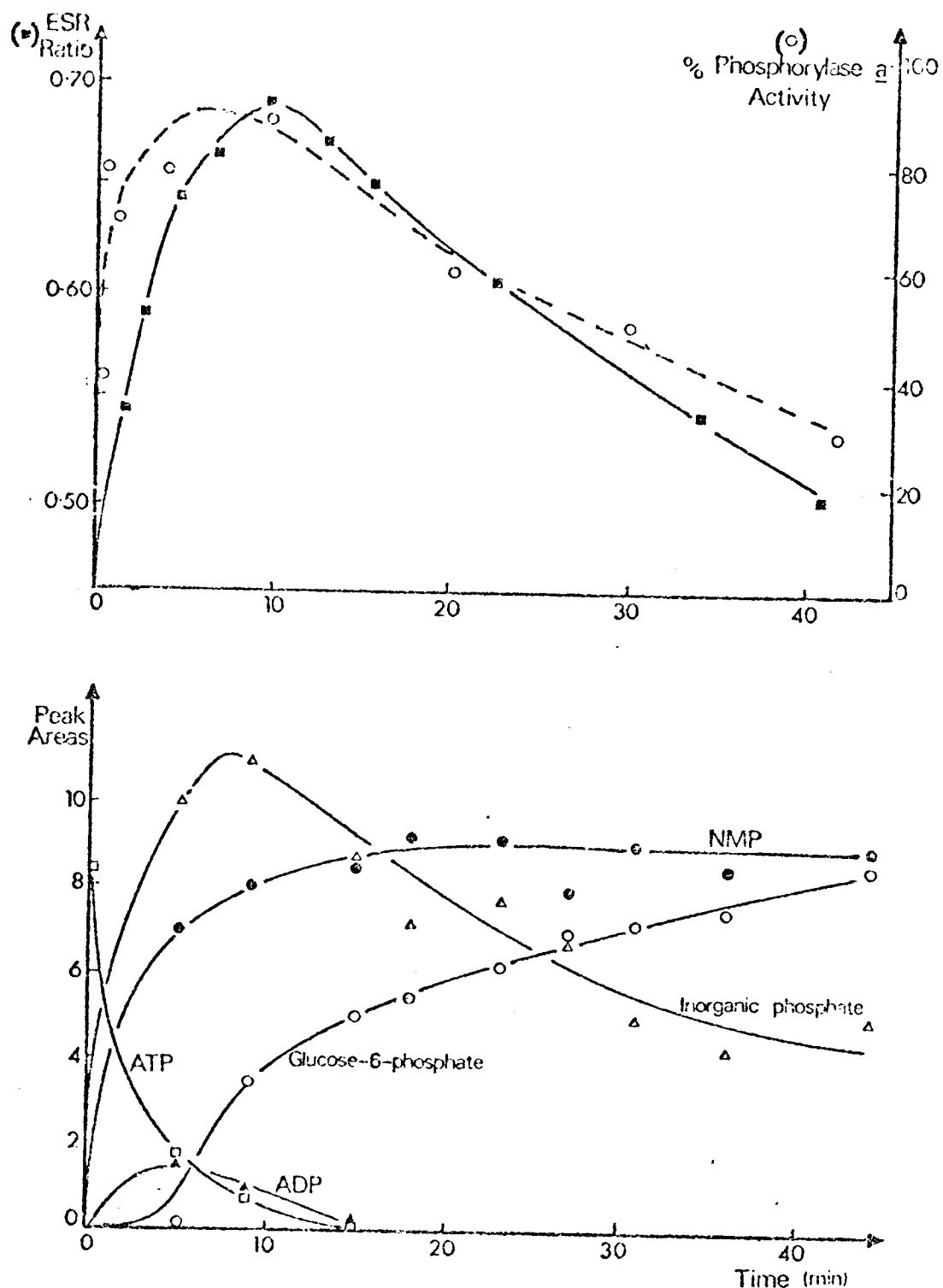


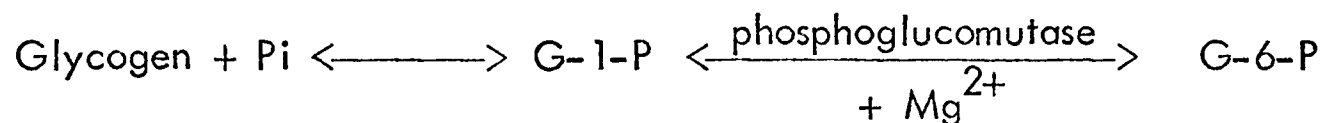
Figure 7.3

Changes in ESR ratio, phosphorylase α activity and ligand concentrations during Ca^{2+} dependent transient activation at high Mg^{2+} and ATP concentration

$42 \mu\text{M}$ spin labelled phosphorylase b was added to a glycogen particle suspension (in the triethanolamine buffer described in the Appendix). 25 mM MgCl_2 , 2 mM CaCl_2 , and 27 mM ATP (added at $t = 0$) were used for transient activation. The upper graph shows changes in the ESR ratio (\blacksquare) and phosphorylase α activity (\circ) (expressed as a % of maximum phosphorylase α activity). The lower set of curves show the relative concentration of each metabolite throughout activation as detected by ^{31}P NMR: NMP is the sum of the "concentrations" of AMP and IMP, which cannot be separated by this technique. Phosphorus NMR spectra were recorded at 129 MHz . Sweep width 5 KHz ; pulse interval 3 s . Each spectrum was 50 scans.

Other experimental details are given in Appendix 2G.

The inorganic phosphate level rises rapidly due to the degradation of ATP but then falls as a result of the breakdown of glycogen by phosphorylase a. Glucose-1-phosphate and hence glucose-6-phosphate are formed:



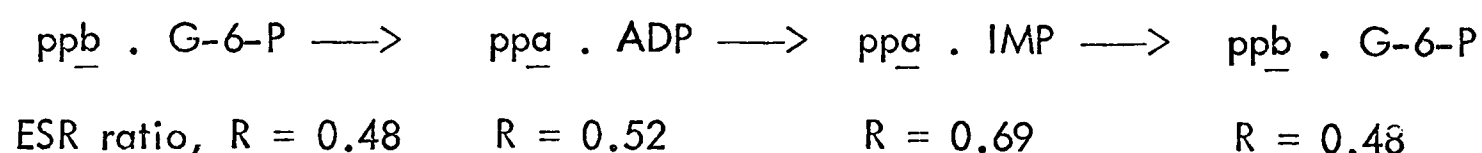
The concentration of glucose-1-phosphate remains low as the equilibrium of the reaction catalysed by phosphoglucomutase is 17:1 in favour of glucose-6-phosphate. The glucose-1-phosphate resonance in the NMR spectrum occurs as a small shoulder slightly downfield of the inorganic phosphate resonance, and cannot be measured accurately.

The glycogen particulate preparation, even when prepared using the triethanolamine buffer system described above, contains 300-500 μM glucose-6-phosphate and phosphate. Since the dissociation constant of glucose-6-phosphate and phosphorylase b is 50 μM , phosphorylase b in the glycogen particulate preparation will have glucose-6-phosphate bound to it. This is indicated by the ESR ratio from spin labelled phosphorylase b in this medium (Fig. 7.3 and Table 7.11). The ratio (0.48) is characteristic of the phosphorylase b - glucose-6-phosphate - glycogen complex rather than the phosphorylase b glycogen complex which is formed after addition of phosphorylase to the dialysed glycogen particulate fraction (Table 7.11).

Addition of ATP, Mg^{2+} and Ca^{2+} causes 80% conversion of phosphorylase b to a in $\frac{1}{2}$ minute. This active phosphorylase a level is maintained for 10 minutes. When the ATP has been exhausted, dephosphorylation and reconversion to phosphorylase b takes place. Although the phosphorylase b to a conversion occurs within $\frac{1}{2}$ minute of addition of ATP, the ESR ratio does

not rise to the value characteristic of phosphorylase a in the glycogen particle mixture until 7 minutes after the initiation of transient activation (Fig. 7.3 and Table 7.11).

Over the period 1-10 minutes activity measurements indicate that 80-90% of the phosphorylase is in the a form whereas the ESR ratio exhibited by the spin labelled phosphorylase is variable. This is due to alterations in the ligand binding to phosphorylase a during this period. The binding constants of phosphorylase a for glucose-6-phosphate, ADP and IMP are 6 mM, 35 μ M and 6 mM respectively (11). Because glucose-6-phosphate binding to phosphorylase a is 120 times weaker than to phosphorylase b, phosphorylation is associated with a loss of glucose-6-phosphate from the enzyme. From a comparison of the characteristic ESR ratios for the various phosphorylase a ligand complexes and the relative metabolite levels at various stages of the transient activation cycle, the following sequence of ligand/enzyme interactions is proposed:



In this treatment it is assumed that nucleotides compete for the same site on phosphorylase a as has been demonstrated for the isolated enzyme (101). Thus the rise in the ESR ratio between 2 or 6 minutes (Fig. 7.3) is due to an increasing concentration of phosphorylase a/IMP complex ($R = 0.69$) replacing the phosphorylase a/ADP complex ($R = 0.52$). Since a large amount of ATP (25 mM) is added in the experiments a high concentration of IMP is formed in the later stages of transient activation, eventually saturating phosphorylase a.

There was no evidence of formation of phospho-dephospho phosphorylase hybrids (the ab form) during transient activation. This species is active in the

absence of AMP but, like phosphorylase b, is inhibited by glucose-6-phosphate (153). No inhibition was caused by 1 mM glucose-6-phosphate when the active form of phosphorylase from a transiently activated glycogen particle suspension was assayed at 75 mM glucose-1-phosphate. It is concluded that the ab form of phosphorylase does not accumulate, even during the early stages of transient activation.

Fig. 7.4 shows a typical transient activation at low ATP concentrations. Changes in phosphorylase activity and in the ESR readout from added spin labelled phosphorylase were recorded. The lag of the ESR response behind the rise in phosphorylase activity is smaller than that observed in Fig. 7.3. Because of the difficulty of obtaining ESR spectra in the first two minutes of transient activation, it is sometimes impossible to observe this lag at very low ATP concentrations. By analogy with the experiment at high concentrations one can interpret this lag as due to transient binding of ADP to newly formed phosphorylase a. At this and lower concentrations of ATP, the IMP formed will not be sufficient to saturate all the phosphorylase a but since the ESR ratio from unliganded and IMP bound phosphorylase a in the glycogen particles is identical, the ESR spectrum gives no definitive indication of the presence of unliganded phosphorylase a (Table 7.11).

D. Transient Activation at Lower Mg^{2+}/Ca^{2+} Ratios

Whilst it has been shown that the transient phosphorylation of phosphorylase b is physiologically significant, the rapid turnover of nucleotides in the glycogen particle fraction is not. Tissue ATP, ADP, AMP and IMP

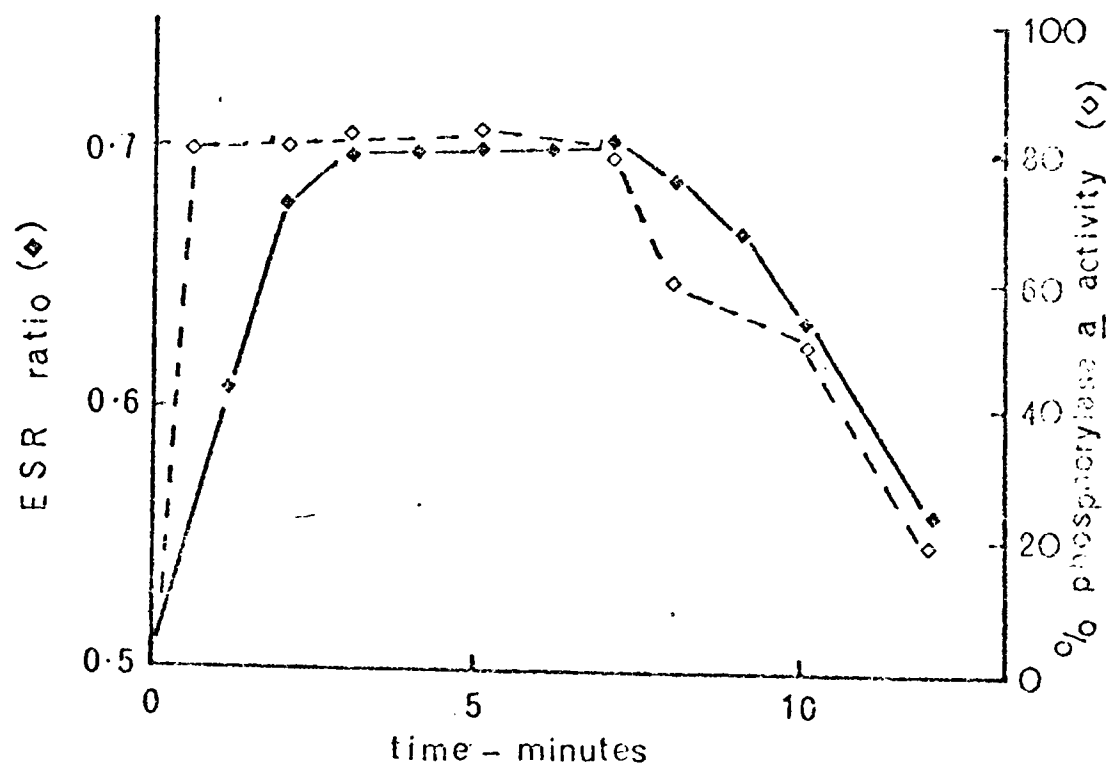


Figure 7.4

Changes in ESR ratio and phosphorylase a activity during Ca^{2+} dependent transient activation at low ATP concentrations

$50 \mu\text{M}$ labelled phosphorylase b was added to a glycogen particle suspension. Transient activation was initiated by the addition of 10 mM MgCl_2 , 2 mM CaCl_2 and 6 mM ATP , at $t = 0$. The ESR ratio (◊) and phosphorylase a activity (◊) were followed as a function of time. Phosphorylase a activity is expressed as % of the maximum.

FLASH ACTIVATION OF PHOSPHORYLASE IN GLYCOGEN PARTICLES

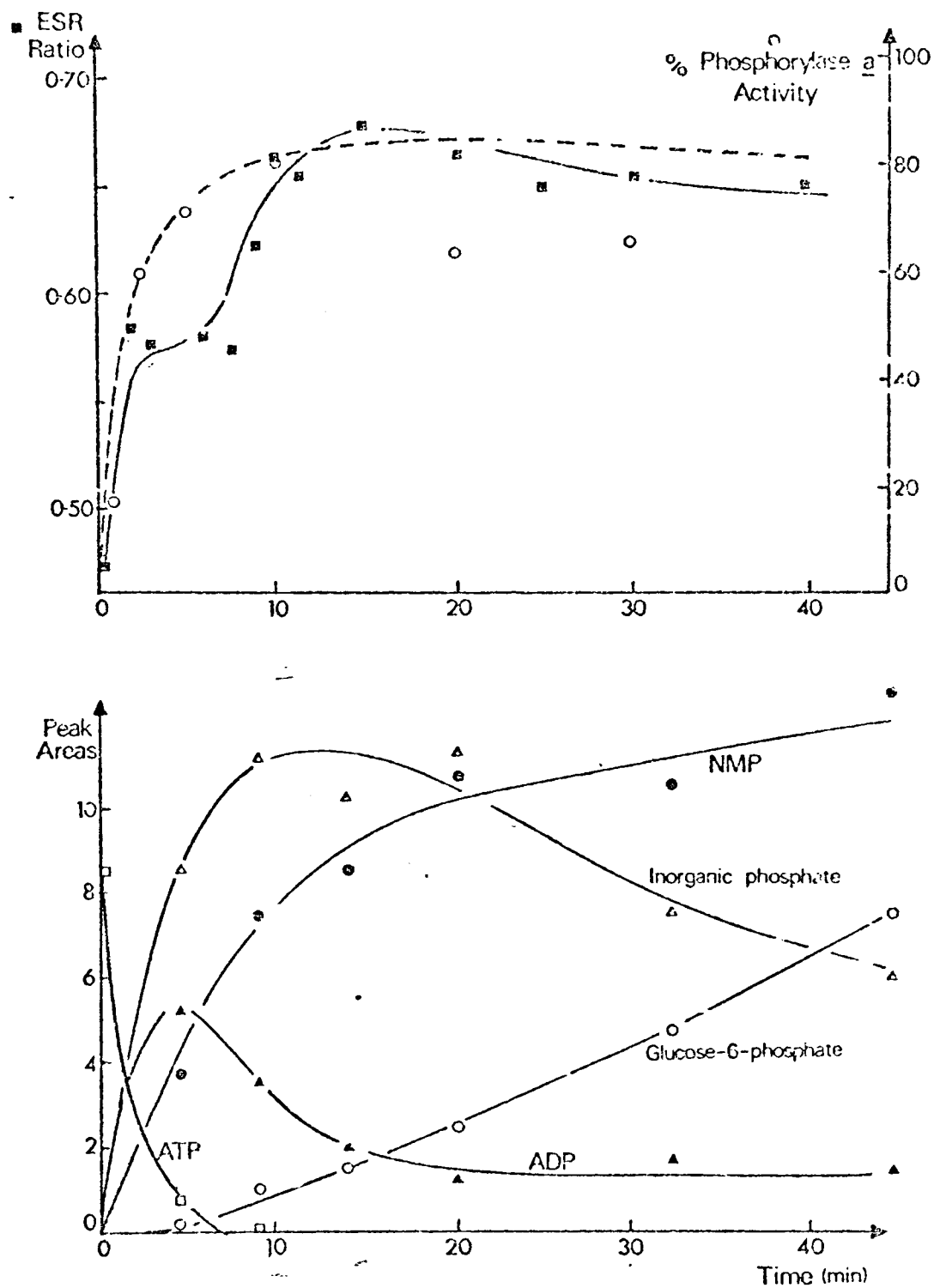


Figure 7.5 Changes in the ESR ratio, phosphorylase a activity and ligand concentrations during Ca^{2+} dependent transient activation at low Mg^{2+} concentration

Conditions as in Fig. 7.3 except that 5 mM MgCl_2 is used

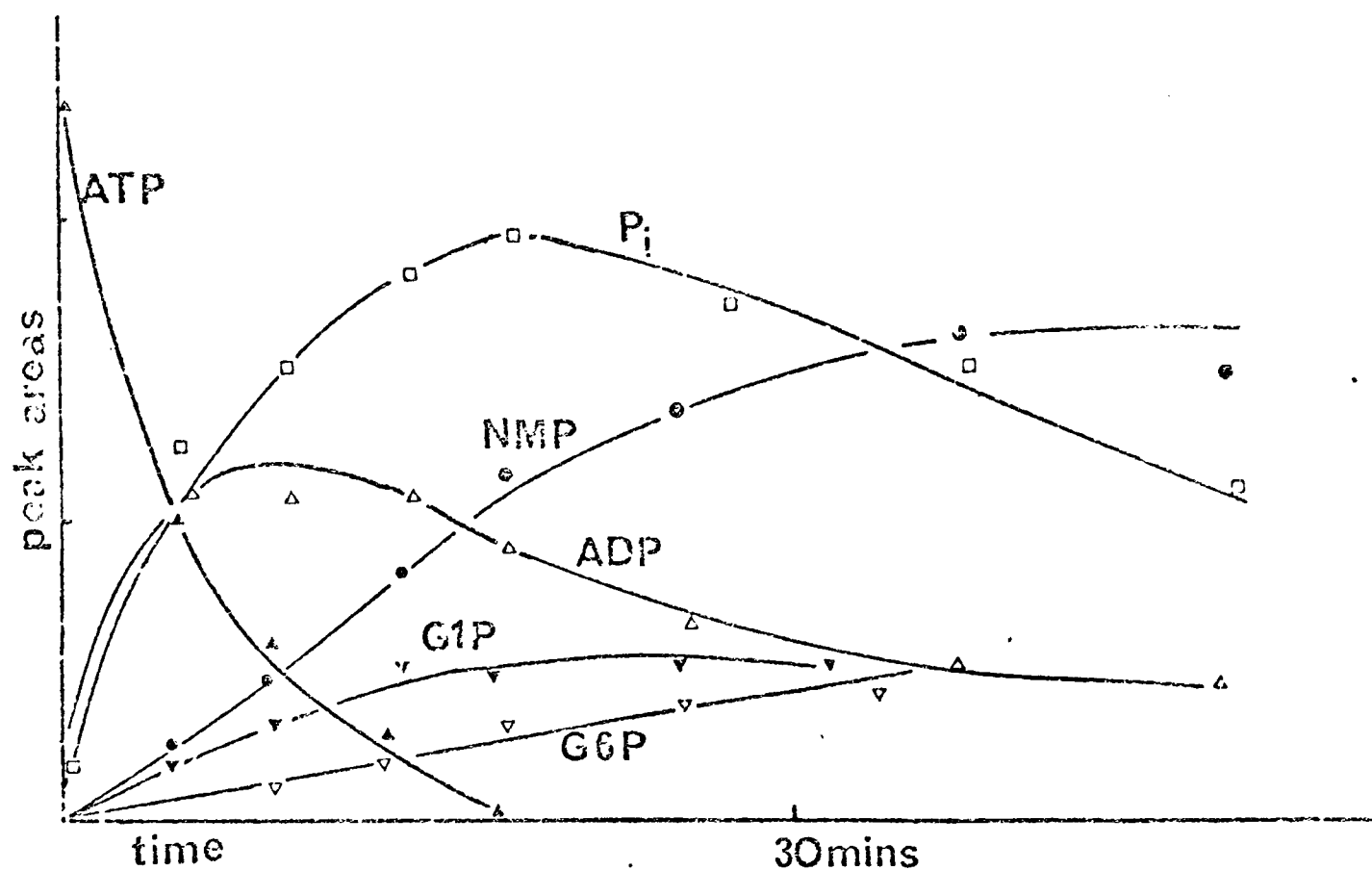


Figure 7.6 Changes in ligand-concentrations during transient activation at low Mg^{2+} and high Ca^{2+} concentration
 Conditions as in Fig. 7.3, except that 5 mM $MgCl_2$ and 5 mM $CaCl_2$ is used

levels alter on excitation of muscle but do not "drain" to IMP as in Fig. 7.3 (179). In vivo the myokinase equilibrium is maintained whereas in the glycogen particle fraction, this equilibrium is displaced by the action of 5'-adenylic acid deaminase. As no specific 5'-adenylic acid deaminase inhibitor is available, an attempt to find less direct methods to stabilize the nucleotide levels in the glycogen particle fraction was made. Decreasing the magnesium ion to calcium ion ratio in the transient activation mixture causes stabilization of the nucleotide levels.

Fig. 7.5 shows the nucleotide turnover in glycogen particles flash activated with 27 mM ATP 5 mM Mg^{2+} and 2 mM Ca^{2+} . Compared to Fig. 7.3, it is clear that the ADP level is stabilized. The activation of phosphorylase b is somewhat slower than in Fig. 7.3, but there is a very much longer lag in the rise of the ESR ratio. This is due to the longer maintenance of the phosphorylase a.ADP glycogen complex before ADP is replaced by IMP.

The change in the metal ion concentrations also leads to a reduction in the rate of glucose-6-phosphate production (compare Fig. 7.3, Fig. 7.5 and 7.4). This is because phosphoglucomutase activity is reduced at the higher Ca^{2+}/Mg^{2+} ratio (29). In Fig. 7.6 changes in metabolite levels during transient activation at almost equimolar Ca^{2+} and Mg^{2+} levels are shown. Under these conditions the ADP level is stabilized even longer than in Fig. 7.5.

E. Does transient activation in the glycogen particle fraction tell us anything about transient activation in vivo?

It is generally accepted that there are two distinct mechanisms of phosphorylase regulation; covalent phosphorylation and interaction with regulator ligands. Correlation of NMR, ESR and activity measurements, shows that under a variety of effector conditions, covalent phosphorylation is associated with a change in occupancy of the various ligand binding sites on phosphorylase. The continuous variation in ligand binding can then provide additional fine control of enzyme activities and thus modify the relation between ATP availability and the time course of the transient activation.

The ligand composition of the glycogen particle fraction during transient activation is not similar to that in the physiological environment. Even under conditions of severe exercise, the concentration of adenine nucleotides is not greatly reduced by 'draining' to IMP (179). This chapter, however, demonstrates that in the glycogen particle fraction, any nucleotide which accumulates can bind to phosphorylase a. Binding of AMP and ADP to purified phosphorylase a is tight and positively cooperative. The dissociation constants are 10 and 2 μM for AMP and 35 μM for ADP (101, 144). Since muscle AMP levels are in the range of 50-400 μM and ADP levels range up to 1 mM (180), it is likely that in vivo phosphorylase a binds these effectors. Parmeggiani and Morgan have suggested that phosphorylase b in resting muscle is inhibited by ATP and glucose-6-phosphate (181). Thus it is likely that the phosphorylase b to a conversion in vivo is associated with expulsion of glucose-6-phosphate and ATP and a take-up of ADP and AMP. Although it is well known that nucleotides inhibit phosphorylase phosphatase activity in purified enzyme systems

by binding to phosphorylase a (173), it has been suggested that such inhibition does not take place in the glycogen particle fraction (171). Chapter 8 is a detailed discussion of the relation between nucleotide binding to phosphorylase a and phosphorylase phosphatase inhibition in the glycogen particle fraction.

F. Ligand Induced Changes in Phosphorylase Conformation without Activation

Transient phosphorylation of phosphorylase b in the glycogen particle fraction is a Ca^{2+} dependent effect. If no Ca^{2+} is present, no phosphorylation takes place. However, added ATP is slowly hydrolysed to ADP by magnesium dependent ATPases in the fraction. Subsequent conversion of ADP to AMP and IMP ensues. Glucose-6-phosphate is competitive with AMP, ADP, ATP and IMP binding to phosphorylase b (101, 89). However, AMP and ADP bind more tightly to phosphorylase b than IMP and ATP and hence have a greater tendency to reverse glucose-6-phosphate binding.

Fig. 7.7 shows the change in the ESR ratio when ATP and magnesium ions are added to spin labelled phosphorylase b in the glycogen particle fraction. The transient rise in the ESR ratio is associated with the accumulation of ADP that is subsequently converted to IMP.

G. Trypsin Treatment of Glycogen Particles

The effect of limited trypsin attack on the glycogen particle fraction was examined. A suspension of glycogen particles was incubated with trypsin (1 mg/ml) at 25° . After 45 minutes two equivalents of trypsin inhibitor

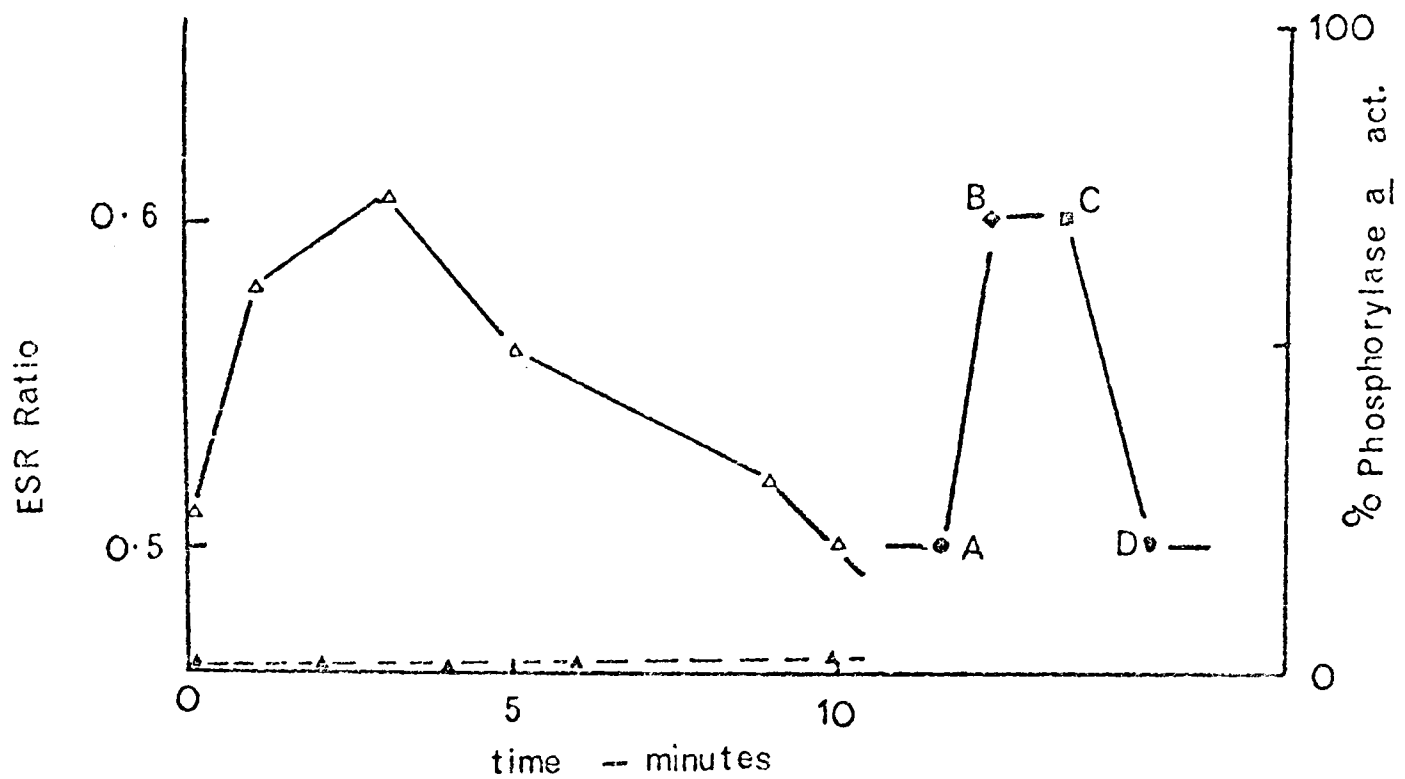


Figure 7.7 Changes in activity (Δ) and ESR ratio (Δ) on addition of ATP and MgCl₂ to glycogen particles

50 μM spin labelled phosphorylase b, 10 mM MgCl₂ and 3 mM ATP (as at t = 0) are added to a glycogen particulate suspension. Phosphorylase a activity (Δ) and the ESR ratio (Δ) are monitored. Points A-D represent: A, D - the characteristic ESR ratio for phosphorylase b / glucose-6-phosphate complex and B, C the ratio for the phosphorylase b / ADP complex (see Table 7.2).

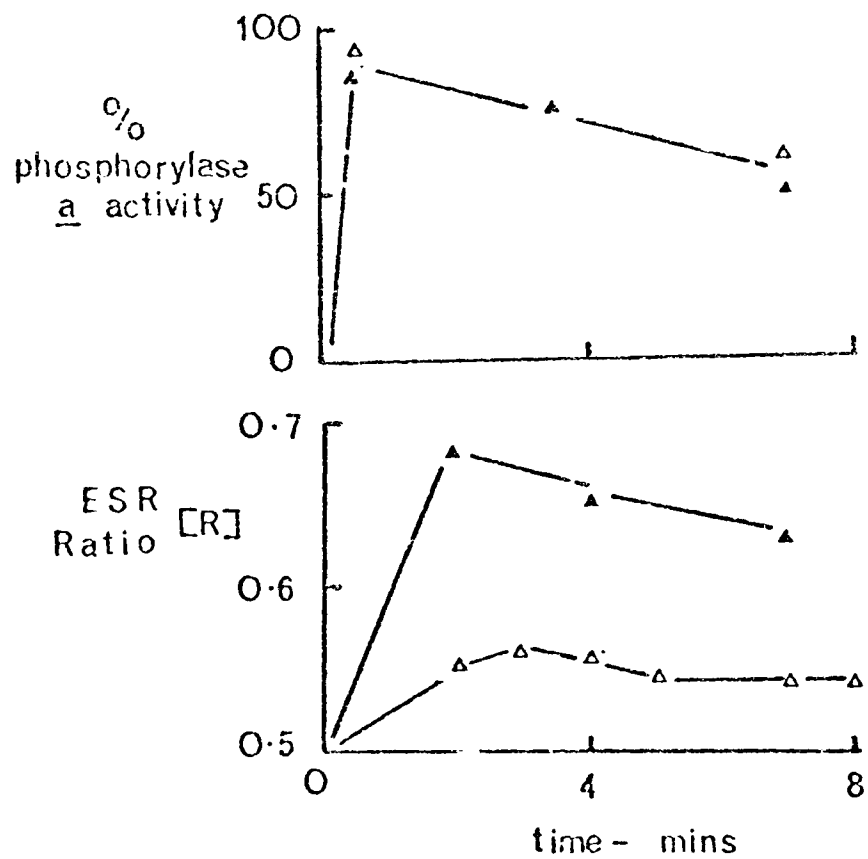


Figure 7.8

Effect of tryptic digestion on transient activation of glycogen particles

The change in ESR ratio and phosphorylase a activity before (▲) and after (Δ) treatment with trypsin as described in the text. $110 \mu\text{M}$ spin labelled phosphorylase b is transiently activated by the addition of 9 mM MgCl_2 , 2 mM CoCl_2 and 15 mM ATP (at $t = 0$). Phosphorylase a activity is expressed as % of maximum.

were added. After the treatment, phosphorylase and myokinase activities were absent whereas phosphorylase b kinase, phosphorylase phosphatase and 5'-adenylic acid deaminase activities remained. $110 \mu\text{M}$ spin labelled phosphorylase b was added to the trypsin treated particle suspension and the mixture was transiently activated. Fig. 7.8 shows the activity changes observed and the associated changes in the ESR ratio before and after trypsin treatment.

Full phosphorylase b to a conversion takes place in both cases within $\frac{1}{2}$ minute. However with the trypsin treated glycogen particle fraction the ESR ratio indicates the presence of the phosphorylase a. ADP complex rather than the phosphorylase a.IMP complex (as in the case of untreated particles). Because, after trypsin treatment, myokinase activity is inhibited, the ADP formed after phosphorylase kinase activity is not converted to AMP and IMP.

H. I strain mice glycogen particles

A comparison of the properties of spin labelled phosphorylase when incorporated in the glycogen/protein complexes of normal and I strain mice was made. Lyon has reported a strain of mice deficient in phosphorylase b kinase activity (182). Cohen and Cohen have demonstrated that muscle extracts from I strain mice contain a protein similar to phosphorylase b kinase but without activity (183). Hence the phosphorylase in their glycogen/protein complex may only be non-covalently activated, although some authors have reported trace kinase activity (184). Glycogen/protein fractions from normal and I strain mice have been isolated by using a scaled-down version of Meyer's acid precipitation method (74).

The glycogen particulate fraction from normal mice is similar to that from

rabbit except that the level of phosphorylase phosphatase in it is very low.

Transient activation of mouse phosphorylase is calcium dependent in this fraction.

The spectral readout from added spin labelled rabbit muscle phosphorylase b in

the mouse and rabbit glycogen fraction during activation is similar. The only

major difference is that the anomalous ratio from phosphorylase a in the mouse

fraction persists because of the low phosphorylase phosphatase levels. When

rabbit muscle spin labelled phosphorylase a is added to the particle suspension

and a simulated medium it is seen that the ratio in the particle suspension rises

to a higher value than that in the simulated medium. The rise to an "anomalous"

ratio, however, is slow compared to the immediate change with rabbit muscle

particles (see Fig. 7.9).

In the I strain mouse glycogen particles, phosphorylase cannot be transiently activated. It is interesting that spin labelled phosphorylase a added to these glycogen particles does not give rise to the "anomalous" ratio found with normal particles. Presumably this is a reflection of the fact that I strain mouse particles have a different gross structure from ordinary mouse glycogen particles. Thus phosphorylase a bound to I strain mouse glycogen particles does not "see" the same molecular interactions as phosphorylase a attached to normal mouse glycogen.

From the studies on glycogen particles it is clear that their properties are not simply the sum of the properties of the component parts. Clearly incorporation of certain components into the fraction does confer special properties upon these components. In order to understand the in vivo regulation of the system it is clearly necessary to define the importance of these interactions.

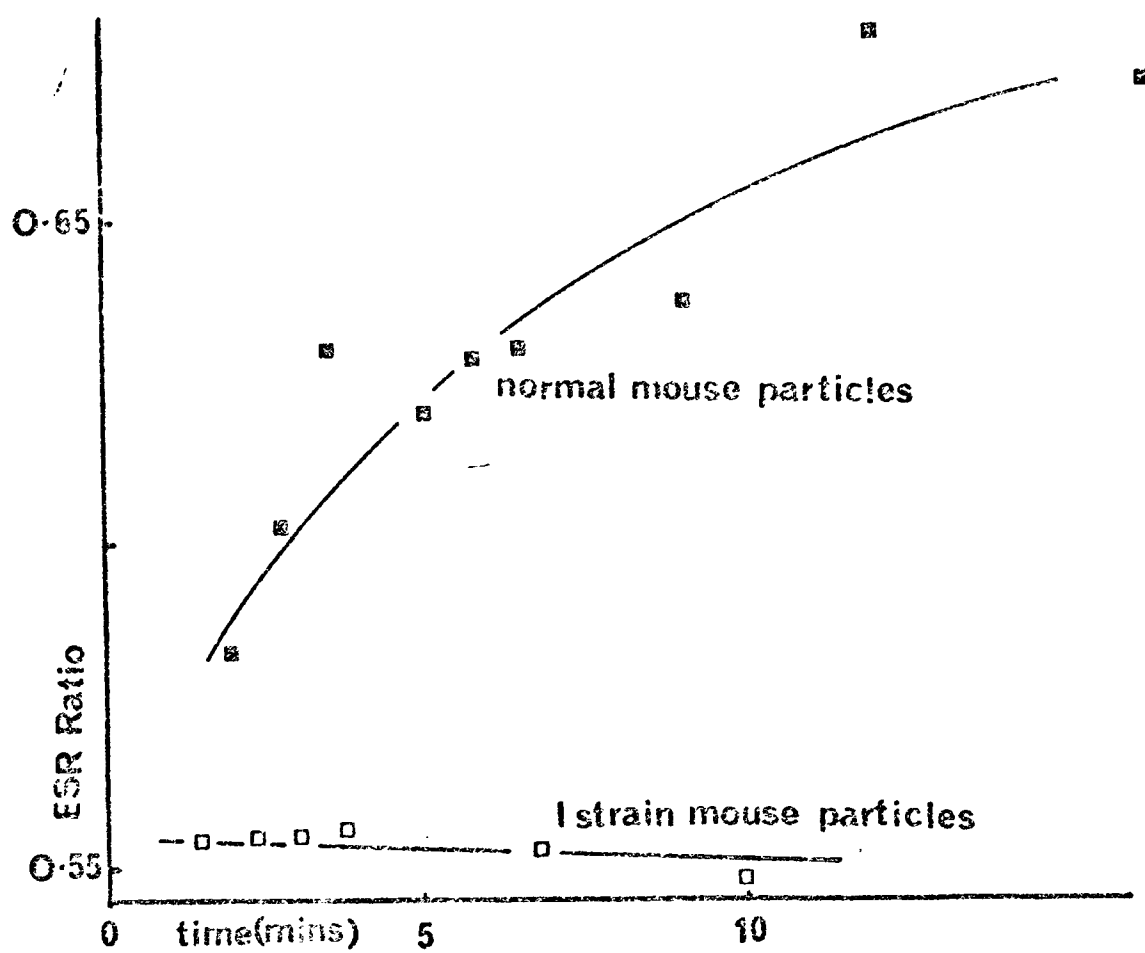


Figure 7.9 Changes in the ESR ratio when spin labelled rabbit phosphorylase α is added (at $t = 0$) to glycogen particles from normal mouse glycogen particles (\blacksquare) or I strain mouse glycogen particles (\square).

Chapter 8

THE CONTROL OF PHOSPHATASE ACTIVITY IN THE GLYCOGEN PARTICLE FRACTION

The regulation of phosphorylase phosphatase activity in vivo and in the glycogen particle fraction must now be discussed. It has already been noted that in vitro phosphatase activity is inhibited by nucleotide binding to the substrate phosphorylase a. As nucleotide binding to phosphorylase a is very tight there has been some doubt as to whether such inhibition takes place in vivo and in the glycogen particle fraction (172). A nucleotide-phosphorylase a complex which was resistant to phosphatase activity would be inconsistent with the speed of a to b conversion reported in glycogen particles and in intact relaxing muscles (75).

Chapter 7 described experiments which showed that in circumstances where nucleotide levels in the glycogen particles were stabilised, phosphorylase a - nucleotide complexes were formed. It was, therefore, proposed that in vivo, where nucleotide levels are stable, transient activation is not only associated with phosphorylation of phosphorylase but also a flux of G-6-P off the b form and a flux of tight binding nucleotides (AMP and/or ADP) on to the a form. If indeed, nucleotide-phosphorylase a complexes are formed in vivo, are they important in regulating phosphatase activity?

This chapter presents an examination of the effects of some nucleotides on phosphatase activity in the glycogen particle fraction. In the case of ADP, phosphatase inhibition is compared with ligand binding to phosphorylase a by using the spin label technique described in the preceding chapter.

Several factors had to be considered before the appropriate measurements could be made.

(a) The glycogen particle fraction contains the contaminant enzymes, myokinase, 5'-adenylic acid deaminase, phosphoglucomutase and sarcoplasmic reticulum ATPase. It is therefore impossible to maintain concentrations of AMP, Mg^{2+}/ADP , Mg^{2+}/ATP or glucose-1-phosphate in order to examine their effect on phosphorylase phosphatase in the glycogen particle fraction. Only the effect of ADP, IMP and glucose-6-phosphate on phosphatase activity could be examined.

(b) Dephosphorylation of phosphorylase a added exogenously to the glycogen particle fraction may be monitored. It is necessary to compare this process to dephosphorylation of phosphorylase a produced by transient activation of the intrinsic phosphorylase b in the glycogen particle mixture. The comparison must be performed under controlled conditions as transient activation initiates a series of ligand fluxes. ADP formed after hydrolysis of ATP is converted to AMP and IMP by the action of myokinase and 5'-adenylic acid deaminase.

(c) The commonly used buffer, glycerophosphate, inhibits purified phosphorylase phosphatase (67,68). A triethanolamine buffer system was therefore selected for these studies.

(d) There are two alternative methods of monitoring glycogen particle phosphorylase phosphatase activity. Release of radioactive phosphate from exogenously added ^{32}P labelled phosphorylase a or decay of AMP independent phosphorylase activity may be monitored. Since with the former method, 'cold' endogenous phosphorylase a is liable to produce apparent inhibition of

phosphorylase phosphatase activity, the latter method was adopted.

A. The Dephosphorylation of Extrinsically added Phosphorylase α

Fig. 8.1 shows the time course of dephosphorylation of phosphorylase α in glycogen particles, after transient activation with 1 mM ATP. The time course of dephosphorylation of an equivalent amount of extrinsically added phosphorylase α is also shown. In both experiments, the magnesium and calcium ion levels were identical. The two rates of dephosphorylation are within 10% of each other, indicating that extrinsically added phosphorylase α is dephosphorylated at a rate similar to intrinsic phosphorylase α (the 1 mM IMP formed from the 1 mM ATP used for the transient activation of phosphorylase causes a slight inhibition of phosphorylase activity).

Fig. 8.2 (curves A and B) shows the rate of dephosphorylation of phosphorylase α , added to the glycogen particle fraction, at different ADP and IMP concentrations. Inhibition takes place as the levels of the two nucleotides are raised, ADP being a more potent inhibitor than IMP. Under these conditions, a 50% decrease in the initial rate of dephosphorylation of added phosphorylase α (or spin labelled phosphorylase α) occurs at 3 mM ADP or 6 mM IMP. Fig. 2 curve C shows the rate of dephosphorylation of phosphorylase α added to a glycogen particle fraction which has been diluted 20 times, at different ADP concentrations. It is apparent that ADP inhibition of phosphatase activity is stronger in the diluted glycogen particle fraction, where dissociation of some of the components occurs. This is confirmed by the

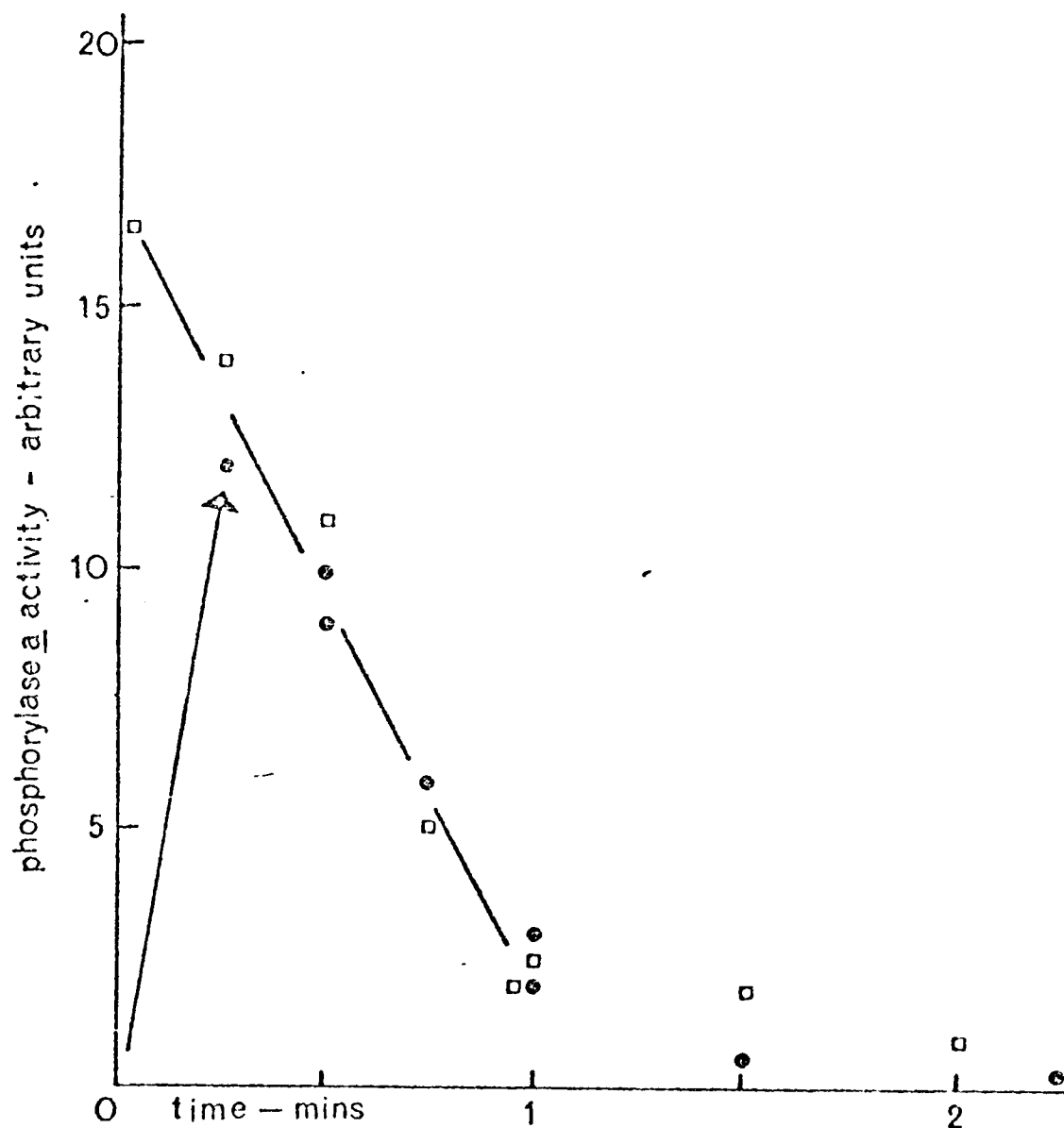


Figure 8.1

Dephosphorylation of intrinsic (●) and extrinsic (□) phosphorylase a

Glycogen particles containing $50 \mu\text{M}$ phosphorylase were transiently activated with 10 mM MgCl_2 , 2 mM CaCl_2 and 1 mM ATP (added at $t = 0$). Phosphorylase a activity was assayed at various time intervals (●) as described in Appendix 2G.

$25 \mu\text{M}$ phosphorylase a was added to a glycogen particle suspension containing 10 mM MgCl_2 and 2 mM CaCl_2 at $t = 0$. Phosphorylase a activity was assayed as above (□).

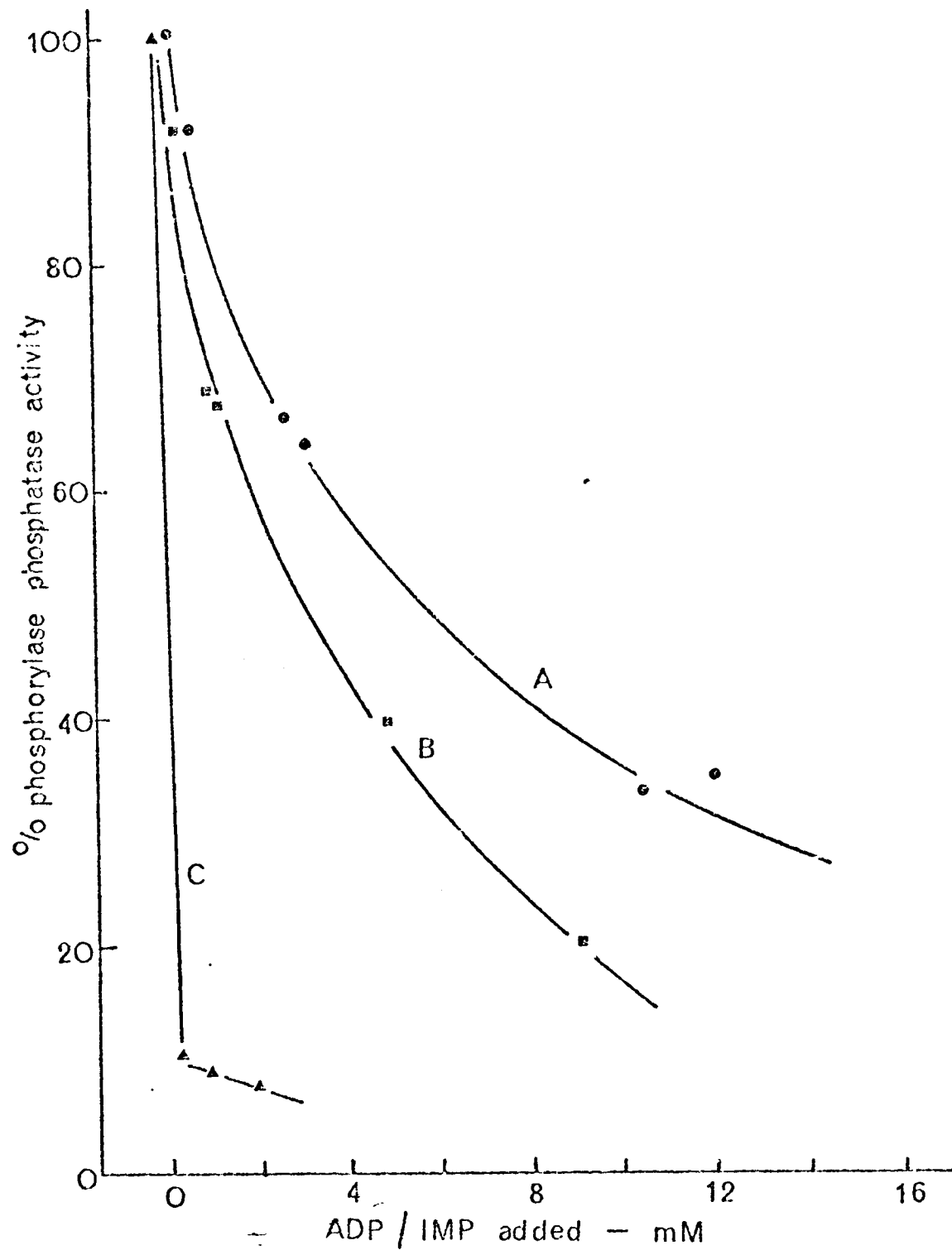


Figure 8.2

Inhibition of phosphorylase phosphatase activity by nucleotides

At $t = 0$, $40 \mu\text{M}$ phosphorylase α was added to: (A) the glycogen particle fraction containing various concentrations of IMP (\bullet): (B) the glycogen particle fraction containing various concentrations of ADP (\square): (C) the glycogen particle fraction diluted 20 times in 50 mM triethanolamine 100 mM potassium chloride, 1 mM EDTA pH 7.0 buffer, in the presence of various concentrations of ADP (\blacktriangle).

Phosphorylase α levels were measured as a function of time in each case. From the rate of disappearance of phosphorylase α , the phosphorylase phosphatase activity was deduced and in case A, B and C is expressed in the figure as a % of the phosphorylase phosphatase activity observed with no added nucleotide.

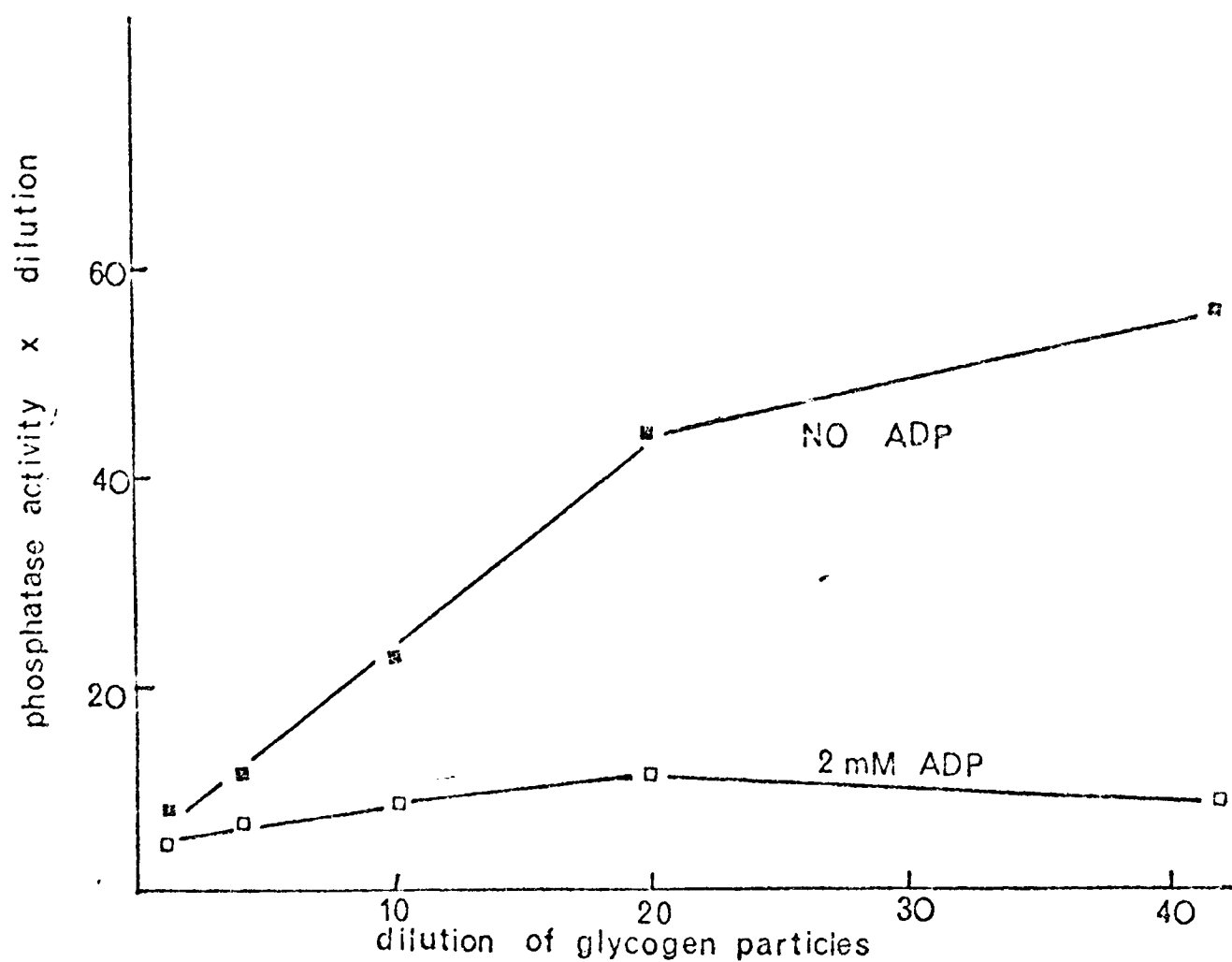


Figure 8.3

Changes in phosphorylase phosphatase activity on dilution of the glycogen particle fraction

40 μ M phosphorylase a was added to various dilutions of the glycogen particulate fraction. Phosphorylase phosphatase activity was measured. Activity \times dilution (i.e. net phosphatase activity) is plotted as a function of dilution with (\square) or without (\blacksquare) 2 mM ADP. The glycogen particulate fraction was diluted into 50 mM triethanolamine, 100 mM potassium chloride, 1 mM EDTA buffer, pH 7.0.

experiment illustrated in Fig. 8.3. Net phosphatase activity in glycogen particles at different dilutions was assayed with or without 2 mM ADP. The proportion of phosphatase activity inhibited by 2 mM ADP at high dilution of particles was greater than at low dilution. In addition dilution was associated with a net increase in specific activity of phosphorylase phosphatase. Addition of 2% glycogen to the diluted glycogen particle fraction did not overcome the ADP inhibition of phosphatase activity. Similar results were obtained using 5 mM IMP instead of 2 mM ADP.

To investigate the nature of inhibition of dephosphorylation of phosphorylase by ADP in the glycogen particles, the experiment illustrated in Fig. 8.2 was repeated using spin labelled phosphorylase a. Fig. 8.4 shows the change in the characteristic ESR ratio (R) at various times after 40 μ M spin labelled phosphorylase a had been added to the glycogen particle fraction in the presence of varying amounts of ADP. When no ADP is present the ratio changes from that for unliganded phosphorylase a in the glycogen particles (0.70) to that for phosphorylase b-glucose-6-phosphate complex (0.48). When ADP is present, since glucose-6-phosphate and ADP bind competitively to phosphorylase b, the final ratio is between 0.48 and 0.63 (the ratio for the phosphorylase b-ADP complex). When ADP is present the starting ratio (obtained from extrapolation to $t = 0$) is between 0.70 and 0.52 (the ratio for the phosphorylase a-ADP complex). As the exact value reflects the amount of phosphorylase a-ADP complex present an apparent binding constant for ADP and phosphorylase a in the glycogen particle fraction may be obtained. From experiments at seven different ADP concentrations, a value for the K_D of ADP of $65 \pm 15 \mu$ M was obtained.

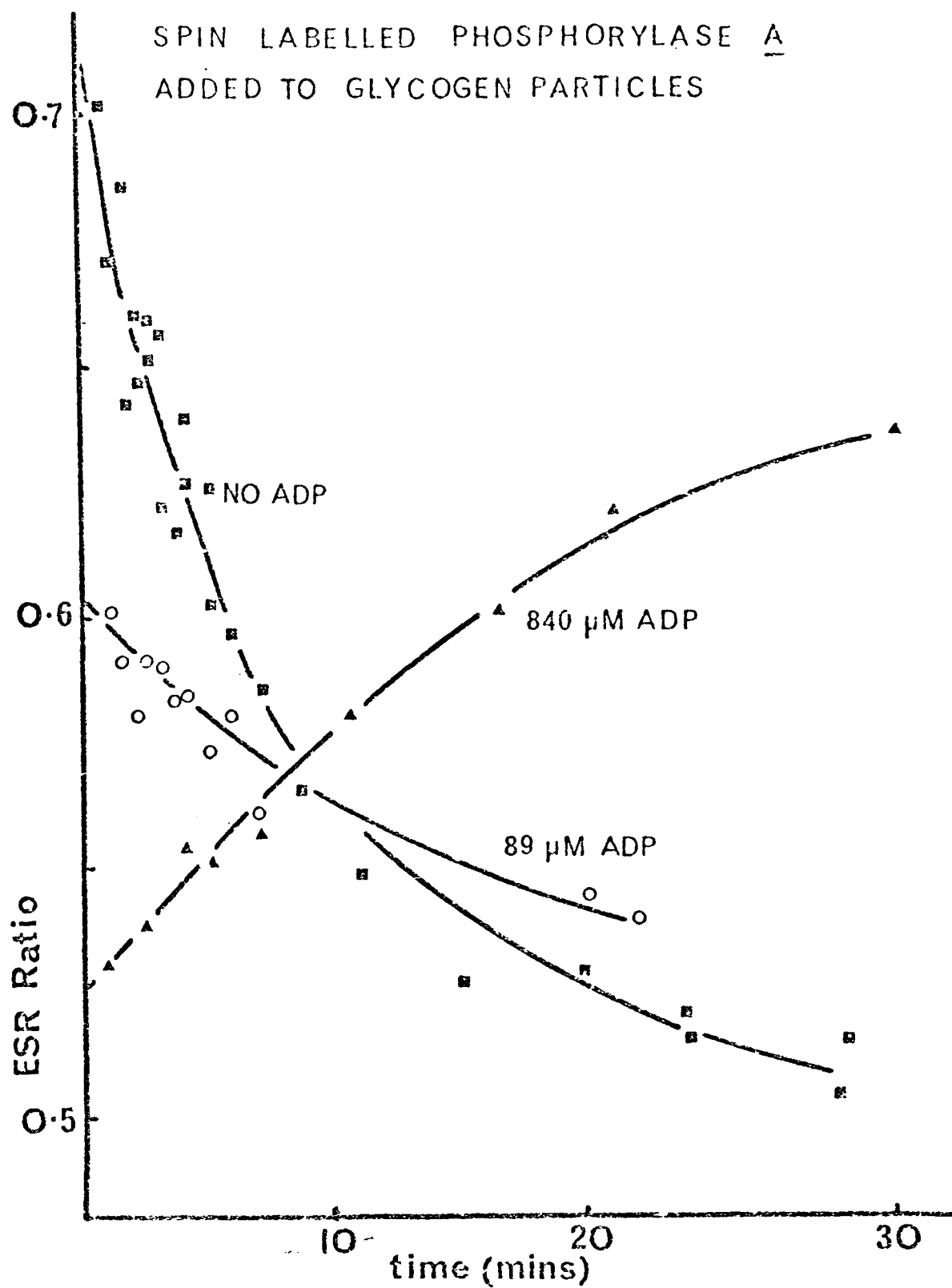


Figure 8.4

Changes in the ESR ratio when spin labelled phosphorylase a is added to the glycogen particulate fraction in the presence of various concentrations of ADP

40 μM spin labelled phosphorylase a was added (at $t = 0$) to the glycogen particulate fraction containing no ADP (\square), 89 μM ADP (\circ) or 840 μM ADP (\triangle). The ESR ratio observed is plotted as a function of time.

Since in the glycogen particle fraction, the K_i for inhibition of phosphatase activity by ADP is 3 mM, it is clear that, in contrast to the situation with purified enzymes, the inhibition is not due to formation of a nucleotide-phosphorylase α complex. For example, at 840 μ M ADP, over 95% of the phosphorylase α is complexed to nucleotide and yet phosphatase activity is less than 30% inhibited (Fig. 8.2 and Fig. 8.4). Unfortunately, it is impossible to determine a dissociation constant for IMP and phosphorylase α as both non-liganded and IMP-binding phosphorylase α exhibit the same ESR ratio in the glycogen particle fraction.

B. The dephosphorylation of phosphorylase intrinsic to the glycogen particle fraction

A second approach which has been adopted is that of monitoring the rate of dephosphorylation of phosphorylase α produced as a result of transient activation in the glycogen particle fraction. Fig. 8.5 shows the time course of transient activation of phosphorylase in the glycogen particle fraction, in the presence of various concentrations of IMP. The dephosphorylation phase of transient activation is slower at higher IMP concentrations. After $\frac{1}{2}$ minute, the added ATP has been exhausted and is rapidly converted to IMP. Since the conversion of AMP to IMP catalysed by 5'-adenylic acid deaminase is irreversible, it is clear that IMP is the species inhibiting phosphorylase phosphatase activity.

A similar experiment was carried out to examine the time course of transient activation initiated by various concentrations of ATP (Fig. 8.6). Previously it has been shown that net decay of phosphorylase α does not

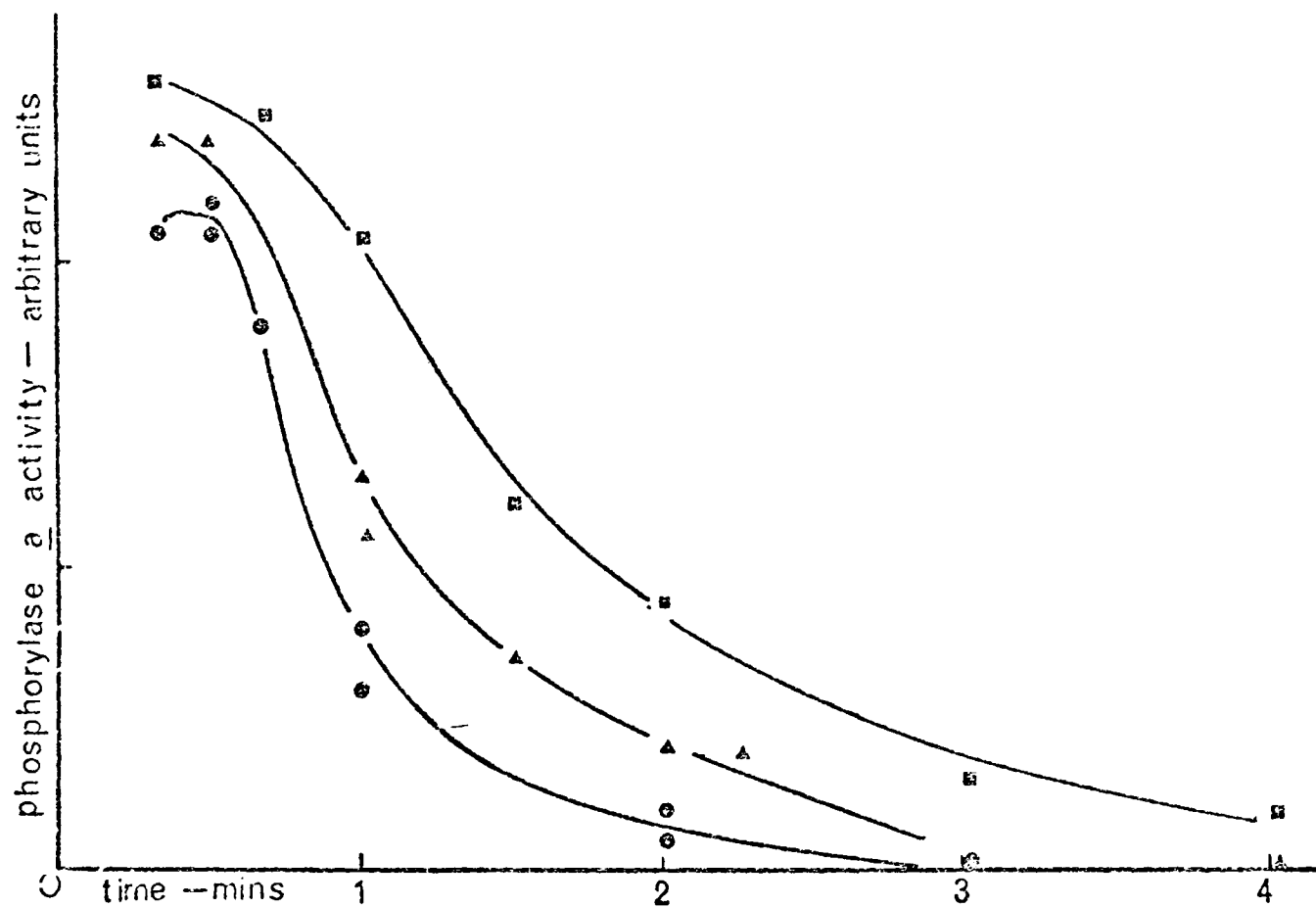


Figure 8.5

Transient activation of the glycogen particulate fraction in the presence of increasing levels of IMP

The glycogen particulate fraction was transiently activated with 2 mM CaCl_2 , 10 mM MgCl_2 and 1.2 mM ATP (added at $t = 0$) in the presence of no IMP (\odot), 2.6 mM IMP (\blacktriangle) and 10.4 mM IMP (\blacksquare). Phosphorylase a activity is plotted as a function of time.

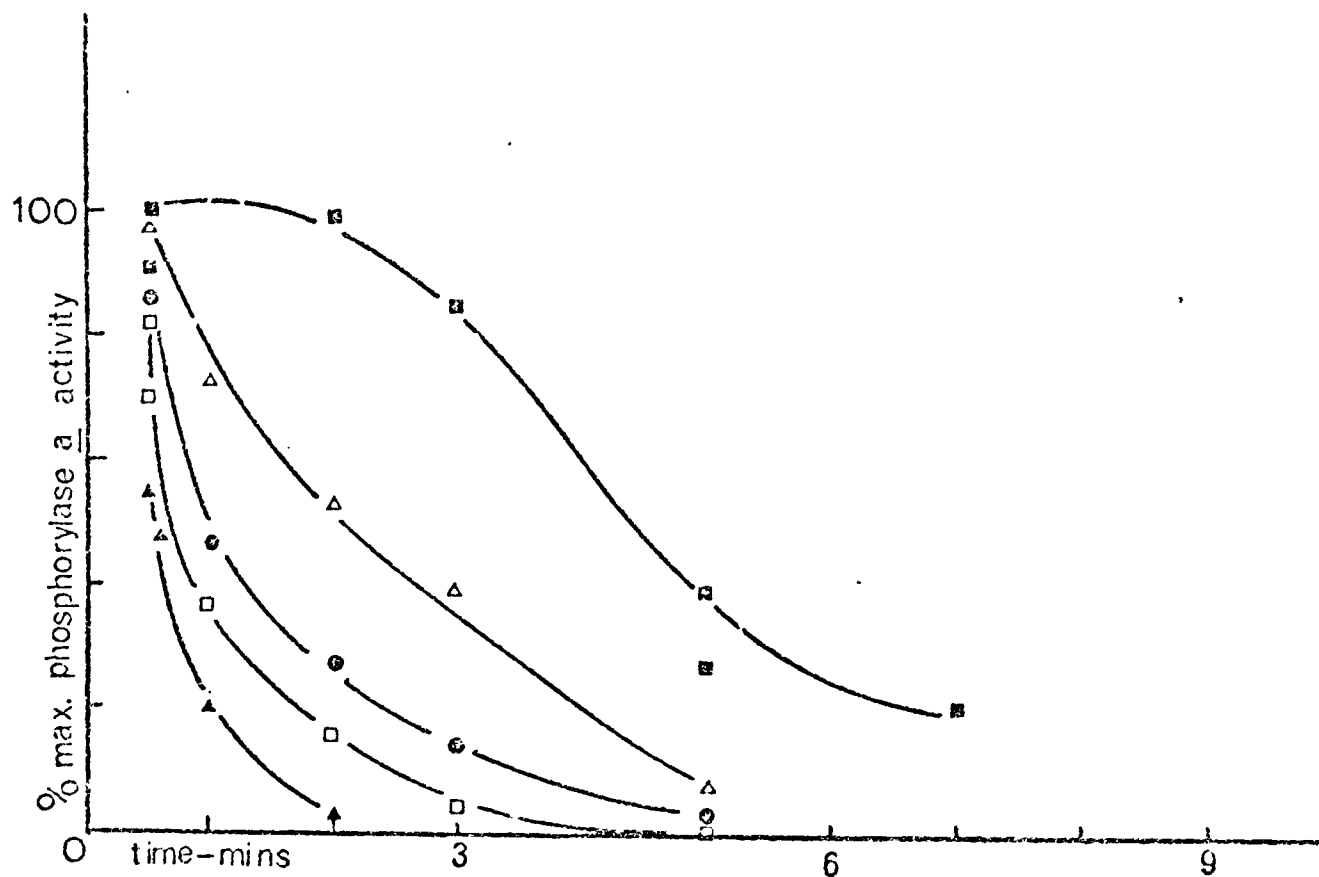


Figure 8.6 Transient activation of the glycogen particulate fraction with increasing levels of ATP

The glycogen particulate fraction was transiently activated with 2.3 mM CaCl_2 , 11.6 mM MgCl_2 and 1.1 mM ATP (▲), 2.2 mM ATP (□), 4.4 mM ATP (●), 8.3 mM ATP (Δ) or 17 mM ATP (⊙). Phosphorylase α activity is plotted as a function of time and is expressed as a % of maximum possible activity.

commence until the ATP supply has been exhausted (164). The dephosphorylation phase of transient activation is slower when activation has been initiated with higher ATP concentrations. This effect could be due to ADP, AMP or IMP accumulation after ATP hydrolysis.

Fig. 8.7 shows the time course of transient activation at high nucleotide concentrations in the presence and absence of glucose-6-phosphate. Glucose-6-phosphate appears to stimulate phosphorylase phosphatase activity, in agreement with the results of Martenson et al. (67,68).

Transient activations have been carried out under conditions where decay of ADP to AMP and IMP is inhibited. Raising the calcium ion concentration and lowering the magnesium ion concentration during transient activation, leads to maintenance of the ADP level in the activation mixture (see Chapter 7). Fig. 8.8 shows the time course of transient activation under different magnesium and calcium ion concentrations. While lowering the magnesium to calcium ion ratio causes inhibition of phosphorylase b kinase, the phosphorylase phosphatase activity in the mixture is also reduced. The inset to Fig. 8.8 shows that lowering the magnesium to calcium ion ratio causes a stimulation of the activity of phosphorylase phosphatase on extrinsically added phosphorylase a (in agreement with Martenson et al. (67,68) who show that magnesium ions inhibit phosphatase activity). This result suggests that inhibition of phosphorylase phosphatase during transient activation at low magnesium / calcium ratios is due to the ADP build up that takes place. A similar result is described in Chapter 7 by Figs. 7.3 and 7.5, which show transient activation at two magnesium to calcium concentration ratios. Lowering the magnesium to calcium ion ratio (Fig. 7.5) results in a

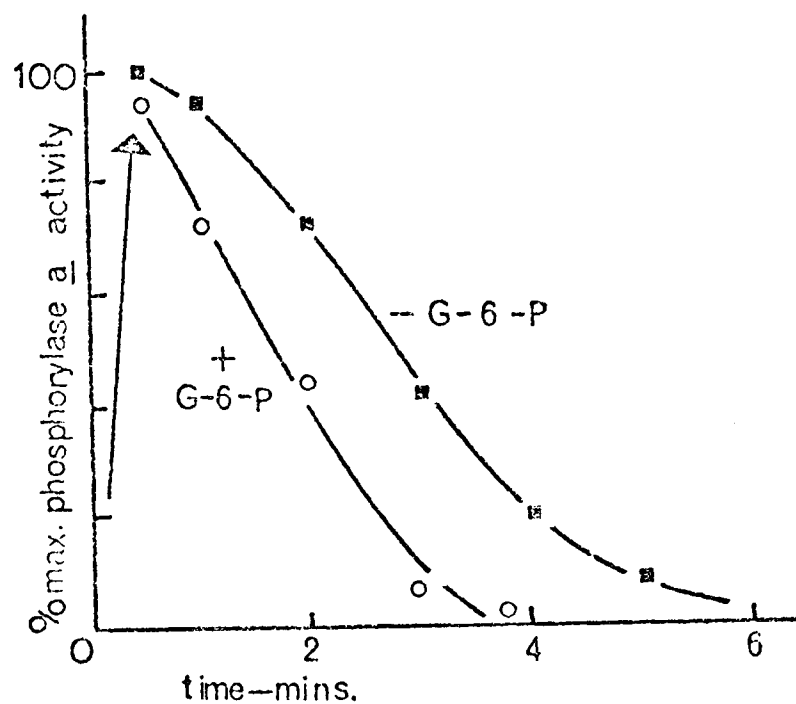


Figure 8.7

The effect of glucose-6-phosphate on transient activation

The glycogen particulate fraction was transiently activated with 10 mM $MgCl_2$, 2 mM $CaCl_2$ and 8.3 mM ATP (added at $t = 0$) with (o) or without (■) 4.4 mM glucose-6-phosphate.

Phosphorylase a activity was measured as a function of time and is expressed as a % of maximum possible activity.

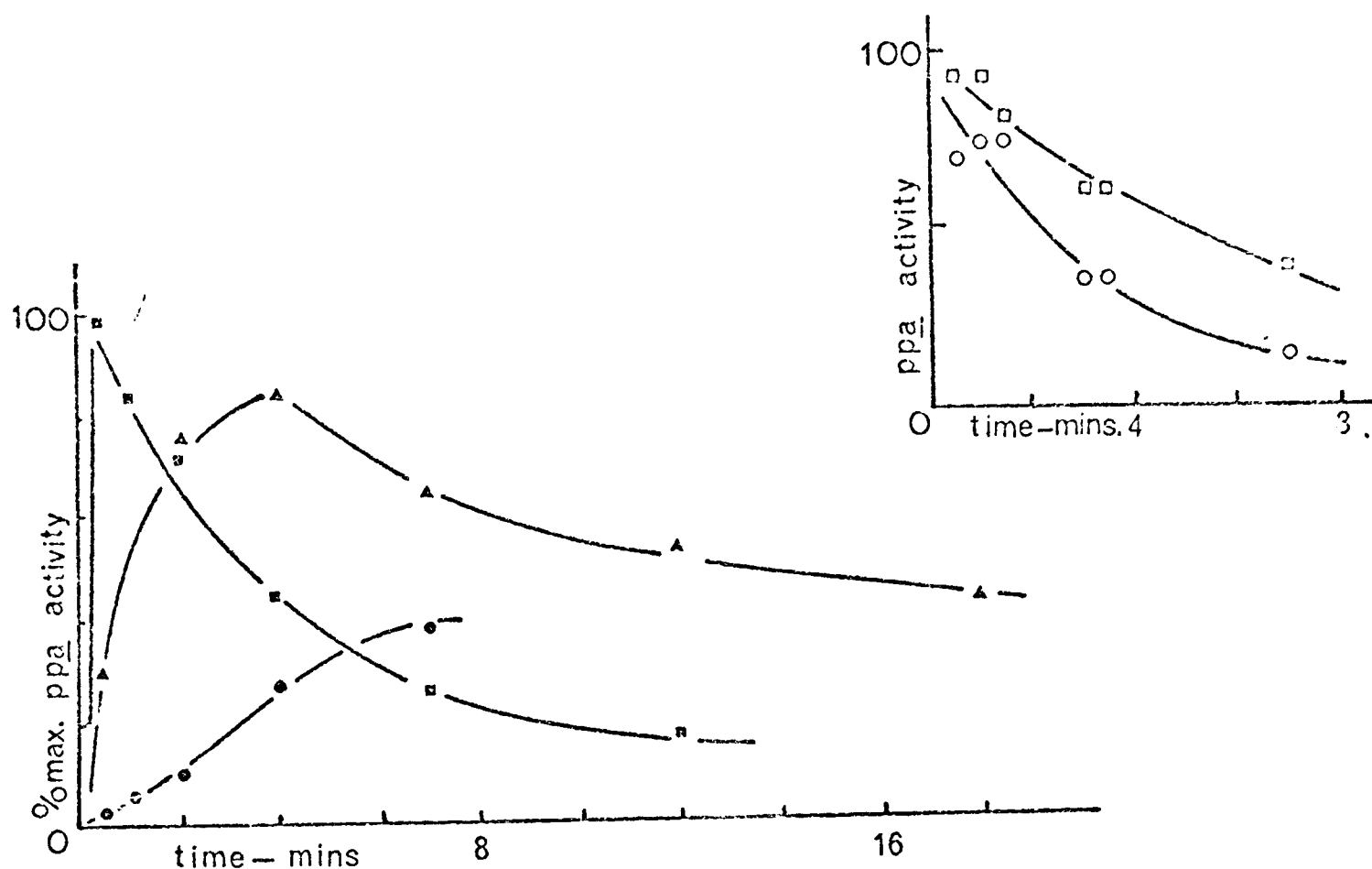


Figure 8.8 Transient activation at different Mg^{2+} / Ca^{2+} ratios

The glycogen particulate fraction was transiently activated with 18 mM ATP (added at $t = 0$) and 9.6 mM $MgCl_2$ and 1.9 mM $CaCl_2$ (□) or 4.8 mM $MgCl_2$ and 3.8 mM $CaCl_2$ (△) or 2.4 mM $MgCl_2$ and 7.6 mM $CaCl_2$ (○). Phosphorylase a activity is plotted as a function of time and is expressed as a % of maximum possible activity.

The inset shows the dephosphorylation of 50 μM extrinsically added phosphorylase a in the glycogen particulate fraction in the presence of 10 mM $MgCl_2$ and 2.1 mM $CaCl_2$ (□) or 2.4 mM $MgCl_2$ and 7.6 mM $CaCl_2$ (○). Phosphorylase a activity is expressed as % of initially added activity.

decrease of phosphatase activity. Fig. 7.5 also clearly shows the ADP build up associated with the alteration in the metal ion concentrations.

C. Discussion and Speculations

This chapter demonstrates that incorporation of phosphatase and phosphorylase into the glycogen particle fraction alters some properties of these enzymes. Firstly, incorporation of these enzymes into the glycogen particle fraction weakens the inhibition of phosphatase activity by ADP and IMP. Secondly, in the glycogen particle fraction, there is an overall inhibition of phosphatase activity. In addition, it is evident that in the glycogen particle fraction the ADP-phosphorylase α complex is susceptible to phosphatase action. With purified enzymes or in a diluted glycogen particle fraction (67, 185, 186) phosphatase activity is inhibited when nucleotides bind to phosphorylase α . The ADP inhibition of phosphatase, observed in the glycogen particles, must therefore be due to weaker ADP binding to a second site on phosphorylase α or to direct ADP binding to phosphatase. The dissociation constant for ADP and glycogen particle bound phosphorylase α is $65 \mu\text{M}$ and is significantly weaker than that obtained for ADP and purified phosphorylase α in the presence of glycogen ($35 \mu\text{M}$ (101)).

It has been suggested that the apparent alterations in the properties of phosphatase and phosphorylase as they are incorporated into the glycogen particles are due to protein interactions in this multi-enzyme complex (135, 159, 187, 191). For example Bot et al. showed that the apparent inhibition of phosphatase in the glycogen particle is due to a specific interaction with phosphorylase β kinase. (159). These experiments do not provide any explanation

for the above effects, but do emphasize the fact that interactions observed using purified enzyme systems must be checked in a more 'life like' situation before extrapolation to the cell. In the glycogen particle fraction the activity of phosphorylase phosphatase, and hence the length of transient activation, may be regulated by nucleotide or sugar phosphate levels. Whilst it is likely that in vivo phosphorylase a binds nucleotides tightly during transient activation, this binding does not lead to the inhibition of phosphatase activity, and thus rapid deactivation of phosphorylase a may take place after phosphorylase kinase is switched off.

Why is it necessary to inhibit phosphorylase phosphatase activity during transient activation in vivo? If phosphorylase kinase and phosphorylase phosphatase both operated at their maximal activities in vivo, maintenance of an adequate level of phosphorylase a even for a short time would require too much ATP. A futile cycle would be produced, similar to that possible between phosphofructokinase and fructose-1-6-diphosphatase (188). Since phosphorylase kinase in the particle fraction acts well below its maximum specific activity, it is doubly important to modulate phosphatase activity in order to maintain phosphorylase a levels. Ideally the cell would adopt a flip-flop mechanism turning off phosphorylase phosphatase when phosphorylase kinase is active (i.e. when Ca^{2+} is present) and vice versa. However, if tight binding of nucleotides to phosphorylase a did inhibit dephosphorylation, in vivo, it is difficult to see how dephosphorylation could ever take place as the phosphorylase a-nucleotide complex would be locked in a phosphatase resistant "active" state. Hence it is proposed that a finer modulation of activity takes place due to a balance between weaker direct inhibition by

nucleotides and, as noted by Martenson et al., activation by sugar phosphates (69). Since phosphorylase is present in such large concentrations, it is certain that very small changes in phosphatase activity can produce large changes in glycolytic flux, the product of which can act as a feedback activator of the phosphatase. On this basis, low energy charge and depletion of glycolytic intermediates cause inhibition of phosphatase and hence potentiation of phosphorylase activity, whilst high energy charge and build up of glycolytic intermediates activate phosphatase and cause phosphorylase activity to be switched off.

Chapter 9THE OBSERVATION OF TISSUE METABOLITES BY
PHOSPHORUS NMR

"...men are invisible nearnesses in the dark, sending out magnetic vibrations of warning..." (235)

Much has been written about the state of the various enzymes involved in the glycogen phosphorylase system in vivo. Many studies have been made of their interaction with ligands, effectors and modifiers. However little has been said about the nature of these ligands inside the muscle or the way in which their "activity" is expressed. Current data rely heavily upon freeze clamp studies (189) and upon equilibrium methods (190). Both methods have built-in disadvantages - the former requires assumptions about compartmentation and sheds no light on metal binding or intracellular pH, whereas the latter method relies on accurate knowledge of the distribution of specific enzymes between different membrane enclosed regions in the cell. It is clear that, to date, no satisfactory method of directly observing the state of metabolites in vivo has been reported.

It has already been shown that phosphorus NMR can give information on the nature of complex mixtures of phosphate containing glycolytic intermediates in subcellular fractions. This chapter shows that phosphorus NMR may be used to observe such metabolites in intact tissue.

The results described in this chapter are obtained using a ^{31}P NMR machine operating at 7.5 Tesla, which was built by Drs. D.I. Hoult and

R.E. Richards. Most of the experiments described here were performed in conjunction with Drs. D.G. Gadian and P.J. Seeley, and have relied heavily on these gentlemen's expertise in magnetic resonance. They follow from the unexpected observation, made with Dr. D.G. Gadian in March 1974, that useful spectra could be obtained from freshly excised intact rabbit muscle tissue. Although the full potential of many of the experiments reported in this chapter has not yet been realised, they are included as they indicate new approaches in the investigation of real physiological situations with physical techniques.

A. Model Studies

Fig. 9.1 shows a phosphorus NMR spectrum of a mixture of phosphorus containing metabolites. Resolution of the resonances is due to differences in the groups attached to the phosphorus atoms in the metabolites. The line positions are sensitive to pH and coordination of the metabolites to magnesium ions. Fig. 9.2 shows a pH titration of the resonances from the α and γ phosphates of ATP in the presence or absence of magnesium ions. Increasing pH causes the resonances to move to a higher frequency. Similar pH titrations of the positions of phosphorus resonances from creatine phosphate, inorganic phosphate and glucose-6-phosphate are shown in Fig. 9.3. These data and the results of titrations of a wide range of phosphorus containing metabolites have been tabulated by Dr. D.G. Gadian (93).

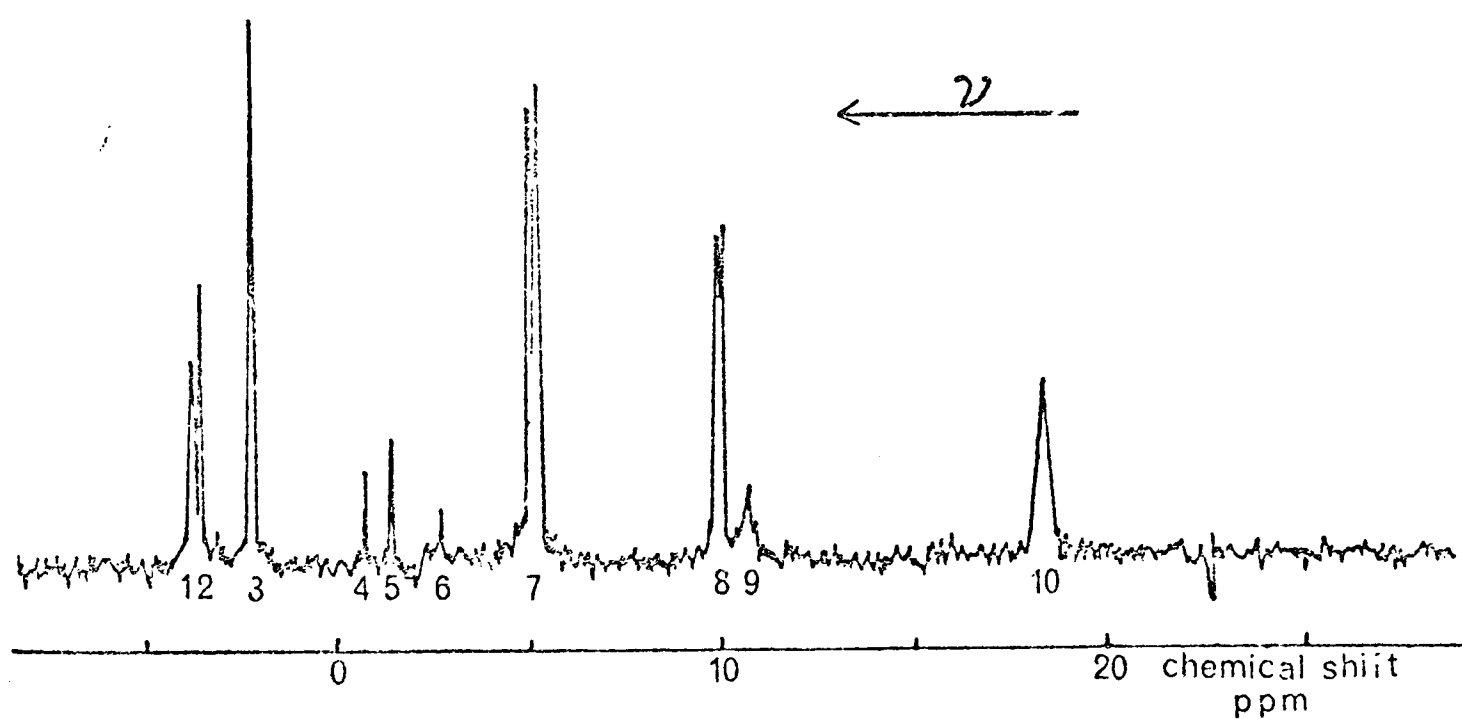


Figure 9.1 Observation of Glycolytic Intermediates by ^{31}P NMR at 129 MHz:

Spectrum width - 5 KHz. Assignments: 1 - 3-Phosphoglycerate, 2 - 2-Phosphoglycerate, 1 & 5 - 1,3-Diphosphoglycerate, 3 - Inorganic Phosphate, 4 - Phosphoenolpyruvate, 6 - Creatine Phosphate, 7,8 and 10 - ATP, 9 - NAD^+ . Zero of the chemical shift scale is the line position from 85% phosphoric acid in water + 5 mM EDTA at 20°C . ν indicates the direction of increasing frequency.

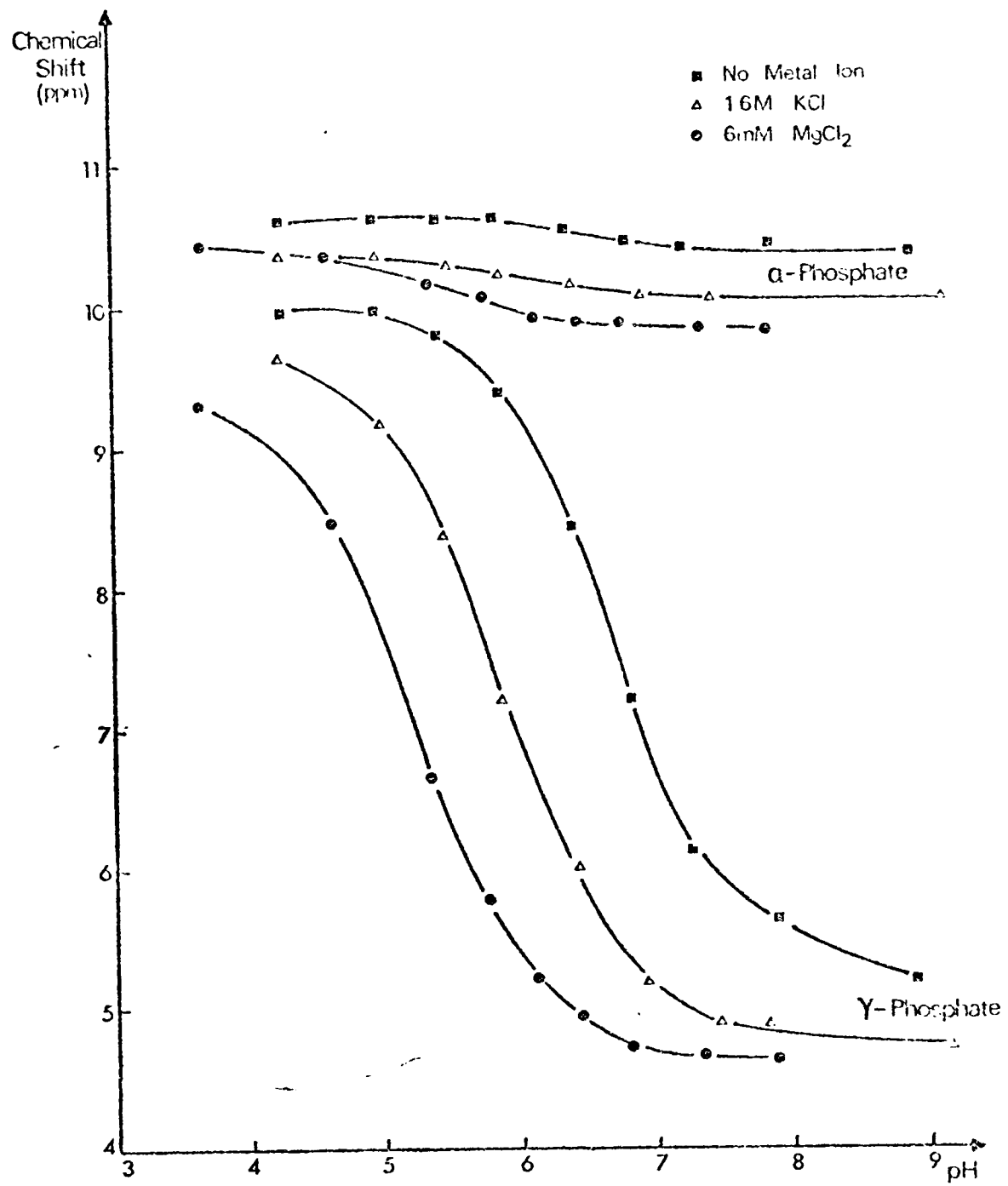


Figure 9.2 pH titrations of 5 mM ATP at 129 MHz

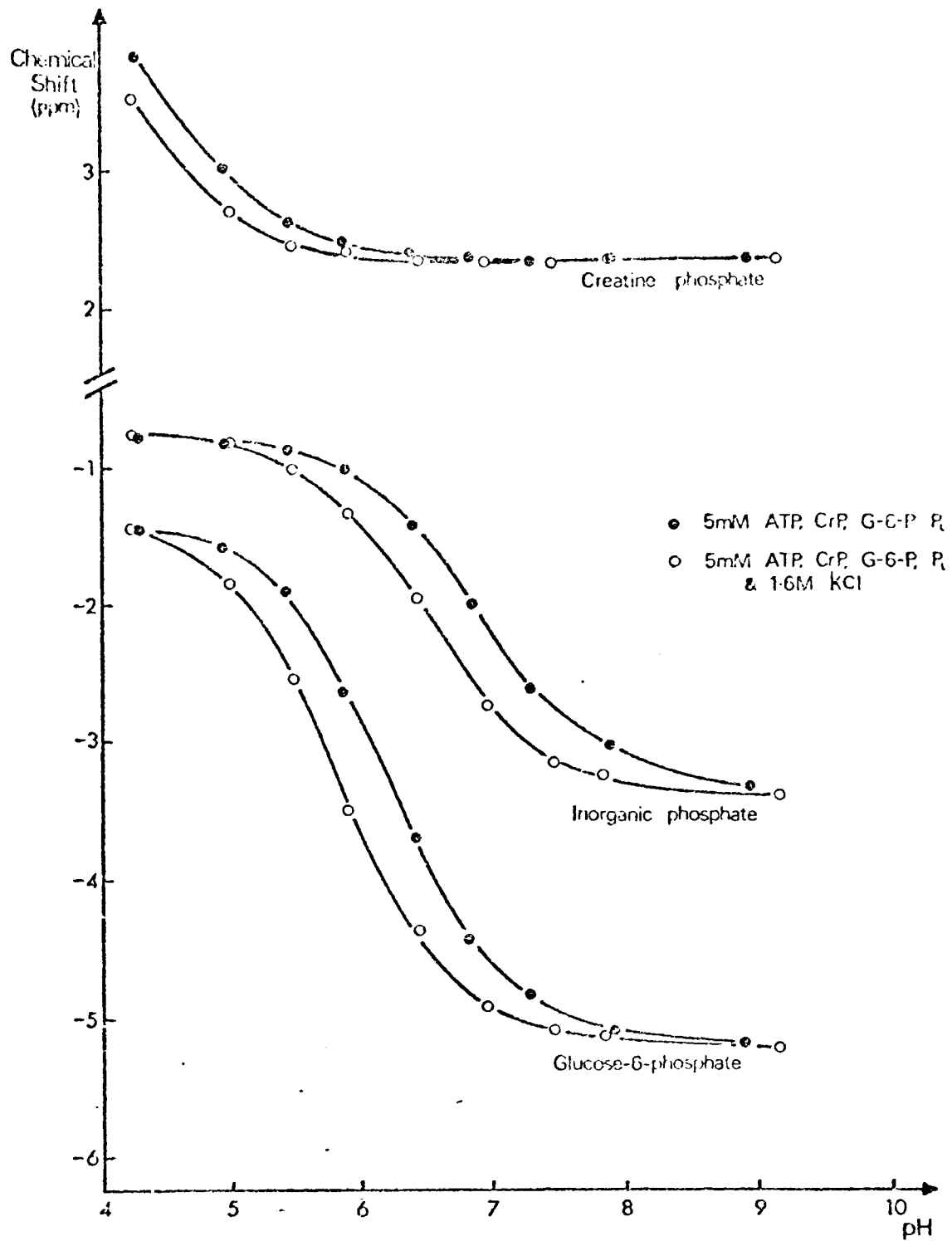


Figure 9.3

pH titrations of Creatine Phosphate, Inorganic Phosphate and Glucose-6-Phosphate

B. Spectra of Intact Tissue

Fig. 9.4 shows the ^{31}P NMR spectrum of an intact, relaxed white muscle, freshly excised from the hind leg of a rat, killed by etheration. Assignments are made on the basis of pH titrations such as those described by Figs. 9.2 and 9.3. Spectra recorded at various times after excision of the muscle are shown. From the spectra several deductions may be made:

(i) The approximate concentrations ($\pm 10\%$) of phosphorus-containing metabolites in the intact muscle may be measured by integration of the NMR spectra, using a sample of known concentration as a standard. Care was taken to avoid saturation of the resonances. There is some variation from muscle to muscle, and the creatine phosphate : phosphate ratio proves to be a sensitive index of the degree of stimulation of the rat muscle before the animal's death. There is a high creatine phosphate : phosphate ratio in rats killed without excessive stimulation. The concentrations of sugar phosphate, inorganic phosphate, creatine phosphate and ATP at intervals between 16 and 170 minutes from excision of the muscle have been measured (Fig. 9.5). Extrapolation along the time axis shows the metabolite levels at the time the muscle was excised to be: sugar phosphate + phospholipid, 6 mM; inorganic phosphate, 6 mM; creatine phosphate, 15 mM; and ATP, 6.5 mM.

Creatine kinase maintains the ATP level constant at the expense of creatine phosphate until all the latter substrate has been used up, demonstrating the ability of the kinase to buffer the muscle ATP concentration.

These results can only be obtained with intact muscle. Samples which are lacerated during handling have only an inorganic phosphate peak in the phosphorus spectrum. Breakdown of organic phosphates by phosphatases is

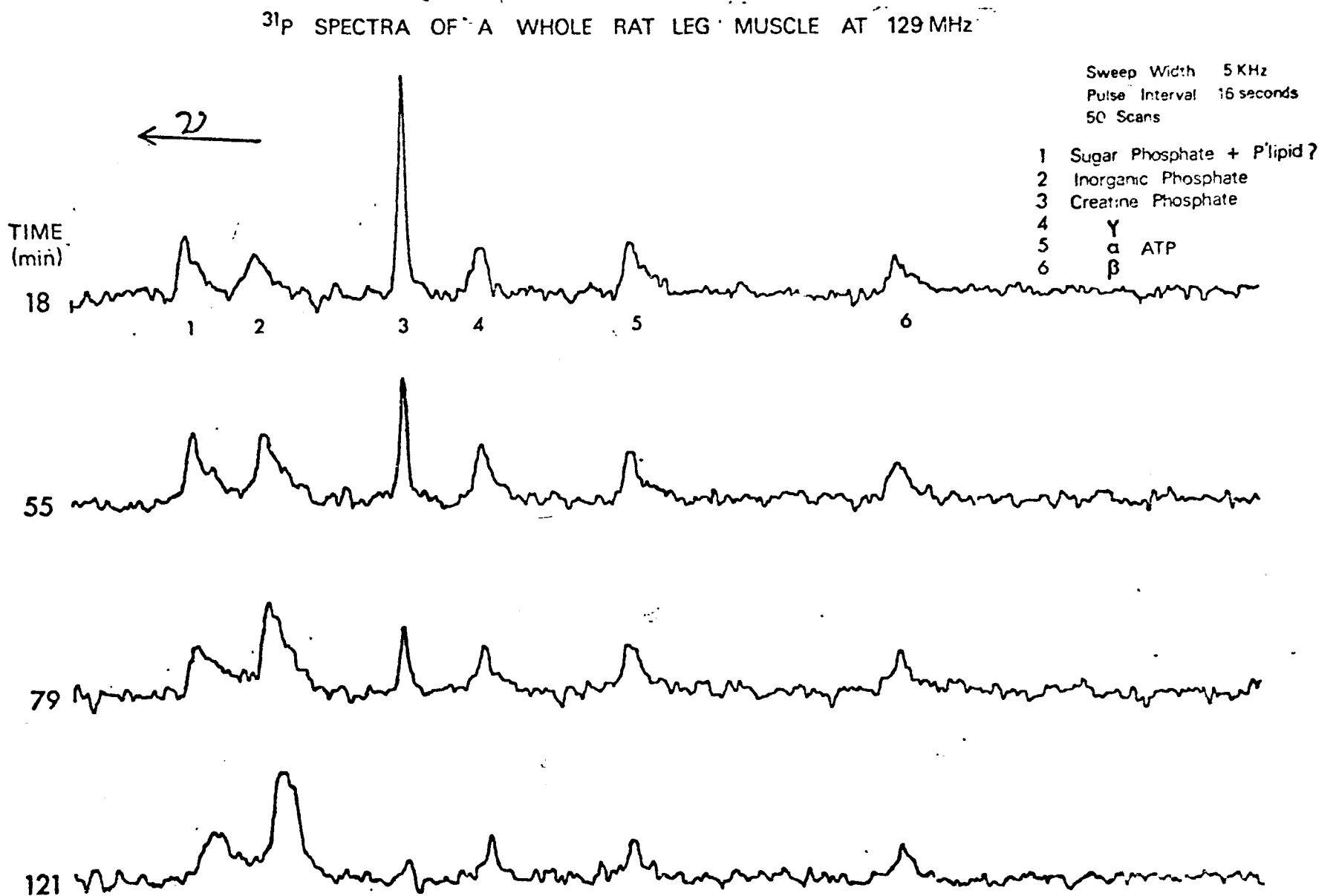


Figure 9.4 ^{31}P NMR spectrum of an intact muscle from the hind leg of the rat recorded at 129 MHz, without proton irradiation. Temperature 20°C and pulse interval 16 s. Peak assignments: 1, sugar phosphate and phospholipid; 2, inorganic phosphate; 3, creatine phosphate; 4, γ ATP; 5, α ATP; 6, β ATP. The times are the midpoints of the 50 scan spectral accumulations (referred to excision time as zero). The muscle was bathed in a minimum volume of calcium-free Locke ringer.

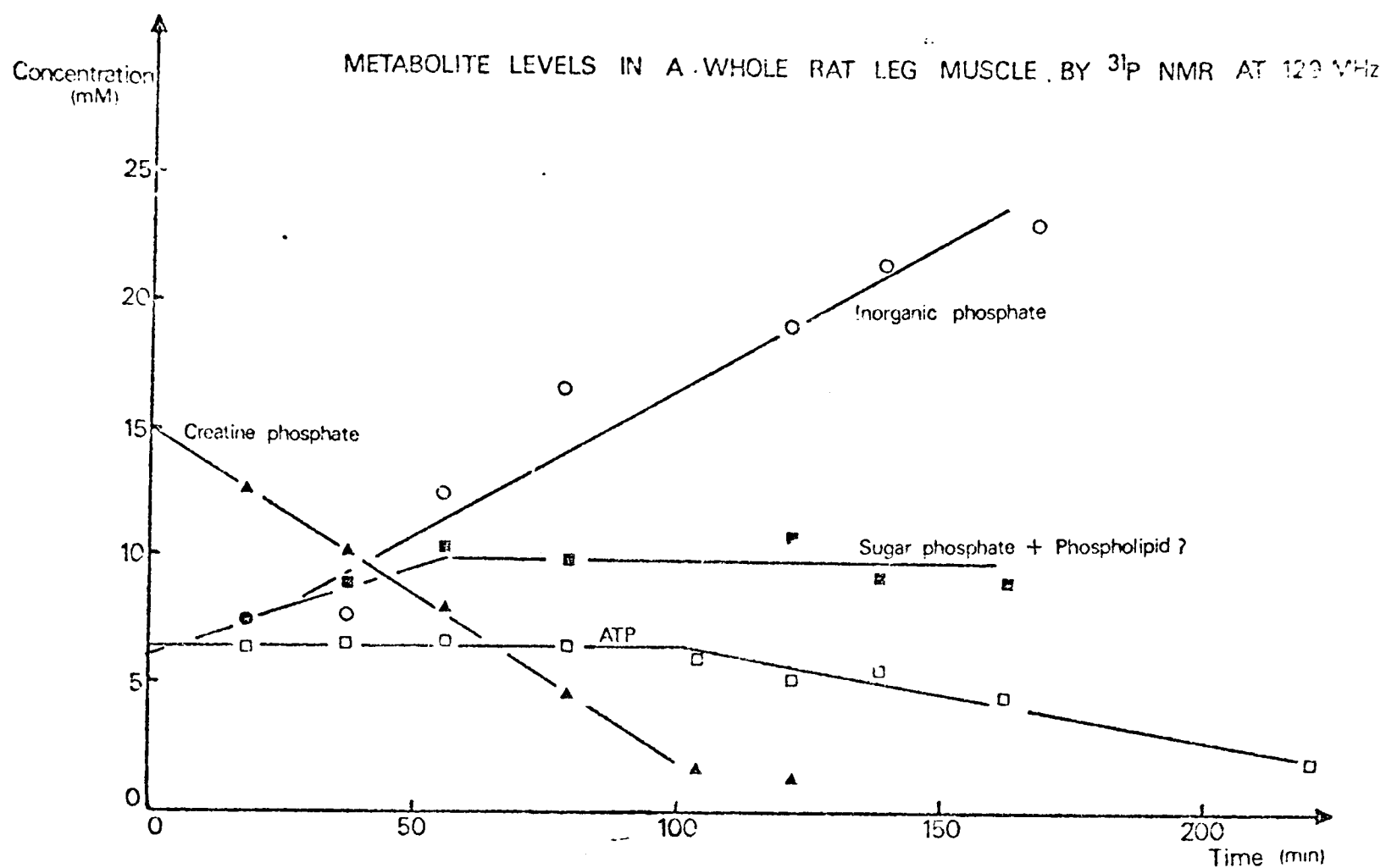


Figure 9.5 Variation of phosphorus metabolite levels in an intact rat leg muscle with time after excision.

The integrals of spectra shown in Fig. 9.4 are plotted in this graph. \circ , Inorganic phosphate; \blacktriangle , creatine phosphate; \blacksquare , sugar phosphate and phospholipid; \square , ATP. An absolute concentration scale was established by running a standard sample of 10 mM phosphate in the same conditions as the muscle.

assumed to have occurred in the damaged muscle.

(ii) The frequency of the inorganic phosphate resonance defines the apparent pH of its environment (7.1 in this spectrum) and the frequencies of the ATP peaks correspond to those for the Mg^{2+} -ATP complex at the phosphate pH.

(The frequency of the creatine phosphate resonance is independent of pH around

7.) In vitro studies of Mg^{2+} binding to ATP show that there are large shifts (2-3 p.p.m.) in the β - and γ -phosphate resonances on complex formation.

These shifts show that the ATP observed in muscle is almost entirely complexed to magnesium ion. Changes in ionic strength also produce measurable spectral shifts, but these are much too small to alter the assignments for the intact muscle spectrum.

(iii) Ageing of the muscle is accompanied by a fall in pH which is monitored by changes in the frequencies of the phosphate and ATP resonances. The pH at the start of data accumulation is 7.1 but after 160 min it falls to 6.2.

Acid accumulation seems to accelerate at the time when the creatine phosphate concentration falls to zero.

(iv) The signal peaks of the muscle phosphates are broader than those for the corresponding compounds free in solution, and the inorganic phosphate peak is markedly broader than the creatine phosphate resonance. The explanation for this phosphate broadening cannot lie in a disturbance of magnetic field homogeneity caused by the nature of the sample as the width of the creatine phosphate signal gives an upper limit for the field inhomogeneity. This observation is confirmed by the experiment shown in Fig. 9.6 where the spectrum of an intact white muscle is compared to the spectrum of an extract from a similar muscle which had been freeze clamped. The main difference

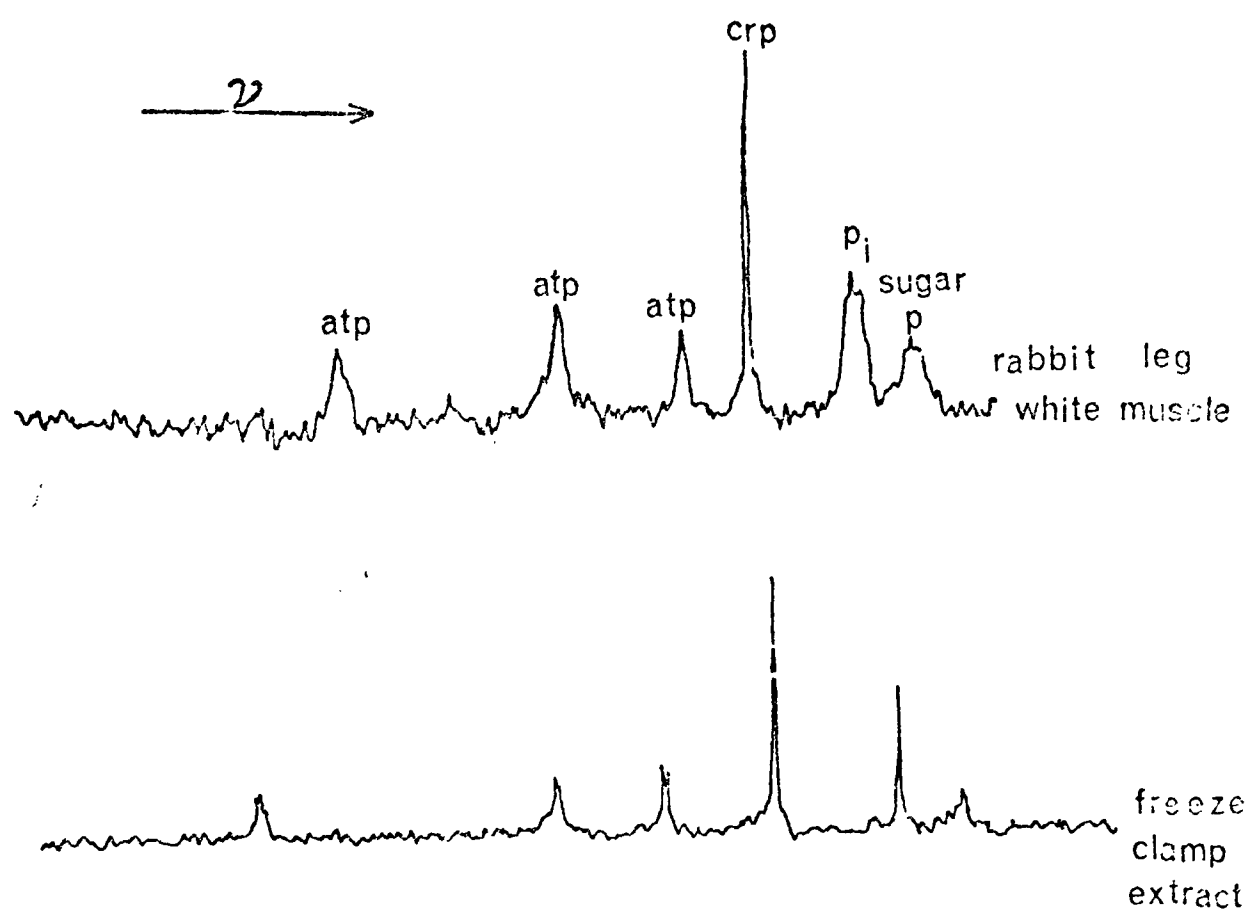


Figure 9.6

^{31}P NMR spectra of an intact rabbit white muscle and an extract from a freeze clamped muscle

The spectra were recorded at 129 MHz without proton irradiation. Spectrum width 5 KHz. ν indicates the direction of increasing frequency. The spectra represent the accumulated magnetisation after 160 90° pulses had been applied to the sample at 6 second intervals. 20°C .

between the two spectra is in the width of the phosphate resonance, this resonance being greatly broadened in the intact tissue. This could be due to compartmentation of phosphate between two or more environments, the chemical shift for phosphate in each environment being different. For example, since the frequency of the phosphate resonance is strongly pH dependent around pH 7, the large width of the line could be due to a distribution of pH within the muscle. The pH range that would account for the line width is about 0.5 pH units.

In Chapter 2, it was noted that for a nucleus in one chemical environment the line width of its resonance was related to the measured T_2 relaxation time. Drs. D.G. Gadian and P.J. Seeley have shown that although the signal from phosphate in muscle has a line width of 150-200 Hz, the measured T_2 relaxation time is 150 ms, which corresponds to a line width of only 2 Hz. This indicates that the observed resonance consists of a superposition of relatively narrow resonances which are slightly shifted from one another. It may therefore be concluded that phosphate in muscle (i) experiences many different environments and (ii) is not in fast exchange between these environments relative to the NMR time scale. These measurements rule out the possibility that the broadening of the bulk phosphate is exclusively due to fast exchange on and off phosphate binding sites, say, on proteins.

C. Studies on Dialysed Muscle

In order to study the factors affecting the line shape of resonances from phosphate in muscle, it is necessary to apply chemical

perturbations to the system. To facilitate this, all phosphate-containing ligands were removed from pieces of muscle by dialysis. Inorganic phosphate in various media was then dialysed back into the muscle and the NMR spectra of phosphate in these muscles were examined.

^{32}P radioactive phosphate was used to check that externally added phosphate equilibrated with phosphate in muscle samples. 10 mM ^{32}P phosphate, pH 7 was dialysed into a 2.69 gm. muscle, from which all phosphorus containing metabolites had been removed by overnight dialysis into 50 mM TEA pH 7. The muscle was removed from the hot phosphate and transferred to 4 litres of "cold" 10 mM phosphate buffer, pH 7 which was stirred continuously. At various times after the transfer, aliquots of the buffer were removed and assayed for radioactivity. The time course of appearance of radioactivity is shown in Fig. 9.7. In addition, 100 mg samples were cut from the muscle before and after the dialysis into "cold" phosphate buffer. After solubilisation, the radioactive content of the tissues was assayed. The results showed that the dialysis had removed more than 99.5% of the radioactive phosphate.

Fig. 9.8 shows the ^{31}P NMR spectra of muscles into which 10 mM phosphate at pH 6, 7 or 8 was dialysed. The phosphate resonance consists of two or more components. In freshly excised muscle it is possible that the multicomponent phosphate resonance is due to pH differences between cells in the same muscle. For example varying rates of lactate production in different cells could cause pH differences between, say, outer and inner cells. In dialysed muscle this is not possible and any variation in the environment of phosphate from one cell to another must be due to intrinsic structural differences between individual cells in the same tissue. Alternatively the

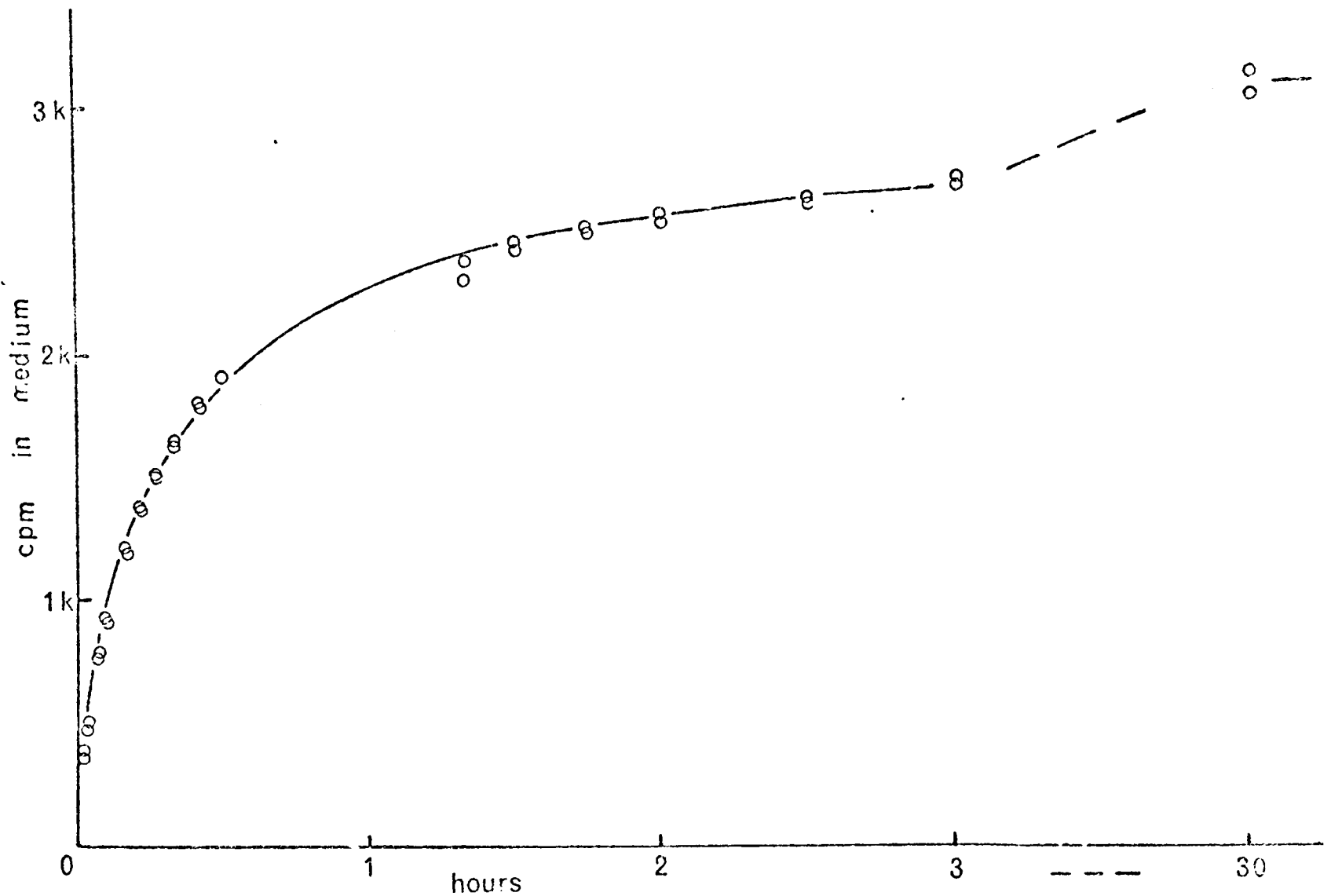


Figure 9.7 Dialysis of hot Phosphate in and out of Muscle

A 2.69 gm sample of rat white hind leg muscle was gently shaken in a solution of 10 mM ^{32}P inorganic phosphate pH 7. After 4 hours the muscle was transferred to 4 litres of 10 mM phosphate buffer, pH 7. Aliquots were removed at intervals, from the buffer, which was vigorously stirred. ^{32}P inorganic phosphate in the aliquots was measured and is plotted as a function of time in the figure.

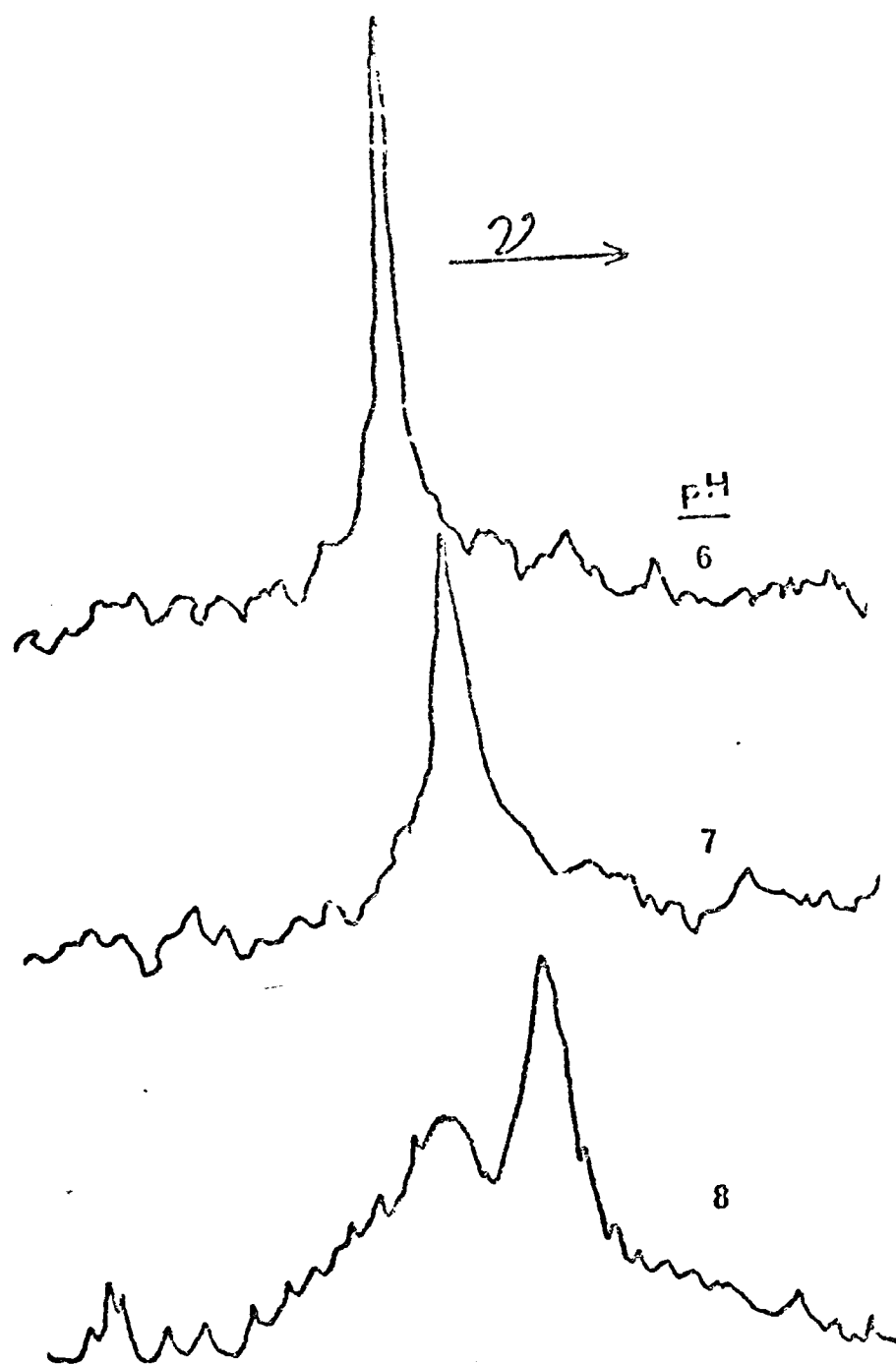


Figure 9.8

^{31}P NMR spectrum of phosphate dialysed into muscle

10 mM inorganic phosphate, 50 mM triethanolamine hydrochloride, 1 mM EDTA pH 6, 7 or 8 was dialysed into rat hind leg muscle from which all metabolites had been removed. Spectrum recorded at 129 MHz - sweep width 1.26 KHz. 20°C.

complex signals may be due to phosphate "seeing" more than one environment in each cell.

The spectra in Fig. 9.8 can most simply be described in terms of two sets of resonances. The position of one set of resonances appears to be sensitive to pH and corresponds to the pH of the phosphate buffer used in each dialysis. In contrast, the position of the second set of resonances is not pH sensitive and "reports" an apparent pH of 6.1 - 6.4. As chemical shifts can be induced by mechanisms other than protonation, however, it is not possible to state dogmatically that the phosphate responsible for the second set of resonances is protonated.

In the presence of excess arsenate, the resonance from phosphate dialysed into muscle has only one component (corresponding in position to the pH of the buffer used) (Fig. 9.9). Other treatments which remove the multiple line shape of phosphate in white muscle include glycerol treatment (Fig. 9.10) or homogenisation with a "Silverson" Shredder (Fig. 9.11). Glycerol treatment disrupts some of the sarcoplasmic membranes of muscle, whilst leaving the actin and myosin filaments intact (198-200), whereas homogenisation breaks up the overall structure of the tissue.

As muscle has a complex intracellular structure it is not surprising that phosphate in muscle cells can be found in a variety of environments and that it cannot exchange rapidly between these different environments. Although the structural basis of this partition is not yet understood, it is clear that it is critically dependent upon the maintenance of the complex intracellular muscle structure. This "compartmentation" need not necessarily be due to the presence of distinct membrane bound enclosures, as is often

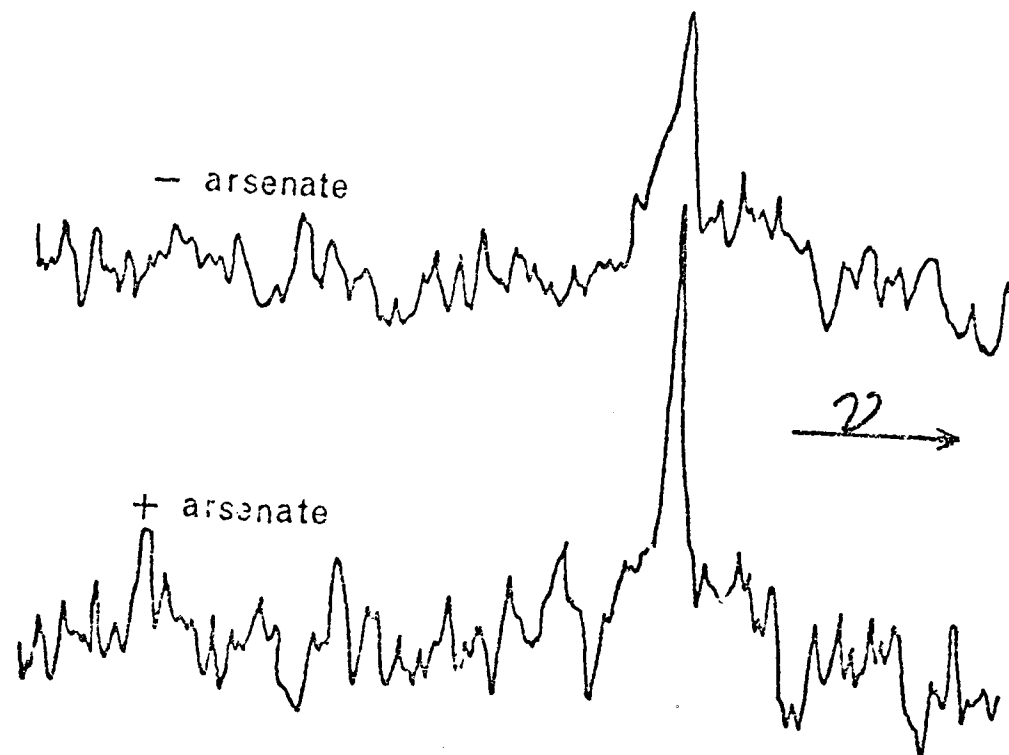


Figure 9.9

^{31}P NMR spectra of phosphate in muscle in the presence or absence of arsenate

Either 5 mM inorganic phosphate, 400 mM KCl, 50 mM triethanolamine hydrochloride, 1 mM EDTA pH 8 or 5 mM inorganic phosphate, 200 mM arsenate, 50 mM triethanolamine hydrochloride, 1 mM EDTA pH 8 was dialysed into a rat white hind leg muscle, from which all metabolites had been removed. Spectra were recorded at 129 MHz. Sweep width 2.5 KHz. 20°C.

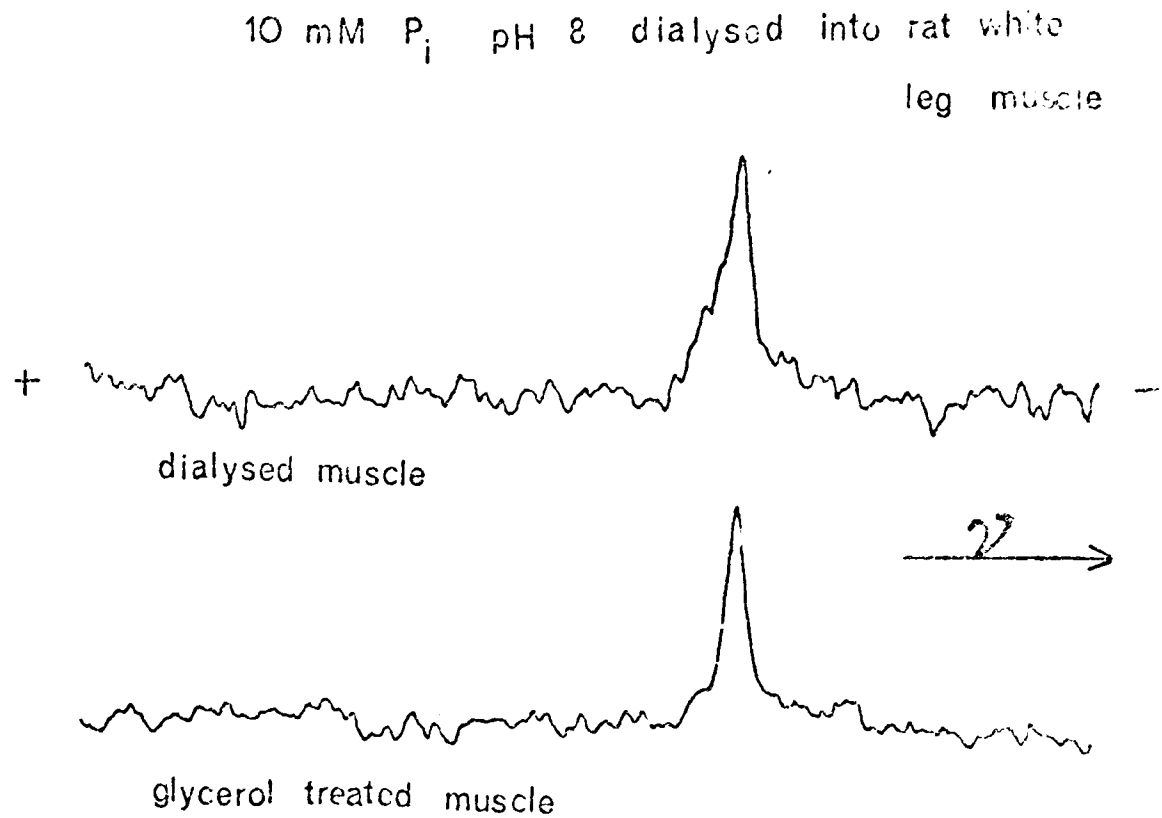


Figure 9.10 ^{31}P NMR spectra of phosphate in glycerol treated muscle

Rat hind leg muscle from which metabolites had been removed by dialysis was gently shaken overnight in 50% glycerol 50% 50 mM TEA pH 7 buffer, by volume. After removal of glycerol by dialysis, the muscle was further dialysed against 10 mM phosphate 50 mM TEA, 1 mM EDTA pH 8 buffer. Spectra of this muscle, and a similar muscle which had not been glycerol treated, were recorded at 129 MHz, and are shown in the figure. Spectrum width - 2.5 KHz.

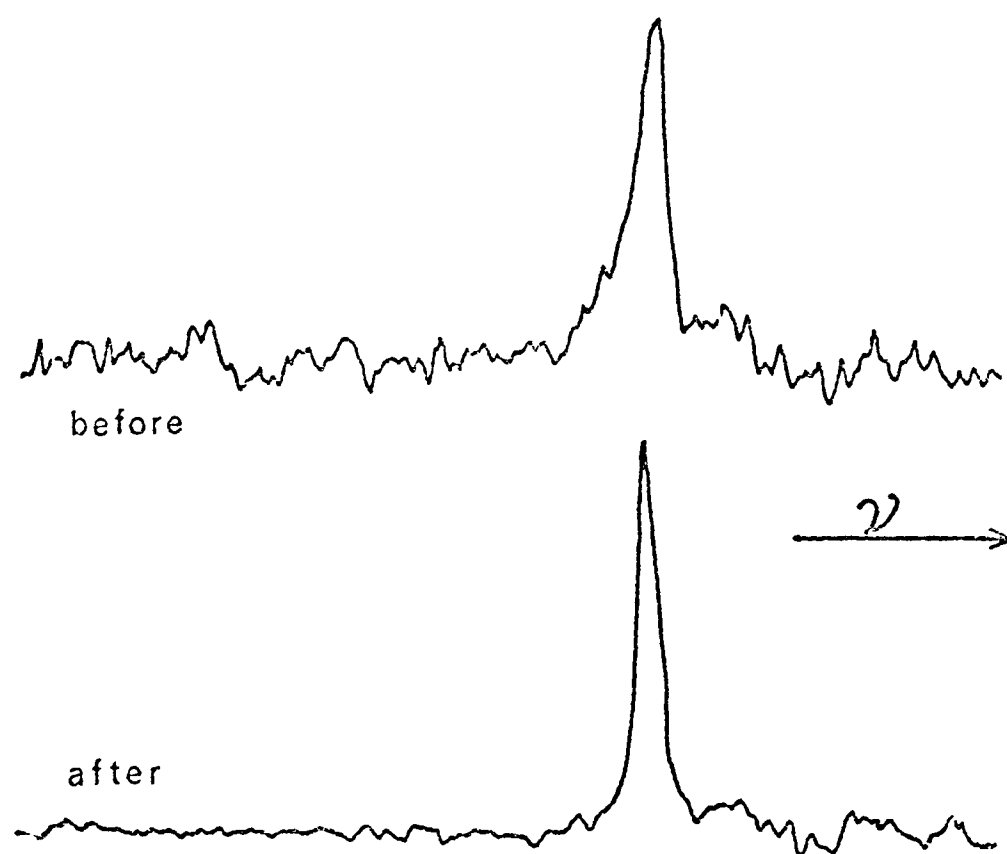


Figure 9.11 ^{31}P NMR spectra of phosphate in dialysed muscle and homogenised muscle

5 mM inorganic phosphate in 50 mM triethanolamine hydrochloride 1 mM EDTA pH 8 buffer was dialysed into rat white hind leg muscle, from which metabolites had been removed. A 129 MHz spectrum was recorded (upper spectrum). This sample was then homogenised in a "Silverson Shredder" and the spectrum was re-recorded (lower spectrum). Spectrum width - 2.5 KHz.

envisaged. It may be due to large amounts of phosphate being protein (or otherwise) bound, to differences in cytoplasmic structure in particular regions of the cells (e.g. around the myofibrils or the plasmalemma), or to differences between cells in the same muscle.

This thesis has discussed the mechanisms of activation and deactivation of phosphorylase at great length. However, although in certain circumstances, the enzyme may be in an "active conformation", the actual in vivo activity expressed will depend on the phosphate concentration in the environment of the glycogen particles. Clearly any partition of phosphate between various environments will affect the actual activity expressed.

D. Red Muscle and the Unassigned Metabolite

Most muscles may be assigned to one of three classes: white, red, and smooth (192). White muscles, such as those used in the experiments described above, usually are employed for short bursts of intense activity, and hence have an extensive sarcoplasmic reticulum (193). As their main source of energy is anaerobic glycolysis, they have very few mitochondria and their blood supply is not well developed. In contrast, red muscles contain many mitochondria and their main source of energy is oxidative phosphorylation. Their blood supply is well developed and they are generally used wherever continuous low-power muscular activity is required (e.g. the heart) (194).

Although most hind leg muscles are white, several red muscles, which are used in the maintenance of posture, can be located. The semitendinosus muscle from the hind leg of rabbit is a convenient red muscle for phosphorus NMR studies (195).

Fig. 9.12 compares the phosphorus NMR spectrum of a freshly excised rabbit semitendinosus muscle to a spectrum of a rabbit white hind leg muscle (according to phosphorus NMR rabbit and rat white hind leg muscles are very similar). Several differences are apparent:

(i) the red muscle contains a lower concentration of creatine phosphate.

This is consistent with the currently accepted view that high levels of creatine phosphate are stored for use in short intense bursts of muscular activity.

(ii) in red muscle, the inorganic phosphate resonance is narrower than in white muscle. This signifies that phosphate in the red muscle is not partitioned between different environments as in white muscle. This result also infers that the compartmentation discussed in the previous section is not due to mitochondrial binding of phosphate. However the nature of the specific factor which occurs in white but not in red muscle and which causes the phosphate resonance to broaden, is not clear.

(iii) in the red muscle spectrum, an additional peak occurs between the phosphate and creatine phosphate resonances. The molecules responsible for this peak were present in an extract of freeze clamped semitendinosus muscle (Fig. 9.13). From the resonance frequency of this metabolite, it was deduced that it was likely to be a phosphodiester; no other commonly occurring phosphate linkages gave resonances at this position. Consistent with this was the observation that its resonance frequency was independent of pH in the range 2 - 10. Treatment of the extract from freeze clamped red muscle with E. coli alkaline phosphatase destroyed ATP, creatine phosphate and sugar phosphates but did not affect the resonance from the unassigned metabolite (196) (Fig. 9.13). This resonance was also unaffected by prolonged

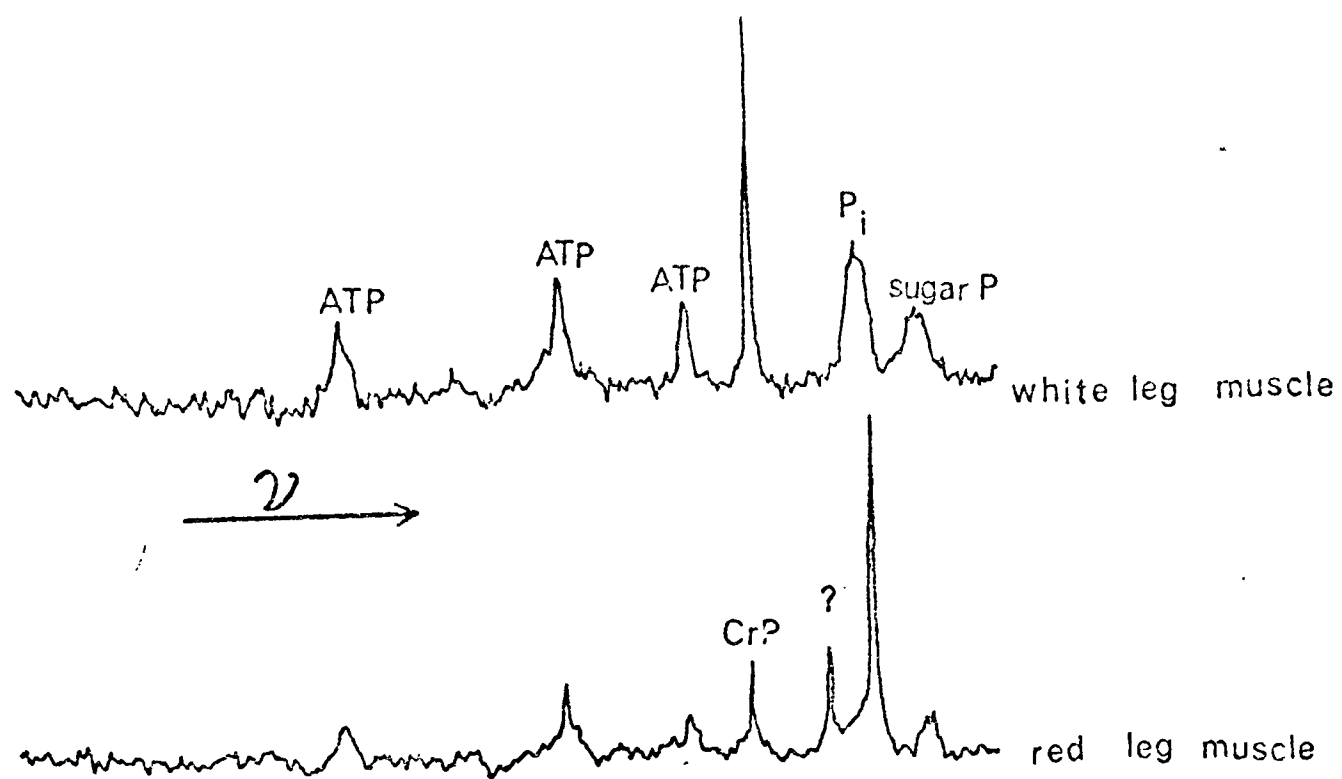


Figure 9.12 ^{31}P NMR spectra of Red and White leg muscles

This figure shows 129 MHz spectra of a rabbit white hind leg muscle and a rabbit red semitendinosus muscle. Both spectra were recorded under identical conditions - given in Fig. 9.6. Spectrum width - 5 KHz. The question mark indicates the unassigned metabolite.

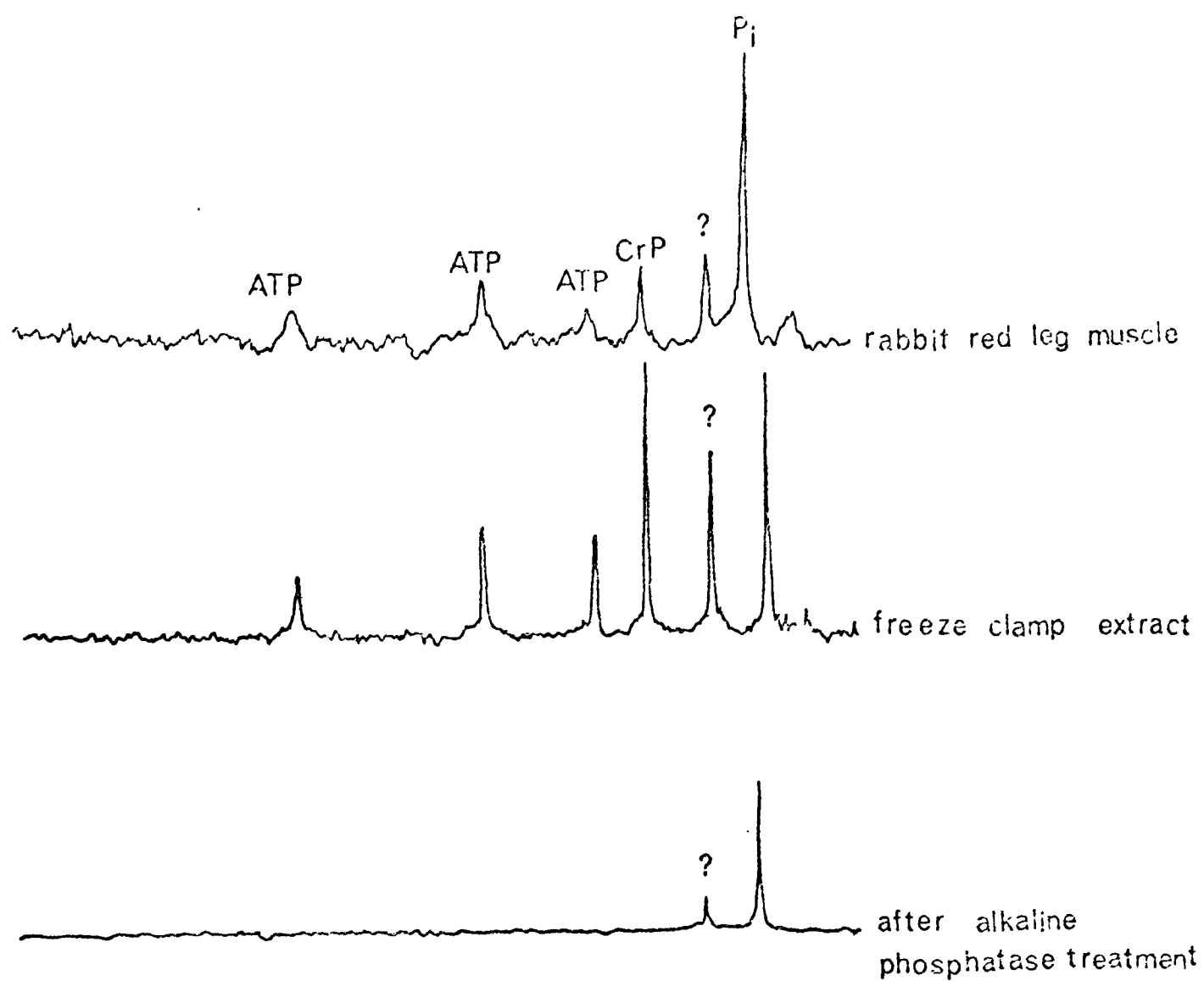


Figure 9.13 ^{31}P NMR spectra of Red muscle and Extracts

129 MHz spectra of (i) a rabbit semitendinosus muscle (ii) an extract from a freeze clamped semitendinosus and (iii) an extract which had been treated with *E. Coli* alkaline phosphatase, are shown in the figure. Conditions as in Fig. 9.6. Spectra width - 5 KHz.

incubation of the freeze-clamp extract with pancreatic RNase or Crotalus
Adamanteus venom phosphodiesterase (oligonucleotide 5'-nucleotido hydrolase)
 (197). This inferred that the unassigned metabolite was unlikely to be RNA.

The metabolite has not been unambiguously identified, to date. The most commonly occurring physiological molecules whose properties are consistent with the above data are the glycerol phosphoryl derivatives and related compounds (e.g. glycerophosphoryl choline, cardiolipin etc.).

Leaving aside the difficult question of the nature of the unassigned metabolite, several matters concerning its existence must be considered.

- (a) Is it an artefact? - phosphorus spectra of rabbit blood, beef heart mitochondria or the tendon attached to the semitendinosus muscle have not revealed any resonances at the frequency characteristic of the unassigned metabolite. The metabolite appears to be an integral component of the muscle.
- (b) What is its metabolic role? - electrical stimulation to exhaustion, or ageing of an excised semitendinosus muscle does not cause destruction of the unassigned metabolite, as revealed by phosphorus NMR. It is not known why the metabolite is present or why it is found in the rabbit red muscle but not in the rabbit white muscle.
- (c) Is it found in other systems? - the range of tissues which may be studied by phosphorus NMR is limited. As the metabolites in the tissue have to be reasonably stable, studies to date have been restricted to muscle. A resonance which corresponds in frequency to the position of the unassigned metabolite has been detected in frog gastrocnemius, a white muscle (see Fig. 9.14). However, as this component has not been extracted from the muscle, there is no evidence that the unassigned resonance in the

^{31}P NMR spectra of frog gastrocnemius

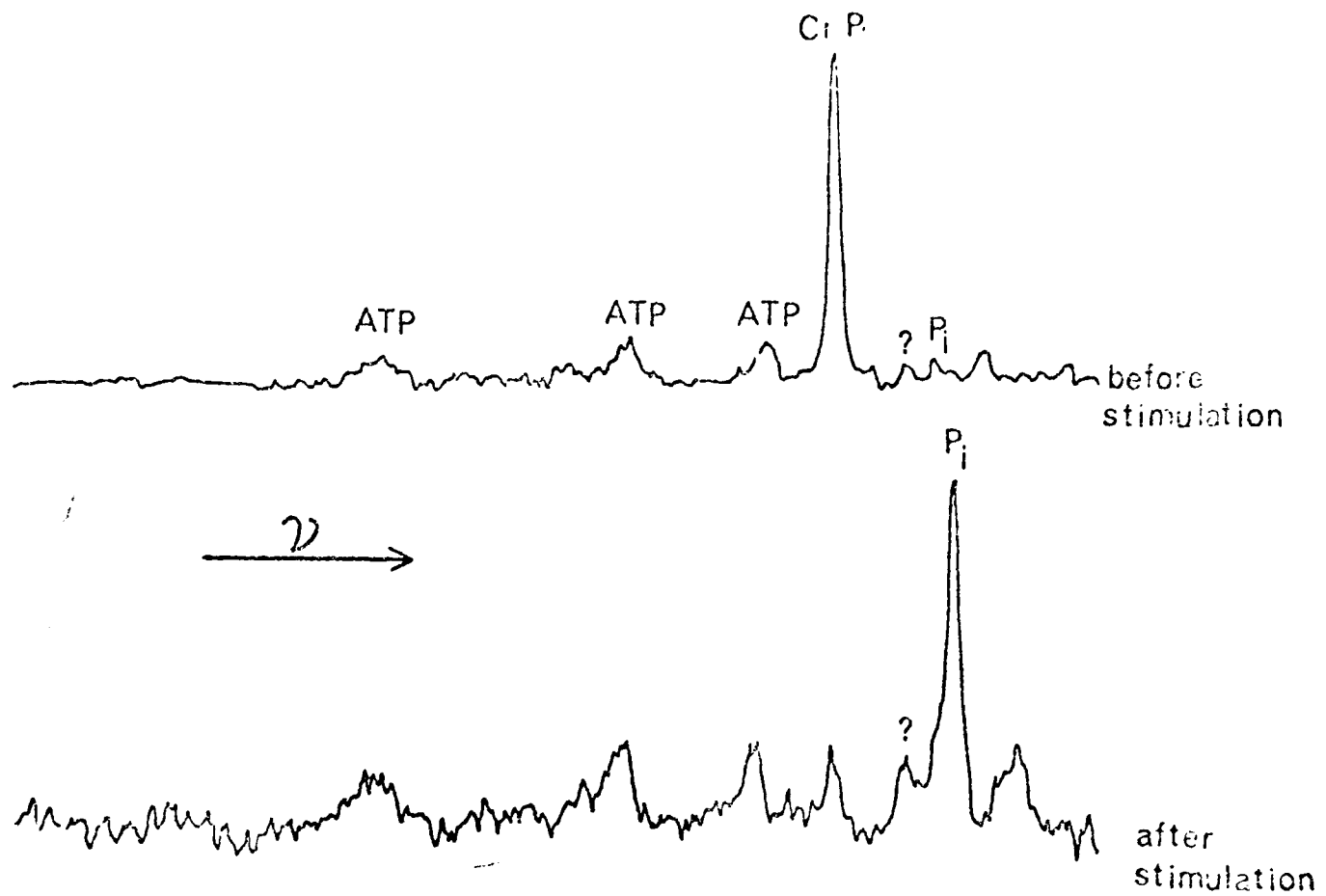


Figure 9.14 ^{31}P NMR spectra of frog gastrocnemius muscle

Spectra of a freshly excised muscle were recorded, at 129 MHz, before and after electrical stimulation. Conditions as in Fig. 9.6. Spectrum width 5 KHz. The question mark indicates the position of the unassigned metabolite.

gastrocnemius is due to the same metabolite as in the semitendinosus muscle. Indeed, it is possible that the resonance in both tissues, could be due to several metabolites, all containing phosphodiester groups.

Clearly the existence of this unassigned metabolite poses many problems which cannot be fully investigated until its chemical nature is determined. The interesting aspect of this, as yet unfinished, piece of work is that it is a useful demonstration of the potential of NMR. Whilst the freeze clamp technique can only detect metabolites for which a specific assay is arranged, phosphorus NMR can give a direct picture of phosphorus containing metabolites, with the minimum of effort. Obviously the most serious drawback of the method is that it cannot detect phosphorus containing metabolites at concentrations of less than 1 mM. However the applications described in this section clearly demonstrate its usefulness and potential.

E. Partial Purification of the Unassigned Metabolite

The unassigned metabolite has been partially purified from the extract of several freeze-clamped rabbit semitendinosus muscles. After treatment with alkaline phosphatase (see Fig. 9.13), the extract was diluted 5 times into 25 mM Tris buffer pH 8.4 and applied to a DEAE column pre-equilibrated in this buffer. The column was first washed with 25 mM Tris buffer pH 8.4, and then with steps of 100 mM Tris, 100 mM Tris + 100 mM KCl, 100 mM Tris + 500 mM KCl, 100 mM Tris + 1 M KCl and 100 mM Tris + 2.5 M KCl. A ^{31}P NMR spectrum of each eluate was recorded after concentration by freeze drying. The unassigned metabolite did not stick to the column and was detected in the 25 mM Tris eluate, whereas inorganic

phosphate was found in the 500 mM KCl eluate (see Fig. 9.15). The 25 mM Tris eluate was transferred to D_2O and a proton NMR spectrum was recorded (Fig. 9.16). Although the only phosphorus containing compound in this sample was the unassigned metabolite, the proton spectrum was complex and suggested that further purification was required.

The concentrated 25 mM Tris eluate from the DEAE column was diluted into a solution of 25 mM oxalate buffer pH 4 and passed through a Dowex 50 cation exchange column. As the unassigned metabolite did not stick to this column under these conditions, it was then absorbed onto Krimsky Racker activated charcoal (201). After elution from charcoal with 20% alcohol in water, the sample containing the metabolite was freeze dried and suspended in a 5 mM Sodium Borate, 5 mM Ammonium formate buffer at pH 8.2. The unassigned metabolite was then attached to a Dowex Anion exchange column which had been equilibrated in this buffer (202). The metabolite was eluted from this column in 20 mM Ammonium formate pH 8.2. This eluate was freeze dried, suspended in D_2O , its pD was adjusted to 7.1 and a proton NMR spectrum was recorded (Fig. 9.17). Although the spectrum indicated that a substantial purification had been made, it was impossible to assign a structure to the metabolite on the basis of this spectrum alone.

Proton spectra of glycerophosphoryl derivatives have been recorded. Comparison of such spectra with Fig. 9.17 does not contradict the suggestion that the unassigned metabolite is a glycerophosphoryl derivative or a related compound. For example, the peak marked X in Fig. 9.17 corresponds in frequency to the N-trimethyl resonance from choline or glycerophosphoryl choline. However, as the partially purified extract may contain free choline, it is unwise to make any conclusions on the basis of these data.

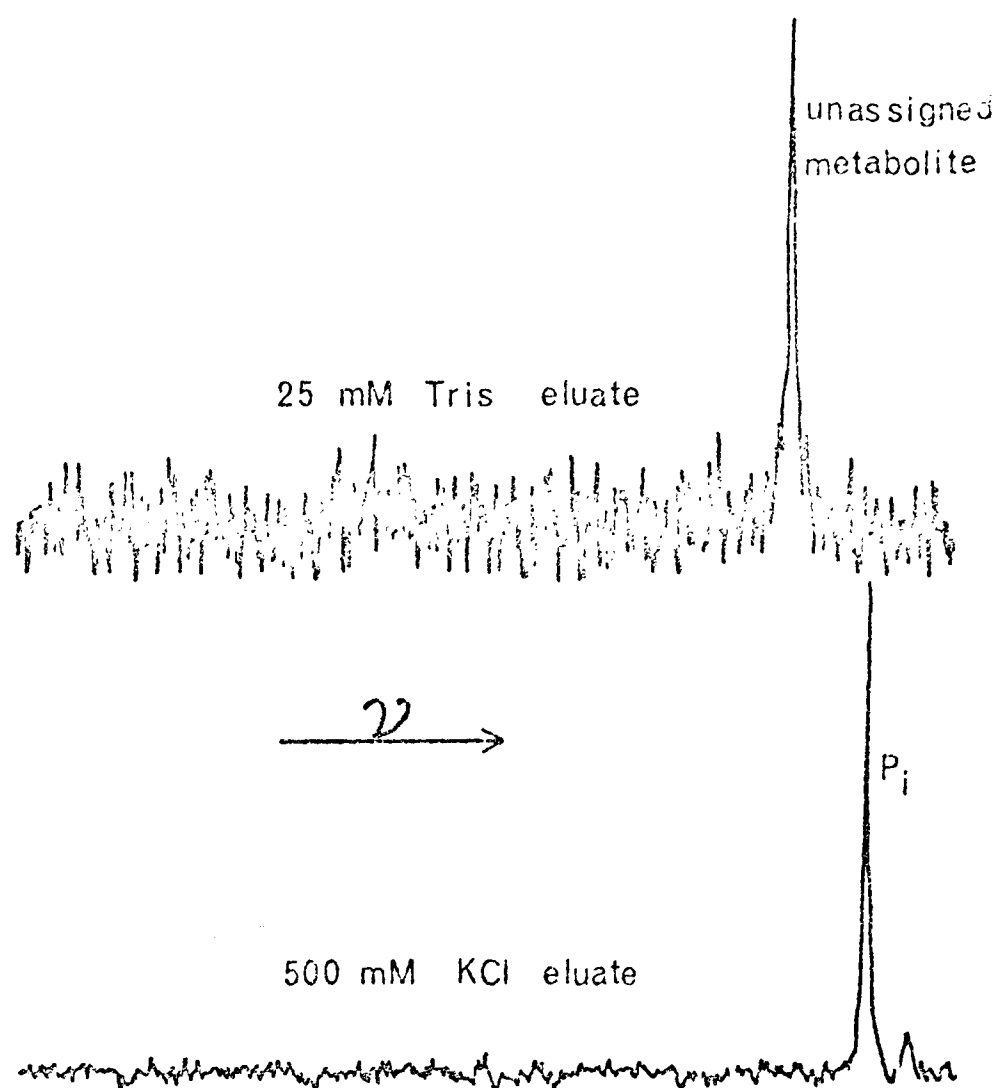


Figure 9.15 Assay for the unassigned metabolite by ^{31}P NMR

The 25 mM Tris eluate and the 500 mM KCl eluate from the DEAE column described in the text were concentrated by freeze drying. Spectra were recorded at 129 MHz and are shown in the figure. Spectrum width - 5 KHz.

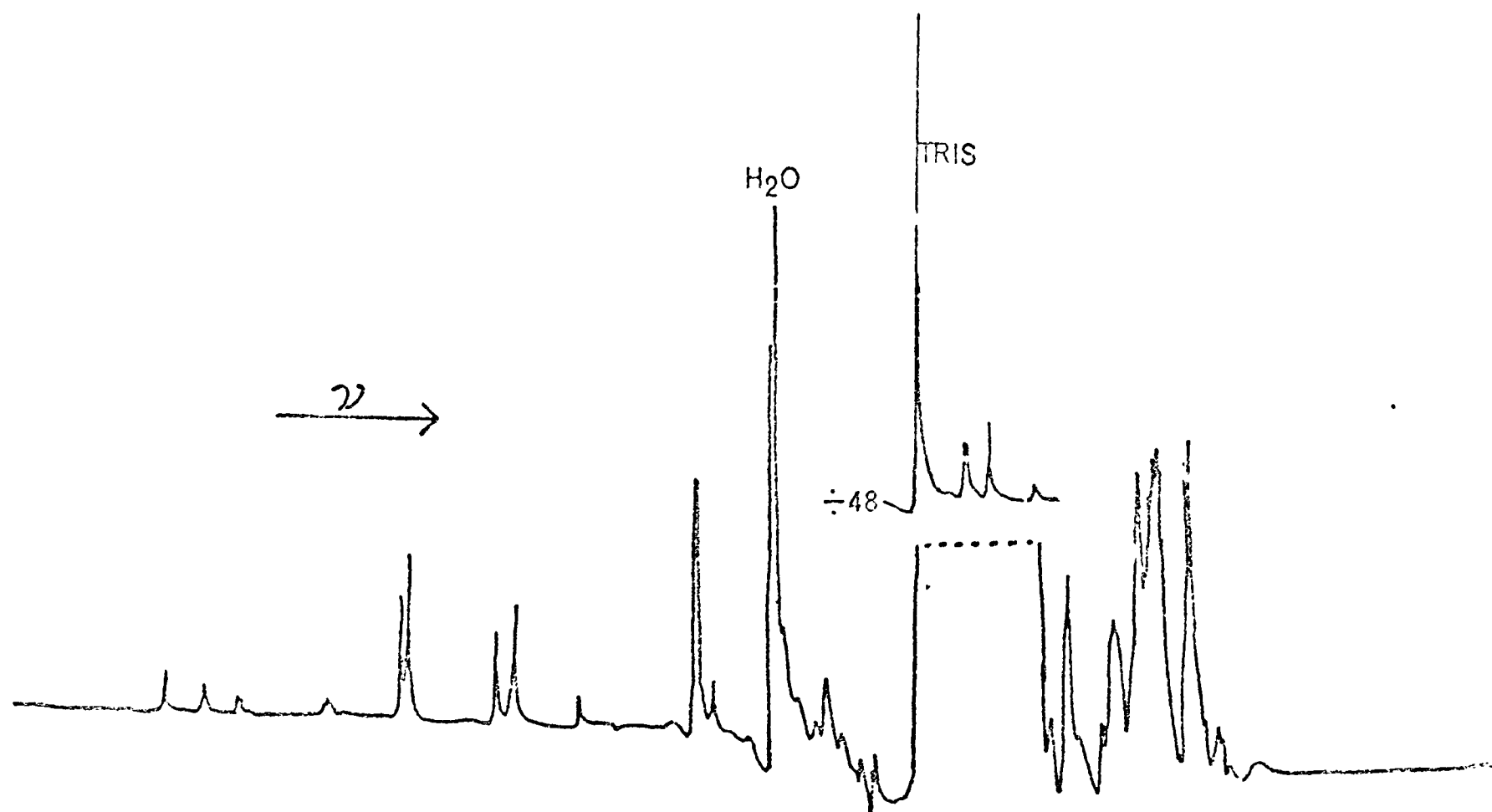


Figure 9.16 Proton Spectrum of eluate containing the unassigned metabolite
The 25 mM Tris eluate described in Fig. 9.15 was freeze dried, suspended in D₂O and adjusted to pH 7. A 270 MHz proton spectrum was recorded and is shown in the figure. Spectrum width - 4 KHz. Part of the spectrum is vertically contracted 48 times.

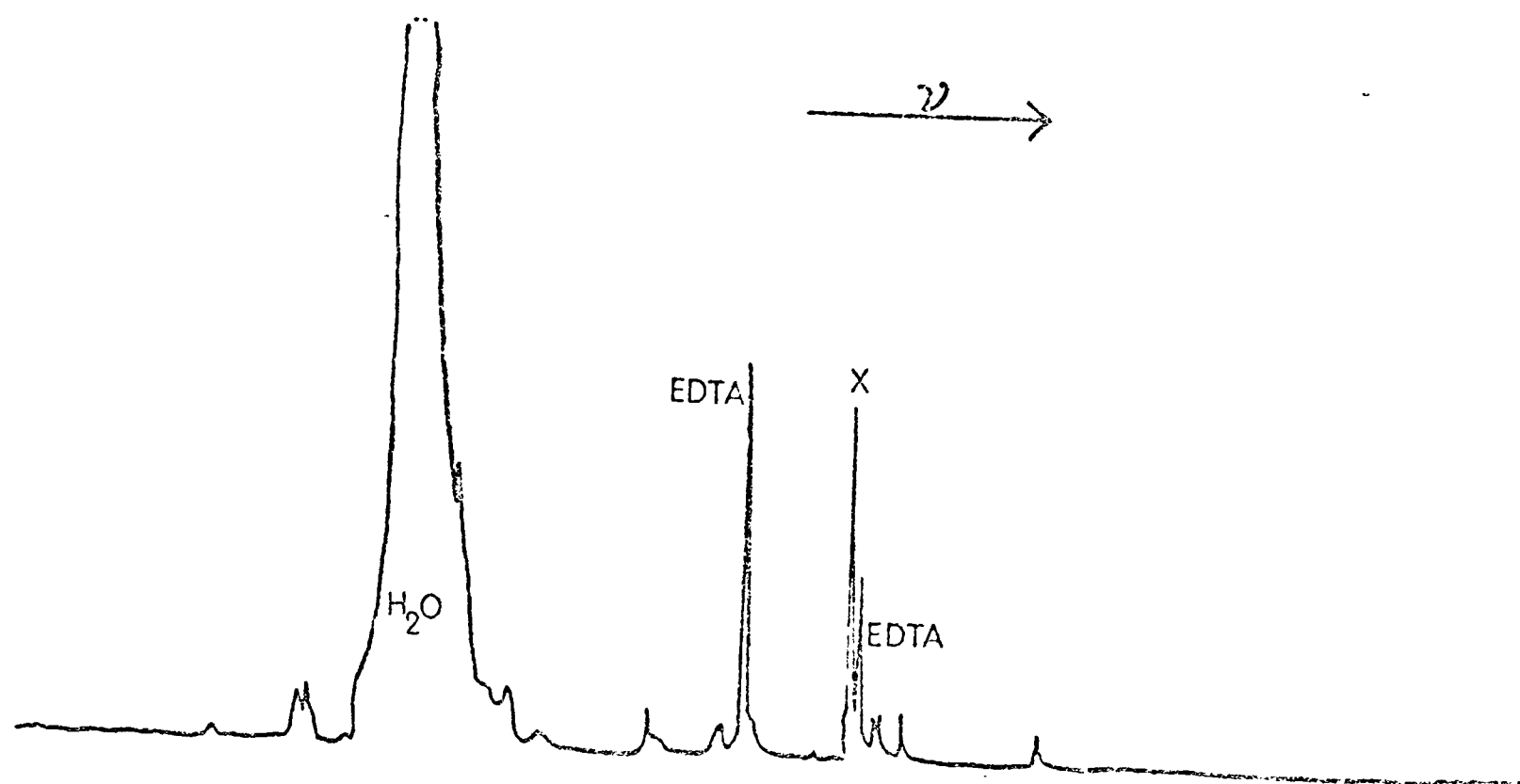


Figure 9.17 Proton Spectrum of purified fraction containing the unassigned metabolite

The 25 mM Tris eluate described in Fig. 9.15 was treated as described in the text. The fraction from the Dowex anion exchange column, containing the unassigned metabolite, was freeze dried, suspended in D_2O and adjusted to pH 7. A 270 MHz proton spectrum was recorded and is shown in the figure. Spectrum width - 2 KHz.

Chapter 10NON COVALENT REGULATION OF PHOSPHORYLASE ACTIVITY∴ UNKNOWN AND INCONSISTENCIESA. Non Covalent Phosphorylase Inhibition

Phosphorylase is present in white skeletal muscle at concentrations of about 6–8 mgs/ml. Although it is obviously important for it to be activated during periods of muscle contraction, it is also imperative that it is inhibited during periods of rest. As glucose-1-phosphate, glycogen, and inorganic phosphate are not in equilibrium in resting muscle (188), flux of glucose units into the glycolytic pathway must be arrested by constraints on phosphorylase activation. Freeze clamp data indicate that in relaxed white muscle, 95–100% of the total phosphorylase is in the b form (217,225). Therefore two questions immediately arise. Firstly, what prevents the 50 μ M AMP present in the resting cell from activating the phosphorylase b? Secondly, how can the resting cell tolerate 0–5% phosphorylase a? While the residual phosphorylase a activity has been largely ignored in the literature, considerable attention has been given to the question of the interaction of small ligands with phosphorylase b in resting muscle. In particular, Morgan and Parmeggiani showed that, in rat heart, most of the AMP activation of phosphorylase b could be blocked by the presence of ATP and glucose-6-phosphate (181,218). Thus the main point discussed in this section is the effectiveness of these and other ligands in inhibiting skeletal muscle phosphorylase b activity, when 50–60 μ M AMP is present (see 219–221).

To understand the non-covalent activation of phosphorylase b, it is necessary to be able to estimate which ligands will be phosphorylase-bound at any point in the tissue's activation cycle. An attempt to do this has been made by using the available muscle ligand concentrations, determined from freeze clamp experiments, in conjunction with the apparent binding constants of these ligands to phosphorylase, determined from measurements with probe-labelled enzyme. Any phosphorylase b molecule may bind only one of the ligands, Glucose-6-phosphate, AMP, ADP or ATP, at any instant. It is therefore possible to estimate the percentage of the total phosphorylase which will bind any of these ligands when the tissue is in any particular metabolic state.

Fig. 10.1 a shows the result of such a calculation. It illustrates the proportion of phosphorylase molecules which will bind either AMP, ADP, ATP or glucose-6-phosphate if a small number of enzyme molecules are placed in a medium containing these ligands, in concentrations equivalent to those estimated from freeze clamp data of resting white muscle (180). It is evident that AMP is prevented from activating phosphorylase b by the levels of glucose-6-phosphate, ADP and ATP.

There are, obviously, several deficiencies in this model. Firstly, this model assumes that the presence of the enzyme does not perturb the concentrations of free ligand. Clearly this is not the case in vivo, where up to 80 μ M phosphorylase is present. The proportion of enzyme which binds AMP could be reduced by a factor of 2 by this effect.

As myofibrils bind ADP very tightly, another major source of error in such a calculation is the estimation of the free ADP level. Whereas freeze

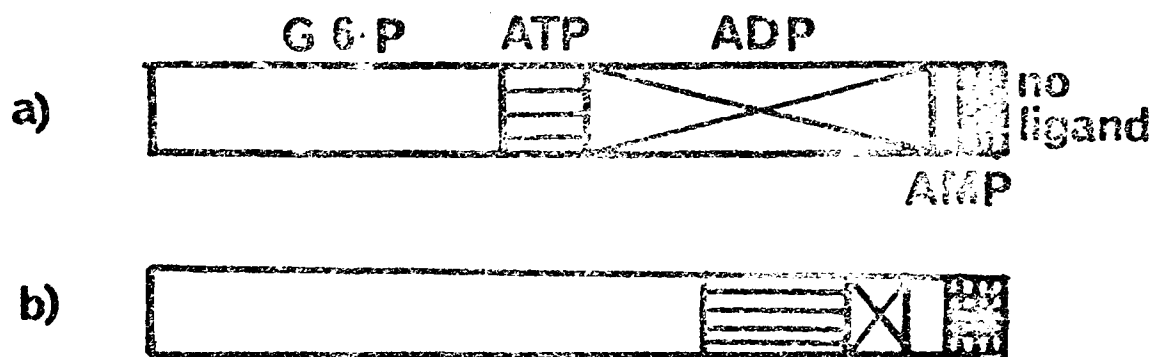


Figure 10.1 The proportions of cellular phosphorylase b which will have G-6-P, ATP, ADP, AMP or no ligand bound.

The whole bar represents 100% phosphorylase b (a) in resting muscle assuming no ADP compartmentation (b) assuming 90% ADP compartmentation. Concentrations taken: $[G-6-P] = 400 \mu M$; $[ATP] = 5 \text{ mM}$; $[ADP] = 1 \text{ mM}$; $[AMP] = 50 \mu M$ (180). Binding constants as in the text.

clamp data quantify the total ADP content of the muscle (222) it may be estimated that up to 90% of the total ADP in the muscle is reversibly or irreversibly bound (223,224). This "compartmented" ADP is not, therefore, available to sarcoplasmic enzymes.

Figs. 10.1 a and b show the percentage of the total phosphorylase which will have each of the four ligands bound, in skeletal muscle in the resting state. Fig. 10.1 a assumes no ADP compartmentation and Fig. 10.1 b assumes that 90% of the total ADP is bound and is not "seen" by phosphorylase. ADP compartmentation causes glucose-6-phosphate to become the principal inhibitor.

The main deficiency in these estimates is that they ignore homotropic and intersubunit heterotropic allosteric effects involving AMP, ADP, ATP and glucose-6-phosphate. The calculation merely takes the apparent dissociation constants for each ligand and uses them as if they represented the constants for simple equilibria. Unfortunately this difficulty cannot be overcome until a more detailed study of these allosteric effects has been made. It is clear that these calculations need much refinement.

The calculations indicate that the proportion of phosphorylase b which will bind AMP is in the range of 1 - 4%. It is at this point that a serious problem arises. The maximum specific activity of phosphorylase is 80 units/mg. If 1% of the phosphorylase present was maximally active, about 4 units (i.e. 4 micromoles of glucose-1-phosphate per minute per ml. of tissue) of enzyme activity would be observed (218,226). As the measured lactate output of perfused resting muscle is only 5 nanomoles/minute per ml. of tissue, it is evident that phosphorylase activity must be additionally suppressed in some way (227). Several possible effects which could cause suppression of phosphorylase b activity are listed here - it is likely that all of these factors

contribute to some degree, to maintaining low phosphorylase activity in resting tissue.

(i) although 1 - 4% of the phosphorylase b may be in an active conformation, it may not be fully active. This is because the concentration of phosphate in the muscle (1-5 mM) never exceeds the K_m value of phosphorylase for phosphate (5-15 mM, depending upon the exact conditions) (218,227). In addition, any compartmentation of phosphate into an environment not "seen" by phosphorylase will further reduce the actual activity expressed.

(ii) homotropic and heterotropic allosteric effects between subunits could lead to the exclusion of AMP from the enzyme over the appropriate concentration range of metabolites. Many workers have expended much effort in designing simplified allosteric models which would be consistent with the known experimental facts concerning phosphorylase b (see 76).

The model which would result in the most effective inhibition of AMP binding is an MWC model in which the activator bound to one conformation of phosphorylase and the three inhibitors could bind simultaneously to another conformation. Dr. J.R. Griffiths has calculated that, if phosphorylase b obeyed this model, the percentage of phosphorylase b activated by AMP would be about 0.01% in resting muscle (i.e. a maximal activity of 40 nanomoles of glucose-1-phosphate per minute per ml. of tissue) (228). In fact, several experimental observations concerning phosphorylase allostery show that this model cannot apply without modification e.g. ADP weakens glucose-6-phosphate binding.

The true allosteric situation is likely to lie somewhere between the simple competition model of Fig. 10.1 and the MWC model.

(iii) The possibility of extensive compartmentation of ADP has been referred to already. Many authors have suggested that the bulk of the AMP present could be similarly compartmented (see 110). Although no direct experimental evidence has been produced for this suggestion, there are several good reasons for suggesting that the actual concentration of free AMP in resting muscle may be in the range of 1 - 10 μM rather than 50 - 60 μM . Firstly, a lower AMP level in resting tissue would be more consistent with the low observed phosphorylase activity. Secondly, when the tissue is activated a large amplification in the AMP level would be generated. Indirect evidence for some degree of AMP compartmentation has come from consideration of the myokinase equilibrium. If it is assumed that (a) equilibrium is maintained in resting tissue, (b) the magnesium/ATP level "seen" by myokinase is about 5 mM and (c) a considerable proportion of the cell's ADP is myofibril-bound, it is necessary to postulate that the AMP level "seen" by myokinase is in the range 1 - 10 μM . Unfortunately, the literature contains no conclusive evidence on this point, and it is difficult to think of direct experimental approaches to the problem.

(iv) It is possible that some of the glucose-1-phosphate produced by phosphorylase action is recycled to glycogen via UDPG. This is, obviously, a very inefficient method of reducing net glycogen breakdown, as the reverse reaction, via UDPG, requires one UTP molecule for each cycled glucose residue.

(v) Several workers (172, 187, 191) have suggested that, in the glycogen particle fraction, inhibitor proteins are present which suppress phosphorylase b activity. Haschke and Heilmeyer reported a preparation of this inhibitor (133)

but the report was never confirmed.

Clearly there are many factors which could cause very low phosphorylase activity in resting muscle. Because of the difficulty of quantifying these factors, it is difficult to estimate their relative importance. It should, however, be remembered that many of these factors do not affect the expression of the residual phosphorylase a activity. This activity is a puzzle which must be reinvestigated and reconfirmed before firm conclusions can be made about it.

B. Non-covalent phosphorylase activation

Resting muscle contains numerous effectors of phosphorylase b - the inhibitors ADP, ATP, G-6-P and UDPG and the activator AMP. In resting muscle, where glycolysis is operating at a low level, interaction with ADP, ATP and G-6-P inhibits phosphorylase b activity. As discussed previously, AMP, ADP and ATP compete for the same site on phosphorylase. G-6-P, while binding to a different site on the enzyme, competes with the adenine nucleotides. Non-covalent activation of phosphorylase, therefore, takes place when the AMP level rises so as to overcome the inhibition caused by ATP, ADP and G-6-P. In addition to AMP levels, phosphorylase b activity is determined by the inorganic phosphate level. There are two situations where such non-covalent activation has been unambiguously identified:

1. Anaerobic rat heart

Anaerobiosis in variously treated perfused rat hearts led to increased glycolytic flux without phosphorylase b to a conversion. After measurement of the tissues' metabolite levels in the various states, it was

concluded that the increase in phosphorylase activity was, indeed, due to AMP overcoming ATP and G-6-P inhibition and also to the rise in the inorganic phosphate level (218).

2. I strain mice

In I strain mice muscle contraction and glycolytic flux is activated by electrical stimulation, without concomitant phosphorylase b to a conversion (182). The initial rate of production of glycolytic intermediates is slower than normal mice whereas the inotropic response is the same (229). Glycogenolysis only starts when muscular action leads to the appropriate changes in nucleotide and phosphate concentrations.

Fig. 10.2 a shows the calculated ligand distribution on phosphorylase b in normal excited muscle. This figure indicates that in activated muscle, if phosphorylase remains in the b form, increased AMP stimulated activity occurs. This is due to an increase in the AMP concentrations relative to the other adenine nucleotide concentrations as the "energy charge" (230) drops in activated muscle. However, only 10-14% of the phosphorylase is activated in this situation. It is therefore clear that the energy charge in I strain mouse activated muscle must be further reduced to give rise to increased glycogenolysis. It seems likely that, when the data becomes available, it will be found that the energy charge in activated I strain mouse muscle will be lower than that in activated normal mouse muscle.

Fig. 10.2 b shows the ligand occupancy of phosphorylase a in normal activated muscle. Most of the phosphorylase a now has AMP or ADP bound to it and almost all the G-6-P is expelled. This is consistent with the experimental

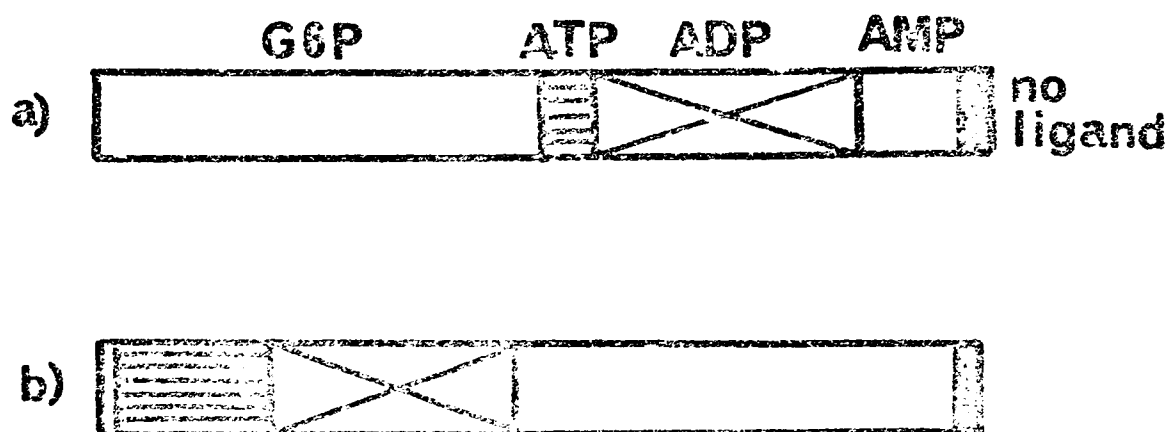


Figure 10.2 The proportions of cellular phosphorylase which will have G-6-P, ATP, ADP, AMP or no ligand bound.

The whole bar represents 100% phosphorylase in excited muscle. (a) where no phosphorylase b to a conversion occurs (b) where 100 % phosphorylase b to a conversion occurs. Concentrations taken: [G-6-P] = 800 μ M; [ATP] = 4.5 mM; [ADP] = 1.2 mM; [AMP] = 300 μ M (no compartmentation is assumed) (180, 227).

data obtained from phosphorylase a in the glycogen particle fraction.

From these studies it is apparent that the information obtained from probe-labelled phosphorylase in vitro can be applied to the situation in vivo. However the state of the enzymes in vivo is always complicated by interaction and information transfer between the glycogen phosphorylase system and other complex regulatory systems. This is very simply illustrated here with a brief description of the factors which determine the tissue AMP level.

The level of AMP relative to the other nucleotides, is determined by the energy charge and the creatine kinase and myokinase equilibria (Fig. 10.3). Skeletal muscle contains high levels of the enzyme AMP deaminase. As this catalyses the irreversible deamination of AMP, tissue nucleotide levels must also be determined by the activity of this enzyme. As resting muscle contains $50 \mu\text{M}$ AMP, AMP deaminase must be "turned off" under these conditions. Deaminase activity is regulated by interaction with various phosphate containing ligands. At physiological pH and potassium ion concentration it is activated by ADP whereas ATP, GTP, inorganic phosphate and creatine phosphate inhibit its action (231) (Fig. 10.3). In resting muscle the levels of these metabolites inhibit the enzyme's action completely. As the enzyme's action is controlled by nucleotides and is linked to the myokinase equilibrium, it is likely that the presence of the enzyme determines the exact resting tissue nucleotide levels. When the ADP level in the tissue rises (as a result of, say, exercise), the AMP deaminase is activated and the ammonium ion level in the tissue rises (232). Adenine nucleotides "drained" from the pool are eventually replaced by cycling of the IMP via succinyl AMP (233,234).

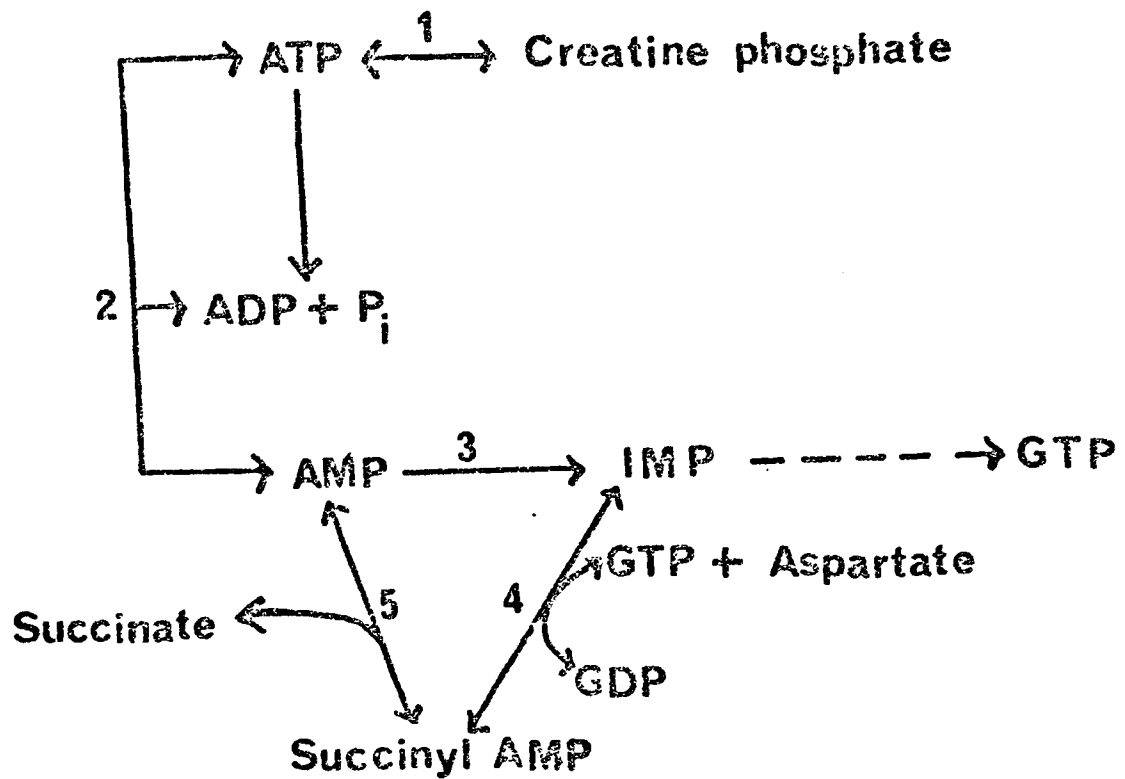


Figure 10.3 Nucleotide interconversions in muscle catalysed by (1) creatine kinase (2) myokinase (3) AMP deaminase (4) adenyly succinate synthetase (5) succinyl AMP hydrolase.

The same regulatory ligands control phosphorylase, glycogen synthase, AMP deaminase and phosphofructo kinase. One may envisage, therefore, that in vivo glycolysis is controlled by a very sensitive balance between these ligands. Hence, in order to fully understand the control of phosphorylase, the factors raised in this chapter must also be applied to the other regulatory systems.

POSTSCRIPT

There can be little doubt that the techniques which have been described give a unique view of the glycogen-phosphorylase system. However a good deal of manipulation, interpretation and extrapolation must be applied to the data before any coherent picture of the system emerges. The techniques often do not directly provide the investigator with discrete pieces of biochemical information.

Biochemistry is a diverging subject. Therefore, one does not need to apologise for a thesis which creates almost as many problems as it solves. "A little learning is a dangerous thing: Drink deep, or taste not the spring: There shallow draughts intoxicate the brain, And drinking largely sobers us again." (236)

APPENDIX 1 - MATERIALS

A) ENZYMES

Phosphorylase b was prepared from frozen rabbit skeletal muscle by the method of Fischer and Krebs (125) substituting dithiothreitol for cysteine. Phosphorylase b was regularly obtained from the enzyme preparation laboratory of the Oxford Enzyme Group in batches of 10-15 grammes. The crystals were freeze dried and stored at -20°C in a dessicated container. Phosphorylase a was prepared from phosphorylase b using the method described by Griffiths (101).

Phosphorylase kinase and AMP deaminase were prepared from fresh rabbit skeletal muscle by the methods of Cohen (52) and Smiley et al. (203) respectively. Phosphorylase kinase, which was activated by phosphorylation, was prepared as described in ref. 52.

Hexokinase (yeast), Glucose 6 phosphate dehydrogenase (yeast), myokinase (rabbit muscle), and pancreatic trypsin, trypsin inhibitor, amylase and RNase were obtained from Sigma Ltd. E. coli alkaline phosphatase and Crotalus phosphodiesterase were purchased from Boehringer Ltd.

Enzyme purity was checked by electrophoresis in $7\frac{1}{2}\%$ polyacrylamide gels containing sodium dodecyl sulphate, according to the method of Weber and Osborn (204).

B) BUFFERS

Triethanolamine hydrochloride, Potassium chloride, EDTA, Tris(hydroxymethyl)-methylamine and β -glycerophosphate (disodium salt) were obtained from

Sigma Ltd. The standard triethanolamine buffer referred to throughout this thesis consists of 50 mM triethanolamine hydrochloride, 100 mM Potassium Chloride and 1 mM EDTA adjusted to pH 7.5 with concentrated hydrochloric acid. Sulphydryl protecting reagents were added when appropriate.

The glycerophosphate buffers used are described in ref. 52.

Tris and phosphate buffers were prepared according to McKenzie (205) using salts obtained from Sigma Ltd., Fisons Ltd. (analytical grade) or BDH (Analar grade).

C. REAGENTS FOR PROTEIN MODIFICATION

Iodoacetamide was purchased from BDH Ltd. and was purified by recrystallisation from petroleum ether (80-100° fraction). 4 iodoacetamidosalicylic acid was purchased from KochLightLtd. Spin labels were obtained from Synvar Ltd. and 4 chloro 7 nitrobenzofurazan was purchased from Serva Ltd. DTNB and cystine were obtained from BDH Ltd.

All these reagents were stored in the dark in sealed dessicated containers.

D. MATERIALS FOR ENZYME ASSAYS

Oyster glycogen was purchased from BDH Ltd. and freed of nucleotides by the method of Metzger et al. (30). Glucose 1-phosphate dipotassium salt was obtained from Boehringer Ltd.

The materials for the Hurst phosphate assay, Ammonium Molybdate, Hydrazine Sulphate and Sulphuric acid were purchased from BDH Ltd.

Nucleotides and sugar phosphate effectors were obtained from Boehringer

or Sigma Ltd. (depending upon availability). Nucleotide concentrations were checked using the extinction coefficients published in "Data for Biochemical Research" (206).

E. MISCELLANEOUS REAGENTS

- (i) Doubly distilled water was used in all experiments.
- (ii) Deuterium oxide and other deuterated chemicals were purchased from Ryvan Ltd.
- (iii) Dithiothreitol, β mercaptoethanol and cysteine were purchased from BDH Ltd.
- (iv) Imidazole was recrystallized 2 or 3 times from water before use.
- (v) Radioactively labelled reagents and materials for scintillation counting were purchased from Radiochemicals Ltd and Kochlite Ltd. respectively.
- (vi) Pyridoxalphosphate and derivatives were obtained from Sigma Ltd.

APPENDIX 2 TECHNICAL DETAILS

A) PHOSPHORYLASE ASSAYS

Phosphorylase activity in the presence or absence of AMP was determined using the autoanalyser method described by Salmon (124), which assays the rate of phosphate release from glucose-1-phosphate in the presence of glycogen. The assay mixture usually consisted of 10 mgs/ml glycogen, 16 mM glucose-1-phosphate, + 1 mM AMP in triethanolamine KCl EDTA buffer at pH 7.0. The assays, which were performed at 30°C were linear for at least 10 minutes.

Phosphorylase kinase activity was assayed by measuring the rate of production of AMP independent phosphorylase activity, using the above assay system.

B) THE MOLAR CONCENTRATION OF PHOSPHORYLASE

Phosphorylase concentrations were determined using the published 280 nm absorption of 1.32 for a 1 mg/ml solution (131). A subunit molecular weight of 100,000 was used in all calculations concerning stoichiometry (207).

C. RADIOACTIVITY MEASUREMENTS

0.5 ml samples containing radioactive material were added to 10 ml aliquots of scintillation fluid (5 gms PPO, 0.1 gms POPOP, 250 ml Tritan X100 made up to 1 litre with Analar Toluene) in glass vials. Rates of 10,000 - 80,000 c.p.m. were recorded on a Beckman LS-233 Liquid Scintillation System (208-210). Duplicate dilutions and measurements were

made and the results were corrected for background radiation using vials containing no "hot" material.

Count rates were converted to molar terms by measuring count rates of standard solutions of radioactive reagents. In some experiments small amounts of protein or other reagents were added to these standard solutions to verify that artefactual quenching effects were minimal.

D) ABSORPTION MEASUREMENTS

Routine optical density measurements were made on a Unicam SP500 Series 2 spectrophotometer. Time dependent changes in optical density were recorded on a Hilger-Gilford spectrophotometer with a thermostatted cell holder and an automatic cell changer. This system was used to monitor the kinetics of the reaction of Nbf-Cl with phosphorylase, and in AMP deaminase and Glucose-6-phosphate dehydrogenase assays.

E. METHODS SUPPLEMENT TO CHAPTERS 4 AND 6

Phosphorylase adducts were prepared as described in the following references:

acetamidosalicylate phosphorylase <u>b</u> and <u>a</u>	- reference 79
spin labelled phosphorylase <u>b</u>	- reference 101
spin labelled phosphorylase <u>a</u>	- reference 144
Nbf phosphorylase <u>b</u>	- reference 124
5 diazo 1H tetrazole(DHT)phosphorylase <u>b</u> (provided by Dr. O. Avramovic-Zikic)	- reference 145
spin and acetamidosalicylate labelled DHT phosphorylase <u>b</u>	- reference 149
FDNB modified phosphorylase <u>b</u>	- reference 137 and text.

The spin labelled derivative [N^6 -(2,2,6,6-tetramethylpiperidin-4-yl-l-oxy)adenosine-5'-monophosphate] was prepared by Drs. W. Trommer and H. Wenzel (211). The diamagnetic analogue N^6 -(2,2,6,6-tetramethylpiperidin-4-yl)adenosine-5'-monophosphate was prepared by Dr Wenzel from the barium salt of 6-chloro-9- β -D-ribofuranosylpurine-5'-monophosphate by treatment with a two molar excess of 4-amino-2,2,6,6-tetramethylpiperidine in aqueous solution for 16 h at room temperature. The crude product was applied to a column of DEAE Sephadex A 25 in the acetate form and was eluted first with water and subsequently with a linear gradient of water and 0.2M acetic acid. A molar extinction coefficient of 20,000 units at 260 nm was taken for both AMP derivatives.

All ESR experiments were carried out on a JEOLCO JES-PE-1X X-band spectrometer using an aqueous solution cell. A small syringe was fitted to the bottom end of the cell in order to mix the solutions during the titrations without removing the cell from the cavity. The ESR instrument settings were usually: scan range 100 Gauss, modulation amplitude 1-2 Gauss, microwave power 40-50 mW, time constant 0.3 sec and scan time 4-8 minutes.

Fluorescence experiments, utilising the quenching of light emission from acetamidosalicylate phosphorylase b and a by ligands were carried out using 1-5 μ M enzyme on a Hitachi-Perkin Elmer recording spectrofluorimeter (model MPF-2A). All experiments were carried out in a buffer system at 20°C containing 50 mM triethanolamine hydrochloride, 100 mM KCl and 1 mM EDTA adjusted to pH 7.0- 8.4 with concentrated KOH.

Ultracentrifugation measurements were made using a Beckman analytical centrifuge (model E) operated by Mrs L. Butterfield. In sedimentation

experiments 5-10 mg/ml phosphorylase was used, the boundary being detected by Schlieren optics. Data from photographic plates were measured with a Nikon Profile Projector Model 6C and analysed using an Olivetti Programme provided by Dr. J.E. Hyde (212). Deductions about the aggregation states of the various phosphorylase species present were made by comparing the measured sedimentation coefficients with the sedimentation values given in references 28-30 for monomeric, dimeric and tetrameric enzyme.

F. NMR SPECTROMETERS

Phosphorus NMR spectra at 129 MHz (7.5 Tesla) were obtained on an instrument constructed by D.I. Hoult (213) using quadrature Fourier Transform with an Ordered Phase Sequence (CYCLOPS) of transmitter pulses, and appropriate hardware routing in the computer store in order to ortho-normalise the two free induction decays. A Bruker WH-90 spectrometer operating in the Fourier Transform mode was used to record phosphorus spectra at 36.43 MHz (2.1 Tesla). Both spectrometers were operated without proton decoupling.

Proton NMR spectra were recorded on a Bruker 270 MHz spectrometer with an Oxford Instrument Co. Superconducting magnet. The Fourier Transform mode was adopted for all spectra shown in this thesis.

G) METHODS SUPPLEMENT TO CHAPTER 7 AND 8

The glycogen particulate fraction from rabbit muscle was prepared by the acid precipitation method described by Meyer et al. (74). In most experiments glycerophosphate buffer was replaced by a triethanolamine buffer system as the former interfered with the ^{31}P NMR assay of ligands. After acid

precipitation of the crude muscle extract from one rabbit, the precipitate was suspended in 50 ml of 50 mM triethanolamine 100 mM KCl 1 mM EDTA buffer at pH 8.0. If necessary the pH was adjusted to 7.0 by adding the above triethanolamine buffer at pH 6.8. The final glycogen particulate suspension was adjusted to contain about 20 mg/ml glycogen using the above triethanolamine buffer at pH 7.0.

Routinely, glycogen particles from 1 rabbit were prepared for immediate use. All the experiments reported in this thesis were performed on freshly prepared particles.

Glycogen particles from normal and l strain mice were prepared by a scaled down version of the Meyer et al method (74). For each precipitation, the hind leg muscles from 12 freshly killed mice were used.

Phosphorylase activation in the glycogen particle fraction was measured as described by Heilmeyer et al. (164) and the test for ab hybrids was performed as described by Hurd et al. (153).

Phosphorylase phosphatase activity in the glycogen particle fraction was assayed by monitoring phosphorylase a activity as a function of time. The procedure for assaying phosphorylase a in the glycogen particles was as follows: 10 λ aliquots of the appropriate glycogen particle mixture were taken at different times and added to 0.5 ml aliquots of 100 mM sodium glycerophosphate, 40 mM β mercaptoethanol, 1 mg/ml bovine serum albumin, 2 mM EDTA, 25 mM sodium fluoride pH 6.8 at 2°C. 10-20 λ aliquots were then taken and added to 1 ml aliquots of 16 mM glucose-1-phosphate, 1% glycogen in 50 mM triethanolamine buffer pH 6.8. Phosphate release was measured using a Technicon autoanalyser by the method described by Salmon (124).

^{31}P NMR spectra were recorded on a Fourier Transform spectrometer operating at 129 MHz (213). Spectra were accumulated for 4-5 minutes on a Nicolet BNC12 computer and then stored on a magnetic disc. Metabolite levels were measured from the peaks using the assignments made by Hoult et al. (175).

Using this technique levels of ATP, ADP, nucleotide monophosphate (AMP and IMP), glucose-6-phosphate, glucose-1-phosphate and inorganic phosphate could be monitored continuously throughout the transient activation.

In order to optimise the signal to noise ratio of the NMR spectra, it is necessary to apply radio frequency pulses at time intervals approximately equal to the spin-lattice relaxation time (T_1), of the resonances. Consequently the peak areas are only proportional to the concentrations of the metabolites if all their resonances have the same T_1 . However, regardless of the relative T_1 values, the change in area of any given peak always reflects the change in concentration of the metabolite responsible for that peak. The total peak area is stable to within 20% during the transient activation process. It is therefore reasonable to assume that the T_1 values for all the ligands are very similar so that the peak areas do reflect the relative concentrations of the metabolites.

Glycogen was assayed by the Montgomery method (214). Glucose-6-phosphate was measured using glucose-6-phosphate dehydrogenase as described by Kuby and Noltmann (215). Myokinase was assayed by the method of Kalckar (216) using 5'-adenylic acid deaminase purified by the method of Smiley et al. (203).

H) FREEZE CLAMP PROCEDURES

The method adopted for freeze clamping tissues was as follows: Immediately after excision, the rat or rabbit intact muscle was clamped between tongs which had been cooled in liquid nitrogen. The frozen muscle was then transferred to a liquid nitrogen cooled percussive mortar and broken to a powder. The powder was tipped into an ice cooled mortar containing 6% perchloric acid and ground with a pestle for about 5-10 minutes. About 4 parts of acid to one part of muscle, by volume, was used. After a short low speed centrifugation to remove the muscle debris, the extract was neutralised with KOH. Using phosphorus NMR, it was checked that the debris contained a minimal quantity of phosphate containing ligands. After further centrifugation, the neutralised extract was freeze dried. The powder was stored at -20°C and could be hydrated in appropriate buffers when required.

I. MUSCLE DIALYSIS

In most studies, the Vastus lateralis or Gastrocnemius white muscles were used. All phosphate containing ligands were removed from freshly excised pieces of muscle by overnight dialysis at room temperature into 50 mM triethanolamine hydrochloride 1 mM dithiothreitol, 1 mM EDTA pH 7.0. During dialysis 1-5 gm samples of muscle were placed in 2-3 litre buffer samples, which were slowly stirred. Various combinations of phosphate / arsenate etc. were subsequently added to the buffer and dialysed into the pieces of muscle.

The presence or absence of phosphate containing metabolites in the muscle could be determined using phosphorus NMR.

APPENDIX 3 ARE CHANGES IN THE ESR RATIO ALWAYS PROPORTIONAL
TO SATURATION FUNCTIONS?

Suppose the free spin labelled enzyme exhibits a ratio $R_A = \frac{h_{1A}}{h_{2A}}$ and ligand saturated spin labelled enzyme exhibits a ratio

$R_B = \frac{h_{1B}}{h_{2B}}$, where $h_{1A,B}$ and $h_{2A,B}$ refer to the heights of the low field

and centre lines in the ESR spectra respectively.

If f is the fraction of enzyme with ligand bound, the ratio observed:

$$R_f = \frac{(1-f) h_{1A} + f h_{1B}}{(1-f) h_{2A} + f h_{2B}}$$

Consider an extreme case where $R_A = 0.8$ and $R_B = 0.5$.

Case 1 If the centre line does not alter in magnitude during the titration $h_{2A} = h_{2B} = 10$, $h_{1A} = 8$ and $h_{1B} = 5$.

$$\therefore f = \frac{8 - 10R}{3} \quad \text{i.e. the fraction of enzyme with ligand}$$

bound is linearly proportional to R .

Case 2 If the centre line does alter in magnitude during the titration

by, say 20%, then $h_{2A} = 10$, $h_{2B} = 8$, $h_{1A} = 8$, $h_{1B} = 4$.

In this case:

$$f = \frac{5R - 4}{R - 2}$$

i.e. the fraction of enzyme with ligand bound is not linearly related to R .

During titrations of ligands into spin labelled enzyme, it is always assumed that changes in the ESR ratio are proportional to f . If this assumption

is made and, during the titration, the centre peak height decreases, an error in f will occur. The error will be given by the difference between the expressions for f in cases 1 and 2.

$$\text{Error in } f, \Delta f = \frac{5R - 4}{R - 2} - \frac{8 - 10R}{3}$$

Over practical values of R , values of f calculated assuming linearity between R and f will be underestimates by up to 10%. As $\frac{5R - 4}{R - 2} > \frac{8 - 10R}{3}$, in the range $R = 0.5 - 0.8$, calculated values of n (see Chapter 4 section D ii) will always be underestimates rather than overestimates.

Conclusion - If it is assumed that changes in the ESR ratio are proportional to the amount of ligand-bound enzyme (f), changes in the centre peak height during ESR titrations can cause an error of up to 10% in the calculated values of f . In most of the cases discussed in this thesis the error is likely to be much less as (i) the decrease in the centre peak height during the titration is less than 20% and (ii) $R_A - R_B < 0.3$.

REFERENCES

1. Hughes J.T., Jerrome D., and Krebs H.A., (1972) Exp. Eye Res. 14 189-195
2. McLuhan M. (1964) in "Understanding Media" ch.2 Routledge and Kegan-Paul, London.
3. Cori G.T. and Cori C.F. (1931) J. Biol. Chem. 94 561-579.
4. Embden G. and Zimmerman M. (1924) Z. Physiol. Chem. 141 225-232
5. Embden G., Schmitz E. and Meincke P. (1921) Z. Physiol. Chem. 113 10-66.
6. Cori C.F., Colowick S.P. and Cori G.T. (1937) J. Biol. Chem. 121 465-477.
7. Cori G.T., Colowick S.P. and Cori C.F. (1938) J. Biol. Chem. 124 543-555.
8. Cori C.F. and Cori G.T. (1936) Proc. Soc. Exper. Biol. Med. 34 702-705.
9. Cori G.T., Colowick S.P. and Cori C.F. (1938) J. Biol. Chem. 123 381-389.
10. Parnas M.J.K. and Mochnocka I. (1936) Compt. rend. Soc. Biol. 123 1173-1175.
11. Green A.A., Cori G.T. and Cori C.F. (1942) J. Biol. Chem. 142 447-448.
12. Green A.A. and Cori G.T. (1943) J. Biol. Chem. 151 21-29.
13. Cori G.T. and Green A.A. (1943) J. Biol. Chem. 151 31-38.
14. Krebs E.G. and Fischer E.H. (1953) J. Biol. Chem. 216 113-120.
15. Fischer E.H. and Krebs E.G. (1955) J. Biol. Chem. 216 121-132.

16. Krebs E.G. and Fischer E.H. (1956) *Biochim. Biophys. Acta* 20 150-157.
17. Krebs E.G. and Fischer E.H. (1958) *J. Biol. Chem.* 231 73-78.
18. Fischer E.H., Graves D.J., Crittenden E.R.S. and Krebs E.G. (1959) *J. Biol. Chem.* 234 1698-1704.
19. Brostrom C.O., Hunkeler F.L. and Krebs E.G. (1971) *J. Biol. Chem.* 246 1961-1967.
20. Ashley C.C. (1970) *Endeavour* 30 18-25.
21. Danforth W.H., Helmreich E., and Cori C.F. (1962) *Proc. Nat. Acad. Sci. USA.* 48 1191-1199.
22. Stull J.T. and Mayer S.E. (1971) *J. Biol. Chem.* 246 5716-5723.
23. Yeaman S.J. and Cohen P. (1975) *Eur. J. Biochem.* 51 93-104.
24. Walsh D., Perkins J.P. and Krebs E.G. (1968) *J. Biol. Chem.* 243 3763-3774.
25. Larner J. and Vilar-Palasi C. (1971) In "Current Topics in Cellular Regulation" (Horecker B.L. and Stadtman E.R. eds.) 3 196-236. Academic Press, New York.
26. Leloir L.F. and Cardini C.E. (1957) *J. Amer. Chem. Soc.* 79 6340-6341.
27. Cohen P., Duewer T. and Fischer E.H. (1971) *Biochem.* 10 2683-2694.
28. Birkett D.J. (1971) D.Phil. Thesis, Oxford University.
29. Wang J.H., Shonka M.L. and Graves D.J. (1965) *Biochem. Biophys. Res. Comm.* 18 131-135.
30. Metzger B., Helmreich E. and Glaser L. (1967) *Proc. Nat. Acad. Sci. USA.* 59 994-1001.

31. Birkett D.J., Radda G.K., and Salmon A.G. (1971)
FEBS letters 11 295-297.
32. Hedrick J.L., Shaltiel S., and Fischer E.H. (1969)
Biochem. 8 2422-2429.
33. Baronowski T., Illingworth B., Brown D.H. and Cori C.F.
(1951) Biochim. Biophys. Acta 25 16-21.
34. Forrey A.W., Sevilla C.L., Saari J.C. and Fischer E.H.
(1971) Biochem. 10 3132-3140.
35. Shaltiel S., Hedrick J.L. and Fischer E.H. (1966)
Biochem. 5 2108-2116.
36. Fischer E.H., Kent A.B., Snyder E.R. and Krebs E.G.
(1958) J. Amer. Chem. Soc. 80 2906-2907.
37. Shaltiel S., Hedrick J.L., Pocker A. and Fischer E.H.
(1969) Biochem. 8 5189-5196.
38. Feldman K., Ziesel H. and Helmreich E. (1972) Proc.
Nat. Acad. Sci. USA. 69 2278-2282.
39. Bresler S., Firsov L., and Glasunov E. (1966) Nature
211 1262-1265.
40. Buc-Caron M-H., Faure F., Oudin L.C., Morange M.,
Vandenbunder B., and Buc H. (1974) Biochimie 56
477-489.
41. Honikel K.O. and Madsen N.B. (1973) Can. J. Biochem. 51
344-356.
42. Shaltiel S. and Cortijo M. (1970) Biochem. Biophys.
Res. Comm. 41 594-600.
43. Cortijo M., Steinberg I.Z. and Shaltiel S. (1971)
J. Biol. Chem. 246 933-938.
44. Nolan C., Novoa W.B., Krebs E.G. and Fischer E.H. (1964)
Biochem. 3 542-551.
45. Fasold H., Ortanderl F., Huber R., Bartels K. and
Schwager P. (1972) FEBS letters 21 229-232.

46. Eagles P.A.M. and Johnson L.N. (1972) *J.Mol.Biol.* 64 693-695.
47. Madsen N.B.(1972) in "The Molecular Basis of Biological Activity" pp.13-52. Academic Press, New York.
48. Eagles P.A.M.,Iqbal M.,Johnson L.N.,Mosley J. and Wilson K.S. (1970) *J.Mol.Biol.* 71 803-806.
49. Johnson L.N.,Madsen N.B.,Mosley J. and Wilson K.S. (1974) *J.Mol.Biol.* 90 703-718.
50. England P.J.,Stull J.T., and Krebs E.G.(1972) *J. Biol.Chem.* 247 5275-5277.
51. Tessmer G. and Graves D.J.(1973) *Biochem.Biophys. Res. Comm.* 50 1-7.
52. Cohen P.(1973) *Eur.J.Biochem.*34 1-14.
53. Hayakawa T.,Perkins J.P.,Walsh D.A., and Krebs E.G. (1973) *Biochem.* 12 567-573.
54. Hayakawa T.,Perkins J.P. and Krebs E.G.(1973) *Biochem.* 12 574-580.
55. Cohen P.(1974) *Biochem.Soc.Symp.* 39 51-73.
56. Krebs E.G.,Huston R.B. and Hunkeler F.L.(1967) In "Advances in Enzyme Regulation" (Weber G. ed.) 6 245-255.
57. Krebs E.G.,Love D.S.,Bratvold G.E.,Trayser K.A., Meyer W.L., and Fischer E.H. (1964) *Biochem.*3 1022-1032.
58. Huston R.B. and Krebs E.G. (1968) *Biochem.*7 2116-2122.
59. Meyer W.L.,Fischer E.H. and Krebs E.G. (1964) *Biochem.* 3 1033-1039.
60. Walsh D. and Krebs E.G. (1973) In "The Enzymes" 3rd. ed.(Boyer P.D.ed.) VIII 555-582. Academic Press, New York.

61. Gill G.N. and Garren L.D. (1971) Proc.Nat.Acad. Sci. USA. 68 786-790.
62. Soderling T.R., Hickenbottom J.P., Reimann E.M. , Hunkeler F.L., Walsh D.A., and Krebs E.G. (1970) J.Biol.Chem. 245 6317-6328.
63. Rasmussen H., Goodman D.B.P. and Tenerhouse A. (1972) Critical Reviews in Biochem. 1 95-148.
64. Robison G.A., Butcher R.W. and Sutherland E.W. (1971) "Cyclic AMP". Academic Press, New York.
65. Kato K. and Bishop J.S. (1972) J.Biol. Chem. 247 7420-7429.
66. Cohen P. and Antoniow J.F. (1973) FEBS letters 34 43-47.
67. Martenson T. M. , Brotherton J.E. and Graves D.J. (1973) J.Biol.Chem. 248 8323-8328.
68. Martenson T.M., Brotherton J.E., and Graves D.J. (1973) J.Biol.Chem. 248 8329-8333.
69. Martenson T.M., and Graves D.J. (1973) J.Biol.Chem. 248 8333-8336.
70. Manners D.J. and Wright A. (1962) J.Chem.Soc. 1597-1602.
71. Walker G. and Whelan W.J. (1960) Biochem.J. 76 264-268.
72. Wanson J.C. and Drochmans P. (1968) J.Cell Biol. 38 130-150.
73. Greenleaf J., Olsson K.E. and Saltin B. (1969) Acta Physiol. Scand. Suppl. 330 86 Abstr. 125.
74. Meyer F., Heilmeyer L.M.G., Haschke R.H. and Fischer E.H. (1970) J.Biol.Chem. 245 6642-6648.
75. Fischer E.H., Heilmeyer L.M.G. and Haschke R.H. (1971) in "Current Topics in Cellular Regulation" (Horecker B.L. and Stadtman E.R. eds.) 4 211-251. Academic Press, New York.

76. Graves D.J. and Wang J.H. (1973) in "The Enzymes" 3rd.ed. (Boyer P.D.ed.) 7 435-482. Academic Press, New York.
77. Radda G.K. (1971) Biochem J. 122 385-396.
78. Birkett D.J., Dwek R.A., Radda G.K., Richards R.E., and Salmon A.G. (1971) Eur.J.Biochem. 20 494-508.
79. Brooks D.J., Busby S.J.W., and Radda G.K. (1974) Eur. J.Biochem. 48 571-578.
80. Brooks D.J., Busby S.J.W. and Radda G.K. (1974) Unpublished observations.
81. Förster T. (1959) Disc.Faraday Soc. 27 7-27.
82. Roberts H. (1972) D.Phil.thesis, Oxford University.
83. Hamilton C.L. and McConnell H.M. (1968) "Spin Labels" in "Structural Chemistry and Molecular Biology" (Rich A. and Davidson N. eds.) pp.115-149. W.H.Freeman, San Francisco.
84. Jost P. and Griffiths O.H. (1972) in "Methods in Pharmacology" 2 (Chignell C.F. ed.) Appleton-Century-Croft, New York.
85. Hemminga M.A. (1974) "Spin Labels in Orientated Membranes", University of Groningen.
86. Campbell I.D., Dwek R.A., Price N.C., and Radda G.K. (1972) Eur.J.Biochem. 30 339-347.
87. Crutchfield M.M., Dungan C.H., Leitcher J.H., Mark V., and Van Wazer J.R. (1967) Topics in Phosphorus Chemistry 5. Wiley Interscience, London.
88. Griffiths J.R., Dwek R.A. and Radda G.K. (1975) Eur. J.Biochem. In press.
89. Griffiths J.R., Dwek R.A. and Radda G.K. (1975) Eur. J.Biochem. In press.
90. Griffiths J.R., Price N.C. and Radda G.K. (1975) Biochem. J. 147 609-613.

91. Busby S.J.W., Hemminga M.A. and Radda G.K. (1975)
Biochem.J. Paper submitted.
92. Coxon B. (1972) in "Advances in Carbohydrate Chemistry and Biochemistry" 27 (Tipson R.S. and Horton D. eds.) pp.7-83. Academic Press, New York.
93. Gadian D.G. (1974) D.Phil. Thesis, Oxford University.
94. Carrington A. and McLachlan A.D. (1967) "Introduction to Magnetic Resonance". Harper and Row, New York.
95. Karplus M. (1963) J.Amer.Chem.Soc. 85 2870-2871.
96. Campbell I.D., Dobson C.M., Williams R.J.P. and Xavier A.V. (1973) Ann.N.Y.Acad.Sci. 222 163-174.
97. Black W.J. and Wang J.H. (1968) J.Biol.Chem. 243 5892-5898.
98. Madsen N.B. and Schechovsky S. (1967) J.Biol. Chem. 242 3301-3307.
99. Madsen N.B. (1961) Biochem. Biophys. Res. Comm. 6 310-315.
100. Tu J.I., Jacobson G.R. and Graves D.G. (1971) Biochem. 10 1229-1236.
101. Griffiths J.R. (1974) D.Phil. thesis, Oxford University.
102. Huang C.Y. and Graves D.J. (1970) Biochem. 9 660-671.
103. Bot G. and Dosa I. (1971) Acta Biochim. et Biophys. Acad. Sci. Hung. 6 73-87.
104. Seery V.L., Fischer E.H. and Teller D.C. (1967) Biochem. 6 3315-3327.
105. Madsen N.B. (1972) in "The Molecular Basis of Biological Activity". pp.13-52. Academic Press, New York.
106. Madsen N.B. and Cori C.F. (1958) J.Biol.Chem. 233 1251-1256.
107. "Fluorescence Techniques in Cell Biology" (1973) (Thaer A.A. and Sernetz M. eds.) Springer-Verlag, New York.

108. Williams D.H. and Fleming I.(1966) "Spectroscopic Methods in Organic Chemistry". McGraw-Hill,London.
109. Seeley P.J.(1975) D.Phil. thesis, Oxford University.
110. Dwek R.A.(1974) "NMR in Biochemistry".Clarendon Press, Oxford.
111. Radda G.K.(1971) in "Current Topics in Bioenergetics" (Sanadi D.R. ed.) 4 81-126. Academic Press, New York. see also 84.
112. Brooks D.J.,Busby S.J.W.,Dwek R.A.,Griffiths J.R., and Radda G.K. (1973) in "Metabolic Interconversion of Enzymes"(Fischer E.H.,Krebs E.G.,Neurath H. and Stadtman E.R.) pp.7-19. Springer-Verlag, Berlin.
113. Battell M.L.,Smillie L.B. and Madsen N.B. (1968) Can. J.Biochem. 46 609-615.
114. Zarkadas C.G.,Smillie L.B. and Madsen N.B. (1968) J.Mol.Biol. 38 245-247.
115. Jokay I.,Damjanovich S.,and Toth S.(1965) Arch. Biochem. Biophys. 112 471-475.
116. Appleman M.M.,Yunis A.A., Krebs E.G. and Fischer E.H. (1967) J.Biol. Chem. 238 1358-1361.
117. Avramovic-Zikic O.,Smillie L.B. and Madsen N.B.(1970) J.Biol. Chem. 245 1558-1565.
118. Zarkadas C.G.,Smillie L.B. and Madsen N.B. (1969) Can. J.Biochem. 48 763-776.
119. Buc-Caron M-H.(1969) D.Sc. thesis, University of Paris.
120. Kleppe K. and Damjanovich S.(1969) Biochim.Biophys. Acta 185 88-102.
121. Sanner T. and Tron L.(1975) Biochem.14 230-235.
122. Johnson P.(1972) Part 2 thesis, Oxford University.
123. Robinson G.B.(1973) Part 2 thesis, Oxford University.
124. Salmon A.G. (1972) D.Phil. thesis, Oxford University.
125. Fischer E.H. and Krebs E.G. (1962) Methods in Enzymology. 5 369-373.

126. "Tables of Physical and Chemical Constants" (Kaye G.W.C. and Laby T.H. eds.) Thirteenth ed. (1966) Longmans, London.
127. Birkett D.J., Price N.C., Radda G.K. and Salmon A.G. (1970) FEBS letters 6 346-348.
128. Ellman G.L. (1959) Arch. Biochem. Biophys. 82 70-77.
129. Freedman R.B. and Radda G.K. (1968) Biochem. J. 108 383-391.
130. Buc M-H and Buc H. (1967) in "Regulation of Enzyme Activity and Allosteric Interactions" 4th FEBS Symposium, Oslo. pp. 109-130. Academic Press, London.
131. Kastenschmidt L.L., Kastenschmidt J. and Helmreich E. (1968) Biochem. 7 4543-4556.
132. Fischer E.H., Hurd S.S., Koh P., Seery V.C. and Teller D.C. (1968) in "Control of Glycogen Metabolism" pp. 19-33. Universitetsfolaget, Oslo.
133. Heilmeyer L.M.G. and Haschke R.H. (1972) in "Protein-Protein Interactions" (Jaenicke R. and Helmreich E. eds.) pp. 299-315. Springer-Verlag, Berlin.
134. Helmreich E., Michaelides M.C. and Cori C.F. (1967) Biochem. 6 3695-3710.
135. Buc H., Buc M-H., Garcia Blanco F., Morange M. and Winkler H. (1975) in "Proc. 3rd. Int. Conf. on Interconvertible Enzymes" (Fischer E.H., Krebs E.G., Neurath H. and Stadtman E.R. eds.) Springer-Verlag, Berlin.
136. Fasold H., Keller F., Halbach M. and Helmreich E. (1969) Fed. Proc. 28 847.
137. Baumert H.G., Fasold H., Keller F., Halbach M., and Ortanderl F. (1973) FEBS letters 31 23-26.
138. Monod J., Wyman J. and Changeux J-P. (1965) J. Mol. Biol. 12 88-118.

139. Koshland D.E., Némethy G., and Filmer P. (1966)
Biochem. 5 365-385.
140. Weber G. (1972) Biochem. 11 864-878.
141. Bell J.E. and Dalziel K. (1973) Biochim Biophys.
Acta 309 237-242.
142. Bennick A., Campbell I.D., Dwek R.A., Price N.C.,
Radda G.K. and Salmon A.G. (1971) Nature 234
140-143.
143. Black W.J. and Wang J.H. (1970) Biochim. Biophys .
Acta 212 257-268.
144. Griffiths J.R., Price N.C. and Radda G.K. (1974)
Biochim. Biophys. Acta 358 275-280.
145. Avramovic-Zikic O., Briedenbach W.C. and Madsen N.B.
(1974) Can. J. Biochem. 52 146-148.
146. Avramovic- Zikic O., Jurasek L., Madsen N.B., and
Shechovsky S. (1975) Abstr. No. 928. 10th. Int.
FEBS Meeting, Paris.
147. Lowry O.H., Schulz D.W., and Passonneau J.V. (1964)
J. Biol. Chem. 239 1947-1953.
148. Busby S.J.W., Hemminga M.A., Radda G.K., Trommer W.E.,
and Wenzel H. (1975) Eur. J. Biochem. In Press.
149. Brooks D.J., Busby S.J.W., Griffiths J.R., Radda G.K.,
and Avramovic-Zikic O. (1975) Can. J. Biochem. Paper
Submitted.
150. Berden J.A., Cullis P.R., Houtt D.I., McLaughlin A.C.,
Radda G.K. and Richards R.E. (1975) FEBS letters
46 55-58.
151. Farrar T.C. and Becker E.D. (1971) "Pulse and
Fourier Transform NMR" Academic Press , New York.
152. Busby S.J.W., Gadian D.G., Radda G.K., Richards R.E.,
and Seeley P.J. (1975) FEBS letters 55 14-117.

153. Hurd S.S., Teller D., and Fischer E.H. (1966) *Biochem. Biophys. Res. Comm.* 24 79-84.
154. Bot G., Kovacs E.F., and Gergely P. (1974) *Biochim. Biophys. Acta* 370 70-77.
155. Gergely P., Bot G., and Kovacs E.F. (1974) *Biochim. Biophys. Acta* 370 78-84.
156. Livanova N.B., Eronina T.B. and Silanova G.V. (1972) *Doklady Biochemistry* 207 533-535.
157. Eisenger J. and Dale R.E. (1973) *J. Mol. Biol.* 84 643-647.
158. Dwek R.A., Griffiths J.R., Radda G.K. and Strauss U. (1972) *FEBS letters* 28 161-164.
159. Bot G., Varsanyi M., and Gergely P. (1975) *FEBS letters* 50 351-354.
160. Brooks D.J., Busby S.J.W., Dwek R.A., Griffiths J.R., Radda G.K. and Seeley P.J. (1973) Unpublished Data.
161. Jennissen H.P. and Heilmeyer L.M.G. (1974) *Anal. Biochem.* 57 118-126.
162. Kim G. and Graves D.G. (1973) *Biochem.* 12 2090-2095.
163. Stull J.T. and Mayer S.E. (1971) *J. Biol. Chem.* 246 5716-5723.
164. Heilmeyer L.M.G., Meyer F., Haschke R.H. and Fischer E.H. (1970) *J. Biol. Chem.* 245 6649-6656.
165. Wanson J-C. and Drochmans P. (1968) *J. Cell Biol.* 38 130-150.
166. Wanson J-C. and Drochmans P. (1972) *J. Cell Biol.* 54 206-224.
167. Higashi Y., Strominger J.L., and Sweeley C.C. (1967) *Proc. Nat. Acad. Sci. USA.* 57 1878-1884.
168. Sentandreu R. and Lampen J.O. (1971) *FEBS letters* 14 109-113.
169. Northcote D.H. (1969) *Proc. Roy. Soc. B.* 173 21-30

170. Takagi A., Schotland D.L., Dimauro S. and Rowland L.P. (1973) *Neurology* 23 1008-1016.
171. Haschke R.H., Heilmeyer L.M.G., Meyer F. and Fischer E.H. (1970) *J. Biol. Chem.* 245 6657-6663.
172. Haschke R.H., Grätz K.W. and Heilmeyer L.M.G. (1972) *J. Biol. Chem.* 247 5351-5356.
173. Gratecos D., Detwiler T., and Fischer E.H. (1973) in "Metabolic Interconversion of Enzymes" (Fischer E.H.,
174. Krebs E.G., Neurath H., and Stadtman E.R. eds.) pp. 43-52. Springer-Verlag, Berlin.
175. Busby S.J.W., Griffiths J.R. and Radda G.K. (1973) *FEBS letters* 42 296-300.
176. Hoult D.I., Busby S.J.W., Gadian D.G., Radda G.K., Richards R.E. and Seeley P.J. (1974) *Nature* 252 285-287.
177. Brody T.G. and Costello J.F. (1974) *Biochim. Biophys. Acta* 350 455-460.
178. Illsley N.P. and Radda G.K. (1975) Unpublished Data. Lee Y-P. (1957) *J. Biol. Chem.* 227 999-1007.
179. Piras R. and Staneloni R. (1970) *Biochem.* 8 2153-2160.
180. Beis I.D. (1973) D.Phil. thesis, Oxford University.
181. Parmeggiani A. and Morgan H.E. (1962) *Biochem. Biophys. Res. Comm.* 9 252-256.
182. Lyon J.B. and Porter J. (1963) *J. Biol. Chem.* 238 1-11.
183. Cohen P. and Cohen P.T.W. (1973) *FEBS letters* 29 113-116.
184. Gross S.R. and Mayer S.E. (1974) *J. Biol. Chem.* 249 6410-6418.
185. Bot G. and Dósa I. (1971) *Acta Biochim. et Biophys. Acad. Sci. Hung.* 6 73-87.
186. Varsányi M. and Bot G. (1973) *Acta Biochim. et Biophys. Acad. Sci. Hung.* 8 23-31.

187. Mejbaum-Katzenellenbogen W., Lomako J., and Makosch D.
(1971) *Acta Biochem. Pol.* 18 271-276.
188. Newsholme E.A. and Start C. (1973) "Regulation in Metabolism". John Wiley, London.
189. Wollenberger A., Ristau O. and Schoffa G. (1960)
Pflügers Arch. Ges. Physiol. 270 399-412.
190. Gumaa K.A., McLean P. and Greenbaum A.L. (1971) in
"Essays in Biochemistry" 7 (Campbell P.N. and Dickens F. eds.) pp. 39-86. Academic Press, London.
191. Brandt H., Killilea D. and Lee E.Y.C. (1974) *Biochem. Biophys. Res. Comm.* 61 598-604.
192. Ranvier L. (1874) *Arch. Physiol. Norm. Path. Paris* 1 5-15.
193. Needham D.M. (1971) "Machina Carnis". Cambridge University Press.
194. Beatty C.H. and Bocek R.M. (1970) in "Physiology and Biochemistry of Muscle as a Food". 2 (Briskey E.J., Cussero R.G. and Marsh B.B. eds.) pp. 151-191. Madison: University of Wisconsin Press.
195. Young V.R. (1970) in "Mammalian Protein Metabolism" IV (Munro H.N. ed.) pp. 585-674. Academic Press, New York.
196. Bergmeyer H.U. (1974) in "Methods of Enzymatic Analysis" pp. 496-497. Academic Press, New York.
197. Bergmeyer H.U. (1974) in "Methods of Enzymatic Analysis" pp. 498-499. Academic Press, New York.
198. Szent-Györgyi A. (1949) *Biol. Bull.* 96 140-161.
199. Rome E. (1972) *J. Mol. Biol.* 65 331-345.
200. Bendall J.R. in "Muscles, Molecules and Movement" pp. 58-73. Heineman Educational Books, London.
201. Krimsky I. and Racker E. (1963) *Biochem.* 2 512-518.
202. Hawthorne J.N. and Hubscher G. (1959) *Biochem. J.* 71 195-200.

203. Smiley K.C., Berry A.J. and Suelter C.H. (1967) *J. Biol. Chem.* 242 2502-2506.
204. Weber K. and Osborn M. (1969) *J. Biol. Chem.* 244 4406-4412.
205. McKenzie H.A. and Dawson R.M.C. (1969) in "Data for Biochemical Research" (Dawson R.M.C., Elliot D.C., Elliot W.H. and Jones K.M. eds.) 2nd. ed. 476-508. Clarendon Press, Oxford.
206. Burton K. (1969) in "Data for Biochemical Research" (Dawson R.M.C., Elliot D.C., Elliot W.H. and Jones K.M. eds.) pp. 169-179. Clarendon Press, Oxford.
207. Cohen P., Duewer T., and Fischer E.H. (1971) *Biochem.* 10 2683-2694.
208. Birks J.B. (1972) "An Introduction to Liquid Scintillation Counting". Koch-Lite Laboratories Ltd.
209. Birks J.B. (1972) "Solutes and Solvents for Liquid Scintillation Counting". Koch-Lite Laboratories Ltd.
210. Price N.C. (1973) *FEBS letters* 36 351-354.
211. Trommer W.E., Wenzel H. and Pfeleiderer G. (1974) *Leibigs Ann. Chem.* 1974 1357-1359.
212. Hyde J.E. (1975) Personal Communication.
213. Houlst D.I. and Richards R.E. (1975) *Proc. Roy. Soc. A.* 344 311-340.
214. Montgomery R. (1957) *Arch. Biochem. Biophys.* 67 378-386.
215. Kuby S.A. and Noltmann E.A. (1966) in "Methods in Enzymology" IX (Wood W.A. ed.) Academic Press, New York.
216. Kalckar H.M. (1947) *J. Biol. Chem.* 167 461-475.
217. Danforth W.H., Helmreich E. and Cori C.F. (1962) *Proc. Nat. Acad. Sci. USA.* 48 1191-1199.

218. Morgan H.E. and Parmeggiani A.(1964) J.Biol. Chem. 239 2440-2445.
219. Cori C.F.(1956) in "Enzymes: Units of Biological Structure and Function". (Gaebler O.H. ed.) Academic Press, New York.
220. Cori G.T.(1945) J.Biol.Chem. 158 333-339.
221. Gerbach E., Deuticke B. and Dreisbach R.H.(1963) Naturwissenschaften 50 228-229.
222. Marston S.(1973) Biochim. Biophys.Acta 305 397-412.
223. Seraydarian K., Mommaerts W.F.H.M. and Wallner A.(1962) Biochim.Biophys.Acta 65 443-460.
224. Mommaerts W.F.H.M.(1952) J.Biol.Chem. 198 469-475.
225. Guillory R.J. and Mommaerts W.F.H.M.(1962) Biochim. Biophys.Acta 65 316-325.
226. Childress C.C. and Sacktor B.(1970) J.Biol.Chem.245 2927-2936.
227. Helmreich E. and Cori C.F.(1965) Adv. Enz. Regulation 3 91-107.
228. Griffiths J.R.(1975) Unpublished calculations.
229. Danforth W.H. and Lyon J.B.(1964) J.Biol.Chem. 239 4047-4050.
230. Atkinson D.E.(1968) Biochem. 7 4030-4034.
231. Zielke C.L. and Suelter C.H.(1971) in "The Enzymes" 3rd.ed. (Boyer P.D. ed.) pp.47-78.Academic Press, New York.
232. Kalckar H.M. and Rittenberg D.(1947) J.Biol.Chem. 170 455-459.
233. Lowenstein J.M.(1972) Physiol.Rev. 52 382-414.
234. Muirhead K.M. and Bishop S.H.(1974) J.Biol.Chem. 249 459-465.
235. Lawrence D.H. in "Selected Poems". Penguin Books, London.
- 236 . Pope A. in "Essay on Criticism".